Université de Montréal

Diencephalic and mesencephalic substrate for brain stimulation reward

Par

Marc Fakhoury

Département de Neurosciences

Faculté de Médecine

Thèse présentée

en vue de l'obtention du grade de

doctorat en neurosciences

Avril 2018

Université de Montréal
Faculté des études supérieures

Cette thèse intitulée:

Diencephalic and mesencephalic substrate for brain stimulation reward

présentée par :

Marc Fakhoury

a été évaluée par un jury composé des personnes suivantes :

John Kalaska, président-rapporteur

Pierre-Paul Rompré, directeur de recherche

Stéphanie Fulton, membre du jury

Andreas Arvanitogiannis, examinateur externe

René Cardinal, représentant du doyen

Résumé

La stimulation électrique de certains sites cérébraux chez les animaux de laboratoire induit un effet de récompense suffisamment fort pour obtenir une réponse opérante; par exemple, les rats apprendront à appuyer sur un levier pour recevoir une salve de pulsions électriques dans ces régions. Ce comportement, appelé autostimulation intracérébrale (ASI), a été largement étudié pour caractériser les substrats neuronaux de la récompense et des comportements dirigés. Plusieurs études au cours des dernières années suggèrent que le système dorsal diencéphalique (SDC) ainsi que la queue de l'aire tegmentale ventrale (qATV) sont impliqués dans le phénomène de récompense induit par l'ASI. Cependant, malgré des progrès significatifs dans la recherche, les mécanismes par lesquels le SDC et qATV participent à la transmission du signal de récompense induit par l'ASI restent largement inconnus.

Le principal objectif de cette thèse est d'étudier le rôle du SDC et du qATV dans la récompense induite par stimulation intracérébrale. Trois articles de recherche sont présentés dans cette thèse. Le premier article évalue l'effet de lésions électrolytiques au niveau du SDC et du faisceau médian prosencéphalique (FMP) dans le phénomène de récompense induit par la stimulation électrique de l'hypothalamus latéral (HL) et du raphé dorsal (RD) chez le rat. Les résultats montrent que des lésions effectuées au niveau du SDC et du FMP produisent une plus grande atténuation du phénomène de récompense induit par l'ASI que des lésions effectuées sur une seule de ces voies seulement, et ont un effet plus important sur le signal de récompense induit par la stimulation électrique du HL. Dans le deuxième article de cette thèse, la technique de marquage immuno-histochimique pour la protéine Fos a été utilisée en combinaison avec l'ASI et des lésions électrolytiques du SDC pour déterminer si les mêmes noyaux qui sont actifs chez des rats n'ayant pas reçu de lésion continuent à être actif après une lésion du SDC. Les résultats montrent que des

lésions du SDC réduisent l'expression de la protéine Fos induite par la stimulation électrique du HL dans certains sites du cerveau antérieur, du mésencéphale et du tronc cérébral. Enfin, le troisième article de cette thèse examine le rôle du qATV dans le phénomène de récompense induit par l'ASI et dans l'activité locomotrice. Une attention particulière a été accordée aux fonctions comportementales des récepteurs glutamatergique AMPA et NMDA, ainsi que les récepteurs opioïdes de type mu exprimés au niveau du qATV. Les résultats montrent que le blocage pharmacologique des récepteurs AMPA et NMDA, ainsi que l'activation des récepteurs opioïdes de type mu, dans certains sites du qATV entrainent une augmentation de l'activité locomotrice et de la récompense induite par l'ASI. Les résultats montrent aussi que la diminution de l'expression des récepteurs NMDA du qATV avec les petits ARN interférents ne modifie pas la récompense induite par l'ASI mais provoque une diminution marquée de la réponse opérante maximale.

Les résultats obtenus dans cette thèse apportent une meilleure compréhension du substrat neuronal de la récompense induite par l'ASI, et suggèrent que (i) le SDC constitue une voie fiable pour la transmission de la récompense induite par l'ASI, (ii) le SDC est connecté avec certaines régions du cerveau antérieur, du mésencéphale et du tronc cérébral, et que (iii) la transmission glutaminergique et opioïde au niveau du qATV régule l'activité locomotrice et le phénomène de récompense induit par l'ASI. Ce travail pourrait avoir d'importantes répercussions sur la compréhension des comportements appétitifs, tels que l'alimentation et la consommation d'alcool, ainsi que sur les troubles psychiatriques, tels que la dépression, la schizophrénie, et les troubles liés à l'utilisation de substances.

Mots-clés: activité locomotrice; autostimulation intracérébrale; queue de l'aire tegmentale ventrale; récompense; système dorsal diencéphalique

Abstract

Electrical stimulation of certain brain regions in laboratory animals induces a rewarding effect that is strong enough to support operant responding; for instance, rats will learn to press a lever to receive a short train of electrical pulses in these regions. This behavior, termed intracranial-self-stimulation (ICSS), has been extensively employed to characterize the neural substrate underlying reward and goal-directed behaviors. Evidence over the past few years suggests that the dorsal diencephalic conduction system (DDC) and the tail of the ventral tegmental area (tVTA) are involved in the rewarding effect of ICSS (or brain stimulation reward). However, despite significant progress in research, the underlying mechanisms remain largely unknown.

The overarching goal of this thesis is to investigate the role of the DDC and the tVTA in brain stimulation reward. Three research articles are presented in this thesis. The first article evaluates the effect of serial electrolytic lesions at the DDC and the medial forebrain bundle (MFB)—another pathway involved in brain stimulation reward—on the reward signal triggered by ICSS of the lateral hypothalamus (LH) and the dorsal raphe (DR) in rats. Results show that lesions at both the DDC and MFB produce larger and longer-lasting attenuations in brain stimulation reward than individual lesions at either pathway alone, and are more effective in attenuating the reward signal induced by LH self-stimulation. In the second article of the thesis, stimulation-induced Fos-like immunoreactivity (FLIR), a marker of cellular activity, was combined with electrolytic lesions at the DDC to determine whether the same nuclei that are active in lesion-naïve rats continue to be active following the lesions. Results show that electrolytic lesions at the DDC cause a marked reduction in stimulation-induced FLIR in certain forebrain, midbrain and brainstem regions that are activated by ICSS. Finally, the third article of the present thesis examines the role of the tVTA in brain stimulation reward and locomotor activity. Special attention was given to the behavioral

functions of the glutamate receptors AMPA and NMDA, as well as the mu opioid receptors (MORs) expressed in the tVTA. Results show that pharmacological blockade of AMPA and NMDA receptors as well as activation of MORs in certain sites of the tVTA produce rewarding and locomotor stimulant effects. Results also show that downregulation of NMDA receptors in the tVTA using the small interfering RNA (siRNA) technique fails to alter brain stimulation reward, but causes a marked decrease in the maximal rate of operant responding for ICSS.

The findings obtained from this thesis shed new light on the neural substrate underlying brain stimulation reward with respect to brain regions, connectivity, and neurotransmitter systems. They suggest that (i) the DDC constitutes a viable route for the transmission of brain stimulation reward and merges with the MFB on a common reward integrator, (ii) the DDC is functionally connected to forebrain, midbrain and brainstem regions that are activated by ICSS, and that (iii) glutamate and opioid transmission in the tVTA are major regulators of brain stimulation reward and locomotor activity. This work could have important implications for understanding appetitive behaviors, such as eating and drinking, and psychiatric conditions, such as substance use disorder, depression and schizophrenia.

Keywords: brain stimulation reward; dorsal diencephalic conduction system; intracranial self-stimulation; locomotor activity; tail of the ventral tegmental area

TABLE OF CONTENTS

Résumé……...iv

Abstract……..vi

List of tables……xiii

List of figures……..xiv

List of initials and abbreviations……...xvi

Acknowledgments…….....xxii

CHAPTER 1: GENERAL INTRODUCTION……1

1.1 Intracranial self-stimulation: a putative model to study the brain reward system….1

1.1.1 Context and discovery……..1

1.1.2 Reinforcing properties of ICSS……...……3

1.1.3 Response-frequency function and the curve-shift paradigm……...6

1.1.4 Methodological and technical considerations……10

1.2 Anatomy, neurochemistry, and pharmacology of the brain reward system……..10

1.2.1 Brain regions and neural pathways……10

1.2.2 Central role of dopamine in reward……...14

1.2.3 Glutamate transmission: overview and implication in reward processing……18

1.2.4 The opioid system: overview and implication in reward processing…….24

1.3 The dorsal diencephalic conduction system in the brain reward circuitry: spotlight on the anatomy and function of the habenular complex (Adapted from the review paper Fakhoury 2018. *Behavioral Brain Research,* Accepted in Press)……...28

1.3.1 The habenula: morphological, cellular and electrophysiological profile……...29

1.3.2 Afferent and efferent pathways of the habenula……32

1.3.3 The habenula: a major regulator of monoaminergic systems……36

1.3.3.1 The habenula and the DA system.……37

1.3.3.2 The habenula and the 5-HT system.……...40

1.3.4 The DDC in reward and aversion.……..43

1.3.4.1 Electrophysiological and neuroimaging studies……43

1.3.4.2 Electrical stimulation studies…….....46

1.3.4.3 Optogenetic stimulation studies…….....49

1.4 The tail of the ventral tegmental area in behavioral processes and in the effect of psychostimulants and drugs of abuse (Adapted from the review paper Fakhoury 2018. *Prog Neuropsychopharmacol Biol Psychiatry,* 84:30-38)…….…….54

1.4.1 Context and overview……54

1.4.2 Cellular, synaptic and electrophysiological profile of the tVTA……...56

1.4.3 Afferents and efferents of the tVTA……..57

1.4.4 The tVTA: a source of negative reward signals…….61

1.4.5 The tVTA: from aversion expectation value to avoidance behavior…….64

1.4.6 The tVTA in responses to psychostimulants and drugs of abuse……..66

1.4.7 Summary and perspectives……...74

1.5 Thesis proposal: overview, hypotheses and objectives…….76

1.5.1 Article 1: Serial lesions at the DDC and MFB……..76

1.5.2 Article 2: Anatomical disconnection following a single lesion at the DDC……..77

1.5.3 Article 3: Manipulation of glutamate and opioid transmission in the tVTA…….79

CHAPTER 2: RESULTS OF ORIGINAL CONTRIBUTIONS…….81

2.1 ARTICLE 1: Role of the dorsal diencephalic conduction system in the brain reward circuitry (Published in *Behavioral Brain Research,* 2016)……..…...81

Author contributions……..81

Abstract……..82

Introduction……83

Material and Methods……86

Results……90

Discussion……..96

Conclusion……...101

Acknowledgments……101

Figure legends……..103

Figures……..105

References……...113

2.2 ARTICLE 2: Effect of electrolytic lesions of the dorsal diencephalic conduction system on the distribution of Fos-like immunoreactivity induced by rewarding electrical stimulation (Published in *Neuroscience,* 2016)……...118

Author contributions……118

Abstract……119

Introduction……..120

Material and Methods……..122

Results……..129

Discussion……131

Conclusion……...137

Acknowledgments..……..138

Figure and table legends……..139

Tables……...……141

Figures……..142

References…..……...149

2.3 ARTICLE 3: Modulation of brain stimulation reward and locomotor activity by ionotropic glutamate and mu opioid receptors in the tail of the ventral tegmental area (in preparation)……157

Author contributions……157

Abstract……158

Introduction…….....159

Material and Methods……..161

Results……..166

Discussion……170

Acknowledgment……175

Supplementary methods……...176

Figure legends……..179

Figures……..183

Supplementary figures……188

References……....193

CHAPTER 3: GENERAL DISCUSSION AND CONCLUSION……..202

3.1 The DDC constitutes a route for the transmission of the reward signal triggered by ICSS…….....202

3.2 The DDC and MFB are functionally interconnected and merge on common reward-relevant neural elements……205

3.3 The DDC is functionally connected to brain regions activated by ICSS……..207

3.4 AMPA and NMDA receptors of the tVTA are major inhibitors of brain stimulation reward and locomotor activity……..210

3.5 MORs of the tVTA are major enhancers of brain stimulation reward and locomotor activity……...……..214

3.6 NMDA receptors of the tVTA are involved in incentive salience and brain stimulation reward…...……..217

3.7 Conclusion: implications for psychiatric diseases……...219

BIBLIOGRAPHY...……...224

List of tables

General introduction

Table 1. The DDC in reward processing…….51

Table 2. The tVTA and the effect of drugs……70

Results of original contributions

Article 2

Table 1…….....141

List of figures

General introduction

Figure 1. ICSS apparatus and properties……...5

Figure 2. Schematic illustration of representative parameters used during an ICSS paradigm…….7

Figure 3. Schematic illustration of the theoretical functions that relate response rates to stimulation frequency under different current intensities and effort requirements….....8

Figure 4. Non-exhaustive illustration of regions involved in brain stimulation reward……..12

Figure 5. Ionotropic and metabotropic glutamate receptors……20

Figure 6. Glutamate transmission in the ventral midbrain exerts opposite roles……23

Figure 7. Model of opposing tonic effects of opioid receptors on mesolimbic dopaminergic cells.26

Figure 8. Habenula afferents and efferents connections……..35

Figure 9. Main afferents and efferents of the tVTA……59

Results of original contributions

Article 1

Figure 1……..……...105

Figure 2…..……..106

Figure 3……...…….107

Figure 4……..……...108

Figure 5……..……...109

Figure 6……..……...110

Figure 7……..……...111

Figure 8……..……...112

Article 2

Figure 1……..……..142

Figure 2……..……..143

Figure 3……..……..…144

Figure 4……..……..145

Figure 5……..……..146

Figure 6……..……..147

Figure 7……..……..148

Article 3

Figure 1……..……..183

Figure 2……..……..184

Figure 3……..……..185

Figure 4……..……..186

Figure 5……..……..187

Supplementary Figure 1……...188

Supplementary Figure 2……...189

Supplementary Figure 3……...190

Supplementary Figure 4……...191

Supplementary Figure 5……...192

General discussion and conclusion

Figure 1. Schematic overview of article 1, 2, and 3 of the present thesis……220

List of initials and abbreviations

6-OHDA	6-hydroxydopamine
β-EP	β-endorphin
A cyclase	Adenylyl cyclase
ADHD	Attention deficit hyperactivity disorder
Amy	Amygdala
AMPA	Amino-3-hydroxy-5-methyl-4-isoxazolepropionate
AMPAR	AMPA receptor
ATP	Adenosine triphosphate
B.C.	Before Christ
BLA	Basolateral amygdala
BNST	Bed nucleus of the stria terminalis
cAMP	Cyclic adenosine monophosphate
Cg	Cingulate cortex
CNS	Central nervous system
CPu	Caudate putamen
DA	Dopamine
DBS	Deep brain stimulation
DDC	Dorsal diencephalic conduction system
DMTg	Dorsomedial tegmental area
DNQX	6,7-dinitroquinoxaline-2,3-dione
DR	Dorsal raphe
DOPAC	3,4-dihydroxyphenylacetic acid

DOR	Delta opioid receptor
DP	Dynorphin
DPC	Dorsal peduncular cortex
EAAT	Excitatory amino acid transporter
EM-1	Endomorphin-1
EM-2	Endomorphin-2
EPSC	Excitatory postsynaptic current
GABA	Gamma-aminobutyric acid
GHB	γ-hydroxybutyric acid sodium salt
Gi	Inhibitory G protein
Glu	Glutamate
Gly	Glycine
GTP	Guanosine triphosphate
I	Intensity
ICSS	Intracranial self-stimulation
IL	Infralimbic cortex
IPN	Interpeduncular nucleus
IPSC	Inhibitory post-synaptic current
Hb	Habenula
HVA	Homovanillic acid
Hz	Hertz
k	Current density
KOR	Kappa opioid receptors

KAR	Kainate receptor
LC	Locus coeruleus
LH	Lateral hypothalamus
LHb	Lateral habenula
log	Logarithm
LPO	Lateral preoptic area
LTDg	Laterodorsal tegmental nucleus
M50	Stimulation frequency that maintains half-maximal responding
MFB	Medial forebrain bundle
mGLuR	Metabotropic glutamate receptor
mGlut	Metabotropic glutamate
MOR	mu-opioid receptor
MR	Median raphe
ms	Millisecond
mPFC	Medial prefrontal cortex
Nac	Nucleus accumbens
nAChR	Nicotinic acetylcholine receptor antagonist
NBQX	2,3,-Dioxo-6-nitro-1,2,3,4-tetrahydrobenzo(f)quinoxaline-7-sulfonamide
NMDA	N-methyl-D-aspartate
NMDAR	NMDA receptor
OFC	Orbitofrontal cortex
Pa	Parafascicular thalamic nucleus
PAG	Periaqueductal gray

PCP	Phencyclidine
PLC	Phospholipase C
PM	Posterior mesencephalon
PMnR	Paramedian raphe nucleus
Pn	Pontine reticular nucleus
PN	Pontine nuclei
PPPA	(2R,4S)-4-(3-Phosphonopropyl)-2-piperidinecarboxylic acid
PPTg	Pedunculopontine tegmental nucleus
PrL	Prelimbic cortex
R/F	Response/Frequency
r	Radius of stimulation
RMTg	Rostromedial tegmental nucleus
RN	Red nucleus
RRF	Retrorubral field
RT-PCR	Reverse transcription-polymerase chain reaction
s	Second
SC	Superior colliculus
SI	Substantia innominate
siRNA	Small interferon RNA
SNc	Substantia nigra pars compacta
SNr	Substantia nigra pars reticulata
T_0	Theoretical point at which the stimulation becomes rewarding
tVTA	Tail of the ventral tegmental area

VGLUT	Vesicular glutamate transporter
VGLUT1	Vesicular glutamate transporter 1
VGLUT2	Vesicular glutamate transporter 2
VM	Ventral midbrain
VP	Ventral pallidum
VTA	Ventral tegmental area
ZI	Zona incerta

To my father

For his unconditional love and support

Acknowledgments

Well, here it is. This thesis represents one of the major early milestones of my career as a scientist. It is the product of tireless efforts and an act of dedication, but also one of pride. This thesis would not have been completed without the support and encouragement of many special individuals.

First and foremost, I would like to thank Dr. Sandra Boye, with whom I initially started my doctoral research. The unparalleled excellence of the creative scientist and humble person that she was gave me the inspiration to strive for perfection. I am truly grateful to her for her full support in applying for a doctoral scholarship, which eventually helped me receive an award from the Centre de Recherche en Neuropsychologie et Cognition (CERNEC) and the prestigious Alexander Graham Bell Canada Graduate Scholarship award from the Natural Sciences and Engineering Research Council of Canada (NSERC). Thank you Sandra! Wherever you are, I hope you will find this thesis as a true reflection of the inspiring vision and dream that we shared.

I am also immensely indebted to my current supervisor, Dr. Pierre-Paul Rompré. I don't have words enough to express my gratitude to him for allowing me to continue my research under his supervision. He has instilled in me a strong sense of passion and discipline, and has helped me grow as an independent scientist. His invaluable advice and scientific insight have been very instrumental in guiding my research towards its successful completion. I feel truly privileged for being able to work with him!

I wish to thank the staff and veterinarians of the animal research facility, and all of my colleagues, in particular Giovanni Hernandez, Claude Bouchard, Sergio Dominguez Lopez and David Voyer for their help in performing the intricate experimental procedures. Many thanks also go to my PhD

committee members, Dr. John Kalaska and Dr. Anne-noël Samaha, for their continuous support and invaluable feedbacks throughout the course of my research.

This thesis would not have seen the light without the financial support from generous contributors. All the work presented in this thesis was supported by NSERC. I also gratefully acknowledge the doctoral scholarships from CERNEC, NSERC and the Faculté des études supérieures et postdoctorales (FESP). These scholarships not only encouraged me to work harder, but also enabled me to focus entirely on my research without having to worry about my finances. Over the course of my doctoral studies, I was able to contribute to 31 research articles/reviews in peer-reviewed journals with 25 as first author, 15 abstracts/presentations, and 1 book chapter. I hope anyone who is reading this can take this personal accomplishment as an example of how anything is possible with the right mindset.

Last but not least, I would like to thank my family. My father's unconditional support is the main reason I was able to pursue my education in Canada. He has stimulated and inspired me immensely, and continues to do so every day. I know he is up there right now smiling at me with pride. I would also like to thank my mother and two brothers who gave me continued encouragement and love throughout the years. None of this would have been possible without you.

CHAPTER 1: GENERAL INTRODUCTION

1.1 Intracranial self-stimulation: a putative model to study the brain reward system

1.1.1 Context and discovery

Throughout their lives, humans learn different patterns of behavior to adapt to their environment and meet their vital needs. One of the most fundamental processes of learning is the ability to effectively associate different stimuli for acquiring or strengthening a behavior. In the early 20th century, Ivan Pavlov, a Russian physiologist, introduced the notion of classical conditioning, in which subjects learn to associate a previously neutral stimulus to an unconditioned stimulus that reliably elicits a response (Pavlov, 1927). In his experiments, he observed that dogs would normally salivate upon presentation of food (the unconditioned stimulus). However, dogs would also drool whenever they saw the lab coats that were worn by the technicians who normally feed them, even when there was no food in sight. Pavlov therefore conducted an experiment in which a bell was rung every time food was presented to the animals. As predicted, the sound of the bell (the neutral stimulus) was able to trigger the salivation response in dogs. Pavlov concluded that any event or object that the animals learn to associate with a reward (in this case food) would trigger the same behavioral response obtained upon presentation of the reward itself. Pavlov's research on classical conditioning have set the ground for much of the subsequent research on conditioning, and stills serves as a historical backdrop for current learning theories. Influenced by Pavlov's experiments on classical conditioning, John B. Watson, an American psychologist, established the first basic principles of behaviorism, which are described in the article “Psychology as the behaviorist views it” (Watson, 1913). In this article, Watson argued that psychology should be viewed as an objective experimental branch of science whose theoretical goal is the understanding of the behavior of humans or animals, rather than their consciousness or internal

state. Watson's theory of behaviorism played a significant role in paving the way for the changes in psychological research that ensued. In 1938, Burrhus F. Skinner introduced the notion of operant conditioning based on the observation that animals would quickly learn to press a lever (the operant response) in order to receive food (Skinner, 1938). He coined the terms positive reinforcers for stimuli that increase the likelihood of the operant response to occur, and punishers for stimuli that decrease the likelihood of the operant response to occur. Most of Skinner's ideas, however, are built upon Edward Thorndike's law of effect, which states that the behavioral responses that are followed by pleasant consequences are more likely to occur again in the same situation, while the behavioral responses that are followed by unpleasant consequences are less likely to be repeated (Thorndike, 1911). Nonetheless, Skinner's theories on conditioning behavior differ from those of Thorndike insofar as they established a distinction between positive and negative reinforcers, the latter being defined by stimuli whose removal increases the likelihood of the operant response to occur. An example of negative reinforcement is when animals need to press a lever to avoid receiving aversive stimuli such as electrical foot shocks. Skinner also found that the way in which reinforcers are scheduled can significantly affect the rate of lever press (or operant response rate) and the rate at which the operant response is extinguished (or extinction rate) (Fesrter and Skinner, 1957). For instance, a continuous reinforcement, where food is delivered after every lever press, would produce a slow rate of responding and a relatively fast extinction rate, whereas a variable ratio reinforcement, where food is delivered after an unpredictable number of lever presses, will tend to sustain high rates of responding with relatively slow extinction rates (Fesrter and Skinner, 1957).

Although research on classical and operant conditioning in the first half of the 20th century has shaped our understanding of motivated behaviors, it failed to characterize its underlying neural

basis. One of the first studies that provided insights into the neural substrate underlying reward and motivated behaviors was by James Olds and Peter Milner in the early 1950s. In their experiments, the electrode that was initially intended to be implanted into the reticular formation missed its target and ended up in the septal area. They discovered that the subject would readily press a lever to receive trains of electrical stimulation within this region, implying that the stimulation was intrinsically rewarding (Olds and Milner, 1954). In additional experiments, Olds and Milner demonstrated that rats would also press the lever for stimulation of other brain areas, including the tegmentum, subthalamus, and cingulate gyrus of the cortex (Olds and Milner, 1954). This behavioral paradigm was termed intracranial-self stimulation (ICSS) on the basis that rats had to perform a specific response to receive a train of electrical pulses. The discovery that ICSS of certain brain areas could serve as a reinforcer spurred intense interest among psychologists and neuroscientists, and led to a wide array of subsequent experiments on the neural substrate underlying brain stimulation reward. An urgent requirement at that time was to discover all the brain areas that could support ICSS, and to determine whether this behavior could be reproduced in other species (Milner, 1991). Following Olds and Milner's observations, the reinforcing properties of ICSS have been described in numerous brain regions (Milner, 1991) and in several species, including monkeys (Bursten and Delgado, 1958), dogs (Sadowski, 1972), cats (Wilkinson and Peele, 1963), chicks (Andrew, 1967), and humans (Bishop et al., 1963).

1.1.2 Reinforcing properties of ICSS

The usefulness of the ICSS paradigm stems from the fact that the rewarding effectiveness of the electrical stimulation can by-pass sensory systems and natural physiological processes such as satiation, thus providing a powerful tool to directly study the brain reward system (Wise, 2002).

Electrical stimulation of certain brain regions triggers a remarkably strong operant behavior in rodents, so strong that they will continuously press a lever over a long period of time to receive the rewarding stimulation (Olds, 1958a). When given the choice between palatable food and electrical stimulation, rats will vigorously work for the rewarding stimulation to the point of self-starvation (Routtenberg and Lindy, 1965). Rats will also exert extra effort, such as crossing a foot-shock-delivering floor grid (Olds, 1958b) or galloping uphill along a runway (Edmonds and Gallistel, 1974) to access the lever that elicits the delivery of the rewarding stimulation.

In a typical ICSS paradigm, rodents are individually placed in stimulation chambers and trained to self-administer a rewarding electrical stimulation through electrodes implanted in certain regions of their brain **(Figure 1A)**. Operants such as nose poke or lever press can be used to study the behavior of the animal in response to the rewarding electrical stimulation. Only neural elements that are located directly around the uninsulated electrode tip and within a certain radius will be stimulated. A common first step in the ICSS procedure is the adjustment of the current intensity for each subject. A reliable estimation of the suprathreshold radius of stimulation for a given current intensity can be obtained by the equation $r^2 = I/k$, where I is the current intensity of the stimulation in µAmp, k the current density in µAmp/mm^2, and r = the radius of stimulation around the electrode tip in mm^2 (Fouriezos and Wise, 1984; Yeomans et al., 1986). This estimation is, however, only valid for reward-relevant axons and for selected values of k, and provided that each pulse generates a single action potential, and that the impedance around the electrode as well as the density of activated neurons remain homogeneous within a given radius (Fouriezos and Wise, 1984; Yeomans et al., 1986). An electrical stimulation of high current intensity will activate a high proportion of reward-relevant neurons, but may also activate neural elements that are not involved in reward **(Figure 1B)**, thus resulting in unwanted motoric effects. Conversely, a stimulation of

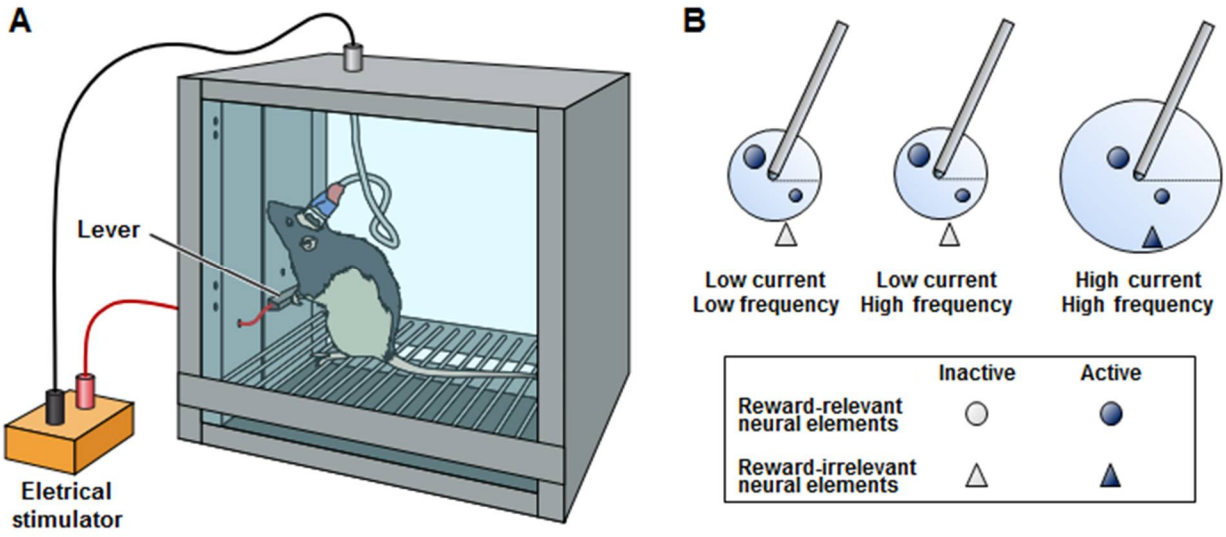

Figure 1: ICSS apparatus and properties. (**A)** Operant self-stimulation chamber. Each lever press triggers the delivery of a short train of electrical pulses to a specific brain region through an implanted electrode. The stimulation electrode is electrically insulated except for the dome-shaped tip. Reproduced from Schultz, 2015. (**B)** Influence of the current intensity and frequency of the stimulation on the activation of neural elements. The current intensity determines the population of neurons that are activated, while the frequency determines the number of times a given neuron is activated.

low current intensity will activate a small proportion of reward-relevant neurons **(Figure 1B)**. Therefore, caution should be taken while choosing the current intensity of the stimulation during an ICSS test. Ideal parameters of stimulation should be able to sustain a reliable rate of responding with minimal motoric effects.

The reinforcing properties of ICSS also depend on the stimulation frequency (Gallistel and Leon, 1991; Mark and Gallistel, 1993). Increasing the frequency of the stimulation will trigger more action potentials in the directly stimulated neurons, which will then increase the rewarding value of the stimulation. One fundamental property of the rewarding electrical stimulation is the ability to add the reinforcing effect of several pulses arriving over a short period of time; a property referred to as temporal summation (Gallistel, 1974; Milner, 1991). When the duration of the

stimulation is constant, the total number of firings in the population of the directly stimulated neurons is determined by the product of the pulse frequency and the current intensity (Gallistel, 1974). Thus, an x-fold increase in current intensity (spatial integration) will have the same effect on the reward intensity as an x-fold increase in pulse frequency (temporal integration) assuming an even density of reward-relevant neurons within the radius of the stimulation. This model of spatial-temporal integration has been dubbed the "counter model" (Gallistel, 1978; Gallistel et al., 1981). When the current intensity of the stimulation remains constant, the rewarding value of the stimulation becomes a function of the pulse frequency; rats will respond more vigorously for stimulation of higher frequencies, and will stop responding at very low stimulation frequencies. The function that describes the relationship between the resulting operant response and the frequency of the stimulation follows a curve of quasi-sigmoidal shape known as the response/frequency (R/F) curve.

1.1.3 Response-frequency function and the curve-shift paradigm

In the curve-shift paradigm of ICSS, animals are tested during several trials of varying stimulation frequencies and a constant current intensity so as to maintain the population of neurons that is stimulated unchanged. Although the parameters used for ICSS can greatly vary from one study to another, each trial typically begins with a 15 s inter-trial interval during which no electrical stimulation is provided, followed by the delivery of 5 trains of non-contingent priming stimulation, and a 5 s adaptation period **(Figure 2)**. The priming trains of stimulation are typically delivered at a rate of 1 Hz, and are used to signal the arrival of discrete 55 s trials during which the animals will be allowed to self-stimulate at constant stimulation parameters **(Figure 2)**. At the end of each trial, the frequency (i.e. the number of pulses per train of stimulation) is lowered by approximately

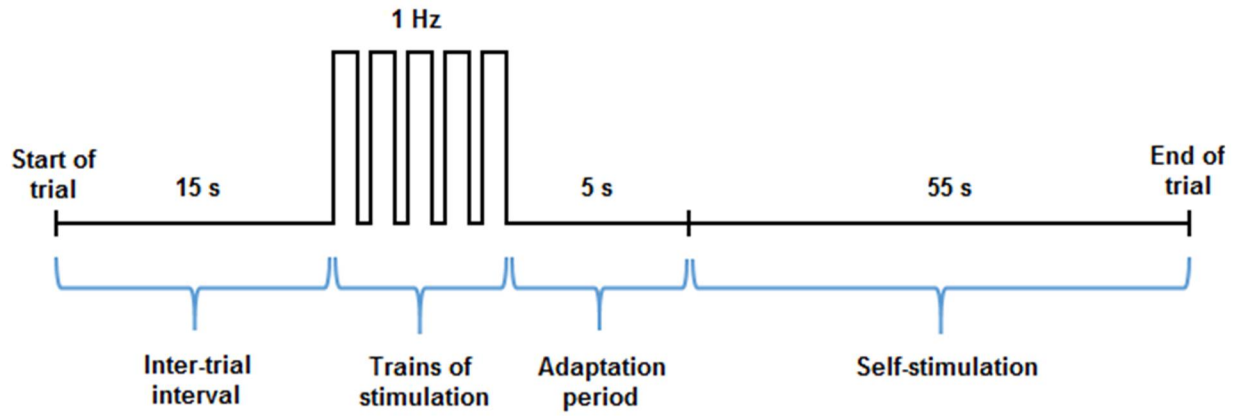

Figure 2: Schematic illustration of representative parameters used during an ICSS paradigm. The nose poke response or number of lever presses of the animal is recorded during discrete 55 s trials. Trials are separated by a 15 s inter-trial interval (or time-out period), followed by the delivery of 5 trains of priming stimulation (delivered over 5 s) and a 5 s adaptation period. The stimulation frequency is reduced by approximately 0.1-log unit after each trial, and at the end of the session, a plot of the response rate as a function of the pulse frequency is generated.

0.1-log units, and at the end of the entire session, a R/F curve illustrating the rate of responding (number of lever presses or nose poke response) versus the stimulation frequency is obtained. During the discrete 55 s trials of ICSS, each operant response triggers the delivery of a single 400 ms train of rectangular cathodal pulses of very short duration (0.1 ms) so as to induce only one action potential per stimulated fiber. Cathodal currents are used instead of anodal currents because they are more effective in triggering action potentials (Ranck, 1975). Moreover, the electrode is connected to ground between deliveries of each pulse so that there is no build up of charge at the tip; building up of charge can be detrimental particularly with anodal stimulation. The delivery of each train of cathodal pulses is followed by a 600 ms period during which the pulse generator could not be triggered. The introduction of a fixed-interval delay after the delivery of each rewarding stimulation prevents the summation between two consecutive trains (Fouriezos, 1995)

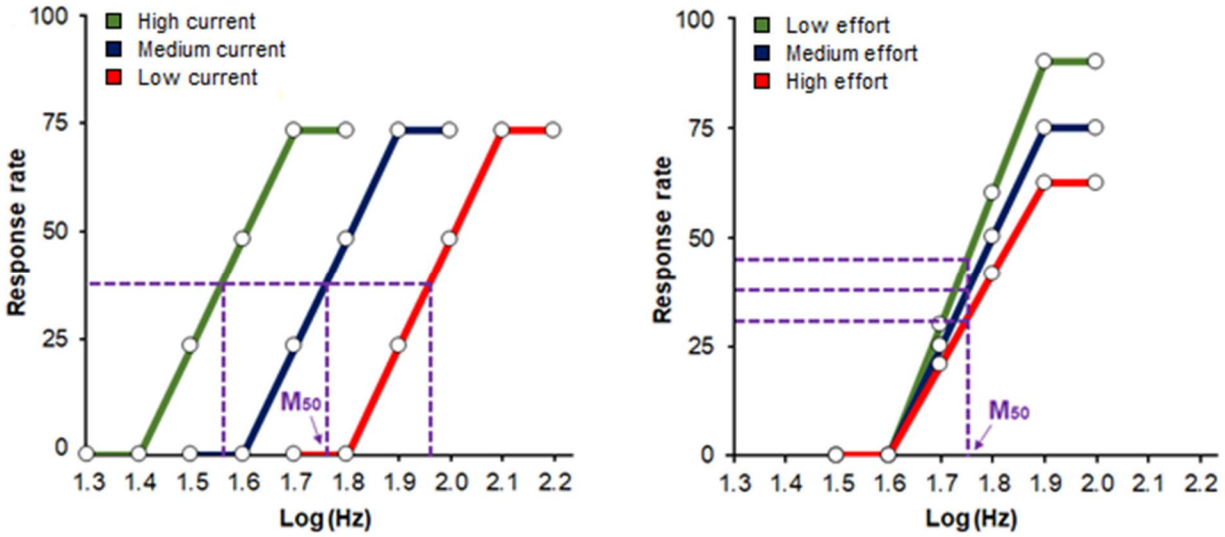

Figure 3: Schematic illustration of the theoretical functions that relate response rates to stimulation frequency under different current intensities **(A)** and effort requirements **(B)**. The stimulation frequency that maintains half-maximal responding (M50) is indicated by the pink arrow. Changes in the current intensity of the stimulation cause a lateral displacement of the R/F curve **(A)** while changes in task difficulty cause a vertical displacement of the R/F curve **(B)**.

and enables a clear control over reward density, thus ensuring that the amount of reward received by the animal does not depend on its speed of responding, but rather on the rewarding effectiveness of the stimulation (Boye and Rompre, 1996).

The plot of the rate of responding of the animal for different pulse frequencies yields an R/F curve of quasi-sigmoidal shape characterized by a bottom portion, a rising portion, and an upper limit (also called plateau). Theoretical examples of R/F curves generated under different experimental conditions are illustrated in **Figure 3A and 3B**. When the current intensities and pulse duration of the stimulation are constant, the magnitude of the reinforcing effect of ICSS is function of the pulse frequency (Gallistel et al., 1981); animals will respond at negligible rates at low frequencies, intermediate rates for moderate frequencies, and maximal or asymptotic rates at high frequencies **(Figure 3A and 3B)**. The most intuitive measure of the reinforcing efficacy of

the stimulation is the brain reward threshold, or M50, which corresponds to the pulse frequency sustaining a half-maximal rate of responding. Manipulations that increase or decrease the rewarding efficacy of ICSS shift the M50 towards lower or higher values, respectively, thereby causing a lateral displacement of the R/F curve (Edmonds and Gallistel, 1974). A decrease in the current intensity of the stimulation increases the M50, while the opposite effect is observed when the current intensity of the stimulation is increased **(Figure 3A)**.

An advantage of using the curve-shift paradigm is that reward threshold that is derived from this method is remarkably stable over several months, thus allowing for multiple testing of each experimental animal over a long period of time (Stoker and Markou, 2011). The curve-shift paradigm also enables experimenters to evaluate the capacity of the subject to self-stimulate. Manipulations that induce a change in the capacity of the animal to self-stimulate (such as increasing or decreasing the effort needed to perform the operant response) lead to upward or downward shifts in the maximum response rate (Miliaressis et al., 1986). Animals will typically have a higher rate of responding when the effort required to self-stimulate is low, and a lower rate of responding when the effort required to self-stimulate is high **(Figure 3B)**. When the reduction in maximum response rate is proportional at each of the pulse frequency tested, the M50 remains the same **(Figure 3B)**. However, the curve shift paradigm does not necessarily enable a clear dissociation between reward threshold and maximum reponse rate since increases in task difficulty can displace the R/F curve laterally (Frank and Williams, 1985; Miliaressis et al., 1986; Fouriezos et al., 1990). The curve-shift paradigm is also insufficient inasmuch as it does not dissociate between the change in the subjective intensity and the cost of reward; this could be better addressed by the "reinforcement mountain" model (Arvanitogiannis and Shizgal, 2008).

1.1.4 Methodological and technical considerations

Since its discovery and implementation, the ICSS paradigm has become a powerful tool to study the neural substrates underlying reward and goal-directed behaviors. A major strength of this paradigm is that the electrical stimulation directly activates the brain reward circuitry, bypassing sensory systems and natural physiological processes like satiation. The ICSS procedure also provides quantitative measurements of brain stimulation reward that are robust and stable over long periods of time, thus allowing the experimenter to perform multiple tests or longitudinal studies on the same subjects (Stoker and Markou, 2011). Another advantage of ICSS is that the stimulation can be delivered to desired regions of the brain with extremely high temporal accuracy (in the order of ms). This can be achieved by controlling external parameters such as the pulse frequency and duration of the stimulation. However, studies employing ICSS with the use of an electrical stimulation have been plagued with a lack of anatomical specificity. The main issue is that the electrical stimulation of the brain does not allow the distinction between reward-relevant neural elements and those that do not play a role in reward, thus making the identification of the neural substrate for brain stimulation reward extremely challenging (Murray and Shizgal, 1996b). However, despite its technical limitations, electrical stimulation is still widely used in rodents for the identification of the neuroanatomical substrates of reward, and has proven valuable in the study of the reinforcing effects of drugs of abuse.

1.2 Anatomy, neurochemistry, and pharmacology of the brain reward system

1.2.1 Brain regions and neural pathways

The discovery by Olds and Milner that rats would readily press a lever to obtain pulses of electrical stimulation in certain brain regions (Olds and Milner, 1954) ushered in a series of

investigations aiming at determining the neuroanatomical substrate underlying brain stimulation reward. Shortly after this discovery, studies showed that electrical stimulation of forebrain and hypothalamic structures (Olds, 1956b, a) could also generate high response rates in an ICSS paradigm, which unequivocally pointed to the medial forebrain bundle (MFB) as a key neural pathway in the brain reward system. The MFB is a large tract of ascending and descending axons that span the entire length of the brain, passing through the basal forebrain and the lateral hypothalamus (LH) in a rostral-caudal direction. MFB fibers also course through midbrain regions including the ventral tegmental area (VTA), to terminate into several nuclei of the brainstem including the dorsal raphe (DR) nucleus (Nieuwenhuys et al., 1982), thus relaying information from one pole of the brain to the other. In the following paragraphs, evidence implicating the MFB in brain stimulation reward are discussed, with an emphasis on mapping, anatomical, and lesion studies. The dorsal diencephalic conduction system (DCC), which is another neural pathway of the brain reward system, will be discussed in details in the next section.

Following the identification of the MFB as a major substrate for ICSS, numerous brain mapping studies, where the anatomical site of the stimulation electrode is manipulated, were conducted to characterize the brain regions that could support ICSS **(Figure 4)**. The emerging picture resulting from these studies suggests that operant responding for ICSS could be obtained along brain regions known to send or receive MFB fibers, including the orbitofrontal cortex (OFC) (Mora et al., 1980), the medial prefrontal cortex (mPFC) (Bielajew and Trzcinska, 1998), the caudate-putamen (Bielajew and Trzcinska, 1998), the lateral preoptic area (Bushnik et al., 2000), the ventral

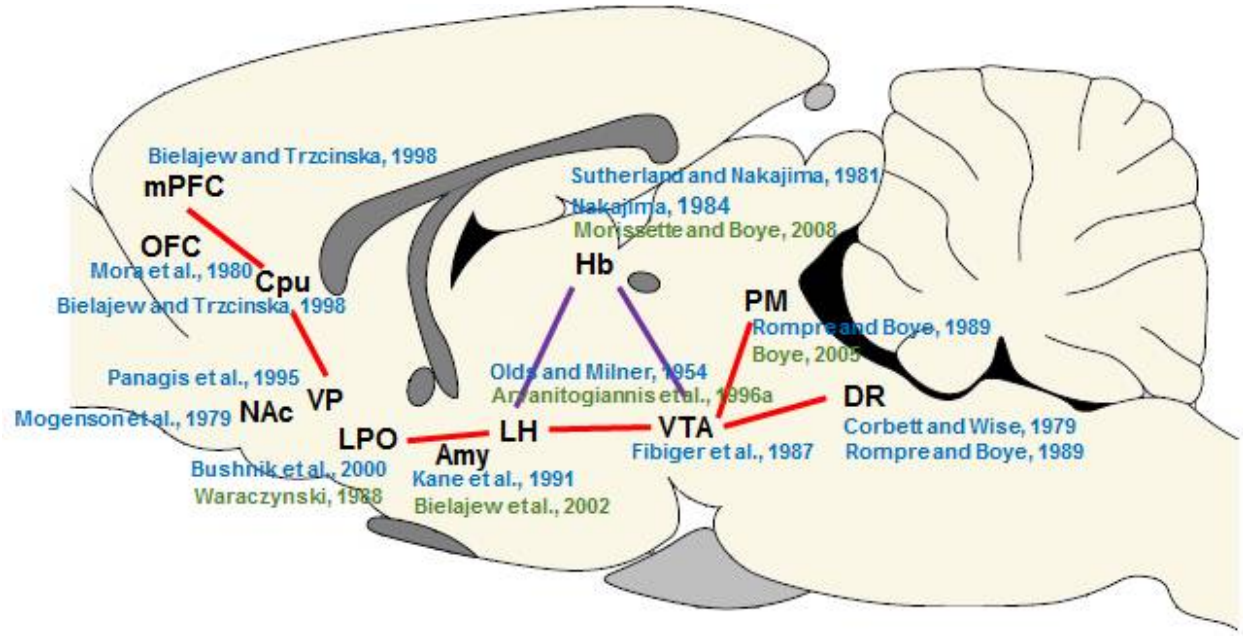

Figure 4: Non-exhaustive illustration of regions involved in brain stimulation reward. This simplified diagram illustrates key brain regions in the MFB (in red) and the DDC (in purple) that support operant responding for ICSS (citation in blue) and/or that result in an attenuation of the rewarding effects of MFB self-stimulation following a lesion (citation in green). Abbreviations: amygdala (Amy); caudate-putamen (CPu); dorsal raphe (DR); habenula (Hb); lateral hypothalamus (LH); lateral preoptic area (LPO); medial prefrontal cortex (mPFC); nucleus accumbens (NAc); orbitofrontal cortex (OFC); posterior mesencephalon (PM); ventral pallidum (VP); ventral tegmental area (VTA).

pallidum (Panagis et al., 1995), the amygdala (Kane et al., 1991), the pontine tegmentum (Rompre and Boye, 1989), the median raphe (MR) (Rompre and Miliaressis, 1985), and the DR (Corbett and Wise, 1979; Rompre and Boye, 1989). ICSS has also been reported in the habenula (Sutherland and Nakajima, 1981; Nakajima, 1984), the olfactory bulbs (Phillips, 1970), the hippocampus (Ursin et al., 1966; Phillips et al., 1977), the nucleus accumbens (NAc) (Mogenson et al., 1979), the VTA (Fibiger et al., 1987), and the cerebellum (Ball et al., 1974; Corbett et al., 1982). However, one of the most extensively studied substrates to date for brain stimulation reward is the LH owing

to its critical role in energy homeostasis and motivated behaviors (Berthoud and Munzberg, 2011; Stuber and Wise, 2016).

The LH is a heterogeneous area of the MFB located posterior to the preoptic area and anterior to the VTA. It resides dorsoventrally between the zona incerta and the base of the brain, and mediolaterally between the optic tract and the fornix. Studies employing electrical or optogenetic stimulation of the LH have implicated this structure in feeding (Delgado and Anand, 1953) and reward-seeking (Olds and Milner, 1954; Kempadoo et al., 2013) behaviors. Anatomically, the LH comprises several distinct nuclear subgroups that receive a wide array of internal and external information, making it well-suited to mediate functions across major output axes (Berthoud and Munzberg, 2011). Afferents to the LH have been classically studied using injections of a retrograde tracer (i.e., transport of the dye occurs in the reverse direction, from the axon terminal back to the cell body), the results of which have demonstrated the existence of projections originating from the bed nucleus of the stria terminalis (BNST), the diagonal tract of Broca, the caudate-putamen, the NAc, the lateral septal nuclei, the lateral preoptic area, the amygdala, and the zona incerta (Barone et al., 1981; Kita and Oomura, 1982). On the other hand, studies employing anterograde tracing techniques (i.e., transport of the dye occurs in the forward direction, from the cell body out to the axon terminal) showed that LH neurons project to distinct areas of the brain including the hypothalamic paraventricular nucleus, the lateral habenula (LHb), the VTA, the mesencephalic and pontine central gray, the lateral parabrachial nucleus, and the raphe nucleus (Kita and Oomura, 1982; Larsen et al., 1994).

Numerous studies have also employed lesions along certain brain structures or pathways in order to evaluate their impact on the reinforcing properties of ICSS **(Figure 4)**. The reasoning behind this technique is based on the assumption that destruction of axons or cellular elements involved

in brain stimulation reward should result in an attenuation of the reinforcing effects obtained from ICSS. Therefore, assessing the strength of the reinforcing effect of ICSS before and after a lesion could help characterize the underlying neural circuit of brain stimulation reward. A common finding is that electrolytic lesions or knife cuts along the MFB cause a rightward shift in R/F curves obtained from LH (Janas and Stellar, 1987; Gallistel et al., 1996) or VTA (Simmons et al., 1998) self-stimulation, indicating a sustained attenuation of the rewarding effectiveness of ICSS. Lesions encompassing the habenula (Morissette and Boye, 2008), the cortical and adjacent amygdaloid subnuclei (Bielajew et al., 2002), the lateral preoptic area (Waraczynski, 1988), and the posterior mesencephalon (PM) (Boye, 2005) also cause a rightward shift in R/F curves for MFB self-stimulation. However, several other studies employing electrolytic lesions failed to observe decreases in the rewarding effectiveness of MFB stimulation. In particular, lesions at the amygdala (Waraczynski et al., 1990), the dorsomedial hypothalamus (Waraczynski et al., 1992), the parabrachial nucleus (Waraczynski and Shizgal, 1995), the rostral LH (Gallistel et al., 1996), and the lateral PM (Boye, 2005) have not resulted in consistent and noticeable changes in the rewarding effectiveness of MFB stimulation. A hypothesis to account for these negative findings is that the neural network subserving ICSS is anatomically diffuse, collateralized, and highly heterogeneous (Lorens, 1966; Simmons et al., 1998), and may be comprised of several pathways that are functionally interconnected. As such, the loss of reward-relevant neurons within one pathway would be compensated by the other, and vice versa, thereby enabling the integration and transmission of reward signals in the brain.

1.2.2 Central role of dopamine in reward

Dopamine (DA) is a neurotransmitter of the catecholamine family and plays a crucial role in a variety of processes within the central nervous system (CNS). In the brain, DA is synthesized from dopaminergic neurons of the VTA, substantia nigra pars compacta (SNc), retrorubral field (RRF), and hypothalamic arcuate and periventricular nuclei, and is transmitted via distinct dopaminergic pathways that play unique functions (Bjorklund and Dunnett, 2007; Luo and Huang, 2016). Dopaminergic neurons of the SNc project into the caudate-putamen via the nigrostriatal pathway, which play a key role in the regulation of voluntary movements (Luo and Huang, 2016). On the other hand, VTA DA neurons project to the NAc and other structures of the limbic system via the mesolimbic pathway, and to the prefrontal cortex via the mesocortical pathway (Luo and Huang, 2016). The mesolimbic and mesocortical pathways are primarily involved in emotion-related behavior and are often collectively referred to as the mesocorticolimbic pathway because of their significant overlap and association (Arias-Carrion and Poppel, 2007). Given the wide range of functions mediated by dopaminergic pathways, it is not surprising that abnormalities in DA transmission have been associated with numerous neuropathological conditions, including schizophrenia, major depressive disorders, substance use disorder, and Parkinson's disease (Birtwistle and Baldwin, 1998; Dunlop and Nemeroff, 2007; Volkow et al., 2009).

Midbrain DA neurons have been extensively studied in the context of reward-related processes owing to their ability to encode information about motivational salience (Bromberg-Martin et al., 2010; Schultz, 2015). In monkeys, these neurons show increased firing rate following the delivery of unpredicted food or liquid rewards, and following the presentation of reward-predicting stimuli (Ljungberg et al., 1992; Schultz et al., 1997; Schultz, 2010). DA neurons not only serve as a global reward signal, but also function as a reward prediction error signal, that is, the degree of discrepancy between the actual reward and its prediction (Schultz, 2016). In the context of ICSS,

early evidence implicating DA in brain stimulation reward comes from studies showing that electrical stimulation of DA-containing cell bodies in the midbrain (Crow, 1972a, b; Wise, 1981) and diencephalic areas that are traversed by DA fiber bundles (Corbett and Wise, 1980) produces positive reinforcement. In the study by Corbett & Wise (1980), reward thresholds obtained from stimulating ascending midbrain dopaminergic pathway were negatively correlated with the density of DA neurons surrounding the tip of the stimulation electrode, suggesting that DA transmission is strongly involved in mediating the rewarding effectiveness of ICSS. Neurochemical studies employing fast-scan cyclic voltammetry and/or in-vivo microdialysis to measure the extracellular release of DA in the brain have also provided robust evidence for the involvement of DA in the rewarding effect of ICSS. These studies reported long-lasting increases in the extracellular concentration of DA in various brain regions, including the NAc (Nakahara et al., 1989; You et al., 2001) and mPFC (Bean and Roth, 1991; Nakahara et al., 1992) following electrical stimulation of the MFB. Increased release of DA metabolites, including 3,4-dihydroxyphenylacetic acid (DOPAC) and homovanillic acid (HVA), were also observed in the striatum, NAc, and olfactory tubercle of rats following VTA self-stimulation (Fibiger et al., 1987). Consistently, DA release in the NAc was significantly increased following VTA self-stimulation (Phillips et al., 1992; Hernandez and Shizgal, 2009), and was found to be inversely correlated with reward thresholds for MFB self-stimulation (Yavich and Tanila, 2007). Last but not least are electrophysiological findings showing that the majority of midbrain DA neurons (>70%) are activated by rewarding electrical stimulation of the PM (Moisan and Rompre, 1998), thus concurring with the view that DA participates in the reinforcing effects of ICSS.

In addition to electrophysiological and neurochemical findings, data from pharmacological studies also provide robust evidence for the role of DA transmission in brain stimulation reward.

DA binds to and activates five different receptor subtypes that are divided into two major subclasses: D_1-like receptors, which include the D_1 and D_5 subtypes, and D_2-like receptors, which include D_2, D_3 and D_4 subtypes (Jaber et al., 1996; Beaulieu and Gainetdinov, 2011). Administration of pimozide and chlorpromazine, two selective antagonists for DA D_2 receptors, produce a rightward shift in ICSS reward thresholds, indicating that the rewarding efficacy of the stimulation is decreased (Gallistel and Karras, 1984; Miliaressis et al., 1986; Gallistel and Freyd, 1987). Reduced brain stimulation reward was also obtained following blockade of DA D_2 receptors (Schaefer and Michael, 1980; Benaliouad et al., 2007) and DA D_1 receptors (Nakajima and McKenzie, 1986), suggesting that DA transmission is critical in the objective reinforcement associated with ICSS. Accordingly, pharmacological manipulations that enhance DA transmission, such as agonist-mediated activation of DA receptors (Gilliss et al., 2002), blockade of DA transporter (Rompre and Bauco, 1990; Maldonado-Irizarry et al., 1994), and administration of psychostimulants such as amphetamine and cocaine (Colle and Wise, 1988; Straub et al., 2010), produce a leftward shift in brain reward thresholds. However, other studies failed to observe changes in the rewarding efficacy of ICSS following administration of DA receptors agonists (Malanga et al., 2008) or antagonists (Fibiger et al., 1976), suggesting that the mechanisms underlying the reinforcing effect of ICSS might not entirely depend on DA transmission. Consistent with this view, rats that received 6-hydroxydopamine (6-OHDA)—a neurotoxin that selectively destroys DA neurons—by intracerebroventricular injection (Sidhu et al., 1993) or bilaterally into the substantia nigra (Ornstein and Huston, 1975) showed normal rates of responding for ICSS. Altogether, the aforementioned studies suggest that although DA transmission plays a crucial role in the reinforcing effects of ICSS, there are most likely other systems involved in brain stimulation reward. Among those, the glutamate and opioid systems

have garnered considerable attention as important mediators of reward-related processes owing to their critical role in controlling DA neuronal activity (Le Merrer et al., 2009; D'Souza, 2015). In the following sections, an overview of evidence implicating these modulatory systems in reward processing is presented.

1.2.3 Glutamate transmission: overview and implication in reward processing

Glutamate is the most abundant excitatory neurotransmitter in the brain and accounts for the majority of synaptic transmission (Niciu et al., 2012). Present in high concentrations in the CNS, glutamate is a non-essential amino acid that can be synthesized from glucose and a variety of other sources (Dingledine and McBain, 1999). Glutamate also serves as a metabolic precursor to gamma-aminobutyric acid (GABA), the main inhibitory neurotransmitter in the brain, the latter being synthesized from the former by the enzyme glutamic acid decarboxylase (Fenalti et al., 2007). As an amino acid and neurotransmitter, glutamate is involved in a wide range of physiological processes, and perturbations in glutamate transmission can result in deleterious effects. For instance, glutamate-mediated excitotoxicity, which occurs as a result of glutamate receptors overactivation and excessive entry of calcium inside the cells, can cause neuronal damage and/or death (Sattler and Tymianski, 2001), and has often been associated with numerous neurodegenerative conditions such as Alzheimer's disease (Hynd et al., 2004), Parkinson's disease (Beal, 1998), and amyotrophic lateral sclerosis (Shaw and Ince, 1997). Because disruptions in glutamate transmission have also been linked to imbalances in the DA system (Kretschmer, 1999) and changes in reward sensitivity (Bechtholt-Gompf et al., 2010), a growing number of studies are focusing on the glutamatergic system as a therapeutic target for psychiatric conditions such as schizophrenia, depression, and substance use disorder (Javitt, 2004; Kerner, 2009).

In order to prevent neuronal damage that might occur as a result of glutamate-mediated excitotoxicity, the extracellular fluid concentration of glutamate is tightly regulated by excitatory amino acid transporters (EAATs) (Zhou and Danbolt, 2014). The EAATs are located on glutamatergic terminals and presynaptic glial cells, and are responsible for the removal of glutamate from the synaptic cleft (D'Souza, 2015). The vesicular glutamate transporters (VGLUTs), which constitute another class of glutamate transporters, are responsible for the uptake and sequestration of glutamate into presynaptic vesicles, and are dependent on a proton gradient that is generated upon the hydrolysis of adenosine triphosphate (ATP) (Liguz-Lecznar and Skangiel-Kramska, 2007). Once stored in vesicles, glutamate gets released into the synaptic cleft by exocytosis, and binds to either metabotropic or ionotropic glutamate receptors **(Figure 5)**. Metabotropic glutamate receptors (mGluR) are slow-acting G-protein coupled receptors located in presynaptic and postsynaptic terminals, which are subclassified into three groups based on anatomical and functional homology: group I includes mGluRs 1 and 5, Group II includes mGluRs 2 and 3, and Group III includes mGluRs 4, 6, 7 and 8 (Niswender and Conn, 2010). Conversely, ionotropic glutamate receptors are fast-acting ligand- gated ion channels which include amino-3-hydroxy-5-methyl-4-isoxazolepropionate (AMPA), N-methyl-D-aspartate (NMDA), and kainate receptors.

AMPA receptors are tetramers composed of four subunits designated as GluR1, GluR2, GluR3 and GluR4 (Ward et al., 2010). Each of the GluR1-4 subunits exists in two different forms (“flip” and “flop”) created by alternative splicing, thus conferring different signalling properties to AMPA receptors (Ozawa et al., 1998). Kainate receptors are also tetramers that form ligand-gated ion channels and that can be assembled from a combination of five different subtypes of subunit: GluK1-3 and GluK4-5 (Fisher and Fisher, 2014). Both AMPA and kainate receptors interact with

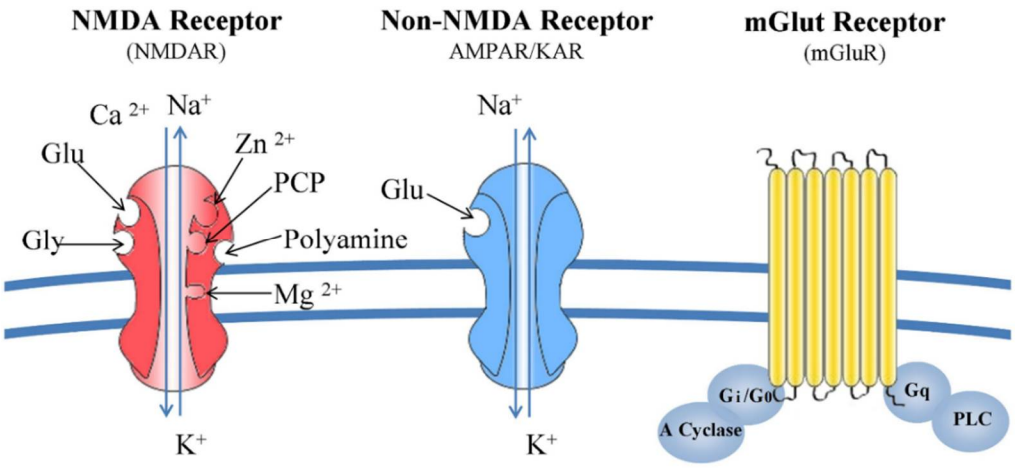

Figure 5: Ionotropic and metabotropic glutamate receptors. NMDA receptors interact with glutamate, glycine, Mg^{2+}, Zn^{2+} and polyamines, and contain a channel that allows the passage of Ca^{2+}, Na^{+} and K^{+} ions. AMPA and kainate receptors interact only with glutamate and their specific agonists, and contain a channel that is permeable to Na^{+} and K^{+} ions. On the other hand, mGluRs are members of the G-protein-coupled receptor superfamily. They regulate ion channels and downstream signalling by activating a guanosine triphosphate (GTP)-binding protein (G_q for Group I, and G_i/G_0 for Group II and Group III mGluRs), which in turn modulates the function of various effector molecules including the enzymes adenylyl cyclase and phospholipase C. Abbreviations: adenylyl cyclase (A cyclase); AMPA receptor (AMPAR); glutamate (Glu); glycine (Gly); kainate receptor (KAR); metabotropic glutamate (mGlut); NMDA receptor (NMDAR); phencyclidine (PCP); phospholipase C (PLC). Adapted from Kritis et al., 2015.

glutamate and their specific agonists, and their associated channels are permeable to various cations including Na^{+} and K^{+} (Kritis et al., 2015). On the other hand, NMDA receptors are tetramers composed of two obligatory GluN1 subunits (for which there are several splice variants), and two of the following subunits: GluN2A, GluN2B, GluN2C, GluN2D, GluN3A and GluN3B (Paoletti et al., 2013). The two non-GluN1 subunits can be identical or different, thus giving rise to di-heteromeric or tri-heteromeric receptors (Paoletti et al., 2013). Unlike AMPA and kainate receptors, NMDA receptors need to be co-activated by two ligands: glutamate and either D-serine

or glycine (Kleckner and Dingledine, 1988). In addition, the NMDA receptor pore is blocked by Mg^{2+} ions in a voltage-dependent manner, however, this block can be dislodged following sufficient membrane depolarization such as opening of AMPA receptor channels (Gass and Olive, 2008). Other regulatory sites on NMDA receptors are recognized by the dissociative anesthetics phencyclidine (PCP), which selectively antagonizes the response to NMDA in a non-competitive manner, and by Zn^{2+} ions, which produce a voltage-independent block.

Converging evidence implicates glutamate transmission in the regulation of DA neuronal activity. Under resting conditions, a small proportion of DA neurons are non-responsive to excitatory inputs, while the majority of DA cells fire spontaneously in two distinctive patterns of activity: (i) a tonic or single spike mode, and (ii) a fast phasic burst firing (Grace and Bunney, 1984a, b). Activation of glutamatergic afferents in the ventral midbrain mediates the switch from pacemaker tonic to phasic burst firing of DA neural activity (Johnson et al., 1992; Chergui et al., 1993; Lodge and Grace, 2006), a mode that is associated with increased DA release (Gonon, 1988; Overton and Clark, 1997). Besides its role in switching the firing mode of DA cells, glutamate afferents also establish synaptic contacts with local GABAergic interneurons of the midbrain, thereby enhancing the inhibitory drive onto DA neurons (Dobi et al., 2010; Omelchenko and Sesack, 2010). In light of these observations, studies examining the capacity of glutamate receptor agonists to alter DA release have reported conflicting results. For instance, both increases and decreases in DA release were observed in the striatum and NAc following activation of metabotropic (Ohno and Watanabe, 1995; Feenstra et al., 1998; Verma and Moghaddam, 1998) and ionotropic (Karreman et al., 1996; Wu et al., 2000) glutamate receptors. Moreover, activation (Kretschmer, 1999) and blockade (Narayanan et al., 1996; Cornish et al., 2001) of ionotropic glutamate receptors in the midbrain enhances locomotor activity, a DA-dependent behavioral

measure. The discrepancies in the results observed concur with the view that glutamate exerts opposite regulatory functions on DA neuron activity, and raise the possibility that such opposite modulation may be mediated by different glutamate receptor subtypes.

Because of its differential role in the regulation of DA neuron activity, glutamate has been proposed to mediate opposite effects on reward by acting on different glutamatergic receptor subtypes. To further clarify the role of midbrain glutamatergic transmission in reward, a series of elegant studies has evaluated the effect of ionotropic glutamatergic receptors blockade on the reinforcing efficacy of ICSS. In rats, intra-VTA injection of the AMPA receptor antagonist, 2,3,-Dioxo-6-nitro-1,2,3,4-tetrahydrobenzo(f)quinoxaline-7-sulfonamide (NBQX), dose-dependently attenuates the rewarding efficacy of ICSS, most likely as a result of reduced glutamatergic excitatory inputs to midbrain DA neurons (Ducrot et al., 2013). The view that AMPA receptor blockade causes a marked reduction in brain stimulation reward is in line with studies showing that injection of AMPA antagonists into the VTA blocks the development of a conditioned place preference to cocaine (Harris and Aston-Jones, 2003) and morphine (Harris et al., 2004). However, it is in contrast with a previous report showing that mice can learn to self-administer the AMPA receptor antagonist, 6,7-dinitroquinoxaline-2,3-dione (DNQX), into the VTA (David et al., 1998). Such discrepancies in the results could be attributable to differences in experimental approaches (i.e., drug and dose used) and injection sites (rostral versus caudal regions of the VTA). A study by Ducrot et al. (2013) also investigated the effect of (2R,4S)-4-(3-Phosphonopropyl)-2-piperidinecarboxylic acid (PPPA)—an NMDA receptor antagonist with a preferred action on GluN2A subunits—on the rewarding efficacy of ICSS, showing that PPPA injection into the VTA produces a time-dependent increase in brain stimulation reward. The reward-enhancing properties of PPPA are very similar to those reported by other studies using the same dose and injection site

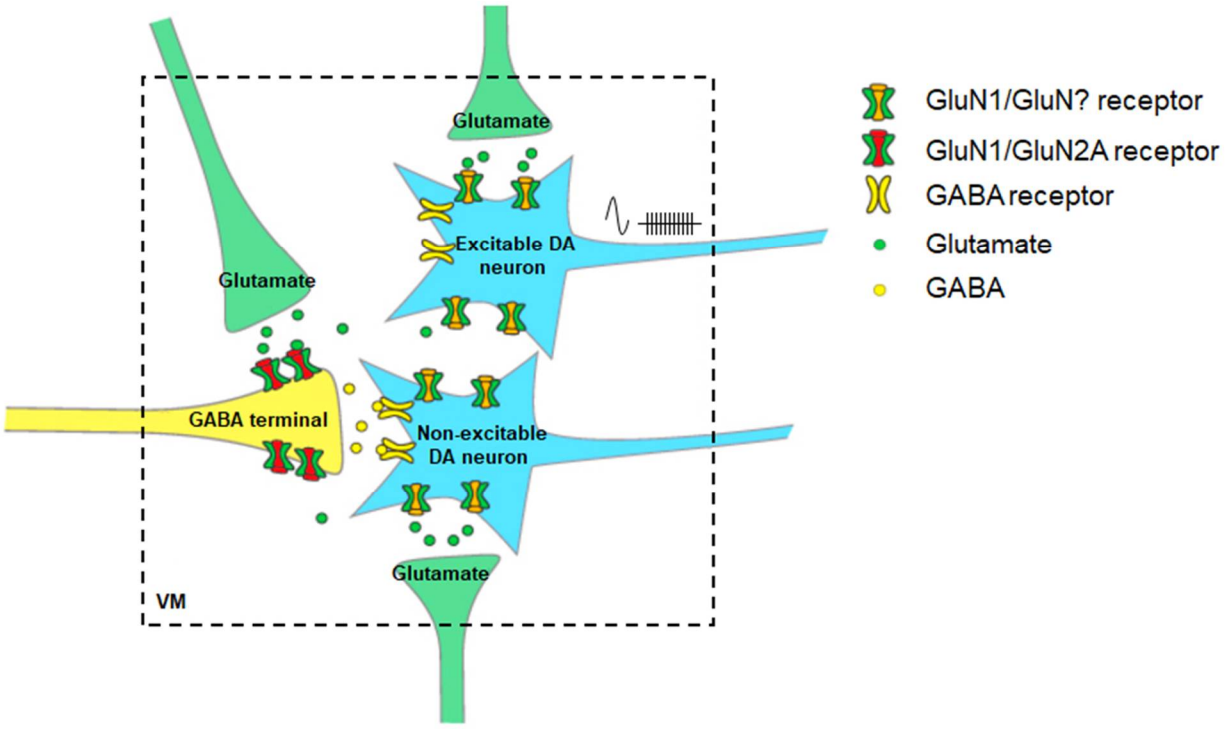

Figure 6: Glutamate transmission in the ventral midbrain exerts opposite roles. On the one hand, glutamate can switch the firing pattern of DA neurons from tonic to phasic burst firing. On the other hand, glutamate afferent terminals can make synaptic contact with local GABAergic interneurons, thereby increasing the inhibitory drive onto DA neurons. The inhibitory effect of glutamate on DA neuronal activity is most likely mediated by GluN2A-containing NMDA receptors located on afferent terminals. Abbreviations: ventral midbrain (VM). Adapted from Hernandez et al., 2015.

(Bergeron and Rompre, 2013; Hernandez et al., 2016), and suggest that GluN2A-containing NMDA receptors are mainly expressed on GABAergic neurons of the VTA. Using the small interferon RNA (siRNA) technique, Hernandez et al. (2015) also showed that downregulation of NMDA receptors in the ventral midbrain attenuates brain stimulation reward, most likely as a result of decreased glutamate-mediated excitability of DA neurons. However, the siRNA-mediated downregulation of NMDA receptors failed to alter the reward-enhancing effect of PPPA,

indicating that GluN2A-containing NMDA receptors are most likely located on glutamate afferent terminals of the ventral midbrain **(Figure 6)** (Hernandez et al., 2015).

Taken together, the aforementioned findings suggest that glutamate signalling is highly implicated in reward and motivational processes as a result of its strong influence over DA neuron activity. This could have important implications for psychiatric conditions such as major depressive disorders, where abnormalities in reward processing are frequently observed (Admon and Pizzagalli, 2015; Whitton et al., 2015). Ketamine, a pharmacological agent that targets glutamate NMDA receptors, has already proven successful in producing rapid and long-lasting attenuations of depressive symptoms in patients (Berman et al., 2000; Messer and Haller, 2017), however, evidence supporting its use as an antidepressant is still very limited and requires further investigation.

1.2.4 The opioid system: overview and implication in reward processing

Early evidence for the existence of an opioid system stems from the use of opium by the Sumerians in 3400 B.C., who called it "gil"—the word for joy (Brownstein, 1993). Opium is obtained from the seed capsules of the opium poppy, *Papaver somniferum,* and is the source of a family of drugs referred to as opiates or opioids. The opioids have been used for both recreational and medicinal purposes for thousands of years due to their principal effect in euphoria and pain reduction. In the beginning of the 19th century, Sertürner isolated the active ingredient of opium, and named it morphine after the Greek god of dreams, Morpheus (Brownstein, 1993). In addition to morphine, opium contains other closely related opioids including codeine and thebaine. However, despite being effective in pain relief, these opium-derived compounds were found to be highly addictive and not very safe to use. In an effort to develop a safer opiate for pain relief,

heroin was chemically synthesized by the Bayer Company in the late 1800s through the addition of two acetyl groups onto the morphine molecule (Pasternak and Pan, 2013). Although heroin was first marketed as a non-addictive painkiller and cough suppressant, its strong addictive properties were soon acknowledged, and resulted in its immediate prohibition from the market (Le Merrer et al., 2009). Today, heroin and morphine are widely used illicit drugs of abuse, and represent a significant public health problem.

The opioid system consists of three major families of G-protein coupled receptors, μ (mu), δ (delta), and κ (kappa), and three major families of endogenous peptides, β-endorphin, enkephalins, and dynorphins. These endogenous peptides derive from the proteolytic cleavage of large protein precursors, which include proopiomelanocortin (the precursor of β-endorphin), preproenkephalin (the precursor of enkephalins), and preprodynorphin (the precursor of dynorphins) (Benarroch, 2012). More recently, two short peptides that display high affinity for mu-opioid receptors (MORs) have been identified and named endomorphin-1 (EM-1) and endomorphin-2 (EM-2), however, their exact function is far from being fully elucidated (Koneru et al., 2009). In the brain and spinal cord, opioid receptors show unique, albeit overlapping, distributions, suggesting that they mediate different physiological functions (Mansour et al., 1987; George et al., 1994; Mansour et al., 1994). MORs are particularly enriched in areas involved in morphine-induced analgesia, such as the thalamus and raphe nuclei, and in areas involved in reward related processes, such as the habenula and the NAc (Mansour et al., 1987; Mansour et al., 1994). Delta opioid receptors (DORs) have a distribution similar to that of MORs, but are more restricted to forebrain regions including the anterior cingulate cortex, neocortex, striatum, and amygdala, suggesting that they may play a role in cognitive functions, motor integration, and reinforcement (Mansour et al., 1987; Mansour et al., 1994). On the other hand, kappa opioid receptors (KORs) exhibit a third pattern of distribution

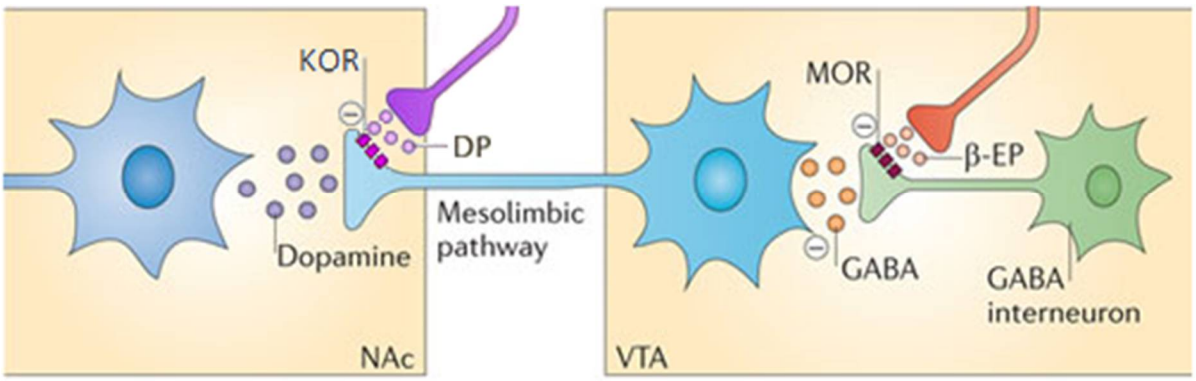

Figure 7: Model of opposing tonic effects of opioid receptors on mesolimbic dopaminergic cells. In the VTA, β-endorphins (via MORs) increase VTA DA neuronal activity by inhibiting the release of GABA from local interneurons. This results in increased release of DA in the NAc. Similarly, activation of DORs by enkephalins increases VTA DA cell firing by inhibiting local GABAergic inhibitory cells (not shown). On the other hand, the release of DA from mesolimbic nerve terminals is tonically inhibited by dynorphins through the activation of KORs, which are located on the terminals of DA neurons. Abbreviation: β-endorphin (β-EP); dynorphin (DP); nucleus accumbens (NAc). Modified from (Heilig et al., 2011).

distinct from that of MORs and DORs, primarily along the hippocampus, dentate gyrus, hypothalamus, amygdala and striatum (Mansour et al., 1987; Tempel and Zukin, 1987), and are mostly involved in the regulation of mood and pain perception (Black and Trevethick, 1998; Bruijnzeel, 2009).

Over the past few decades, there has been increasing evidence showing that the opioid system is involved in processes of reinforcement. It is well established that activation of MORs, and to a lesser extent DORs, produces positive reinforcement, whereas activation of KORs induces aversive effects (Gruber et al., 2007b; Le Merrer et al., 2009). Early studies on opioid self-administration demonstrated that rats (Weeks, 1962; van Ree et al., 1978) and rhesus monkeys

(Thompson and Schuster, 1964; Deneau et al., 1969) would readily press a lever to receive intravenous infusions of morphine, a selective MOR agonist. Similarly, intracranial administration of enkephalins, which primarily bind to DORs, produces positive reinforcement in rodents (Goeders et al., 1984b; Goeders et al., 1984a; Dib, 1985). Consistent with the view that activation of MORs and DORs is reinforcing, agonists for these receptors have been shown to potentiate the rewarding effects of ICSS inasmuch as they produce a leftward shift in the R/F curve (Broekkamp and Phillips, 1979; Bauco et al., 1993; Duvauchelle et al., 1997; Robinson et al., 2012). In addition, several reports have shown that MOR and DOR agonists, including morphine (Wu et al., 2016), heroin (Schlussman et al., 2008), fentanyl (Miller and Nation, 1997), EM-1 (Zangen et al., 2002), and Met-enkephalin (Agmo and Gomez, 1991), produce conditioned place preference; effect that is attributed to their rewarding and addictive properties. However, unlike MOR and DOR agonists, agonists for KORs do not produce reinforcing effects. Instead, activation of KORs produces conditioned place aversion (Land et al., 2009; Robles et al., 2014) and depressive-like behaviors in rodents (Mague et al., 2003; Carlezon et al., 2006), suggesting that these receptors may contribute to negative emotional states. Activation of KORs also decreases the rewarding effectiveness of ICSS inasmuch as systemic administration of the KOR agonist, U-69593, dose-dependently increases reward thresholds for MFB self-stimulation (Todtenkopf et al., 2004; Tomasiewicz et al., 2008).

MORs, DORs and KORs are proteins that possess seven membrane-spanning domains coupled to an inhibitory G protein (Gi). Activation of these receptors inhibit adenylyl cyclase, which normally synthesizes the second messenger cyclic adenosine monophosphate (cAMP). Opioid receptor-mediated cellular changes are inhibitory; their activation reduces membrane excitability and subsequent cell firing by opening K^+ channels, which causes membrane hyperpolarization,

and by closing voltage gated Ca^{2+} channels, which decreases the amount of neurotransmitter released (Meyer and Quenzer, 2005). Opioids mediate their effects through a number of brain areas of the corticomesolimbic system, however, chief among these is the VTA, which houses DA cell bodies that project to the NAc (Wise, 1989). Activation of MORs and DORs in the VTA increases the release of DA in the ventral striatum (Leone et al., 1991; Devine et al., 1993), which suggests that these receptors are localized on GABAergic interneurons and that their activation produces DA cell activation via disinhibition **(Figure 7)**. On the hand, KORs are located on the terminals of VTA DA neurons **(Figure 7)**, and agonists for these receptors decrease striatal DA release when injected systematically (Di Chiara and Imperato, 1988; Maisonneuve et al., 1994) or directly into the NAc (Spanagel et al., 1992). Altogether, these findings concur with the view that opioid receptors mediate distinct and unique roles in reward processing, and highlight the opioid system as a key regulator of goal-directed behaviors.

1.3 The dorsal diencephalic conduction system in reward processing: spotlight on the anatomy and function of the habenular complex (Adapted from the review paper Fakhoury 2018. *Behavioral Brain Research,* Accepted in Press)

The DDC is a neural pathway composed of the stria medullaris (SM), the habenula, and the fasciculus retroflexus (FR) that merges with the MFB at its rostral and caudal poles. The information received by the DDC travels from the anterior portion of the LH to the habenula through the SM, and gets transmitted to midbrain regions via the FR (Sutherland, 1982; Beretta et al., 2012). Sites within the DDC, including the SM and the habenula, have all been shown to support operant responding for ICSS, indicating that this pathway plays crucial roles in the modulation of reward and goal-directed behaviors (Sutherland and Nakajima, 1981; Blander and

Wise, 1989; Vachon and Miliaressis, 1992). However, until recently, the role of the DDC in reward processing has largely been overlooked in favor of the MFB. Following Matsumoto and Hikosaka's seminal work on the LHb as a source of negative reward signals in monkeys (Matsumoto and Hikosaka, 2007), the DDC has undergone a resurgence of scientific interest, paving the ways for many subsequent studies (Batalla et al., 2017; Fakhoury, 2017). Numerous functions have been ascribed to the DDC, including the regulation of sleep homeostasis (Aizawa et al., 2013; Zhang et al., 2016), stress response (Wirtshafter et al., 1994; Jacinto et al., 2017), anxiety (Mathuru and Jesuthasan, 2013), pain (Shelton et al., 2012b) and analgesia (Shelton et al., 2012a). However, the overarching goal of the following sections is to provide an overview of the neuroanatomical and behavioral findings aimed at deciphering the functions of the DDC in reward processing, with a special focus on the habenular complex. A description of the cellular and synaptic profile of habenular neurons and their interconnectivity with monoaminergic systems is first given, followed by an overview of findings delineating the reward-related functions of the DDC.

1.3.1 The habenula: morphological, cellular and electrophysiological profile

Centrally located along the DDC, the habenula acts as an interface between forebrain and mesencephalic regions. It is an evolutionary conserved epithalamic structure that shows striking asymmetry in most groups of vertebrates (Concha and Wilson, 2001; Bianco and Wilson, 2009). In the lamprey, the right habenula is substantially larger than the left, while in most species of cartilaginous fishes, the habenular nucleus is enlarged on the left side (Concha and Wilson, 2001). Size differences between the right and left habenula have also been observed in rodents. In the albino rat, the left habenula is slightly larger compared to the right (Wree et al., 1981), whereas in the albino mouse, the right habenula is markedly enlarged and displays a more complex

arrangement of neurons compared to the left habenula (Zilles et al., 1976). Anatomically, the habenula is divided into two functionally distinct subclei; the medial (MHb) and the lateral (LHb) habenula. The MHb is comprised of a superior (MHbS), inferior (MHbI), central (MHbC), and lateral (MHbL) part, and is characterized by a remarkably high density of cells that show striking differences in somatodendritic and axonal morphology (Kim and Chang, 2005; Aizawa et al., 2012). On the other hand, the LHb is comprised of a medial (LHbM) and lateral (LHbL) part, each one further subdivided into distinct sets of nuclei on morphologic and cytochemical grounds (Andres et al., 1999; Geisler et al., 2003; Aizawa et al., 2012). Morphological analysis also reveal the presence of four major types of cells within the LHb, namely the spherical, fusiform, polymorphic, and vertical cells (Weiss and Veh, 2011), and unlike the MHb, cells in this nucleus are more loosely dispersed (Kim and Chang, 2005). Although morphologically different from each other, LHb neurons share similar electrophysiological profile and intrinsic membrane properties; they have a high input resistance and produce long-lasting discharges in response to transient synaptic hyperpolarization (Chang and Kim, 2004; Weiss and Veh, 2011). Such similarity most likely suggests that the formation of functional entities within the LHb is achieved by specific synaptic inputs to particular neurons rather by individual differences in intrinsic membrane properties (Weiss and Veh, 2011).

LHb neurons are mainly glutamatergic, with enriched expression of the vesicular glutamate transporter VGLUT2 (Aizawa et al., 2012; Vigneault et al., 2015). These neurons exhibit different patterns of spontaneous action potential firing, including tonic regular, tonic irregular and burst firing (Kowski et al., 2009). Electrophysiological evidence suggests that the glutamatergic transmission in the LHb is primarily driven by calcium-permeable AMPA receptors, and to a lesser extent, calcium-impermeable AMPA receptors (Li et al., 2011; Shabel et al., 2012; Meye et al.,

2013). The excitatory glutamatergic transmission in LHb neurons also relies on the activation of NMDA receptors (Li et al., 2011) and mGluR1 (Valentinova and Mameli, 2016), though synaptic currents mediated by these receptors are relatively small compared to those mediated by AMPA receptors. The LHb also receives strong gamma-GABAergic inputs, which are mainly driven by the activation of GABA type-A ($GABA_A$) and type-B ($GABA_B$) receptor subunits (Liang et al., 2000; Meye et al., 2013). These GABAergic projections most likely originate from extrinsic sources since local interneurons are relatively scarce (Smith et al., 1987). Besides glutamate and GABAergic receptors, the LHb contains DA type-2 (D_2) and type-4 (D_4) receptors postsynaptically (Aizawa et al., 2012; Good et al., 2013), as well as serotonin receptor 2C ($5\text{-}HT_{2C}$) (Han et al., 2015), suggesting that it may be subject to dopaminergic and serotonergic modulation.

The cellular and electrophysiological profile of the MHb is very different compared to that of the LHb (Kim and Chang, 2005; Aizawa et al., 2012). A known feature of the MHb is that it has one of the highest concentrations of $GABA_B$ receptors in the brain, indicating the existence of strong inhibitory inputs (Durkin et al., 1999; Liang et al., 2000; Wang et al., 2006; Kim and Chung, 2007). MHb neurons are mostly homogeneous in their electrophysiological profile, exhibiting tonic firing of action potentials (Kim and Chang, 2005). They receive glutamate- and ATP-mediated synaptic inputs (Robertson and Edwards, 1998) and contain functional AMPA receptors of low calcium permeability (Robertson et al., 1999). Recent observations also indicate that the MHb contains glutamate-expressing neurons with enriched expression of VGLUT1 and VGLUT2 (Barroso-Chinea et al., 2007; Qin and Luo, 2009) and with the ability to co-release acetylcholine at synaptic terminals (Ren et al., 2011). Unlike the LHb, which expresses several subunits of $GABA_A$ receptors at both the mRNA and protein level, the MHb only expresses the α2-subunit of $GABA_A$ receptors (Hortnagl et al., 2013). The MHb is also distinctive from the LHb in that it

expresses at very high level the α3, α4, α5, α6, β2, β3 and β4 subunits of the nicotinic acetylcholine receptors (nAChRs) (Grady et al., 2009; Shih et al., 2014), and shows strong immunoreactivity for MORs (Gardon et al., 2014), suggesting that it most likely play a crucial role in modulating the behavioral effects of nicotine and morphine.

Last but not least, evidence indicates some degree of functional specialization within MHb neurons. For instance, gene expression analysis of medial habenular subnuclei in the rat reveal that the superior MHb is glutamatergic, the dorsal-central part of the MHb is both substance P-ergic and glutamatergic, and that the ventral-center and lateral part of the MHb are both cholinergic and glutamatergic (Aizawa et al., 2012). More recently, Chou and colleagues (2016) identified two subregions in the evolutionarily homologous dorsal habenula (dHB) of the zebrafish, namely the lateral subregion of the dHb (dHbL) and the medial subregion of the dHb (dHbM), which antagonistically regulate the outcome of conflict. Silencing the dHbL or dHbM in zebrafish caused a stronger predisposition to lose or win a fight, respectively, indicating that these subregions differentially regulate the resolution of social conflict (Chou et al., 2016).

1.3.2 Afferent and efferent pathways of the habenula

As shown in **Figure 8**, the habenula is an epithalamic structure divided into a lateral and medial component that lie in close proximity to the pineal gland. The connection between the two habenular subnuclei is asymmetrical inasmuch as only the MHb sends axonal projections to the LHb (Kim and Chang, 2005). Despite sharing some sources of afferent inputs and efferent targets, the LHb and MHb are characterized by different connectivity that underlie differences in their functions. In delineating the afferent and efferent circuitry of the habenula, the primary focus will be on the rat, which has been well studied. Some subtle differences in connectivity may exist across

species, however, a description of the comparative neuroanatomy of the habenula is outside the scope of this paper.

Much of the knowledge on the connectivity of the habenula has been acquired through studies employing retrograde and anterograde tracing. Findings from these studies suggest that the LHb receives strong GABAergic inputs from structures of the limbic system including the medial septum, diagonal band of Broca, lateral preoptic area and the substantia innominate (SI) (Herkenham and Nauta, 1977; Araki et al., 1984; Hreib et al., 1988), as well as bilateral and topographically organized inputs from the anterior insular, cingulate, prelimbic and infralimbic cortices (Sesack et al., 1989; Kim and Lee, 2012). By far, the strongest inputs to the LHb originate from the LH and the entopeduncular nucleus (EP), the latter being the internal segment of the globus pallidus in non-primate mammals (Herkenham and Nauta, 1977). Projections from these regions to the LHb are primarily excitatory and glutamatergic, though evidence of a GABAergic input originating from these regions has also been demonstrated (Shabel et al., 2012; Stamatakis et al., 2016). Projections from the BNST, dorsomedial hypothalamic nucleus, periaqueductal gray (PAG), SNc, and VTA (Li et al., 1993) as well as inputs from 5HT-containing neurons of the median (MR) and DR (Conrad et al., 1974; Vertes et al., 1999) also densely innervate the LHb. On the other hand, the LHb innervates a wide range of structures by projecting caudally through the FR or rostrally through the SM. One of the major targets of the LHb efferent pathway is the tail of the VTA (tVTA); a GABAergic region located posterior to the VTA, which is also referred to as rostromedial tegmental nucleus (RMTg) (Jhou et al., 2009a; Kaufling et al., 2009). The dense projections from the LHb to the tVTA are glutamatergic (Brinschwitz et al., 2010), mainly ipsilateral, and organized in a topographical manner, with medial and lateral portions of the LHb targeting medial and lateral portions of the tVTA, respectively (Jhou et al., 2009a; Kaufling et al.,

2009). Direct excitatory projections from the LHb to DA and GABAergic neurons of the VTA have also been reported, though these constitute only a small proportion (~16%) of LHb projecting axons (Omelchenko et al., 2009; Goncalves et al., 2012). Other caudal targets of LHb efferents include the DR and MR (Herkenham and Nauta, 1979), the PAG (Quina et al., 2015), the nucleus incertus (Goto et al., 2001), the pontine reticular formation (Araki et al., 1988), the superior colliculus (SC) (Herkenham and Nauta, 1979), and the pedunculopontine and laterodorsal tegmental nuclei (Semba and Fibiger, 1992). Rostrally, the LHb projects to a wide range of structures, including the NAc, the amygdala, and zona incerta (Akagi and Powell, 1968; Herkenham and Nauta, 1979; Phillipson and Griffiths, 1985). Rostral projections of the LHb also target forebrain and thalamic structures, many of them acting as a source of input to the LHb. For instance, the supramammillary area of the hypothalamus (Hayakawa et al., 1993; Kiss et al., 2002), lateral preoptic area (Akagi and Powell, 1968), LH (Akagi and Powell, 1968; Yamadori, 1969), SI (Herkenham and Nauta, 1979), diagonal band of broca (Akagi and Powell, 1968), and septum (Akagi and Powell, 1968) all share reciprocal connections with the LHb.

The afferent and efferent pathways of the MHb are very distinct to that of the LHb, albeit with some similarities. While the LHb receives the majority of its inputs through the SM, FR and habenular commissure, afferent fibers reach the MHb primarily through the SM and to lesser extent the inferior thalamic peduncle (Sutherland, 1982). Similar to the LHb, the MHb receives inputs from the medial septum, diagonal band of Broca, lateral preoptic area, LH and MR (Herkenham and Nauta, 1977; Qin and Luo, 2009). The most prominent inputs to the MHb arise from two nuclei in the posterior septum; the triangular septal nucleus and the septofimbrial nucleus. While the former primarily innervates the MHb at its caudal part, the latter primarily innervate the MHb at its rostral part (Herkenham and Nauta, 1977). Dopaminergic projections from the VTA

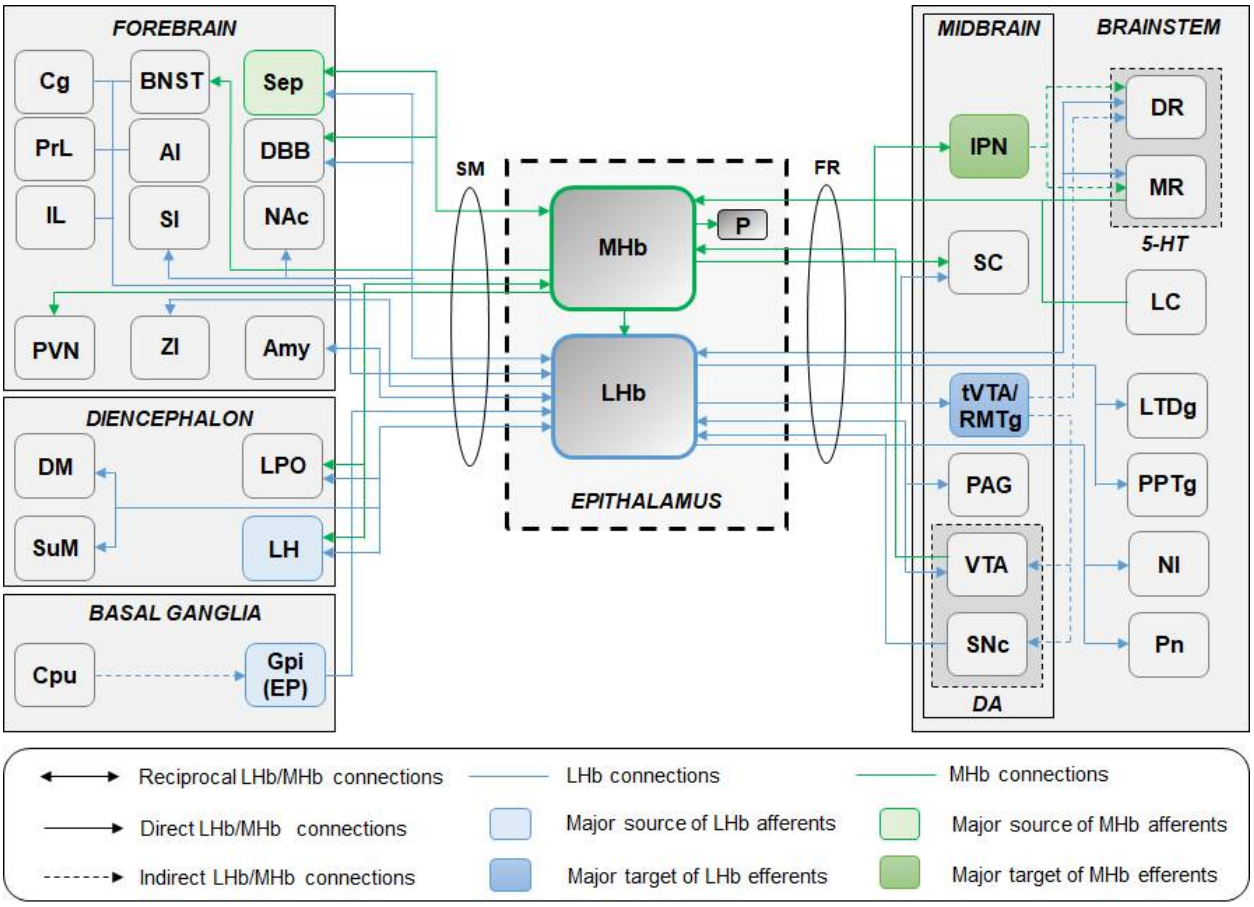

Figure 8: Habenula afferents and efferents connections. This schematic illustrates the major connections of the MHb and LHb as described in the rat and other mammals. Abbreviations: 5-HT, serotonin; AI, anterior insula; Amy, amygdala; BNST, bed nucleus of the stria terminalis; Cg, cingulate cortex; Cpu, caudate putamen; DA, dopamine; DBB, diagonal band of broca; DM, dorsomedial hypothalamic nucleus; EP, entopeduncular nucleus; FR, fasciculus retroflexus; Gpi, internal segment of the globus pallidus; IL, infralimbic cortex; IPN, interpeduncular nucleus; LC, locus cœruleus; LH, lateral hypothalamus; LHb, lateral habenula; LPO, lateral preoptic area; LTDg, laterodorsal tegmental nucleus; MHb, medial habenula; NAc, nucleus accumbens; NI, nucleus incertus; P, pineal gland; PAG, periaqueductal gray; Pn, pontine reticular formation; PPTg, pedunculopontine tegmental nucleus; PrL, prelimbic cortex; PVN, paraventricular nucleus; RMTg, rostromedial tegmental nucleus; SC, superior colliculus; Sep, septum; SI, substantia innominate; SM, stria medullaris; SNc, substantia nigra pars compacta; SuM, supramammillary area of the hypothalamus; tVTA, tail of the ventral tegmental area; VTA, ventral tegmental area; ZI, zona incerta.

(Phillipson and Pycock, 1982) and noradrenergic projections from the locus coeruleus and superior cervical ganglion (Gottesfeld, 1983) also innervate the MHb by travelling anteriorly in the MFB before coursing through the SM. In turn, MHb neurons project to numerous rostrally and caudally located regions by coursing either through the SM or FR, respectively. By far, the majority of MHb axons terminate into the interpeduncular nucleus (IPN), a midbrain region located just anterior to the MR (Herkenham and Nauta, 1979; Shibata et al., 1986). Neurochemical studies of the MHb-IPN tract showed that MHb projecting neurons utilize substance P, acetylcholine, and glutamate as their three major output neurotransmitters (Contestabile et al., 1987; Qin and Luo, 2009). In contrast to LHb projecting neurons, which mainly course through the external portion of the FR, the MHb projects to the IPN through the internal portion of the FR (Herkenham and Nauta, 1979). MHb neurons that project to the IPN terminate into the VTA and raphe nuclei, thus exerting an indirect influence over the DA and 5-HT system (Akagi and Powell, 1968; Cuello et al., 1978; Groenewegen et al., 1986). Last but not least, studies employing electrolytic lesions at the MHb have reported severe degeneration of terminals in the pineal gland of rats (Ronnekleiv and Moller, 1979), and in the SC, LH, paraventricular nucleus, septum, diagonal band of broca, and BNST of cats (Akagi and Powell, 1968), demonstrating that nerve fibers from the MHb may also innervate these regions.

1.3.3 The habenula: a major regulator of monoaminergic systems

In light of anatomical evidence demonstrating the existence of LHb and MHb axonal connections with various brain regions, the habenula is often considered as a relay station between forebrain and brainstem structures. Its connectivity with the limbic system and globus pallidum makes it well suited to participate in a wide range of motivational and emotional states and to modulate

various motor behaviors. In accordance with the diversity of axonal connections between the habenula and monoaminergic nuclei, it is not surprising that the habenula has been implicated in the regulation of neurotransmitter systems, including those for DA and 5-HT. Habenular neurons have also been shown to participate in noradrenaline and acetylcholine transmission (Sastry et al., 1979; Kalen et al., 1989), however, the focus of the following sections will be on the DA and 5-HT systems owing to the well-established evidence implicating these neurotransmitters in reward processing (Wise and Rompre, 1989; Faulkner and Deakin, 2014) and psychiatric conditions (Volkow et al., 2007; Fakhoury, 2016).

1.3.3.1 The habenula and the DA system

The discovery that habenular neurons share reciprocal axonal connections with midbrain DA neurons either directly or indirectly through intermediate structures have ushered in a wide array of studies investigating the functional implication of this connectivity. Findings from these studies suggest that the habenula—in particular the LHb—exerts an inhibitory control over midbrain DA neurons. For instance, electrical stimulation of the LHb inhibits the activity of DA neurons in the VTA and SNc; effect that is abolished following destruction of the FR but not the SM (Christoph et al., 1986; Ji and Shepard, 2007). Conversely, lesions at the habenula and FR (Lisoprawski et al., 1980; Nishikawa et al., 1986), or activation of habenular GABAergic interneurons through deep brain stimulation (DBS) (Meng et al., 2011), increase DA transmission, indicating that habenular efferents exert a tonic inhibitory control over DA neurons. The inhibitory effect of the habenula over midbrain DA neurons is likely mediated by its output target, the tVTA, which in turn sends GABAergic projections to DA neurons of the VTA and SNc (Jhou et al., 2009a), though direct

excitatory LHb projections activating midbrain GABAergic interneurons may also account for this effect (Omelchenko et al., 2009).

The view that the LHb receives direct inputs from midbrain dopaminergic nuclei (Li et al., 1993; Gruber et al., 2007a), together with evidence showing that it expresses DA D_2 and D_4 receptors (Aizawa et al., 2012; Good et al., 2013), suggest that its activity is most likely influenced by changes in DA transmission. Findings in support of this hypothesis come from metabolic studies showing that DA receptor agonists and DA-increasing drugs decrease LHb glucose consumption (Wechsler et al., 1979; McCulloch et al., 1980; Porrino et al., 1988), in contrast to DA receptor antagonists, which increase LHb glucose consumption (McCulloch et al., 1980; Ramm et al., 1984). Although these studies suggest a negative correlation between the functional activity of the LHb and the DA system, the relationship between midbrain DA and LHb neurons appears to be far more complex. Indeed, local and systemic administration of DA receptor agonists increase the neuronal activity (Wirtshafter et al., 1994) and firing rate (Kowski et al., 2009) of LHb neurons, respectively. In addition, LHb neurons were shown to fire at a higher rate following tetanic stimulation of the VTA (Shen et al., 2012), which is inconsistent with prior reports indicating mutually inhibitory relations between the LHb and midbrain DA neurons. In another study, single-pulse stimulation of either the VTA or SNc was shown to inhibit the firing of approximately 90% of LHb neurons (Shen et al., 2012). In light of these findings, sustained and transient activation of midbrain DA neurons may have opposite functional effects on LHb neurons. While the former exerts an excitatory effect on the activity of LHb neurons, the latter appears to play an inhibitory role on the activity of LHb neurons, likely through the activation of local GABAergic interneurons and fibers of passage (Shen et al., 2012).

To date, most of the studies investigating the functional relationship between the habenula and the DA system have focused on the LHb, however, evidence also indicates a role for the MHb in the regulation of DA neuronal activity. For instance, infusion of a cholinergic antagonist into the IPN—the main target of the MHb—increases DA utilization in the mPFC and NAc of rats, suggesting that the habenula-IPN pathway may exert a tonic inhibitory influence on mesocortical and mesolimbic dopaminergic neurons (Nishikawa et al., 1986). The view that MHb neurons exert a control over the activity of DA mesolimbic neurons is also supported by recent studies showing that blockade of nAChRs in the MHb prevents the increase in accumbal DA level induced by systemic injection of nicotine (McCallum et al., 2012), and reduces the sensitization of DA response to repeated morphine treatment in the NAc (Taraschenko et al., 2007). The MHb may also influence the activity of nigrostriatal DA neurons by sending indirect projections to the VTA through the IPN (Groenewegen et al., 1986), or by providing additional inputs to the LHb (Kim and Chang, 2005).

Considering the modulatory role of the habenula over the DA system, together with evidence of a regulatory feedback control, this nucleus has been extensively investigated in the context of substance use disorder (Boulos et al., 2017; Fakhoury, 2017). Drugs of abuse exert their initial reinforcing effects by elevating mesolimbic DA transmission (Adinoff, 2004; Volkow and Morales, 2015). Thus, a bidirectional relationship between the activity of the habenula and the effect of drugs of abuse appears unsurprising. In rodents, self-administration of cocaine increases the excitability of LHb neurons (Neumann et al., 2014), and chronic administration of morphine decreases cholinergic signaling in the MHb (Neugebauer et al., 2013). Because of the reciprocal connections of the LHb with midbrain DA neurons, scientists have also looked at the possibility of using this subnucleus as a modulatory target site for DBS treatment of substance use disorder

(Yadid et al., 2013). DBS of the LHb was shown to reduce cocaine self-administration during drug maintenance, extinction, and reinstatement (Lax et al., 2013) and attenuate cocaine-induced increases in VTA glutamatergic transmission (Friedman et al., 2010). However, despite significant progress in research, the safety and long-term efficacy of this approach are poorly understood and remain to be tested in controlled clinical trials.

1.3.3.2 The habenula and the 5-HT system

Besides it role in the regulation of the DA system, mounting evidence suggests that the habenula strongly modulates the 5-HT system. Electrophysiological studies have repeatedly shown that the habenula provides a powerful regulatory control over 5-HT transmission in different regions of the brain, including the striatum, hippocampus, and substantia nigra (Soubrie et al., 1981; Reisine et al., 1982; Sabatino et al., 1991). The control of the habenula over the 5-HT system is largely mediated through dense projections to raphe nuclei (Herkenham and Nauta, 1979; Pollak Dorocic et al., 2014), in particular the DR, which constitutes the primary source of 5-HT-containing neurons in the brain (Descarries et al., 1982; Vertes and Crane, 1997). The habenula-raphe projection is excitatory, with glutamate and substance P as the main neurotransmitters, and primarily originates from the lateral part of the habenula (Neckers et al., 1979; Kalen et al., 1985; Kalen et al., 1986). LHb neurons that project to the DR are thought to mainly innervate and activate local GABAergic neurons, leading to an indirect inhibition of 5-HT neurons. Evidence in support of this hypothesis comes from studies showing that electrical stimulation of the LHb decreases the firing activity of DR 5-HT neurons (Stern et al., 1979; Park, 1987; Varga et al., 2003), and that this effect is blocked by the administration of GABA receptor antagonists (Wang and Aghajanian, 1977; Ferraro et al., 1996). Also, the inhibition of 5-HT neurons induced by LHb stimulation is

preceded by a rapid onset excitation of non-5HT neurons (12–21 ms latency), suggesting that the LHb primarily influences the activity of DR 5-HT neurons through monosynaptic projections targeting a local network of GABAergic neurons (Varga et al., 2001; Varga et al., 2003). However, the possibility of an indirect polysynaptic projection from the LHb to the DR should not be ruled out inasmuch as neurons of the tVTA, the main output target of the LHb, sends robust GABAergic projections to the DR (Lavezzi et al., 2012; Sego et al., 2014). Also noteworthy to mention is the existence of excitatory projections from the LHb that directly innervate DR 5-HT neurons (Ogawa et al., 2014). Electrical stimulation of the LHb can thus directly activate DR 5-HT neurons, thereby facilitating local serotonergic transmission (Ferraro et al., 1996; Varga et al., 2003). To functionally probe the direct projections of LHb neurons to the DR, Pollak Dorocic and colleagues (2014) have shown that optogenetic stimulation of LHb axon terminals into the DR results in a rapid and marked depolarization of 5-HT neurons. This effect was blocked by the application of an AMPA, but not GABA, receptor antagonist, thus confirming the presence of excitatory and glutamatergic LHb projections onto DR 5-HT neurons (Pollak Dorocic et al., 2014).

Because of its reciprocal anatomical connections with raphe nuclei (Herkenham and Nauta, 1979; Vertes, 1991; Vertes et al., 1999) and its constitutive expression of 5-HT_{2C} receptors postsynaptically (Pompeiano et al., 1994; Han et al., 2015), the LHb has also been subject to a wide array of investigations exploring the possibility of a forward-feedback loop with the 5-HT system. Numerous studies have demonstrated the existence of a 5-HT modulation of both synaptic transmission and intrinsic excitability of LHb neurons (Tchenio et al., 2016). In a set of experiments employing the expression of Channelrhodopsin-2 in the EP, a region of the basal ganglia that sends glutamatergic and GABAergic projections to the LHb, Shabel and colleagues showed that bath application of 5-HT reduces light-evoked EP-LHb inhibitory (IPSCs) and

excitatory (EPSCs) postsynaptic currents (Shabel et al., 2012; Shabel et al., 2014). Although these findings suggest that 5-HT modulates the synaptic transmission of LHb neurons, they failed to identify the subtype of 5-HT receptor involved. In another study, exposure of LHb-containing slices to 5-HT or a 5-HT_{1B} receptor agonist induced a long-term depression of evoked IPSCs and EPSCs (Hwang and Chung, 2014). The latter was prominently blocked in the presence of a $5HT_{1B}$ receptor antagonist, indicating that the 5-HT-induced suppression of excitatory inputs to the LHb occurs through the pre-synaptic activation of 5-HT_{1B} receptors (Hwang and Chung, 2014). However, in contrast to the suppression of EPSCs described by Hwang and Ching (2014), a recent study showed that 5-HT facilitates glutamate transmission in many LHb neurons, and only in a subset of these neurons does it reduce synaptic excitability (Xie et al., 2016). Bath application of 5-HT also accelerates spontaneous firing in the majority of LHb neurons via postsynaptic activation of 5-HT receptors (Zuo et al., 2016). Altogether, the aforementioned findings suggest that 5-HT may exert different effects on the presynaptic and postsynaptic membrane of LHb neurons. However, the subcellular localization and subtype of 5-HT receptors involved in this modulation are still lacking and need to be thoroughly investigated in future studies.

The view that the habenula is functionally related to the 5-HT system is of particular relevance from a psychiatric standpoint, as changes in 5-HT neurotransmission are involved in the pathogenesis of mood disorders (Fakhoury, 2016). One prevailing hypothesis that has been supported by a wide array of animal and human studies is that the habenula is hyperactive in major depressive disorders (Proulx et al., 2014; Fakhoury, 2017). In rodents, metabolic studies point to increased metabolism of the habenula in animal models of depression (Shumake et al., 2003; Mirrione et al., 2014), whereas in humans, functional magnetic resonance imaging (fMRI) findings show increased activity of the habenula in individuals with remitted MDD following tryptophan

depletion (Roiser et al., 2009). Molecular changes in the LHb, including upregulation of β-CamKII, were also shown to increase synaptic efficacy and spike output of LHb neurons and to cause depressive-like behaviors in rodents (Li et al., 2013). The LHb is therefore considered as a potential neuromodulatory target for the treatment of depressive-like symptoms, and has already been the subject of numerous studies with animal models of depression or patients with MDD (for review see Fakhoury, 2017).

1.3.4 The DDC in reward and aversion

Given the wide array of evidence highlighting the existence of reciprocal functional connections between the DDC and the DA and 5-HT systems, this pathway is likely to participate in the control of reward-related processes. To date, most of the studies concerned about the role of DDC in reward processing have eschewed the functions of the MHb in favor of the LHb, in part due to the existence of stronger functional projections between the latter structure and midbrain DA neurons. The following sections, which are summarized in **Table 1**, provide a detailed overview of findings from electrophysiological, neuroimaging, electrical stimulation and optogenetic stimulation studies investigating the role of the DDC in reward and aversion.

1.3.4.1 Electrophysiological and neuroimaging studies

One of the most groundbreaking discoveries on the LHb comes from a study by Matsumoto and Hikosaka (2007) showing that this subnucleus is involved in negative reward processing. In this study, monkeys were trained to perform a visually guided saccade task with biased reward outcomes during which the activity of LHb and SNc DA neurons were monitored (Matsumoto and Hikosaka, 2007). LHb neurons were excited in response to a no reward-predicting target, and inhibited in response to a juice reward-predicting target (Matsumoto and Hikosaka, 2007). In

contrast, DA neurons in the SNc followed the exact opposite pattern of activity; they were excited by reward-predicting targets and inhibited by no-reward-predicting targets (Matsumoto and Hikosaka, 2007). The authors of the study also showed that the excitation of habenular neurons started earlier than the inhibition of DA neurons in unrewarded trials, and that the activity of DA neurons was inhibited by the electrical stimulation of the LHb, hence suggesting that LHb neurons are critical in conveying reward-related information to DA neurons (Matsumoto and Hikosaka, 2007). Similar findings were found in mice; LHb neurons were inhibited by sucrose reward or sucrose-predicting cues (Wang et al., 2017). However, in some LHb neurons, sucrose produced a post-inhibitory rebound in spike firing that could be explained by the termination of reward stimuli (Wang et al., 2017). Notwithstanding the differential effect of reward on LHb neurons, these findings, together with the view that excitation of LHb neurons to a no reward-predicting target starts earlier than the inhibition of DA neurons (Matsumoto and Hikosaka, 2007), suggest that the LHb sends negative reward-related signals to midbrain DA neurons. As a major input station to the LHb, the globus pallidus internal segment (GPi) of the basal ganglia may influence these negative reward signals insofar as many LHb-projecting GPi neurons show reward-dependent changes in phasic activity earlier than LHb neurons (Hong and Hikosaka, 2008). The reward-related signals that reach the LHb could also originate from the OFC and related cortical areas such as the anterior cingulate cortex, which have been proposed to encode reward value and influence the LHb through a basal ganglia and lateral hypothalamic route (Rolls, 2017).

The view that given brain regions follow a different pattern of activity in response to reward- or no reward-predicting cues provides interesting insights into the existence of opposite processes underlying response to salient appetitive and aversive behaviors. Consistently, studies in rats have shown that LHb neurons are excited (Gao et al., 1996; Wang et al., 2017) whereas VTA and SNc

DA neurons are inhibited (Gao et al., 1996; Ungless et al., 2004; Mileykovskiy and Morales, 2011) in response to various aversive stimuli. Likewise, single unit recordings in monkeys conditioned to a Pavlonian procedure showed that LHb neurons are strongly excited by a stimulus associated with the absence of reward or the presence of a punishment, indicating that the information processed by the LHb may participate in both reward-seeking and punishment-avoidance behaviors (Matsumoto and Hikosaka, 2009). More recently, the inhibitory response of VTA DA neurons was shown to be diminished in habenula-lesioned animals during reward omission but not in response to a punishment such as air puff, suggesting that the habenula plays a critical role in instructing midbrain DA neurons the absence of reward, but that additional structures may be involved in the integration of aversive signals (Tian and Uchida, 2015). A likely candidate structure is the tVTA, which receives strong excitatory inputs from the LHb and in turn sends GABAergic inhibitory projections to midbrain DA neurons (Jhou et al., 2009a; Kaufling et al., 2009). Experiments in monkeys showed that tVTA neurons display a pattern of activity that is similar to that of LHb neurons and opposite to that of midbrain DA neurons in response to reward-related cues (Hong et al., 2011). In addition, tVTA neurons are excited following electrical stimulation of the LHb, and electrical stimulation of the former structure inhibits putative midbrain DA neurons (Hong et al., 2011). Thus, the tVTA is likely to act as a relay structure for the transmission of reward-related information from the LHb to midbrain DA neurons.

LHb neurons have also been implicated in reward prediction error, that is, the difference between the expected reward value and the actual reward value. Evidence in support of this view comes from experiments in monkeys showing that LHb neurons show phasic decreases in their firing activity following the unexpected delivery of a reward (Matsumoto and Hikosaka, 2007), and increases in their firing activity following the omission of an expected reward (Matsumoto and

Hikosaka, 2007) or in response to an unpredicted aversive stimulus (Matsumoto and Hikosaka, 2007, 2009). The finding that the LHb encodes negative reward prediction errors has also been extended in humans. Notably, studies using fMRI in healthy participants have shown that the habenula is activated by negative feedback (Ullsperger and von Cramon, 2003; Shepard et al., 2006; Furman and Gotlib, 2016) and during negative prediction error events (Salas et al., 2010). Reinforcement learning coupled to fMRI investigations in humans also demonstrate positive habenula responses to cues signaling painful electric shocks, and negative habenula responses to monetary reward cues (Lawson et al., 2014). These findings not only point to the representation of negative motivational value and negative-reward prediction error by the habenula, but also suggest that this structure might participate in the avoidance of aversive events. These processes are essential for survival as they enable the acquisition of rewarding outcomes and the selection of appropriate defensive responses in the face of threatening situations.

1.3.4.2 Electrical stimulation studies

Early evidence demonstrating the implication of the habenula in the reinforcing effect of ICSS comes from studies by Boyd and colleagues showing that lesions of the habenulo-interpeduncular tract decreases the response rate for LH (Boyd and Gardner, 1967) and septal (Boyd and Celso, 1970) self-stimulation. Subsequent studies have shown that the rewarding electrical stimulation of the MFB increases Fos-like immunoreactivity in the LHb (Arvanitogiannis et al., 1996b; Arvanitogiannis et al., 1997; Hunt and McGregor, 1998; Arvanitogiannis et al., 2000; Hunt and McGregor, 2002) but paradoxically decreases LHb metabolic activity as measured by [^{14}C]-2-deoxyglucose autoradiography (Gomita and Gallistel, 1982; Gallistel et al., 1985), though discrepancies in the observed results could be attributed to differences in methodological approaches. In rats, sites within the DDC, including the SM, FR and the habenula, have all been shown to

support operant responding for ICSS, indicating that electrical stimulation of these regions is rewarding (Sutherland and Nakajima, 1981; Nakajima, 1984; Blander and Wise, 1989; Vachon and Miliaressis, 1992). These observations, however, contradict reports showing that electrical stimulation of the LHb produces an inhibitory effect on sucrose (Friedman et al., 2011) and cocaine (Friedman et al., 2010) self-administration, and that electrical stimulation of the FR decreases the attribution of incentive motivational salience to a reward predictive cue (Danna et al., 2013). One likely explanation for these discrepancies is the use of different stimulation parameters. While the majority of ICSS studies employ a 0.4-s train of rectangular cathodal pulses of fixed intensity (~0.2-1 mA) and duration (0.1 ms), the studies by Friedman and colleagues (2010, 2011) have employed a combined stimulation pattern alternating between high and low frequencies, whereas the study by Danna and colleagues (2013) has used stimulation parameters (0.25 mA; 3 Hz) that have previously been demonstrated to inhibit the activity of midbrain DA neurons (Christoph et al., 1986).

Another approach to assess the role of the DDC in brain stimulation reward is the use of electrolytic lesions along this pathway in combination with ICSS. In a study by Morisette and Boye (2008), rats were trained to self-administer pulses of electrical stimulation at the LH, VTA, DR, or MR before and after receiving an electrolytic lesion at the habenula (Morissette and Boye, 2008). Lesions of the habenula failed to alter the rewarding effectiveness of MR self-stimulation, but produced long-lasting reductions of the reinforcing effects of LH, VTA and DR self-stimulation, suggesting that the DDC constitutes an important component of the neural circuitry underlying brain stimulation reward (Morissette and Boye, 2008). In this study, however, the attenuation of brain stimulation reward following the lesion was only observed in approximately 25% of rats (Morissette and Boye, 2008). The lack of lesion effect observed in the remaining

subjects is most likely attributable to the anatomical diffuse, collateralized, and heterogeneous nature of the reward substrate that makes it difficult to functionally disconnect the pathway between the lesion and stimulation sites (Arvanitogiannis et al., 1996a; Simmons et al., 1998). The involvement of the DDC in brain stimulation reward is also supported by findings showing that electrolytic lesions at the DDC lead to long-lasting attenuations of the reinforcing effect of LH and DR self-stimulation (Fakhoury et al., 2016a), and produce a marked reduction in Fos-like immunoreactivity in several brain regions implicated in reward processing (Fakhoury et al., 2016b).

In contrast to the conspicuous decreases in brain stimulation reward observed following lesions at the DDC, Gifuni et al. (2012) showed that cell-body specific lesions of the LHb fails to alter the reward-enhancing properties of amphetamine in an ICSS paradigm, but markedly enhance the amphetamine-induced locomotor activity. Although findings from this study may suggest that LHb neurons do not directly contribute to the rewarding effectiveness of ICSS, the authors have not tested this hypothesis directly inasmuch as the lesions were performed at the time of surgery and their effects compared to that of sham-lesioned rats and not with baseline values obtained before amphetamine injection (Gifuni et al., 2012). Notwithstanding the lack of effect on the reward-enhancing properties of amphetamine, these findings suggest the contribution of two different DA-mediated behavioral measures (that is, ICSS and locomotor activity) that are functionally independent and that show different sensitivity to habenular control. Work from the same group also showed that D-amphetamine injection into the NAc enhances the rewarding effectiveness and operant rate of responding of electrical stimulation of the PM, while injection into the LHb fails to produce any observable effects, suggesting that the mesoaccumbens and mesohabenular DA

pathways are differentially implicated in the rewarding effects of ICSS (Duchesne and Boye, 2013).

1.3.4.3 Optogenetic stimulation studies

Although electrical stimulation has been effectively used for the identification of the neuroanatomical substrates of reward, studies employing this approach have been plagued by a lack of anatomical specificity. This stimulation typically activates a population of neurons of unknown functions in addition to the group of neurons that give rise to the rewarding effect. The recently developed technique of optogenetics can circumvent this problem by using light to achieve gain- or loss-of-function within specific neurons or pathways, thus enabling a more precise delineation of the neural substrate of behavior (Bernstein and Boyden, 2011; Yizhar et al., 2011). Since its implementation, optogenetics has also been used for a more precise dissection of the role of specific efferent and afferent pathways of the DDC, particularly the LHb, in different behavioral contexts. Notably, a study investigating the behavioral functions of LHb neurons projecting to the tVTA showed that optogenetic activation of the LHb-to-tVTA pathway promotes conditioned behavioral avoidance and disrupts sucrose-induced positive reinforcement, suggesting that tVTA-projecting LHb neurons convey negative reward-related information (Stamatakis and Stuber, 2012). Consistently, optogenetic activation of glutamatergic excitatory inputs to the LHb originating from the basal ganglia (Shabel et al., 2012) or the anterior LH (Stamatakis et al., 2016) produces aversive effects in place preference tests. More recently, a functional GABAergic projection from the basal forebrain to the LHb was shown to participate in the modulation of aggression-related reward behavior, thus providing a novel mechanism into the underlying mechanisms of maladaptive behaviors (Golden et al., 2016).

Besides innervating the tVTA, LHb neurons send direct glutamatergic excitatory projections to the VTA (Brinschwitz et al., 2010; Goncalves et al., 2012). However, these projections mainly terminate on local GABAergic neurons and do not innervate DA neurons (Brinschwitz et al., 2010). Accordingly, optogenetic activation of LHb efferents to the VTA resulted in sparse induction (<12%) of c-fos protein in VTA DA neurons, and high induction (>80%) in the presumably GABAergic neurons of the tVTA, suggesting that the LHb exerts a net inhibitory effect over VTA DA neurons by primarily activating extrinsic GABAergic neurons (Lammel et al., 2012). In addition, optogenetic activation of LHb terminals into the VTA was shown to produce conditioned place aversion (Lammel et al., 2012), thus concurring with previous electrophysiological evidence showing that LHb neurons encode negative motivational value (Matsumoto and Hikosaka, 2007). While the LHb conveys potent inhibitory inputs to VTA DA neurons, the VTA in turn sends feedback dopaminergic projections to the LHb (Phillipson and Pycock, 1982; Gruber et al., 2007a). The behavioral function of the VTA-to-LHb pathway has recently been examined by Stamatakis and colleagues (2013) which showed that optogenetic activation of VTA DA neurons projecting to the LHb produces a strong conditioned place preference and facilitates operant responding for ICSS (Stamatakis et al., 2013). Activation of the VTA-to-LHb pathway was also associated with a marked attenuation of LHb neuronal firing activity; effect that was blocked following intra-LHb microinjections of a $GABA_A$ receptor antagonist (Stamatakis et al., 2013). Thus, the VTA most likely exerts a feedback inhibitory control over the LHb through a hybrid population of neurons expressing both dopaminergic and GABAergic markers (Stamatakis et al., 2013).

Overall, findings obtained from optogenetic studies are in line with electrophysiological evidence showing that the LHb plays a central role in conveying negative reward-related

information (Matsumoto and Hikosaka, 2007, 2009). However, they appear at odds with electrical stimulation studies showing that electrolytic lesions at the habenula diminish the effectiveness of brain stimulation reward (Morissette and Boye, 2008). The inconsistencies in the results observed between these studies are mainly due to the fact that the use of electrolytic lesions may influence different populations of neurons, such as those within the MHb and LHb, which are known to be functionally distinct (Aizawa et al., 2012). Indeed, optogenetic activation of dorsal MHb neurons produces positive reinforcement (Hsu et al., 2014), whereas optogenetic activation of LHb outputs (Stamatakis and Stuber, 2012) or inputs (Stamatakis et al., 2013) produces aversive effects. Therefore, care must be taken while interpreting findings from conventional ICSS studies using electrical stimulation electrodes.

Subject	Main findings	Study
Electrophysiological studies		
Female adult Sprague-Dawley rats	Excitation of LHb neurons following peripheral nociceptive stimulation	Gao et al., 1996
Two adult rhesus monkeys	Inhibition of LHb neurons by reward-predicting cues or after unexpected delivery of a reward; Excitation of LHb neurons by no-reward-predicting cues and after omission of an expected reward	Matsumoto and Hikosaka. 2007
Two adult rhesus monkeys	Inhibition and excitation of LHb-projecting GPi neurons by reward- and no-reward-predicting cues, respectively	Hong and Hikosaka. 2008
Two adult rhesus monkeys	Excitation of LHb neurons in response to punishments or sensory stimuli predicting punishments; Stronger LHb excitation to partially predicted compared to fully predicted punishments	Matsumoto and Hikosaka 2009
Two adult rhesus monkeys	Inhibition and excitation of LHb and tVTA neurons by reward- and no-reward-predictive cues, respectively	Hong et al., 2011
Adult mice	Impaired inhibitory response in VTA DA neurons of habenula-lesioned mice during reward omission	Tan and Uchida 2015
Slc17a6-ires-Cre mice	Excitation of LHb neurons by aversive stimuli and aversion-predicting cue, and inhibition by sucrose reward and sucrose-predicting cues	Wang et al., 2017

Human fMRI studies		
50 right-handed healthy participants	Activation of the habenula during negative prediction error events	Salas et al., 2010
16 healthy right-handed healthy participants	Activation of the habenula by negative feedback	Ullsperger and von Cramon, 2003
5 medicated schizophrenics and 5 healthy participants	Activation of the habenula by negative feedback in healthy, but not schizophrenic, participants	Shepard et al. 2006
27 healthy participants	Activation and inhibition of the habenula to cues signaling painful electric shocks and monetary reward, respectively	Lawson et al., 2014
15 current MDD and 13 healthy participants	Activation of the habenula during the prediction or experience of negative outcomes in healthy, but not MDD, participants	Furman and Gotlib, 2016
Electrical stimulation studies		
Male Wistar rats	Decreased rate of LH self-stimulation following lesion at the habenulo-interpeduncular tract	Boyd and Gardner, 1967
Male Wistar rats	Decreased rate of septal self-stimulation following lesion at the habenulo-interpeduncular tract	Boyd and Celso, 1970
Male Long-Evans rats	Steady operant response following electrical stimulation of the MHb, LHb or FR	Sutherland and Nakajima, 1981
Rats	Decreased metabolic activity in the LHb following rewarding stimulation of the MFB	Gomita and Gallistel, 1982; Gallistel et al., 1985
Adult rats	Steady operant response following electrical stimulation of the LHb; effect that is supressed by the 5-HT receptor blocking agent, metergoline	Nakajima, 1984
Male Long-Evans rats	Steady operant response following electrical stimulation of the SM	Blander and Wise 1989
Male and female Sprague-Dawley rats	Steady operant response following electrical stimulation of the SM, FR or habenula	Vachon and Miliaressis, 1992
Rats	Increased Fos-like immunoreactivity in the LHb following rewarding electrical stimulation of the MFB	Arvanitogiannis et al., 1996b, 1997, 2000; Hunt and McGregor, 1998, 2002
Male Long Evans rats	Attenuation of brain stimulation reward in ~25% following electrolytic lesions at the habenula	Morissette and Boye 2008

Male Sprague-Dawley rats	Reduced and increased cocaine self-administration following DBS and electrolytic lesion of the LHb, respectively	Friedman et al., 2010
Male Sprague-Dawley rats	Reduced and increased positive reward-sucrose self-administration following DBS and lesion of the LHb, respectively	Friedman et al., 2011
Male Sprague-Dawley rats	Enhancement of the locomotor-stimulant effect of amphetamine following neurotoxic lesions of the LHb; No effect on the reward-enhancing properties of amphetamine	Gifuni et al., 2012
Male Sprague-Dawley rats	Decreased and increased incentive salience to reward predictive cues following stimulation and electrolytic lesion of the FR, respectively	Danna et al., 2013
Male Sprague-Dawley rats	Enhanced rewarding effectiveness and operant rate of responding for ICSS following injection of D-amphetamine (4-80 μg/μl) into the NAc, but not the LHb	Duchesne and Boye, 2013
Optogenetic stimulation studies		
Male C57BL/6J mice	Facilitation of active, passive, and conditioned behavioral avoidance following optogenetic activation of LHb projections to the tVTA	Stamatakis and Stuber 2012
Male Sprague-Dawley rats	Development of place aversion following optogenetic activation of LHb inputs from the EP	Shabel et al., 2012
Male adult C57Bl6 mice	Development of conditioned place aversion following optogenetic activation of LHb terminals into the VTA	Lammel et al., 2012
Male TH-IRES-Cre mice	Development of conditioned place preference and positive reinforcement following optogenetic activation of LHb inputs from the VTA	Stamatakis et al. 2013
Adult mice	Positive reinforcement and place aversion following optogenetic activation of dorsal MHb neurons or inhibition of their output, respectively	Hsu et al., 2014
VGLUT2-ires-cre mice	Development of place aversion and preference following optogenetic activation and inhibition of LHb inputs from the anterior LH, respectively	Stamatakis et al., 2016
Male CD-1 and C57BL/6J mice	Decreased LHb neuronal firing and development of conditioned place preference following optogenetic activation of GABAergic BF–LHb terminals of non-aggressors; The opposite effect is observed following optogenetic silencing of GABAergic BF–LHb terminals of aggressors	Golden et al., 2016

Table 1: The DDC in reward processing. This table illustrates the major findings from electrophysiological, neuroimaging, electrical stimulation and optogenetic stimulation studies investigating the role of the DDC in reward-related processes. Abbreviations: BF, basal forebrain;

BLA, basolateral amygdala; BNST, bed nucleus of the stria terminalis; DR, dorsal raphe; EP, entopeduncular nucleus; GPi, globus pallidus internal segment; IPN, interpeduncular nucleus; NAc, nucleus accumbens; PN, pontine nuclei.

1.4 The tail of the ventral tegmental area in behavioral processes and in the effect of psychostimulants and drugs of abuse (Adapted from the review paper Fakhoury, 2018. *Progress in Neuropsychopharmacology & Biological Psychiatry,* 84:30-38)

1.4.1 Context and overview

The tail of the ventral tegmental area (tVTA) has been recently described as a cluster of gamma-aminobutyric acid (GABA)ergic neurons that exerts a major inhibitory drive onto midbrain DA neurons (Jhou et al., 2009a; Kaufling et al., 2009). Anatomically, the tVTA lies within the posterior end of the VTA, where it is restricted dorsolateral to the caudal part of the IPN (Jhou et al., 2009a; Barrot and Thome, 2011). As it extends caudally, the tVTA shifts dorsally and slightly laterally to become embedded within the decussation of the superior cerebellar peduncle, near the rostral edge of the pedunculopontine tegmental nucleus (PPTg) and lateral to the MR nucleus (Kaufling et al., 2009; Bourdy and Barrot, 2012).

First identified in the rat (Perrotti et al., 2005; Kaufling et al., 2009), the tVTA has been described in many species, including mice and monkeys, as a region that receives strong excitatory glutamatergic inputs from the LHb (Jhou et al., 2009a; Kaufling et al., 2009), that encodes negative reward signals (Jhou et al., 2009b; Hong et al., 2011; Stamatakis and Stuber, 2012), and that sends inhibitory GABAergic projections to DA neurons of the VTA and SNc (Jhou et al., 2009a; Kaufling et al., 2010a). Given the wide array of cells projecting from the LHb to the tVTA and from the tVTA to the VTA/SNc complex (Jhou et al., 2009a; Kaufling et al., 2010a), the tVTA has been proposed to act as a relay through which glutamatergic inputs from the LHb inhibit midbrain

DA neuron activity (Balcita-Pedicino et al., 2011). The functional significance of this disynaptic inhibitory circuit is revealed by electrophysiological experiments in monkeys showing that the firing pattern of tVTA neurons is similar to that of LHb neurons, but inversely correlated to that of midbrain DA neurons (Matsumoto and Hikosaka, 2007; Hong et al., 2011).

The pervasive inhibitory influence of tVTA neurons over midbrain DA neurons is also supported by electrophysiological studies in rats showing that opioid-mediated inhibition (Jalabert et al., 2011) and neurotoxic lesions (Brown et al., 2017) of the tVTA increase the firing rate of VTA DA neurons and attenuate the LHb-induced inhibition of midbrain DA cells, respectively, whereas electrical stimulation of the tVTA supresses the activity of midbrain DA neurons (Lecca et al., 2011; Lecca et al., 2012; Bourdy et al., 2014). Consistent with these findings, ex vivo optogenetic stimulation of the tVTA evokes $GABA_A$-mediated IPSCs in DA neurons of the VTA; effect that is inhibited following application of a MOR agonist (Matsui and Williams, 2011). These findings suggest that the tVTA receives excitatory inputs from the LHb, and in turn exerts a tonic inhibitory influence on midbrain DA cells.

LHb and midbrain DA neurons have a crucial role in processing aversive and rewarding outcomes, respectively (Matsumoto and Hikosaka, 2007), and have largely been studied in the context of goal-directed behaviors. Neurotoxic lesions of the LHb increase positive reward-sucrose or cocaine self-administration, whereas the opposite effect is observed following electrical stimulation of the LHb (Friedman et al., 2010; Friedman et al., 2011). On the other hand, pharmacological blockade of DA receptors attenuates the rewarding effectiveness of ICSS (Benaliouad et al., 2007) and inhibits cocaine-seeking behavior (Peng et al., 2009) in rats. As an intermediate structure connecting the LHb to midbrain DA neurons, the tVTA is thus likely to act as a regulatory interface between rewarding and aversive processes, and may be part of the

complex neural circuitry underlying goal-directed behaviors. These processes have important implications for psychiatric diseases, such as substance use disorder, which is characterized by escalating dysregulations of brain reward and aversion mechanisms (Koob and Le Moal, 2008; Volkow and Morales, 2015). In an attempt to shed some light on the current state of knowledge of the tVTA, the following sections highlight the anatomical and functional importance of this structure as a major regulator of reward-related processes and a primary target of psychostimulants and certain drugs of abuse.

1.4.2 Cellular, synaptic and electrophysiological profile of the tVTA

Morphological analysis of the tVTA reveals that this structure is a heterogeneous population of cells comprised of small and medium-sized neurons (Jhou et al., 2009a). The vast majority of these neurons (~70-92%) are GABAergic (Jhou et al., 2009a; Kaufling et al., 2009) and elicit Fos expression in response to aversive stimuli (Jhou et al., 2009b) and psychostimulants (Perrotti et al., 2005; Kaufling et al., 2009; Kaufling et al., 2010b). This dense cluster of Fos-immunoreactive nuclei in the tVTA also shows strong immunoreactivity for MORs that appear to be more prominent in the medial part of the tVTA (Jhou et al., 2009a). Dense immunoreactivity for somatostatin (Jhou et al., 2009a) and in situ hybridization for prepronociceptin (Jhou et al., 2012)—a gene that encodes the opioid-like peptide nociception—have also been reported in the tVTA.

Electron micrographic analysis indicates that almost all of tVTA axons contacting the VTA are unmyelinated, and that these are mostly comprised of small-diameter intervaricose segments or vesicle-containing boutons that do not contact surrounding dendrites (Balcita-Pedicino et al., 2011). The remaining tVTA unmyelinated axons are varicosities in direct contact with surrounding

dendrites forming either synaptic connections or membrane appositions (Balcita-Pedicino et al., 2011). Further analysis of the tVTA also revealed insightful details regarding its intrinsic electrophysiological property. In vivo, the mean firing rate of tVTA neurons is between 11 and 18 Hz, the interspike interval is around 73 ms, and the mean duration of their action potential measured from peak to trough is roughly 1 ms (Jhou et al., 2009b; Jalabert et al., 2011; Lecca et al., 2011). In addition, neurons in the "core" region of the tVTA have different electrophysiological properties compared to neurons in the "periphery" region of the tVTA; while the former fires at an average rate of 20 Hz, the mean firing rate of the latter is significantly lower (11 Hz), thus pointing to functional differences among tVTA neurons (Jhou et al., 2009b). In-vitro, tVTA neurons fire at a relatively lower rate (~5 Hz) than that recorded in vivo, and the EPSC evoked in this region are mediated by AMPA receptors (Lecca et al., 2011).

Taken together, the aforementioned studies have proved extremely fruitful in determining the anatomical and neurophysiological signature of the tVTA. However, despite developing at a rapid pace, research on the tVTA is still in its infancy and many questions remain unanswered. For instance, no information regarding the function of non-GABAergic neurons in the tVTA is currently available in the literature. Detailed anatomical and electrophysiological analysis of tVTA neurons along the rostrocaudal axis is also warranted as this could give new insights on the functional properties of the tVTA.

1.4.3 Afferents and efferents of the tVTA

The discovery that the tVTA consists of a GABAergic population of neurons that conspicuously express Fos in response to various stimuli and psychostimulants led to a wide array of studies aimed at characterizing the input and output circuitry of this region. Although the tVTA has been

studied in several species including the mouse and monkey (Hong et al., 2011; Wasserman et al., 2013), a proper anatomical description of its boundaries and connectivity has been done in rats only (Jhou et al., 2009a; Kaufling et al., 2009). Studies employing retrograde and anterograde tracing show that tVTA afferents are widely dispersed **(Figure 9A)**, with one of the strongest inputs originating from the LHb (Jhou et al., 2009a; Kaufling et al., 2009). LHb projections to the tVTA are mainly ipsilateral, with moderate labeling in the contralateral hemisphere, and are organized in a topographic manner, with inputs from the medial and lateral tVTA primarily originating from the medial and lateral LHb, respectively (Jhou et al., 2009a). Electron microscopic examination of rat brain sections also reveal that 35% of LHb axons projecting to the tVTA are myelinated, while the remaining 65% are unmyelinated axons that appear either as small-diameter fibers or larger diameter varicosities that make no direct contacts onto dendrites (Balcita-Pedicino et al., 2011). These descending pathways originating from the LHb likely exert an excitatory glutamatergic influence on tVTA neurons inasmuch as most LHb neurons contain the VGLUT2 and other markers reminiscent of glutamate signaling (Herzog et al., 2004; Geisler et al., 2007; Brinschwitz et al., 2010; Root et al., 2014). Afferents of the tVTA have also been shown to originate from the VTA/SNc complex, suggesting the existence of feedback projections that reciprocate the strong tVTA projections to these regions (Jhou et al., 2009a). Retrograde and anterograde tracing of tVTA afferents reveal strong labeling in other brain areas, including the prelimbic and infralimbic cortex, lateral preoptic area, LH, SC, zona incerta, PAG, IPN, laterodorsal tegmental nucleus, and DR, and low to moderate labeling in the cingulate cortex, dorsal peduncular cortex, NAc, ventral pallidum, BNST, paraventricular hypothalamic nucleus, red nucleus, MR, PPTg, locus coeruleus, dorsomedial tegmental area, and pontine reticular nucleus **(Figure 9A)** (Jhou et al., 2009a; Kaufling et al., 2009; Yetnikoff et al., 2015). Direct projections

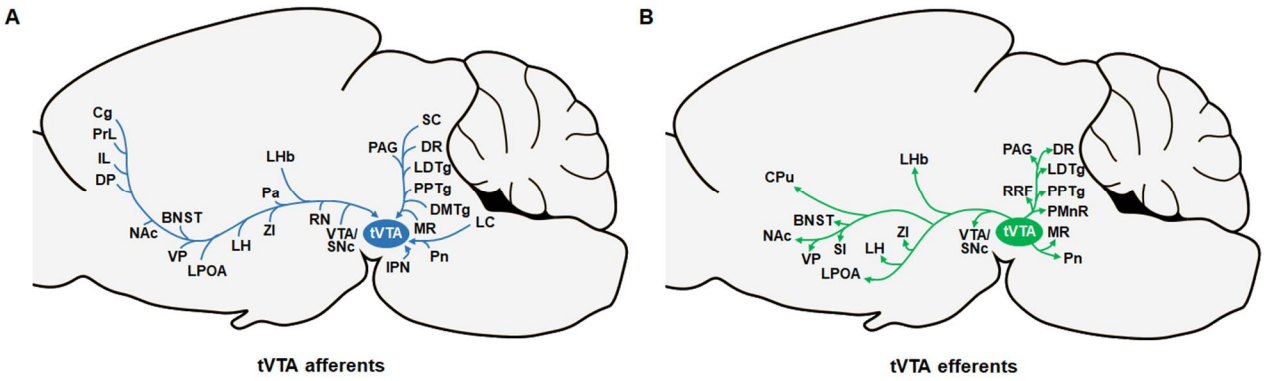

Figure 9: Main afferents and efferents of the tVTA. This schematic illustrates some of the major tVTA inputs and outputs. **(A)** tVTA afferents are widely dispersed and originate from a broad range of structures within the forebrain, diencephalon, midbrain and brainstem. **(B)** tVTA efferents preferentially target dopaminergic neurons of the VTA/SNc complex and neurons of the LH. Abbreviations: bed nucleus of the stria terminalis (BNST); cingulate cortex (Cg); caudate putamen (CPu); dorsomedial tegmental area (DMTg); dorsal peduncular cortex (DPC); dorsal raphe (DR); infralimbic cortex (IL); interpeduncular nucleus (IPN); locus coeruleus (LC); lateral hypothalamus (LH); lateral habenula (LHb); lateral preoptic area (LPO); laterodorsal tegmental nucleus (LDTg); median raphe (MR); nucleus accumbens (NAc); parafascicular thalamic nucleus (Pa); periaqueductal gray (PAG); paramedian raphe nucleus (PMnR); pontine reticular nucleus (Pn); pedunculopontine tegmental nucleus (PPTg); Prelimbic cortex (PrL); red nucleus (RN); retrorubral field (RRF); superior colliculus (SC); substantia innominate (SI); substantia nigra pars compacta (SNc); ventral pallidum (VP); ventral tegmental area (VTA); zona incerta (ZI).

from the hippocampus to the tVTA were not detected by retrograde and anterograde tracings, however, the former may possess indirect connectivity with the latter inasmuch as several structures that are recipient of hippocampus outputs also project to the tVTA; these include the lateral septum, the NAc, the paraventricular thalamic nucleus, the BNST, and the perifornical hypothalamus (Jhou et al., 2009a; Kaufling et al., 2009).

While tVTA afferents are widely dispersed, tVTA efferents are more restricted and primarily target DA neurons of the midbrain **(Figure 9B)**. The majority of these tVTA outputs innervate DA

cell bodies of the VTA/SNc complex, and to a lesser extent the RRF (Jhou et al., 2009a; Kaufling et al., 2010a; Bourdy and Barrot, 2012). Electron microscopic examination of rat brain following injection of an anterograde tracer in the tVTA revealed that more than 80% of tVTA axon terminals form symmetric synapses with tyrosine hydroxylase immunoreactive dendrites in the VTA/SNc complex (Balcita-Pedicino et al., 2011). A topographical organization of tVTA outputs to VTA DA neurons has also been proposed, with lateral parts of the tVTA targeting laterally located neurons of the VTA, and medial parts of the tVTA targeting centrally located neurons of the VTA (Jhou et al., 2009b; Jhou et al., 2009a). In addition, evidence shows that tVTA neurons along the rostrocaudal axis show a different pattern of projections to VTA DA neurons; while the rostral tVTA exhibits a densely packed cluster of GABAergic neurons projecting to VTA DA neurons, this density progressively declines at more caudal levels of the tVTA (Jhou et al., 2009a). Besides midbrain DA-containing cell bodies, other output targets of the tVTA have been reported, including the ventral pallidum, caudate putamen, NAc, BNST, SI, lateral preoptic area, LH, LHb, zona incerta, PAG, paramedian raphe nucleus, MR, laterodorsal tegmental nucleus and pontine reticular nucleus **(Figure 9B)** (Kaufling et al., 2010a). The DR and PPTg, which contain serotonergic and cholinergic neurons respectively, have also been reported as output targets of the tVTA (Lavezzi et al., 2012). Many tVTA neurons that project to the DR or PPTg express Fos upon psychostimulant administration (Lavezzi et al., 2012), and projections to the former are focally directed to a distinctive subdivision poor in serotonin and enriched in glutamatergic neurons (Sego et al., 2014). Double-injection tracer experiments with the VTA, DR and PPTg also indicate that a significant proportion of tVTA neurons may project to more than one of these structures, suggesting that the tVTA likely act as an integrative modulator of multiple neurotransmitter systems (Lavezzi et al., 2012). Last but not least, anterograde tracing studies reveal that tVTA

neurons heavily project to the LH (Kaufling et al., 2010a), leading to speculation that they may be involved in the coordination of physiological processes already associated with this structure, including feeding, reward and energy homeostasis (Seoane-Collazo et al., 2015; Stuber and Wise, 2016).

Altogether, findings from retrograde and anterograde tracing studies suggest that the tVTA may act as a converging hub, processing external information from a wide range of structures, and channeling the output toward midbrain DA neurons. Because of its reciprocal connections with the VTA/SNc complex, the characterization of the tVTA, including its boundaries, connectivity and anatomical properties, has fostered a tremendous growth of scholarly research for better understanding the neural mechanisms underlying reward and aversion.

1.4.4 The tVTA: a source of negative reward signals

In light of previous anatomical evidence showing the existence of dense excitatory glutamatergic projections from the LHb to the tVTA (Brinschwitz et al., 2010), it is not surprising that the tVTA has been implicated in many behavioral functions already reported for the LHb, including negative reward processing and reward-prediction error (i.e., the difference between the expected reward value and the actual reward value) (Matsumoto and Hikosaka, 2007). Convergent evidence indicates that the tVTA exhibits patterns of activity to rewarding and aversive stimuli that are similar to those reported for the LHb and inverse to those of putative midbrain DA neurons (Matsumoto and Hikosaka, 2007; Jhou et al., 2009b; Hong et al., 2011). In rats, most tVTA neurons show phasic activation and/or Fos induction in response to aversive or aversion-predicting stimuli such as food deprivation, shock-predictive cues and footshocks, and inhibition following rewards or reward-predictive stimuli such as sucrose delivery and sucrose-predictive cues (Jhou et al., 2009b; Brown and Shepard, 2013; Sanchez-Catalan et al., 2017). The mechanisms underlying the

activation of tVTA neurons by aversive stimuli largely depend on axons of the FR, the principal output pathway of the habenula, inasmuch as a lesion at this pathway impairs the ability of mild foot shocks to induce Fos expression in the tVTA (Brown and Shepard, 2013). Exposure to an aversive foot-shock also increases the LHb excitatory glutamatergic transmission to the tVTA in mice (Stamatakis and Stuber, 2012), and activation of the AMPA-mediated glutamatergic transmission into the tVTA produces robust conditioned place aversion in rats (Jhou et al., 2013). However, it is important to note that some aversive stimuli, such as lithium chloride, naloxone at high dose, lipopolysaccharide, inflammatory or neuropathic pain, and restraint stress, fail to induce Fos in the tVTA, indicating some degree of complexity in the mechanisms underlying the expression of immediate early genes following exposure to aversive events (Sanchez-Catalan et al., 2017).

Consistent with findings obtained in rodents, experiments in monkeys show that the tVTA mainly consists of what is called “reward-negative” neurons that behave in a similar and opposite way to LHb and midbrain DA neurons respectively; they are inhibited by reward predictive cues and excited by cues predicting the absence of reward (Hong et al., 2011). Although these findings support the view that tVTA neurons primarily encode negative reward signals, it is important to mention that some of these neurons do not show the same pattern of activity in response to rewarding and aversive stimuli. Notably, heterogeneity in neuronal response has been observed when comparing neurons in the core versus periphery region of the tVTA. For instance, Jhou et al. (2009b) showed that acute footshock induces a 5-fold increase in the proportion of Fos-positive neurons in the tVTA core, whereas only a 2-fold increase is observed in the tVTA periphery. Similarly, experiments in monkeys showed that only 67% of tVTA neurons are inhibited and excited following cues that predict reward and reward omission, respectively, and that this

proportion increases to 94% in the core region of the tVTA (Hong et al., 2011). However, whether similar heterogeneity could be observed along the rostrocaudal axis of the tVTA still needs to be addressed.

Similar to LHb neurons, tVTA neurons encode reward prediction error information. Jhou et al. (2009b) showed that some neurons of the tVTA are excited after the omission of an expected reward, and that the majority of these neurons are located in the core region of the tVTA. Consistent with this view, experiments in monkeys suggest that the tVTA is comprised of two populations of neurons that exhibit different reward-related properties; the reward-negative neurons (roughly 2/3) and the reward-positive neurons (roughly 1/3) (Hong et al., 2011). These neurons encode reward-prediction errors, exhibiting either increased (reward-negative neurons) or decreased (reward-positive neurons) activity in the absence of reward when reward was expected (Hong et al., 2011). For the negative-neurons of the tVTA, this pattern of response is similar to that of LHb neurons and opposite to that of midbrain DA neurons (Matsumoto and Hikosaka, 2007; Bromberg-Martin and Hikosaka, 2011), indicating that the tVTA primarily translates the negative reward-prediction error from the LHb into a DA positive reward-prediction error. It is also noteworthy to mention that in the study by Hong et al. (2011), some tVTA neurons responded to reward cues earlier than LHb neurons, suggesting that the tVTA may receive reward-related information that could derive from areas other than the LHb. The ventral pallidum is a potential candidate for mediating this rapid appearance of reward-related signals in the tVTA insofar as prior studies showed that neurons in the ventral pallidum highly project to the tVTA (Jhou et al., 2009a; Kaufling et al., 2009) and respond to reward cues earlier than many LHb neurons (Tachibana and Hikosaka, 2012).

1.4.5 The tVTA: from aversion expectation value to avoidance behavior

Learning to appropriately predict a rewarding or aversive outcome is an important process for survival and adaptive behaviors (Schultz et al., 1997; McNally and Westbrook, 2006). The aversive expectation value encoded by the tVTA is thus likely to contribute to the development of adaptive defensive behaviors related to fear and anxiety. Such behaviors could include active coping strategies when escape from the threat is possible, and passive coping strategies, such as freezing, which are usually characterized by behavioral inhibition (Steimer, 2002). In rats, cell-body specific lesions of the tVTA reduce passive behaviors related to fear including auditory conditioned freezing and unconditioned freezing to a predator odor, while increasing active defensive behaviors such as treading and burying, suggesting a role for tVTA neurons in encoding and recalling aversive consequences (Jhou et al., 2009b). Consistent with this view, lesions of the tVTA were shown to impair the ability of rats to properly shift decision making away from aversive outcomes during a cost-benefit decision task (Vento et al., 2017). In addition, excitotoxic lesions or optogenetic inactivation of the tVTA at a period when cocaine exhibits aversive effects (~15 min post-injection) abolish cocaine-induced avoidance behaviors in a runway operant paradigm (Jhou et al., 2013), whereas optogenetic activation of LHb inputs to the tVTA promotes behavioral avoidance and disrupts positive reinforcement in mice (Stamatakis and Stuber, 2012). These findings, together with evidence that tVTA neurons exhibit increased Fos immunoreactivity following conditioned and unconditioned aversive stimuli (Jhou et al., 2009b; Sanchez-Catalan et al., 2017), lead to speculation that the tVTA is involved in representing negative reward signals and promoting behavioral inhibitory responses.

The loss of behavioral inhibition observed following lesions of the tVTA is consistent with prior findings showing that lesions of the LHb or its efferent pathway increase locomotor activity

(Murphy et al., 1996; Gifuni et al., 2012). However, lesions of the LHb (Heneka et al., 2013) or its efferent pathway (Murphy et al., 1996) fail to replicate the marked decreases in freezing behavior produced by lesions of the tVTA (Jhou et al., 2009b); the effect of the latter is rather more closely related to that produced by lesions of the periaqueductal gray (Kim et al., 1993; Amorapanth et al., 1999), a major afferent to the tVTA. Aside from the LHb and PAG, other tVTA-projecting structures were shown to influence fear-related behaviors, including the BNST (Schulz and Canbeyli, 2000), the mPFC (Giustino and Maren, 2015), the DR (Maier et al., 1993; Berg et al., 2014) and the MR (Wang et al., 2015; Balazsfi et al., 2017). However, whether these afferent projections are integrated simultaneously by the tVTA to influence fear-avoidance behaviors remains to be determined.

Last but not least, a series of studies have shown that lesions of the tVTA produce hyperactivity in a novel environment (Vento et al., 2017) and increase motor performance on a rotarod (Bourdy et al., 2014) or open field (Brown et al., 2017) test. Moreover, lesions of the tVTA were shown to increase time spent in open arms on an elevated plus maze, suggesting a potential involvement of the tVTA in anxiety-like behavior (Jhou et al., 2009b). In addition, owing to its reciprocal anatomical connections with raphe nuclei (Kaufling et al., 2009, 2010a; Lavezzi et al., 2012), where brain 5-HT cell bodies are mainly localized (Charnay and Leger, 2010), the tVTA is likely to play a crucial role in the pathogenesis of depression and other disorders where dysfunctions in the 5-HT system are observed. Thus far, no studies have been conducted to investigate the role of the tVTA in depression, however, manipulation of structures that heavily project to the tVTA, such as the LHb or the PAG, yields antidepressant-like effects in rodents (Berton et al., 2007; Winter et al., 2011; Yang et al., 2018), and DBS of the LHb induces beneficial responses in treatment-resistant depressed patients (Sartorius et al., 2010; Kiening and Sartorius, 2013). Therefore, in light

of these findings, as well as those mentioned above, the tVTA appears as a hub between motor and emotional systems, and as a major regulator of behaviors underlying aversion and fear-like responses. These processes are essential for survival as they enable the acquisition of rewarding outcomes and the selection of appropriate defense responses. They may also help delineate the mechanisms underlying certain psychiatric conditions such as substance use disorder and other addictive behaviors, which are characterized by a failure of aversive outcomes to inhibit behavior despite ongoing detrimental effects.

1.4.6 The tVTA in responses to psychostimulants and drugs of abuse

Drug abuse can be envisaged as a cycle of escalating dysregulation of brain reward and aversion mechanisms resulting in the compulsive use of drugs and a loss of control over drug-taking behaviors (Koob and Le Moal, 2008; Volkow and Morales, 2015). In view of its relationship with brain areas encoding reward and aversion, it seems reasonable to speculate that the tVTA has a role in the complex circuitry mediating the effects of drugs of abuse. Findings from molecular, electrophysiological and behavioral studies highlighting the role of the tVTA in the effect of drugs of abuse and other drugs are illustrated in **Table 2**.

tVTA neurons were first described in the context of their ability to induce Fos expression in response to psychostimulants. Acute (Kaufling et al., 2009; Kaufling et al., 2010b) or chronic (Perrotti et al., 2005; Kaufling et al., 2010a; Zahm et al., 2010) administration of cocaine in a noncontingent manner as well as single (Zahm et al., 2010) or repeated (Geisler et al., 2008; Jhou et al., 2009a; Zahm et al., 2010) administration of cocaine during a self-administration setting induce FosB/ΔFosB or c-Fos expression in the tVTA. Expression of Fos-related genes in the tVTA is also observed following exposure to other psychostimulants, including amphetamine (Perrotti

et al., 2005; Colussi-Mas et al., 2007; Kaufling et al., 2010b; Rotllant et al., 2010; Matsui and Williams, 2011), methamphetamine (Jhou et al., 2009a; Lecca et al., 2011; Cornish et al., 2012; Lavezzi et al., 2012), 3,4-methylenedioxymethamphetamine hydrochloride (MDMA) (Kaufling et al., 2010b) and caffeine (Kaufling et al., 2010b). It is worth mentioning that the expression of Fos and other immediate-early genes in the tVTA following exposure to psychostimulants does not necessarily indicate an activation of the corresponding structure, but is rather indicative of changes in intracellular signaling or neuronal activity (Zahm et al., 2010). The psychostimulant-induced expression of Fos and other related immediate-early genes in the tVTA is likely mediated by the DA system since acute (Kaufling et al., 2010b) or chronic (Perrotti et al., 2005) administration of the DA reuptake inhibitor, GBR-12909, increases Fos-like immunoreactivity in the tVTA, while no such effect is observed with drugs acting on norepinephrine or 5-HT neurotransmission (Perrotti et al., 2005; Kaufling et al., 2010b). However, it is worthwhile to mention that the induction of Fos-related proteins in the tVTA is not limited to psychostimulants with addictive properties. For instance, acute systemic injection of modafinil, a psychostimulant with low addictive properties used for the treatment of narcolepsy, induces Fos-like immunoreactivity in the tVTA (Scammell et al., 2000). On the other hand, acute administration of morphine, ethanol, diazepam, γ-hydroxybutyric acid sodium salt (GHB), ketamine, PCP or Δ9-tetrahydrocannabinol solution (THC) fails to induce Fos-like immunoreactivity in the tVTA, despite their abuse potential (Perrotti et al., 2005; Kaufling et al., 2010b). It thus appears that the capacity of tVTA neurons to express Fos and other related genes in response to psychostimulants is related to their stimulant and arousing properties. Experiments with c-fos immunohistochemistry also show that cocaine induces the activation of the LHb with a delay of approximately 15 min, and that this activation predominantly targets LHb neurons that project to and activate neurons in the tVTA (Jhou et al.,

2013). In addition, acute morphine withdrawal strongly induces Fos in the tVTA (Sanchez-Catalan et al., 2017), while acute (Kaufling et al., 2010b) or chronic (Perrotti et al., 2005) administration of morphine does not, suggesting that Fos-like immunoreactivity in the tVTA following exposure to psychostimulants might not be induced by the drug directly, but rather by its offset.

Studies have also investigated the effect of drugs of abuse on the electrophysiological activity of the tVTA GABAergic neurons, which is more indicative of their functional activation or inhibition. In anesthetized rats, acute administration of cocaine (Lecca et al., 2011) and morphine (Jalabert et al., 2011; Lecca et al., 2011) decreases the firing rate of tVTA neurons, whereas in vitro, bath application of morphine (Lecca et al., 2011) or MOR agonists (Matsui and Williams, 2011) reduces the EPSC and spontaneous activity of tVTA neurons, respectively. The electrophysiological activity of the tVTA is also influenced by the endocannabinoid system inasmuch as administration of the type 1-cannabinoid receptor agonist, WIN55212-2, decreases the discharge frequency of tVTA neurons in anesthetized rats and the EPSC in vitro (Lecca et al., 2011). Conversely, nicotine nearly doubles the firing rate of tVTA neurons in vivo and results in marked increases in EPSC amplitude in vitro (Lecca et al., 2011). The nicotine-induced potentiation of tVTA neurons is likely the result of enhanced glutamate release induced by α7-containing nAChRs, since bath application of methyllycaconitine, a α7-containing nAChR antagonist, blocks the in vitro effect of nicotine (Lecca et al., 2011). The view that GABAergic neurons of the tVTA project to midbrain DA neurons and show changes in their electrophysiological activity after exposure to drugs of abuse strongly implicates the tVTA in drug-induced alterations in DA neurotransmission. In vivo experiments done in anesthetized rats show that tVTA inactivation by muscimol suppresses the excitatory effect of morphine on VTA DA neurons (Jalabert et al., 2011), and that acute administration of morphine or WIN55212-2, but not cocaine or nicotine, blocks the tVTA-evoked

suppression of VTA DA neuron firing (Lecca et al., 2012). In vitro, bath application of the MOR agonist, DAMGO, inhibits $GABA_A$ IPSCs in midbrain DA neurons evoked by electrical or optogenetic stimulation of the tVTA; effect that is not observed with kappa receptor and DOR agonists (Matsui and Williams, 2011). In agreement with these findings, behavioral studies show that intra-tVTA administration of morphine (Wasserman et al., 2013; Wasserman et al., 2016; Steidl et al., 2017) or the MOR agonist, DAMGO (Kotecki et al., 2015), enhances locomotor activity in rodents; an effect that typically correlates with increases in mesolimbic DA neurotransmission (Pijnenburg et al., 1976; Ikemoto, 2002). Moreover, intra-tVTA infusion of EM-1, a selective MOR agonist, produces positive reinforcement in an intracranial self-administration setting, and elicits conditioned place preference (Jhou et al., 2012), whereas intra-tVTA infusion of morphine extends the satiating effects of heroin intake (Steidl et al., 2015).

Through a disinhibition process, the tVTA may thus be an important target for certain drugs of abuse, including opioids and cannabinoids, to influence the activity of midbrain DA neurons. The original disinhibition model of opioid action on midbrain DA neurons posits that opioids, such as morphine and heroin, exert their reinforcing effects by acting on MORs located on GABA-containing interneurons of the VTA, thereby reducing the spontaneous GABA-mediated synaptic input to DA cells (Johnson and North, 1992). In light of the aforementioned findings and given the enriched expression of MORs in tVTA neurons (Jhou et al., 2009a), Bourdy and Barrot (2012) proposed a new model in which opioids act on tVTA cell bodies or terminals to suppress the inhibitory tone exerted by the tVTA on VTA DA neuron activity. The capacity of the tVTA to disinhibit DA cells is impaired after opioid withdrawal inasmuch as tVTA inactivation by local microinjection of a $GABA_A$ agonist increases VTA DA neuron activity in opiate-naive, but not in withdrawn, rats (Kaufling and Aston-Jones, 2015).

Subject	Treatment design	Main findings	Study
Cocaine			
Male Sprague–Dawley rats	Injection of cocaine hydrochloride (15 mg/kg; i.p.) twice-daily for 14 days; Cocaine self-administration (0.5 mg/kg/0.1ml infusion) daily for 14 days	Increased FosB immunoreactivity in the tVTA	Perrotti et al., 2005
Male Sprague–Dawley rats	Cocaine self-administration (500 µg/kg per 30 µl infusion; i.v.) for six consecutive days	Increased Fos immunoreactivity in VTA-projecting tVTA neurons	Geisler et al., 2008; Jhou et al., 2009a
Male Sprague-Dawley rats	Acute injection of cocaine hydrochloride (20 mg/kg; i.p.)	Increased FosB immunoreactivity in the tVTA	Kaufling et al., 2009
Male Sprague Dawley rats	Acute injection of cocaine hydrochloride (2.5-40 mg/kg; i.p.)	Dose-dependent increases in FosB/ΔFosB immunoreactivity in the tVTA	Kaufling et al., 2010b
Male Sprague–Dawley rats	Single or repeated (6 days) cocaine self-administration (500 µg/kg per 30 µl infusion; i.v.); Passive infusions of cocaine for 6 days	Increased Fos immunoreactivity in the tVTA	Zahm et al., 2010
Male Sprague–Dawley rats	Injection of cocaine hydrochloride (20 mg/kg; i.p.) twice daily for 7 days	Increased ΔFosB immunoreactivity	Kaufling et al., 2010a
Male Sprague–Dawley albino rats	Acute injection of cocaine (1 mg/kg; iv)	Decreased firing rate of tVTA neurons in vivo	Lecca et al., 2011
Male Sprague–Dawley albino rats	Acute injection of cocaine (1 mg/kg; iv)	No effect on tVTA-evoked suppression of VTA DA neuron firing	Lecca et al, 2012
Amphetamine			
Male Sprague–Dawley rats	Injection of d-amphetamine (4 mg/kg; i.p.) once daily for 4 days	Increased FosB immunoreactivity in the tVTA	Perrotti et al., 2005
Male Sprague–Dawley rats	Acute injection of d-amphetamine (5 mg/kg; s.c.)	Increased Fos immunoreactivity in the tVTA	Colussi-Mas et al., 2007
Male Sprague–Dawley rats	Acute injection of d-amphetamine (1.5 or 5 mg/kg; s.c.)	Increased Fos-immunoreactivity in the tVTA	Rottlant et al., 2010
Male Sprague–Dawley rats	Acute injection of d-amphetamine (1 mg/kg; i.p.)	Increased FosB/ΔFosB immunoreactivity in the tVTA	Kaufling et al., 2010b
Male and female Sprague–Dawley rats	Acute injection of d-amphetamine (4 mg/kg, s.c.)	Increased Fos immunoreactivity in the tVTA	Matsui and Williams, 2011

Methamphetamine			
Male Sprague–Dawley rats	Acute injection of methamphetamine (10 mg/kg; i.p.)	Increased Fos-immunoreactivity in VTA-projecting tVTA neurons	Jhou et al., 2009a
Male Sprague–Dawley albino rat	Acute injection of methamphetamine (10 mg/kg; i.p.)	Increased Fos-immunoreactivity in the tVTA	Lecca et al., 2011
Male Sprague–Dawley rats	Acute injection of methamphetamine (10 mg/kg; i.p.)	Increased Fos expression in tVTA neurons projecting to the DR or the PPTg pars dissipata, but not to the RtGi	Lavezzi et al., 2012
Male Australian albino Wistar rats	Self-administration or passive injection (yoked delivery) of methamphetamine (0.1 mg/kg/0.05ml infusion) daily for 3 weeks	Increased Fos-immunoreactivity in the tVTA	Cornish et al., 2012
Morphine and morphine-like drugs			
Male Sprague–Dawley rats	Continual (75 mg pellet; s.c. once daily for 5 days) or intermittent (twice daily; s.c.; escalating doses of up to 120 mg/kg for 10 days) injection of morphine	No effect on FosB immunoreactivity in the tVTA	Perrotti et al., 2005
Male Sprague–Dawley rats	Acute injection of morphine sulphate (10 or 50 mg/kg, s.c.)	No effect on FosB/ΔFosB immunoreactivity in the tVTA	Kaufling et al., 2010b
Male and female Sprague–Dawley rats	Bath application of the MOR agonist, DAMGO (1 μM) in tVTA slices	Decreased rhythmic spontaneous firing rate of the tVTA; Reduced tVTA-evoked GABA-A IPSCs in VTA/SN DA neurons	Matsui and Williams, 2011
Male Sprague–Dawley rats	Acute injection of morphine (1 mg/kg; i.v.); Intra-tVTA injection of morphine (1 mg/ml) or muscimol (0.05 mg/ml)	Decreased firing rate of tVTA neurons following systemic or local injection of morphine; Blockade of morphine-induced excitatory effect on VTA-DA neurons following muscimol-mediated inactivation of the tVTA	Jalabert et al., 2011
Male Sprague–Dawley albino rats	Acute morphine injection (4 mg/kg, i.v.) in vivo; Bath application of morphine (1 μM) in tVTA slices	Decreased firing rate of tVTA neurons in vivo and decreased EPSCs in vitro	Lecca et al., 2011
Male Sprague–Dawley albino rats	Acute morphine injection (4 mg/kg, i.v.) in vivo; Bath	Decreased tVTA-evoked suppression of VTA DA neuron firing in vivo and decreased	Lecca et al., 2012

	application of morphine (1 μM) in tVTA slices	IPSCs evoked by tVTA stimulation in vitro	
Male albino Wistar rats	Bilateral intra-tVTA infusion of EM1 (50 or 250 pmol)	Positive reinforcement in a self-administration paradigm; Conditioned place preference	Jhou et al., 2012
Male CD1×129 mice	Bilateral intra-tVTA infusion of morphine (10 and 30 mg/kg)	Increased locomotor activity; effect inhibited by the bilateral transfection of the M5 gene	Wasserman et al., 2013
C57BL/6J mice	Bilateral intra-tVTA infusion of the selective MOR agonist, DAMGO (0.01, 0.1, 1 or 10 nmol)	Increased locomotor activity in a dose-dependent manner; effect potentiated by Girk1 ablation at the two highest doses of DAMGO	Kotecki et al., 2015
Male Long-Evans rats	Bilateral intra-tVTA infusion of morphine (10 mM)	Reduced heroin (0.025 mg/kg/infusion) self-administration	Steidl et al., 2015
Male GAD2::Cre mice	Bilateral intra-tVTA injection of morphine (10 mg/kg)	Increased locomotor activity; effect blocked by the activation of M3 and increased by the activation of M4	Wasserman et al., 2016
C57BL/6 mice	Bilateral intra-tVTA injection of morphine (5 nM)	Increased locomotor activity; effect potentiated by the co-infusion of morphine with M3, but not M4, selective antagonist	Steidl et al., 2017
Male Sprague–Dawley rats	Naloxone injection (1 mg/kg; s.c.) following chronic morphine treatment at escalating doses (10-80 mg/kg; i.p.; twice daily for 7 days)	Increased Fos immunoreactivity in the tVTA following naloxone-precipitated opiate withdrawal	Sanchez-Catalan et al., 2017
Cannabinoids			
Male Sprague–Dawley rats	Acute injection of THC (30%; i.p.)	No effect on FosB/ΔFosB immunoreactivity in the tVTA	Kaufling et al., 2010b
Male Sprague–Dawley albino rat	Acute injection of WIN (0.5 mg/kg, i.v.) in vivo; Bath application of WIN (1 mM) in tVTA slices	Decreased discharge frequency of tVTA neurons in vivo and decreased EPSC amplitude in vitro	Lecca et al., 2011
Male Sprague–Dawley albino rats	Acute injection of WIN (0.5 mg/kg, i.v.) in vivo; Bath application of WIN (1 mM) in tVTA slices	Decreased tVTA-evoked suppression of VTA DA neuron firing in vivo and decreased IPSCs evoked by tVTA stimulation in vitro	Lecca et al., 2012

Nicotine			
Male Sprague–Dawley albino rat	Acute injection of nicotine (0.2 mg/kg, i.v.); Bath application of nicotine (1 μM)	Increased firing rate of tVTA neurons in vivo and increased EPSC amplitude in vitro	Lecca et al., 2011
Male Sprague–Dawley albino rat	Acute injection of nicotine (0.2 mg/kg, i.v.)	No effect on tVTA-evoked suppression of VTA DA neuron firing	Lecca et al, 2012
DA reuptake inhibitor			
Male Sprague–Dawley rats	Injection of GBR-12909 (20 mg/kg; i.p.), twice daily for 7 days	Increased FosB-like immunoreactivity in the tVTA	Perrotti et al., 2005
Male Sprague–Dawley rats	Acute injection of GBR12909 (15 mg/kg, i.p.)	Increased FosB/ΔFosB immunoreactivity in the tVTA	Kaufling et al., 2010b
Norepinephrine and/or 5-HT reuptake inhibitors			
Male Sprague–Dawley rats	Injection of the norepinephrine reuptake inhibitor, nortriptyline (15 mg/kg; i.p.), twice daily for 7 days	No effect on FosB immunoreactivity in the tVTA	Perrotti et al., 2005
Male Sprague–Dawley rats	Injection of the 5-HT reuptake inhibitor, fluoxetine (10 mg/kg; i.p.), twice daily for 7 days	No effect on FosB immunoreactivity in the tVTA	Perrotti et al., 2005
Male Sprague–Dawley rats	Acute injection of either reboxetine mesylate (0.8 mg/kg; i.p.), nortriptyline hydrochloride (15 mg/kg; i.p.), fluoxetine hydrochloride (10 mg/kg; i.p.), venlafaxine hydrochloride (5 mg/kg; i.p.)	No effect on FosB/ΔFosB immunoreactivity in the tVTA	Kaufling et al., 2010b
5-HT releasing drugs			
Male Sprague–Dawley rats	Acute injection of S-(+)-fenfluramine hydrochloride (dexfenfluramine; 4 mg/kg; i.p.)	No effect on FosB/ΔFosB immunoreactivity in the tVTA	Kaufling et al., 2010b

Other drugs			
Male Sprague–Dawley rats	Acute injection modafinil (75 or 150 mg/kg; i.p.)	Increased Fos-immunoreactivity following treatment with the high dose	Scammell et al., 2000
Male Sprague–Dawley rats	Acute injection of either MDMA (5 mg/kg; i.p.), methylphenidate hydrochloride (10 mg/kg; i.p.) or caffeine (2.5-100 mg/kg; i.p.)	Increased FosB/ΔFosB immunoreactivity in the tVTA	Kaufling et al., 2010b
Male Sprague–Dawley rats	Acute injection of either 15% ethanol (1.5-5 g/kg; i.p.), diazepam (1.5 mg/kg, i.p.), GHB (1 g/kg; i.p.), ketamine hydrochloride (50 mg/kg; i.p.), PCP (3 or 10 mg/kg; i.p.), sodium valproic acid (20 mg/kg; i.p.) or gabapentin (50 mg/kg; i.p.)	No effect on FosB/ΔFosB immunoreactivity in the tVTA	Kaufling et al., 2010b

Table 2: The tVTA and the effect of drugs. Abbreviations: serotonin (5-HT); dopamine (DA); dorsal raphe (DR); excitatory postsynaptic current (EPSC); gamma-hydroxybutyric acid sodium salt (GHB); G protein-coupled inwardly-rectifying potassium channel 1 (Girk1); intraperitoneal (i.p.); inhibitory postsynaptic current (IPSC); intravenous (i.v.) ; muscarinic acetylcholine receptor 3 (M3); muscarinic acetylcholine receptor 4 (M4); muscarinic acetylcholine receptor 5 (M5); (+/−)-3,4-methylenedioxymethamphetamine hydrochloride (MDMA); phencyclidine hydrochloride (PCP); pedunculopontine nucleus (PPTg); pontomedullary paramedian gigantocellular reticular formation (RtGi); subcutaneous (s.c.); substantia nigra (SN); Δ9-tetrahydrocannabinol solution (THC); tail of the ventral tegmental area (tVTA); ventral tegmental area (VTA).

1.4.7 Summary and perspectives

Studies in the past few decades have yielded a wealth of information on brain systems encoding reward and aversive stimuli, however, the mechanisms underlying the interaction between these two processes are poorly understood. Recently, the tVTA has been described as a major GABAergic structure that starts within the posterior VTA and extends into the pons, acting as a possible connecting hub between aversion- and reward-responding brain regions. This cluster of

GABAergic cells receives inputs from the LHb and projects to DA neurons of the VTA/SNc complex, with additional projections to brainstem regions including the DR and PPTg (Jhou et al., 2009a; Kaufling et al., 2009; Lavezzi et al., 2012). Electrophysiological studies concerned about the role of the tVTA in reward and aversive processes suggest that tVTA neurons exhibit similar functional properties to those of LHb neurons, but opposite to those of midbrain DA neurons; they are excited following aversive or aversion-predicting stimuli, and inhibited following rewards or reward-predictive stimuli (Matsumoto and Hikosaka, 2007; Jhou et al., 2009b; Hong et al., 2011). Evidence also implicates the tVTA in the representation of negative reward prediction error (Hong et al., 2011) and avoidance behaviors related to fear (Jhou et al., 2009b). The identification of the tVTA as a major regulatory region capable of directly influencing midbrain DA neuron activity (Jalabert et al., 2011; Matsui and Williams, 2011; Brown et al., 2017) has also created avenues for a better understanding of the mechanisms underlying the reinforcing effects of psychostimulants and drugs of abuse. GABAergic cells of the tVTA show increased Fos-like immunoreactivity in response to psychostimulants (Perrotti et al., 2005; Geisler et al., 2008; Jhou et al., 2009a; Kaufling et al., 2009), and marked changes in their electrophysiological activity following exposure to a number of drugs of abuse, including cocaine, cannabinoids, nicotine and opioids (Jalabert et al., 2011; Lecca et al., 2011; Matsui and Williams, 2011). The latter findings have led to an updated disinhibition model of opioid action on VTA DA cells, which posits that opioids act on tVTA cell bodies or terminals to suppress the GABAergic inhibitory tone in midbrain DA neurons (Bourdy and Barrot, 2012). In view of its connectivity with the LHb and the previously reported beneficial effect of DBS of the LHb in depressed patients (Sartorius et al., 2010; Kiening and Sartorius, 2013), the tVTA may also be an interesting modulatory target for treating symptoms of depression. However, because the tVTA is a newly identified structure, relatively little information regarding

its role in reward-related processes and psychiatric disorders are presently available, and additional studies are required to go from fundamental theories to clinical applications. A major gap in the literature that still needs to be addressed is how the manipulation of certain receptors that are pre- or post-synaptically expressed in the tVTA, including those involved in glutamate and opioid transmission, could influence the ability of tVTA neurons to encode aversive stimuli and inhibit midbrain DA neuron activity.

1.5 Thesis proposal: overview, hypotheses and objectives

1.5.1 Article 1: Serial lesions at the DDC and MFB

In an attempt to characterize the neural substrate for brain stimulation reward, initial interest was given to the habenula. Electrical stimulation of the habenula (Sutherland and Nakajima, 1981; Nakajima, 1984; Vachon and Miliaressis, 1992) or its afferent (Blander and Wise, 1989; Vachon and Miliaressis, 1992) and efferent (Sutherland and Nakajima, 1981; Vachon and Miliaressis, 1992) pathway supports operant responding for ICSS. In addition, experiments employing lesions in combination with ICSS have shown that electrolytic lesions at the habenula attenuate the rewarding effectiveness of LH, VTA and DR self-stimulation (Morissette and Boye, 2008). However, the latter findings could not determine whether the habenula is directly involved in the rewarding effectiveness of ICSS because the lesions employed in the study not only destroyed habenular cell bodies, but also fibers of passage. In another set of studies from the same group, bilateral intra-habenula injection of d-amphetamine and cell body-specific lesions of the habenula failed to alter the rewarding effect of ICSS (Duchesne and Boye, 2013) and the reward-enhancing effect of amphetamine (Gifuni et al., 2012), respectively, suggesting that the habenula is perhaps not the key structure responsible for mediating the rewarding effect of ICSS. In light of these

findings and those reported by Morisette and Boye (2008), brain stimulation reward is likely mediated by fibers of passage within the DDC and not intrinsic habenular cell bodies. It is worth mentioning that the attenuation of brain stimulation reward reported by Morisette and Boye (2008) following electrolytic lesions at the habenula was only observed in approximately 25% of all the rats that were tested for ICSS. Although the lack of effect may be explained by the anatomical diffuse, collateralized, and heterogeneous nature of the neural substrate for ICSS (Arvanitogiannis et al., 1996a; Simmons et al., 1998), another plausible explanation may be that the two pathways of the brain reward circuitry, namely the DDC and the MFB, are functionally interconnected and merge on a common reward integrator. Therefore, the loss of reward-relevant neurons within the DDC should be compensated by the MFB, and vice versa. **Objective:** The aim of the present study is to evaluate the effect of single or serial electrolytic lesions along the DDC and MFB on the reward thresholds and maximum response rates obtained from rewarding electrical stimulation of the LH and DR. **Hypothesis:** *If the DDC and MFB merge on a common reward integrator, then sequential lesions of these pathways should produce larger and longer-lasting attenuations of brain stimulation reward than a lesion of either one of these pathways alone.*

1.5.2 Article 2: Anatomical disconnection following a single lesion at the DDC

Once a functional relationship between the MFB and DDC has been established, I will use the latter site and combine electrolytic lesions with immunolabeling for Fos proteins to characterize the reward-relevant neurons that are anatomically connected to the DDC. Synthesis of Fos proteins is regulated by the expression of the immediate early gene, c-fos, and is triggered by a variety of stimuli including rewarding electrical stimulation (Flores et al., 1997; Arvanitogiannis et al., 2000) and single (Kaufling et al., 2009; Lavezzi et al., 2012) or repeated (Perrotti et al., 2005; Zahm et

al., 2010) exposure to drugs of abuse. c-fos is a proto-oncogene that is part of the Fos gene family, which also consists of FosB, Fra-1 and Fra-2 (Milde-Langosch, 2005). The distribution of Fos-like immunoreactivity (FLIR) is a powerful tool to visualize neuronal activity in response to rewarding electrical stimulation owing to its ability to directly stain the cell nucleus (Flores et al., 1997; Arvanitogiannis et al., 2000). In addition to labeling neurons that are antidromically activated by ICSS, FLIR allows the detection of neurons that are transsynaptically activated by the rewarding stimulation, thereby providing a map of functional reward pathways (Sagar et al., 1988; Flores et al., 1997; Arvanitogiannis et al., 2000). Previous studies have shown that FLIR is enhanced in brain regions of rats that were trained to self-administer pulses of electrical stimulation at the LH (Arvanitogiannis et al., 1996b), MFB (Hunt and McGregor, 1998), VTA (Flores et al., 1997), DR (Marcangione and Rompre, 2008) and mPFC (Arvanitogiannis et al., 2000), in particular in the hemisphere that is ipsilateral to the stimulation electrode. However, to our knowledge, no prior studies have combined electrolytic lesions at the DDC with stimulation-induced FLIR. Such work could inform us whether the same nuclei that are active in lesion-naïve animals continue to be active following a lesion at the DDC. **Objective:** The aim of the present study is to evaluate the effect of a single electrolytic lesion at the DDC on the distribution of FLIR triggered by the rewarding electrical stimulation of the LH. The LH stimulation site will be used for ICSS because this region was associated with the larger lesion-induced attenuation of reward in the previous study. For the distribution of FLIR, special attention will be given to regions that are involved in the rewarding effect of ICSS and those that are anatomically connected to the DDC (Herkenham and Nauta, 1977; Araki et al., 1988). **Hypothesis:** *Electrolytic lesions at the DDC should produce significant reward deficits and reduce the stimulation-induced FLIR in brain regions that are subserved by its activity.*

1.5.3 Article 3: Manipulation of glutamate and opioid transmission in the tVTA

The last part of my PhD project is aimed at characterizing the role of the tVTA in brain stimulation reward and locomotor activity with respect to specific receptor systems. The tVTA is a recently identified structure that starts in the midbrain. It is located posterior to the VTA and dorsolateral to the caudal part of the IPN, and it extends into the pons (Barrot and Thome, 2011). It was first identified in the rat as a discrete population of GABAergic neurons that elicits Fos expression in response to psychostimulants (Perrotti et al., 2005). Rationale for investigating the tVTA is threefold. First, the tVTA receives strong glutamatergic inputs from the DDC, in particular from the LHb (Jhou et al., 2009a; Kaufling et al., 2009). Second, GABAergic neurons of the tVTA heavily project to the VTA and SNc (Jhou et al., 2009a) and exert an electrophysiological inhibitory control over midbrain DA neurons (Matsui and Williams, 2011; Brown et al., 2017). Third, tVTA neurons are responsive to reward and aversive cues; they are excited by aversive stimuli or aversive-predicting stimuli, and inhibited by rewards or reward-predicting stimuli (Jhou et al., 2009b; Hong et al., 2011).

The ability of tVTA neurons to encode reward-related signals and inhibit midbrain DA neurons is largely influenced by local glutamate and opioid transmission. Injection of AMPA into the tVTA produces robust conditioned place aversion in rats (Jhou et al., 2013), while lesions of the LHb (Gifuni et al., 2012) or the FR (Murphy et al., 1996), through which most of the glutamatergic inputs to the tVTA are conveyed, increase spontaneous and psychostimulant-induced locomotor activity. In addition, opioid-mediated inhibition of the tVTA with MOR agonists produces positive reinforcement in a self-administration setting (Zangen et al., 2002; Jhou et al., 2012) and increases the firing activity of VTA DA neurons (Jalabert et al., 2011). **Hypothesis 1:** *In light of these findings, I hypothesize that blockade of NMDA and AMPA receptors as well as activation of MORs*

in the tVTA enhance brain stimulation reward and locomotor activity. **Objective 1:** To test this hypothesis, ICSS and locomotor activity will be assessed before and after bilateral intra-tVTA injection of either NBQX, an AMPA receptor antagonist, PPPA, an NMDA receptor antagonist, or the vehicle in a counterbalanced order, followed by an injection of EM-1, a selective MOR agonist. Treatment with EM-1 is administered at the end to confirm (in addition to histology) that that injection was within the tVTA; that is because the tVTA, unlike adjacent structures, shows very strong immunoreactivity for MORs (Jhou et al., 2009a; Jalabert et al., 2011). **Objective 2:** ICSS and locomotor activity will be assessed following siRNA-mediated downregulation of NMDA receptors in the tVTA. The reward-enhancing effect of PPPA will also be assessed following the siRNA treatment. This experiment will tell us whether a reduction in NMDA receptor alters the rewarding efficacy of ICSS and the reward-enhancing effect of PPPA. **Hypothesis 2:** *If GluN2A-containing NMDA receptors are located on presynaptic terminals of the tVTA, then siRNA-mediated downregulation of NMDA receptors in cells that have their cell bodies in the tVTA should not alter the reward-enhancing effect of PPPA.*

CHAPTER 2: RESULTS OF ORIGINAL CONTRIBUTIONS

2.1 ARTICLE 1: Published in *Behavioral Brain Research*. 2016, 296:431-441.

Role of the dorsal diencephalic conduction system in the brain reward circuitry

Marc Fakhoury[1], Pierre-Paul Rompré[1,2], Sandra M. Boye[1]

[1]Department of Neurosciences, Faculty of Medicine, Université de Montréal, Montreal, Quebec, Canada

[2]FRQ-S Research Group in Behavioral Neurobiology, Concordia University, Montreal, Quebec, Canada

AUTHOR CONTRIBUTIONS

I wrote the first draft of the manuscript and conducted all the behavioral experiments in the laboratory of Dr. Sandra Boye and the histological analysis in the laboratory of Dr. Pierre-Paul Rompré.

ABSTRACT

Previous work with psychophysically based studies suggests that electrolytic lesions of the habenula, which lies in the dorsal diencephalic conduction system (DDC), degrade the rewarding effect induced by intracranial self-stimulation (ICSS). This experiment was aimed at studying the importance of the DDC in brain stimulation reward, and its connections with other areas that support operant responding for brain stimulation. For this purpose, rats were implanted with stimulating electrodes at the dorsal raphe (DR) and lateral hypothalamus (LH), and lesioning electrodes in the medial forebrain bundle (MFB) and the DDC. Rats were trained to self-administer the stimulation at three different current intensities and were tested daily for changes in reward thresholds, defined as the pulse frequency required for half-maximal responding. The lesions were done at the DDC and the MFB, and were separated by two weeks interval during which the rats were tested for self-stimulation. At the end of the experiment, rats were transcardially perfused and their brains collected to determine the extent of the lesions and the locations of the stimulation sites. Results show that lesions at both the DDC and MFB produced larger and longer-lasting increases in reward thresholds (up to 0.40 $\log_{10}$ units) than lesions at either pathway alone (up to 0.25 $\log_{10}$ units), and were more effective in attenuating the reward induced by LH self-stimulation. These results suggest that there exist two parallel pathways, the MFB and the DDC, which could constitute a viable route for the reward signal triggered by ICSS.

Keywords: Dorsal raphe; Habenula; Lateral hypothalamus; Reward; Self-stimulation

INTRODUCTION

It is well established that electrical stimulation of certain brain areas such as the lateral hypothalamus (LH) and the dorsal raphe (DR) induces a rewarding effect that is strong enough to support operant responding in laboratory animals; rats will quickly learn to press a lever, for instance, to receive a short train of electrical pulses delivered to these regions (Annau, 1978; Morissette and Boye, 2008). Since its discovery more than 60 years ago, electrical self-stimulation has been extensively used in an attempt to characterize the neural substrates of appetitive behaviors. This animal model has the advantage of bypassing external sensory processes to directly excite the reward circuit of the brain, hence being less affected by variables inherent to these processes. Despite a large amount of research, our knowledge of the reward circuitry and its trajectory within the brain is still largely limited. The main issue in establishing a detailed map of the reward-relevant substrates has been the proper differentiation between the reward-relevant neural elements from other elements that do not play a role in the rewarding effect but are still activated by the electrical stimulation (Murray and Shizgal, 1996a). Studies that made use of psychophysical measures combined with behavioral collision techniques revealed unique anatomical and physiological properties of the reward-relevant neurons (Bielajew and Shizgal, 1986; Murray and Shizgal, 1996a). From these studies, we know that the reward signal initiated by electrical stimulation of the medial forebrain bundle (MFB) travels at moderate velocities (1–8 m/s) along axons that possess short refractory periods (0.4–1.2 ms) and that link anterior regions of the LH to the ventral tegmental area (VTA) (Bielajew and Shizgal, 1986; Murray and Shizgal, 1996a, b). The hypothesis that the reward signal is carried by first-stage neurons traveling between regions anterior to the LH and the VTA led to the prediction that damage to the MFB should decrease the rewarding efficacy of LH and VTA electrical stimulation (Waraczynski, 1988;

Gallistel et al., 1996). Consistently, sustained attenuations of LH (Janas and Stellar, 1987; Murray and Shizgal, 1991; Waraczynski et al., 1998) and VTA (Simmons et al., 1998) self-stimulation threshold were observed following electrolytic lesions, or a knife cut, placed along the MFB. A common finding of these studies, however, is that in the great majority of cases, damage to the anterior MFB failed to attenuate the reward or induced a small transitory attenuation. These negative results were attributed to a highly diffuse neural network that contributes to reduce the probability of functionally disconnecting the pathway between the lesion and the stimulation sites (see (Simmons et al., 1998)). A hypothesis to account for the large number of ineffective lesions is that the reward signal is carried by more than one pathway. Such a hypothesis has been proposed by Murray and Shizgal (Murray and Shizgal, 1994) who used the behavioral version of the collision technique to reassess the physiological properties of the first-stage neurons that link the LH and the VTA. Using a high resolution frequency sampling, they observed collision intervals that were significantly longer than those reported in previous studies. Such long collision intervals imply that the first-stage neurons that they were stimulating had very slow conduction velocities (<1 m/s), a conclusion that was inconsistent with previous findings and with the duration of the refractory period. The discrepancy could be resolved assuming that the relevant neurons do not travel only within the MFB, the shortest course between the LH and the VTA, but also follow the course of the dorsal diencephalic conduction system (DDC), hence increasing the axonal length between the two stimulation sites.

The idea that diencephalic structures are involved in brain stimulation reward comes from early lesions studies showing that rats are still able to self-stimulate at the LH after surgical removal of telencephalic structures (Huston and Borbely, 1973, 1974), and following 6-OHDA injection into the substantia nigra (Ornstein and Huston, 1975). Not only do these studies suggest that the

reinforcing mechanisms of ICSS are independent of dopamine transmission, they also propose the existence of a diencephalic locus of integration of reward (Huston, 1982). The DDC has recently received a lot of attention because electrical stimulation along its trajectory is effectively rewarding, suggesting that it likely contains reward-relevant axons (Sutherland, 1982; Vachon and Miliaressis, 1992). This pathway links structures that serve as a key relay between forebrain and several midbrain and hindbrain sites, and that play an important role in the regulation of reward-seeking behaviors (Wang and Aghajanian, 1977; Bianco and Wilson, 2009; Beretta et al., 2012; Proulx et al., 2014). It has been shown that in response to rewarding stimulation, sites along the DDC show increased expression of the neuronal marker Fos (Arvanitogiannis et al., 1996b; Zhang et al., 2005). Moreover, the DDC receives information through the stria medullaris (sm) from the anterior portion of the MFB, and has efferent projections terminating in the caudal mesencephalon (Beretta et al., 2012). Many of the fibers within this pathway synapse in important regions that support self-stimulation, such as the lateral habenula (LHb) (Morissette and Boye, 2008; Bianco and Wilson, 2009). The LHb, which is located centrally along the DDC, receives dopaminergic innervations that primarily arise from the medial VTA (Omelchenko et al., 2009; Shen et al., 2012; Root et al., 2015), a region that also innervates key structures involved in reward such as the ventral striatum (Ikemoto, 2007). The hypothesis that the DDC plays an important role in brain stimulation reward is further supported by a previous study by Morissette and Boye (Morissette and Boye, 2008), who reported sustained attenuations of the rewarding effectiveness of the median raphe, DR, LH and VTA self-stimulation in more than 25% of tested rats following electrolytic lesions of the habenula. This reinforces the hypothesis that reward-relevant neurons that link mesencephalic and rostral diencephalic regions likely travel through the DDC. The present study was aimed at testing this hypothesis. We trained rats to self-administer electrical stimulation at the

level of the DR and the LH; then we made a small lesion at the DDC followed two weeks later by a second lesion at the MFB (and vice versa). Using the curve-shift paradigm, reward thresholds were measured daily for 2 weeks after each lesion at three different current intensities and for each stimulation site. Results show that the DDC and MFB lesions tend to shift the reward threshold towards higher values, suggesting that these pathways play an important role in brain stimulation reward.

MATERIAL AND METHODS

Subjects

Adult male Long Evans rats, purchased from Charles River Canada, served as experimental subjects. The animals were kept in a temperature (22ºC) and humidity (50%) controlled animal colony lit from 6:30 am to 6:30 pm. They were individually housed in a standard cage with unrestricted access to food and water, and were allowed to habituate to the animal colony for at least 5 days prior to surgery. All procedures followed the Canadian Council on Animal Care guidelines and were approved by the Institutional Animal Care Committee.

Surgery

Rats (300–400 g) were anesthetized with a mixture of isoflurane (2.5–3.5% O_2, 0.6 L/min) and oxygen, and fixed in a stereotaxic apparatus. An analgesic, Ketoprofen (5 mg/kg), was administered by subcutaneous injection at the day of the surgery and 24 h later. After an incision was made on the scalp, an uninsulated stainless steel wire coupled to a male Amphenol connector was wrapped around screws in the skull that served as the anodal current path. Stainless steel electrodes were implanted in the DR (anterior: −7.8, lateral: +0, ventral: −7.0), the LH (anterior:

−2.5, lateral: +1.7, ventral: −8.6), the MFB (anterior: −3.8, lateral: +1.7 ventral: −8.6) and the DDC (anterior: −3.3, lateral: +0.65, ventral: −4.5). All coordinates are expressed in mm in reference to bregma and were taken from the Paxinos and Watson atlas of the rat brain (Paxinos G. and Watson C., 1997). The stimulation and the lesion electrodes were all unilateral and ipsilateral to each other and were made from 0.25 mm diameter rod coated with Epoxylite except for the dome-shaped tip. Dental acrylic cement was used to secure the electrodes assembly to the skull. At the end of the surgery, the rats were housed individually in cages with food and water available ad libitum, and body weight was monitored daily for 6 days after surgery.

Apparatus

All self-stimulation sessions took place in chambers made from Plywood (back and side walls) and Plexiglas (front wall). Operant conditioning chambers (28 cm wide × 29.4 cm deep × 68.6 cm high) were equipped with a non-retractable lever (ENV-116 M, Med Associated Ins, St Albans VT, USA) located on the left wall, 3.4 cm above the metal rod floor. Chambers were encased in sound-attenuating wooden boxes (48.6 cm wide × 50.7 cm deep × 95.4 cm high) insulated with Styrofoam, with a Plexiglas window that allows constant viewing of the rat. The stimulation electrode was connected to a constant current stimulator (PHM-152/2, Med Associates Inc, St Albans, VT, USA), and the current intensity was monitored on an oscilloscope. Depression of the lever delivered a single 400-ms train of rectangular cathodal pulses of 0.1 ms in duration.

Training

ICSS training was performed 1 week after the surgery. Rats were trained to self-administer a train of pulses using a FR1 schedule. Once the response was learned, rats were allowed to self-

stimulate continuously for 1 h at stimulation parameters that support consistent responding. After at least 2 days of training, rats were allowed to self-administer the same stimulation parameters, but during discrete 45 s trials separated by 30 s intervals; each trial began with the delivery of 5 trains of non-contingent stimulation delivered at 1 Hz. The plot of the rate of responding as a function of pulse frequency comprised of a single response-frequency (R/F) curve. The reward threshold, defined as the pulse frequency required for half-maximal responding, was interpolated from a regression line fit to the rising portion of each R/F curve. At the end of each trial, the pulse number, which ranged from 0 to 2.6 Hz in $\log_{10}$ units, was reduced by approximately 0.1 $\log_{10}$ units. Three current intensities, designated as the "low", "medium" and "high" current, were chosen during the trials so as to yield reward thresholds of approximately 25, 50 and 100 Hz respectively.

Behavioral tests

The behavioral tests consisted in administering an electrical stimulation in the DR and the LH of each rat. A stimulation site was considered viable if it could be used to derive R/F curves at three different currents. Three R/F curves were generated from each current and were collected for the DR stimulation site in the morning session, and the LH stimulation site in the afternoon session. Each session was separated by at least 2 h in order to allow enough time for the rats to return to its home cage and get some rest. The first trial consisted of a warm-up phase that was discarded from data analysis. Following the warm-up phase, 3 R/F curves were obtained at each current. Once the three current intensities were determined for each rat, they were tested at each intensity each day for 4 consecutive days. The rats were then lesioned by passing an anodal current (100 µA, 20–30 s) through the lesioning electrode. The lesion was first made in the DDC at the level of the LHb in

half of the rats (group 1), while the other half received the first lesion at the level of the MFB (group 2). After two weeks of daily training, rats that received the first lesion in the DDC received another lesion in the MFB and vice versa.

Histology and tissue processing

At the end of the behavioral tests, rats were anesthetized with an intraperitoneal injection of urethane (1.5 g/kg of bodyweight). The stimulation sites were marked by passing a direct anodal current of 100 μA for approximately 30 s through the DR and LH electrodes. Rats were then transcardially perfused with 60 ml of 0.9% saline followed by 60 ml of a formaldehyde solution containing 3% potassium hexacyanoferrate II, 3% potassium hexacyanoferrate III and 0.5% trichloroacetic acid in order to produce a visible blue staining at the level of the lesions. The brains were then taken out, fixed in 10% formalin, and kept in 30% sucrose solution for at least 1 week. The following day, the brains were removed from the sucrose solution, sliced into 40 μm coronal sections, and mounted onto gelatine-coated slides. Thionin was then used to stain the brain slices for Nissl substance, and the sections were analyzed under light microscopic conditions to verify the placement of the electrodes **(Figure 1)**.

Statistical analysis

The mean of the threshold values and maximum response rates are expressed in $\log_{10}$ units and percentages (%) of baseline respectively, and were obtained before and after each lesion. Statistical comparisons with baseline values were made by constructing 95% confidence intervals around the mean of the measures obtained during the 4 days preceding the first lesion. Confidence intervals were obtained by multiplying the standard deviation of the four baseline means by the t-value

associated with the p = 0.05 level of significance for 3 degrees of freedom (t = 3.182) (Arvanitogiannis et al., 1996a). The mean of the reward threshold and maximum response rate obtained following the first lesion was considered significantly different than baseline values if they lied outside the 95% confidence intervals. In order to determine whether the second lesion alters the results obtained after the first lesion, confidence intervals were constructed around the mean of the measures obtained during the 4 days preceding the second lesion, and statistical comparisons were carried out as described previously.

RESULTS

Changes in reward thresholds during DR stimulation

Of the 34 rats initially prepared for the study, 9 were successfully trained for self-stimulation on both DR and LH electrodes, and had lesions located within the trajectory of the DDC and the MFB. The remaining rats were excluded from data analysis either because they failed to learn the ICSS behavior, because their electrodes were not in the intended regions, or because they failed to complete the experiments (post-surgical death or removal of the electrode assembly). Among the 9 rats that were successfully trained for ICSS, rat 2, 14, 29 and 30 received the first lesion at the DDC (group 1), and rat 5, 9, 25, 26 and 32 received the first lesion at the MFB (group 2). An important observation is that the reward thresholds measured at each current intensity at the DR stimulation site during the four days that preceded the first lesion were highly stable for each rat **(Figure 2)**. A lesion at the DDC in group 1 resulted in increases in reward thresholds at all current intensities; an effect that remained significant in most days following the lesion. Reward threshold shifts varied from 0.02–0.21 $\log_{10}$ units at the high current, 0.06–0.12 $\log_{10}$ units at the medium current, and 0.05–0.23 at the low current. In rats 14, 29 and 30, the increase in reward threshold

was observed 24 h after the lesion and did not change during the next 13 days, except for rat 30 at the highest current where a slight decrease was observed. In rat 2, reward thresholds increased slightly over time and tended to return towards baseline at the end of the second week, more particularly when the high current was used. The second lesion performed at the level of the MFB in the same group of rats had little impact on the rewarding efficacy of the stimulation. For rat 29, there were no significant differences between threshold values obtained before and after the lesion at all current intensities. Although a slight increase in reward threshold was observed in rats 2, 14 and 30, the changes occurred only at selected current intensities and failed to persist during the two weeks of testing.

In group 2, the MFB lesion led to an increase in reward threshold that ranged from 0.02–0.17 $\log_{10}$ units at the high current, 0.01–0.15 $\log_{10}$ units at the medium current and 0.03–0.14 $\log_{10}$ units at the low current **(Figure 2)**. The changes in reward thresholds were more pronounced in rats 25 and 26, and remained significantly higher than baseline values at all current intensities. However, the lesion failed to produce significant increases in reward thresholds in rat 5 at the medium current intensity, and in rat 9 at the high current. The second lesion, aimed at the DDC, was able to further increase the threshold shift obtained after the first lesion, except for rats 5 and 25 at the high and medium currents respectively. For rat 9, the threshold shifts occurred immediately after the DDC lesion when the medium and high currents were used, and gradually after the lesion when the low current was used. Unlike rats 26 and 30, the changes in reward thresholds observed in rat 9 were long-lasting and remained significant until the final day of testing.

Changes in maximal response rates during DR stimulation

The maximum response rate was measured during stimulation of the DR at 1, 11, 15 and 25 days following the first lesion. In group1, the first lesion, which was aimed at the DDC, failed to produce immediate changes in the maximum response rate except for rats 29 and 30 with the low current intensity, where a decrease of up to 9.6 ± 3.19% was observed **(Figure 3)**. At day 11, the maximum response rate remained significantly low in rats 29 and 30 at the low current, but increased in rat 14 when the medium current was used. The second lesion, which was done at the MFB, failed to enhance the shift in the maximum response rates beyond what was observed after the first lesion, except at day 25 for rat 14 at the low and medium currents, and rat 29 at the medium current.

In group 2, the first lesion was able to produce significant changes in the maximum response rate in rat 9 but did not have any immediate effect in rats 5, 25, 26 and 32. In rat 9, the medium and low currents were associated with an increase in the maximum response rate after the first lesion, whereas the high current was characterized by a decrease in the maximum response rate. After the second lesion, the maximal response rate decreased in rat 5 at the medium current, in rat 25 at the high and low currents, and in rat 32 at the low current, but remained unchanged for the other rats and current intensities at day 15. On the last day of testing, the maximal response rates were unaltered compared to values obtained after the first lesion, except for rats 25 and 32 at the low and medium current respectively.

Changes in reward thresholds during LH stimulation

Slightly different results were obtained when the reward was induced by LH electrical stimulation. At this stimulation site, the DDC lesion resulted in significant increases in reward threshold that ranged from 0.04–0.23 $\log_{10}$ units at the high current, 0.05–0.13 $\log_{10}$ units at the medium current, and 0.06–0.18 $\log_{10}$ units at the low current in rats from group 1 **(Figure 4)**. For

rats 14, 29 and 30, the increase in reward threshold occurred 24 h after the lesion and changed little over time; these results are very similar to those seen with DR electrical stimulation. For rat 2, we observed a progressive increase in reward threshold that depended on the current intensity. From day 1 to day 4 post-lesion, the reward threshold increased progressively at the low current and remained elevated over the subsequent testing days, whereas at the medium and high current, the increase in reward threshold was immediate and did not change over time. Contrary to what was seen at the DR stimulation site, the second lesion performed at the level of the MFB had a significant impact; it produced additional increases in reward threshold in most rats, ranging from 0.05 to 0.13 $\log_{10}$ units. It is noteworthy to mention that the changes in reward threshold occurred soon after the lesion and remained elevated and stable over the entire test period for all rats and at each current intensity (except for rat 2 at the low current).

In group 2, increases in reward threshold after a MFB lesion ranged from 0.08 to 0.24, 0.06 to 0.25 and 0.02 to 0.16 $\log_{10}$ units at the high, medium and low currents respectively, and was statistically significant compared to baseline values in most rats **(Figure 4)**. In the case of rats 25, 26, 30 and 32, the maximum increase was observed after 24 h and remained stable over the subsequent days. Rat 9 showed the largest threshold shift but it was progressive over day 2 and day 3 post-lesion. Significant increases in reward threshold were also observed in rat 5, more particularly when the medium and high currents were used. The second lesion performed at the level of the DDC enhanced the threshold shifts produced by the MFB lesion in all rats, with the exception of rats 5, 26 and 32 at the high current. For the remaining rats and current intensities, the increase in reward thresholds was evident 24 h after the lesion and remained stable over the entire test period. Rat 9 displayed the highest increase in reward threshold following both lesions,

more particularly at the medium current where an increase of 0.40 $\log_{10}$ units (124%) relative to baseline values was observed.

Changes in maximal response rates during LH stimulation

The maximum response rates expressed in % baseline were monitored during LH stimulation at several days following the lesions **(Figure 5)**. In group 1, following the first lesion at the DDC, the maximum response rates decreased in rat 14 and 29 at the low current at day 1, and remained significantly lower than baseline values at day 11. One day following the second lesion, the maximum response rate decreased in rat 14 only at the medium current intensity, and remained significantly low at day 25. However, the MFB lesion failed to alter the maximum response rate in the remaining rats and current intensities of group 1.

In group 2, the first lesion at the MFB was the most effective in reducing the maximum response when the low current intensity was used. At this current, the changes in reward thresholds occurred immediately after the lesion in rats 25 and 32, and 11 days after in rats 5, 9 and 26. Decreases in reward thresholds were also observed at the medium current intensity, but only in rats 5, 9 and 26. Conversely, the reward thresholds measured following the first lesion failed to significantly change at the high current intensity, except at day 11 in rat 32 where a slight increase was observed. At day 15, one day following the DDC lesion, the maximal response rate decreased in rat 25 at the low and medium currents, and rat 32 at the low current, but was unaltered in the remaining rats and current intensities. Finally, at day 25, the maximum response rates were significantly lower than values obtained prior to the second lesion at the low and high currents in rat 26, and at the low and medium currents in rats 5, 9, 25 and 32.

Electrodes and lesions location

No major sign of discomfort or pain was observed when doing the lesions, and the rats regained their normal bodyweight after the lesions. Tissue sections of the brain were examined under light microscopy for electrode localization, and drawings of the stimulation site and lesion damage were made. **Figure 6** and **Figure 7** illustrate the histological reconstructions for group 1 and 2 respectively, using the Paxinos and Watson atlas of the rat brain (Paxinos G. and Watson C., 1997). The stimulation site is indicated by the black circle, while the lesion damage is represented in grey. Coronal sections of an individual rat showing the DDC and MFB lesions are illustrated in **Figure 8**. In all rats, the DR stimulation sites were located approximately 7.64–8.30 mm anterior to bregma and 0–0.17 mm lateral to bregma. The anterior coordinates of LH stimulation sites were 2.30–2.80 mm with reference to bregma and 1.20–1.96 mm lateral to the bregma.

Damage to the LHb within the trajectory of the DDC was evident in all subjects. The size of the lesions ranged from 0.19 to 0.62 mm^2 at their maximal cross-sectional area. Some of the fibers of the sm, which sends inputs to the habenular nuclei, were also damaged following DDC lesions. In group 1, the majority of the lesions were centered on the sm and minimally involved the LHb, whereas in group 2, the lesions appeared to substantially damage the LHb in most of the cases. The lesions also appeared to damage part of the medial habenula in some rats (2, 9 and 14) while leaving it intact in others. For the MFB, the lesions were relatively smaller and ranged from 0.11 to 0.30 mm^2. MFB lesions were located within the defined boundaries of the MFB: mediolaterally between the internal cerebral peduncle and the fornix, and dorsoventrally between the zona incerta and the base of the brain. In some cases, structures outside of these boundaries, including the fornix, the perifornical nucleus, and the parasubthalamic nucleus, were also damaged by the lesion.

DISCUSSION

Reward threshold and maximum response rate

In the present study, we investigated the contribution of the DDC and MFB in the transmission of reward signals triggered by stimulation of the DR and LH. The use of two stimulation sites enabled us to study the functional relationship between the DDC and brain structures in different anatomical regions that could support self-stimulation. In order to determine whether a lesion at the DDC and MFB could significantly alter the reward induced by ICSS, we looked at the changes in reward thresholds obtained from R/F curves. The long-lasting increases in reward thresholds observed in most rats after a first lesion at the DDC strongly support the notion that this pathway is functionally linked to reward-relevant sites within the LH and the DR (Varga et al., 2003; Bianco and Wilson, 2009; Poller et al., 2013). In contrast, data obtained from the DR simulation site indicate that a first lesion at the MFB failed to produce significant changes in reward threshold for all rats and current intensities, suggesting that the MFB and the DR share only a modest complement of axons. However, the MFB lesion had a significantly higher influence on the rewarding effectiveness of the LH stimulation. This effect is consistent with the notion that neurons in the MFB have axons that extend from anterior regions of the LH (Gratton and Wise, 1983; Bielajew and Shizgal, 1986; Murray and Shizgal, 1996b). Although there is evidence suggesting that DR axons also descend along the midline within the brainstem and enter the MFB, they do not share a significant amount of axonal connections with the MFB because of their relatively different anatomical localization (Gagnon and Parent, 2014).

Data obtained at the DR stimulation site also indicate that the lesions failed to produce long-lasting changes in the maximum response rate at each current intensity. Although the maximum response rates decreased in some rats following a lesion, no additive effects were observed

between the first and second lesion, except for few rats. On the other hand, data obtained at the LH stimulation site indicate that the lesions were generally more effective in producing higher shifts in the maximal response rates. Although no major changes were observed when the high current intensity was used, the lesions were able to reduce the maximum response rate in most rats at the low and medium currents. Taken together, the results obtained at the LH stimulation site might raise the possibility that the decrease in the maximum response rate is due to a general decrease in reward. However, if this was the case, then we would also expect to see a significant decrease at the high current intensity as well. Changes in maximum response rates are therefore more likely to be the result of other parameters independent of the reward threshold, such as deficits in the performance or general disturbance in behavior. This finding is compatible with earlier pharmacological and electrophysiological studies demonstrating a clear dissociation between the maximum response rate and the reward threshold during ICSS (Boye and Rompre, 2000; Morissette and Boye, 2008; Bergeron and Rompre, 2013).

Electrolytic lesions

Electrolytic lesions of the DDC and MFB resulted in significant attenuations of brain stimulation reward. Although most of the lesions produced immediate long-lasting increases in reward thresholds, the magnitude of the effect observed after the lesions was different among each rat. This difference in effect may be explained by the fact that the location and size of the lesions vary among subjects, and that each rat has a unique and specific trajectory of reward fibers in the brain (Waraczynski et al., 1998). In most rats of group 1, the DDC lesions were located along the sm, and yet were generally more effective in altering brain stimulation reward compared to lesions from group 2, where damage of the LHb was more evident. This observation is highly relevant

with respect to the neural substrate of reward, and could suggest that attenuations in reward thresholds are more likely due to the destruction of DDC fibers and not the LHb. In this study, we also found that the size of a given lesion did not always predict its behavioral effect. For instance, rat 9 had relatively smaller lesions compared to rat 5, but showed a larger and longer lasting increase in reward threshold for the LH stimulation (up to 0.40 $\log_{10}$ units). Such discrepancy is commonly observed in psychophysical studies and could reflect the presence of a highly collateralized and diffuse network of reward-relevant axons. It is also in line with other reports suggesting an inconsistency between the size or location of a lesion and the magnitude of the change in reward thresholds (Murray and Shizgal, 1991, 1996b; Morissette and Boye, 2008).The changes in reward thresholds measured after the lesions also indicate that additive effects were obtained between MFB and DDC lesions during stimulation of the LH, but not the DR. At the DR stimulation site, the first lesion (irrespective of its location) produced significant increases in reward thresholds in most rats and current intensities, whereas the second lesion failed to further increase the reward thresholds in the majority of the rats. In contrast, at the LH stimulation site, the second lesion enhanced the threshold shifts produced by the first lesion in all rats and most current intensities, suggesting that lesions at the MFB and DDC have a greater impact on the rewarding effect obtained at the LH stimulation site. Another interesting observation is that the order of the lesions had a different impact on the reward thresholds depending on which stimulation site was used. Results obtained from the DR stimulation site indicate that the attenuations in reward thresholds were of greater magnitude when the first lesion was done at the DDC, suggesting that the order of the lesions contributed to some of the differences observed between group 1 and group 2. In contrast, results obtained at the LH stimulation site did not reveal major differences in reward attenuation between rats from group1 and group 2.

Current intensities used

In this study, we evaluated the effect of using different current intensities on the behavioral changes observed during the DR and LH stimulation. Our data suggest that there are no clear relationship between the current intensity and the maximum response rate. Some of the current intensities were as low as 120 μA and still did not elicit a significant decrease in the maximum response rate compared to higher current intensities. This finding appears at odds with other studies indicating that the asymptotic level of reward declines at low current intensities (Gallistel et al., 1991; Simmons and Gallistel, 1994). It is very difficult to formulate a clear explanation, but it may be that the animals had to respond more with the low currents in order to generate higher rewarding effects. In other words, the lower the current intensity, the lower the number of relevant axons recruited, and therefore, the higher number of times this reduced population of axons must be activated to produce a significant rewarding effect. On the other hand, a clear correlation was observed between the reward threshold and the current intensities used. With few exceptions, the highest increase in reward threshold was observed at the low and medium currents, suggesting that lower current intensities constitute a more sensitive parameter that could be used for better evaluating the effects of lesions on the reward threshold. This is consistent with other reports suggesting that the highest increase in reward threshold is observed when using low current intensities (Gallistel et al., 1991; Arvanitogiannis et al., 1996a; Gallistel et al., 1996; Morissette and Boye, 2008). If the fibers travel very close to the tip of the stimulation electrode, then their lesion should be more effective in reducing the rewarding effectiveness within the small stimulation field created by low current intensities.

The DDC in the brain reward circuitry: suggested anatomy

In the present study, we demonstrated that lesions at the DDC and MFB produce long-lasting attenuation in brain stimulation reward that was more evident at the LH stimulation site. The attenuations in reward following a lesion at the DDC were not only caused by damage of the LHb, but were also due to destruction of DDC fibers including the sm. These results are highly informative with respect to the trajectory of the circuitry for ICSS, and suggest that the key structure in reward is not the LHb, but rather the DDC. This finding is consistent with studies showing that destruction of the LHb with electrolytic lesions degrades ICSS, while cell-body specific neurotoxic lesions do not (Morissette and Boye, 2008; Gifuni et al., 2012). The summation of lesion effect observed after DDC and MFB lesions also confirms the hypothesis that there exist two complementary routes that the reward signal could take, the DDC and the MFB, and that following lesions of these channels, the rewarding effect is greatly reduced. More particularly, it suggests that the MFB and the DDC are parallel pathways that are separated dorso-ventrally by the thalamus and that provide a functional link between limbic structures such as the habenula, and mesencephalic structures such as the raphe nuclei. The network of reward-relevant axons forming the DDC and MFB act both in serial and parallel fashion to perform various functions important for goal-directed behavior. Descending hypothalamic fibers running along the MFB travel towards the VTA, where they project to the periaqueductal gray and to the vicinity of the decussation of the superior cerebellar peduncle (Huston, 1982). In addition, collateral sprouting of axonal projections traveling along the MFB project caudally along the sm and provide functional inputs to the LHb (Morissette and Boye, 2008). Therefore, sites like the diagonal band of Broca, septal complex, and preoptic areas not only project caudally via the MFB, they also project via the DDC, en route to midbrain sites (Hikosaka, 2010).

CONCLUSION

In summary, this study suggests that brain stimulation reward arises from several structures localized over multiple brain regions that collectively mediate various functions important for goal-directed behavior. We showed that lesions of the DDC and MFB were more effective in attenuating the reward induced by LH self-stimulation, which is consistent with the hypothesis that some first-stage neurons arise in some rostral MFB nuclei, and that they send their projections through the LH (Murray and Shizgal, 1996a). It is also in line with a recent study indicating the existence of glutamatergic projections from the LH to neurons in several structures of the DDC such as the LHb (Poller et al., 2013). Moreover, the additive effects observed between DDC and MFB lesions indicate that these two pathways can compensate for the loss of reward-relevant axons within one or the other, and that they both constitute key components of the neural substrate for ICSS. By providing a functional link between the DDC and reward-relevant axons in the brain, this study helps extend the boundaries of the known reward circuitry in the brain. The identification of the neurobiological bases of reward is a first step towards a better understanding of normal behaviors, such as eating and drinking, and abnormal behaviors such as substance abuse and gambling. To date, few studies have characterized the functional relationship of the DDC to other reward-relevant sites in the brain, and clearly more effort needs to be devoted to the identification of all the players involved in the integration and transmission of reward signals.

ACKNOWLEDGMENTS

This study was supported by a Discovery Grant from the Natural Sciences and Engineering Research Council (NSERC) of Canada to PPR (#119057) and SMB (#298613). The authors also

acknowledge the help of colleagues Sergio Dominguez López and Giovanni Hernandez for data analysis and presentation.

FIGURE LEGENDS

Figure 1: Sagittal view of the rat's brain indicating the stimulation and lesion sites. Each rat was implanted with stimulation electrodes at the LH and DR, and lesion electrodes at the MFB and LHb, which is situated within the DDC.

Figure 2: Changes in reward thresholds during DR stimulation. Data were obtained before and after the lesions and are illustrated by symbols representing the mean ± standard deviation (stdve) of three threshold values in $\log_{10}$ units. The arrows indicate the day and location of the lesions, and the current intensities used are illustrated on top of each graph. Grey symbols represent post-lesion 1 values that are significantly different from baseline values, whereas black symbols represent post-lesion 2 values that are significantly different from post-lesion 1 values.

Figure 3: Changes in maximal response rates during DR stimulation. The maximal response rates were obtained at 1, 11, 15 and 25 days following the first lesion and are expressed in% of baseline values. The arrows indicate the day and location of the lesions, and the current intensities used are illustrated on top of each graph. Each symbol represents the mean ± stdve of three independent values. Grey symbols represent post-lesion 1 values that are significantly different from baseline values, whereas black symbols represent post-lesion 2 values that are significantly different from post-lesion 1 values.

Figure 4: Changes in reward thresholds during LH stimulation. Data were obtained before and after the lesions and are illustrated by symbols representing the mean ± standard deviation (stdve) of three threshold values in $\log_{10}$ units. The arrows indicate the day and location of the lesions, and the current intensities used are illustrated on top of each graph. Grey symbols represent post-lesion 1 values that are significantly different from baseline values, whereas black symbols represent post-lesion 2 values that are significantly different from post-lesion 1 values.

Figure 5: Changes in maximal response rates during LH stimulation. The maximal response rates were obtained at 1, 11, 15 and 25 days following the first lesion and are expressed in% of baseline values. The arrows indicate the day and location of the lesions, and the current intensities used are illustrated on top of each graph. Each symbol represents the mean ± stdve of three independent values. Grey symbols represent post-lesion 1 values that are significantly different from baseline values, whereas black symbols represent post-lesion 2 values that are significantly different from post-lesion 1 values.

Figure 6: Histological reconstructions of the electrolytic lesions and the locations of the tips of the stimulation electrodes of group 1. The number above each graph indicates the distance in mm posterior to bregma (from left to right: MFB, DDC, LH, DR). The lesion damage is illustrated in grey, and the black dots represent the stimulation site. Drawings were taking and adapted from the Paxinos and Watson atlas of the rat brain (Paxinos G. and Watson C., 1997).

Figure 7: Histological reconstructions of the electrolytic lesions and the locations of the tips of the stimulation electrodes of group 2. The number above each graph indicates the distance in mm posterior to bregma (from left to right: MFB, DDC, LH, DR). The lesion damage is illustrated in grey, and the black dots represent the stimulation site. Drawings were taking and adapted from the Paxinos and Watson atlas of the rat brain (Paxinos G. and Watson C., 1997).

Figure 8: Thionin staining of coronal brain sections of an individual rat showing a lesion in the DDC (left) and the MFB (right). Abbreviations: medial habenula (MHb); region of hippocampus proper (CA); zona incerta (ZI).

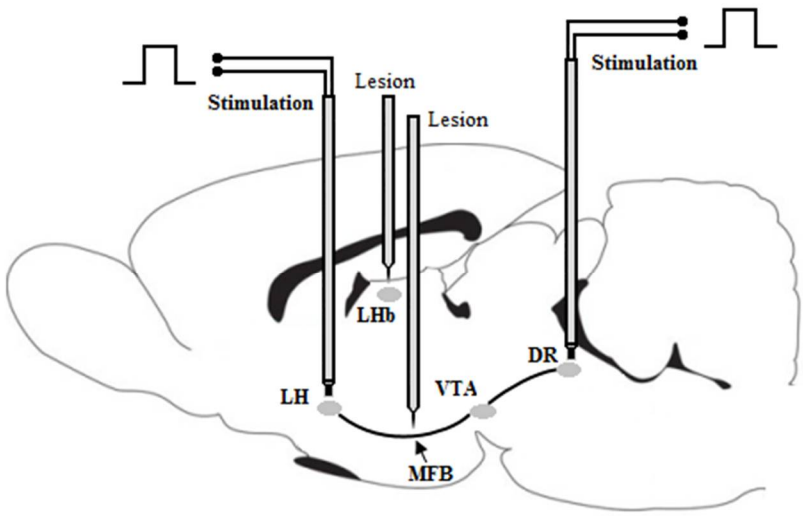

Figure 1

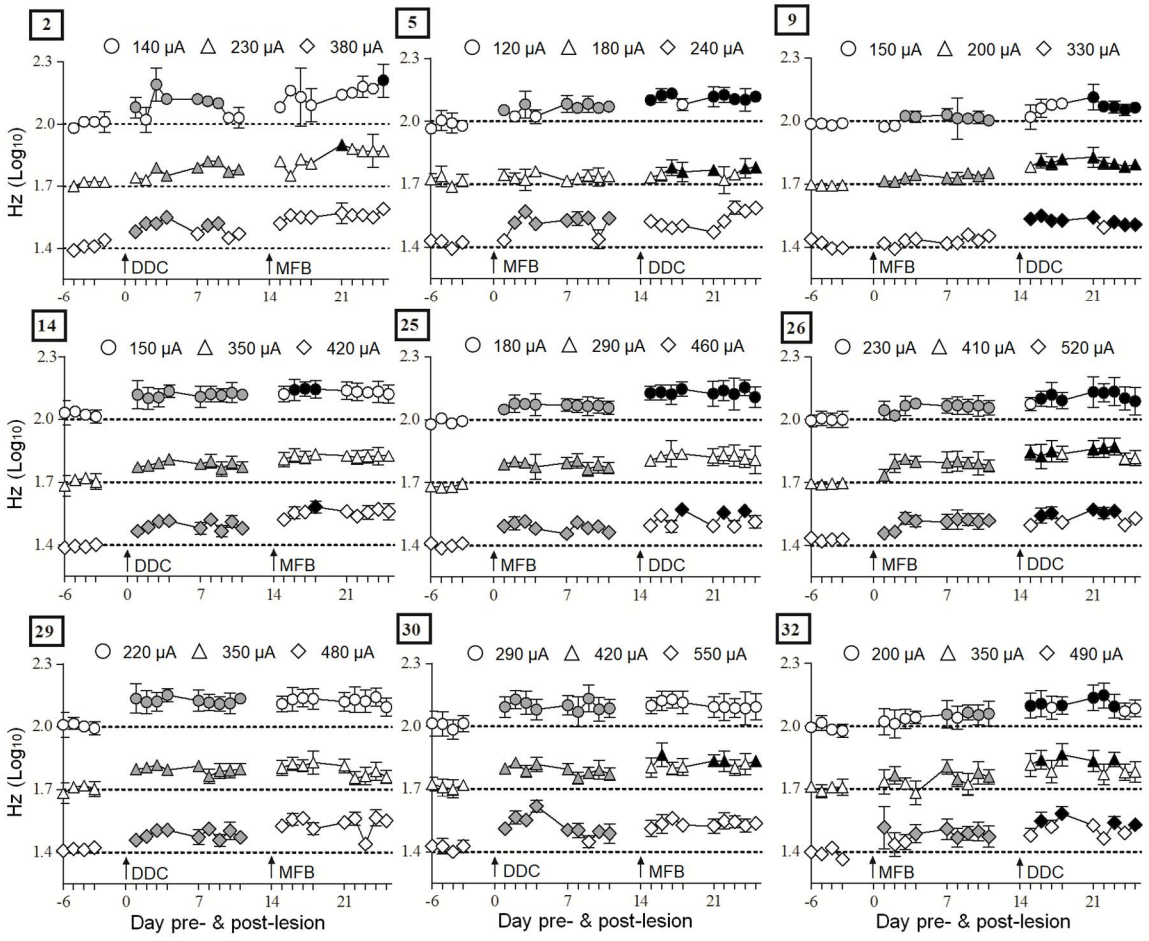
2
140 µA
230 µA
380 µA
5
120 µA
180 µA
240 µA
9
150 µA
200 µA
330 µA
14
150 µA
350 µA
420 µA
25
180 µA
290 µA
460 µA
26
230 µA
410 µA
520 µA
29
220 µA
350 µA
480 µA
30
290 µA
420 µA
550 µA
32
200 µA
350 µA
490 µA
Hz (Log10)
DDC
MFB
Day pre- & post-lesion

Figure 2

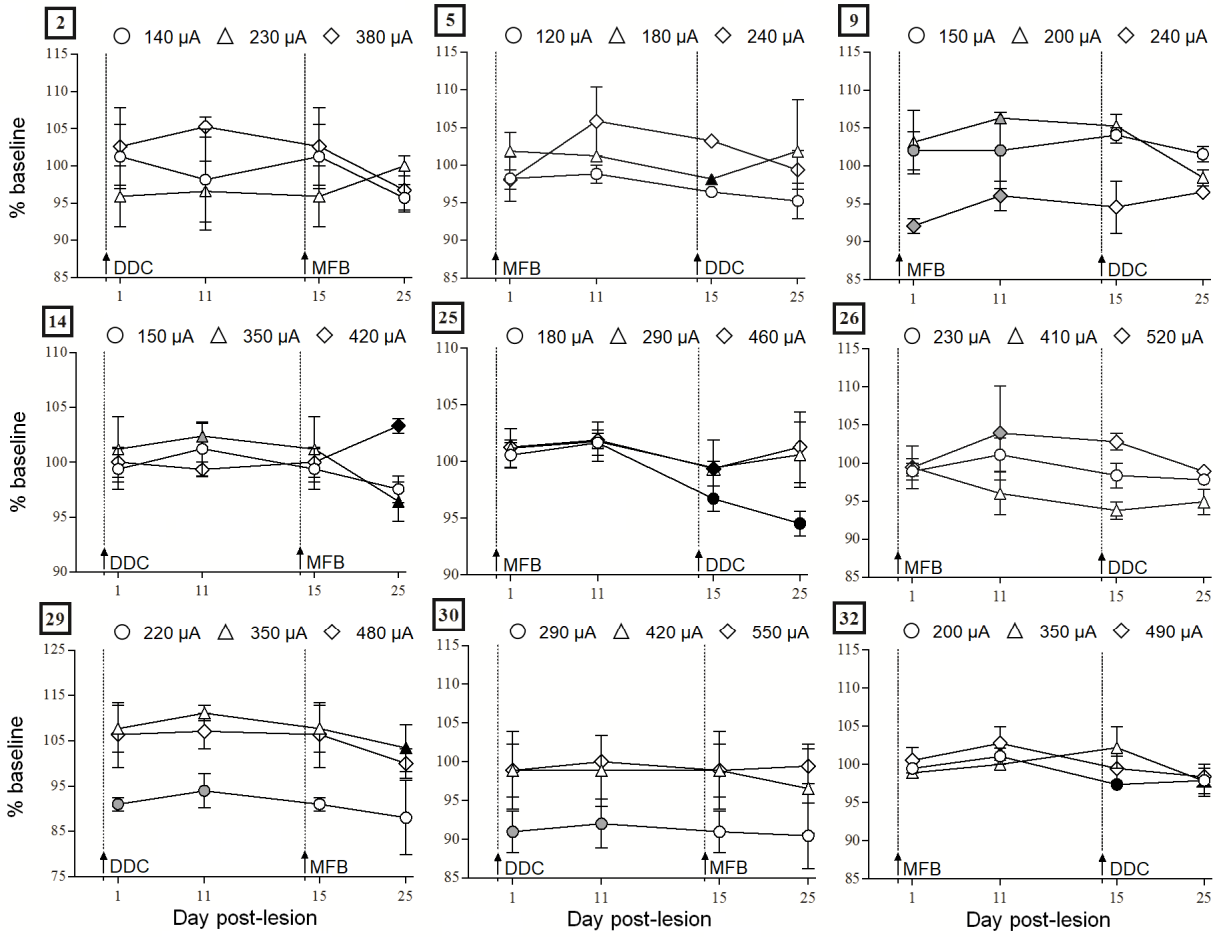
2
140 µA
230 µA
380 µA
5
120 µA
180 µA
240 µA
9
150 µA
200 µA
240 µA
14
150 µA
350 µA
420 µA
25
180 µA
290 µA
460 µA
26
230 µA
410 µA
520 µA
29
220 µA
350 µA
480 µA
30
290 µA
420 µA
550 µA
32
200 µA
350 µA
490 µA
% baseline
DDC
MFB
Day post-lesion

Figure 3

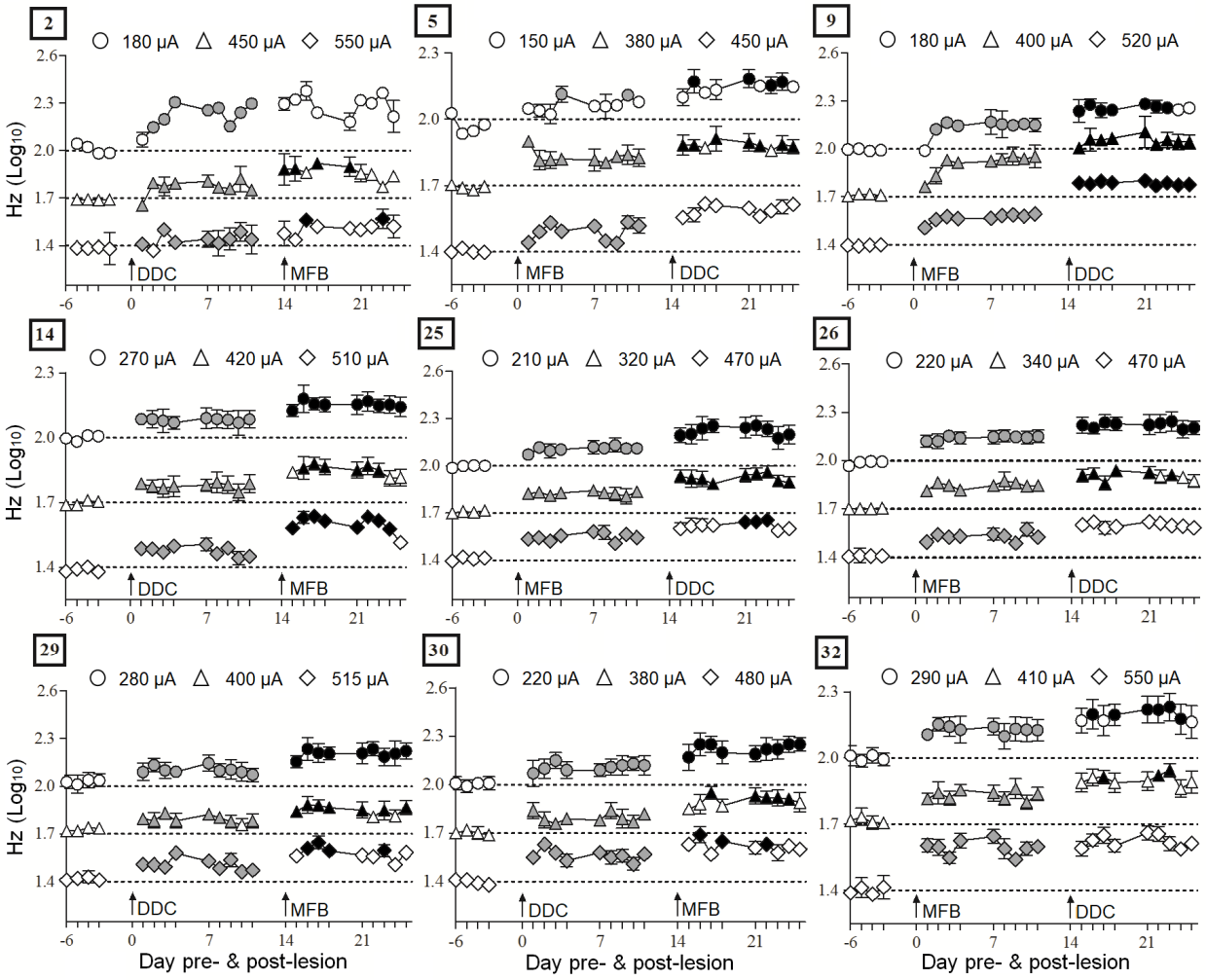
2
180 µA
450 µA
550 µA
5
150 µA
380 µA
450 µA
9
180 µA
400 µA
520 µA
14
270 µA
420 µA
510 µA
25
210 µA
320 µA
470 µA
26
220 µA
340 µA
470 µA
29
280 µA
400 µA
515 µA
30
220 µA
380 µA
480 µA
32
290 µA
410 µA
550 µA
Hz (Log10)
DDC
MFB
Day pre- & post-lesion

Figure 4

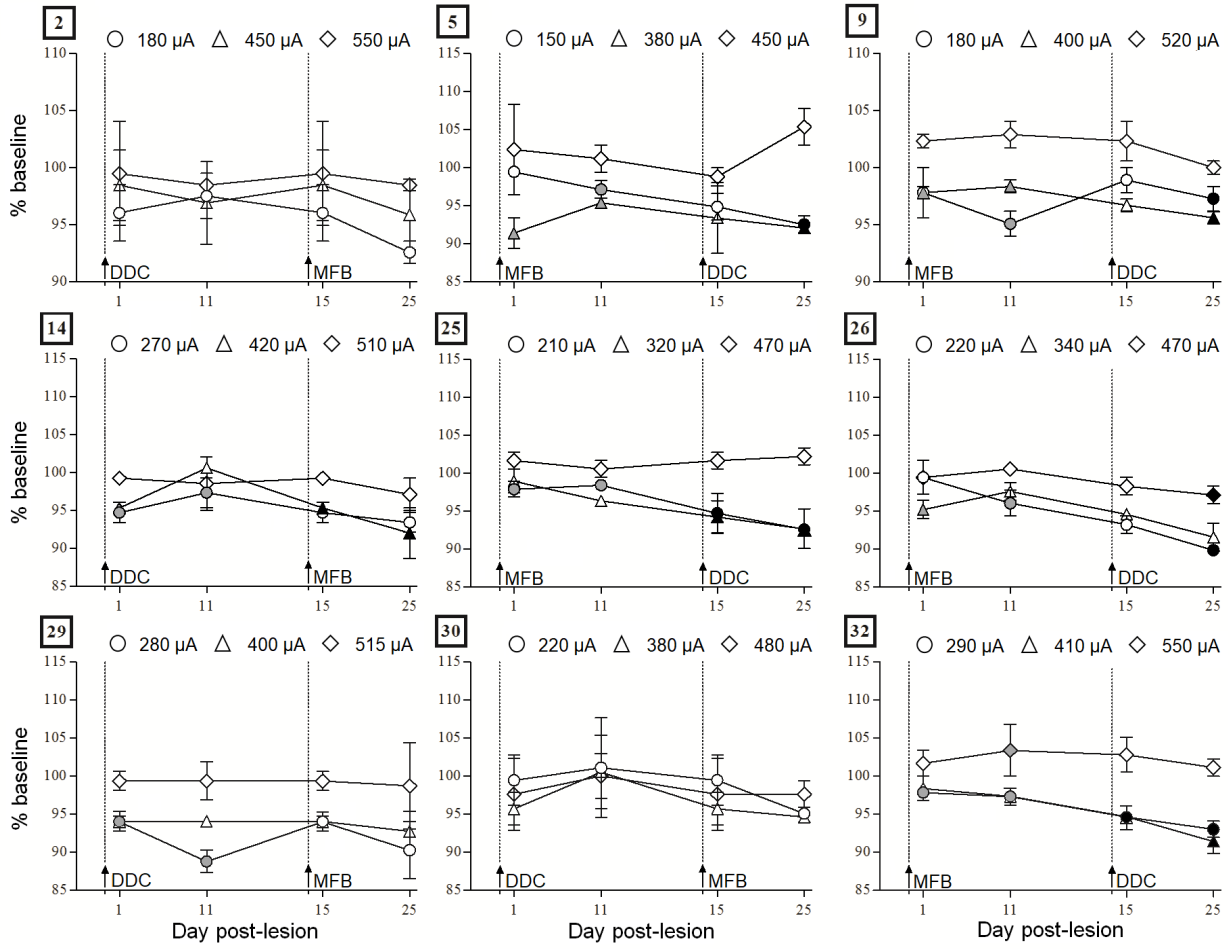
2
180 µA
450 µA
550 µA
5
150 µA
380 µA
450 µA
9
180 µA
400 µA
520 µA
14
270 µA
420 µA
510 µA
25
210 µA
320 µA
470 µA
26
220 µA
340 µA
470 µA
29
280 µA
400 µA
515 µA
30
220 µA
380 µA
480 µA
32
290 µA
410 µA
550 µA
% baseline
DDC
MFB
Day post-lesion

Figure 5

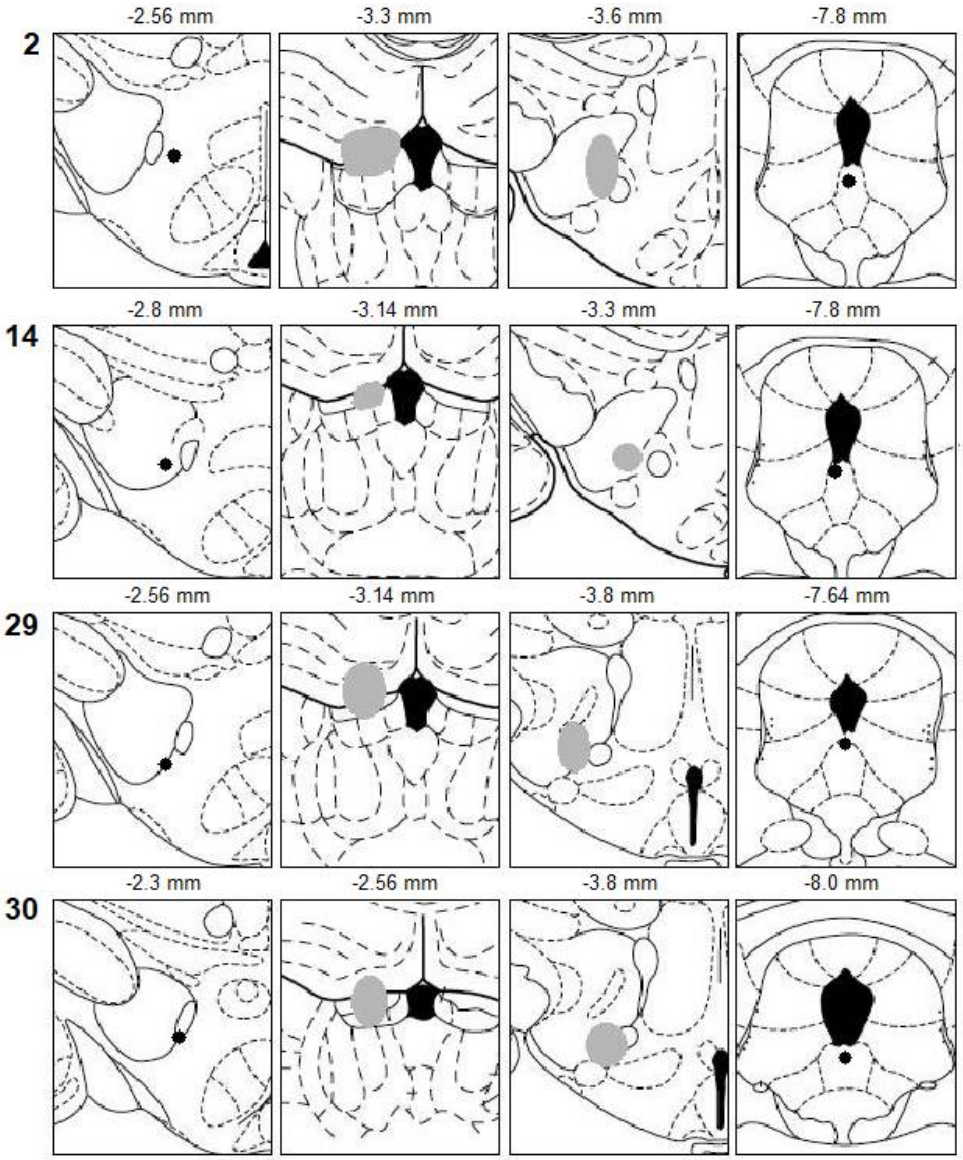
2
-2.56 mm
-3.3 mm
-3.6 mm
-7.8 mm
14
-2.8 mm
-3.14 mm
-3.3 mm
-7.8 mm
29
-2.56 mm
-3.14 mm
-3.8 mm
-7.64 mm
30
-2.3 mm
-2.56 mm
-3.8 mm
-8.0 mm

Figure 6

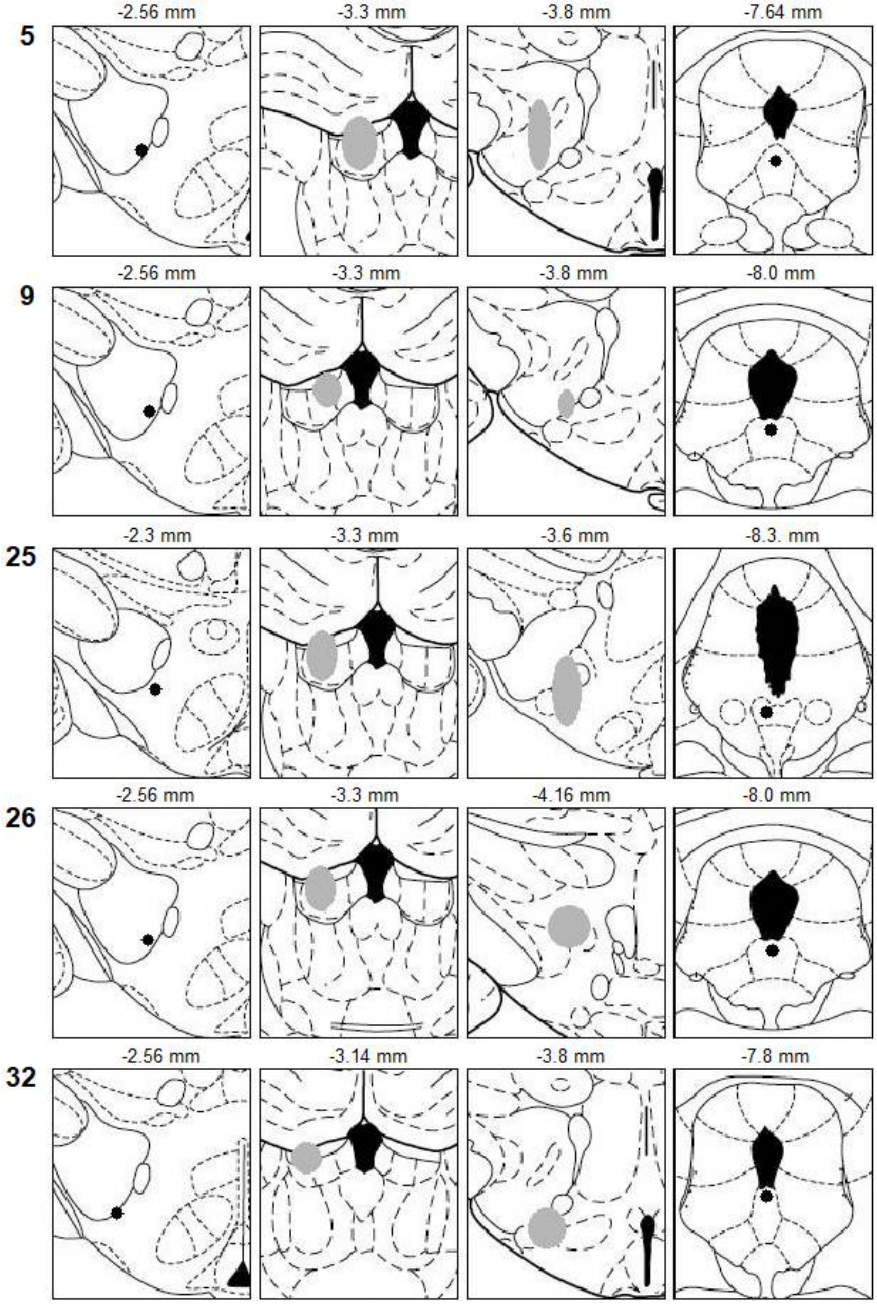
5
-2.56 mm
-3.3 mm
-3.8 mm
-7.64 mm
9
-2.56 mm
-3.3 mm
-3.8 mm
-8.0 mm
25
-2.3 mm
-3.3 mm
-3.6 mm
-8.3. mm
26
-2.56 mm
-3.3 mm
-4.16 mm
-8.0 mm
32
-2.56 mm
-3.14 mm
-3.8 mm
-7.8 mm

Figure 7

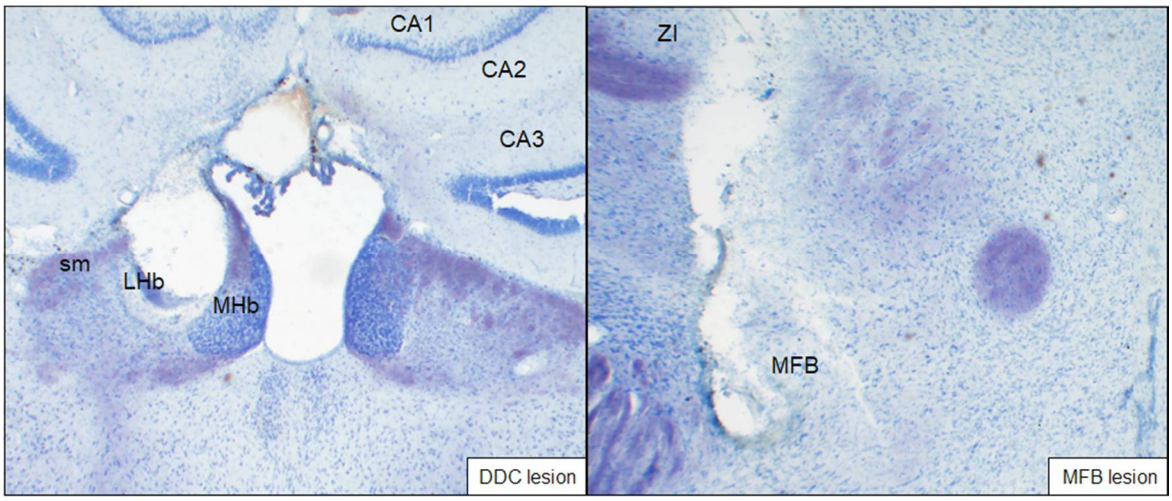

Figure 8

REFERENCES

Annau Z (1978) Electrical self-stimulation of the brain: a model for the behavioral evaluation of toxic agents. Environ Health Perspect 26:59-67.

Arvanitogiannis A, Waraczynski M, Shizgal P (1996a) Effects of excitotoxic lesions of the basal forebrain on MFB self-stimulation. Physiol Behav 59:795-806.

Arvanitogiannis A, Flores C, Pfaus JG, Shizgal P (1996b) Increased ipsilateral expression of Fos following lateral hypothalamic self-stimulation. Brain Res 720:148-154.

Beretta CA, Dross N, Guiterrez-Triana JA, Ryu S, Carl M (2012) Habenula circuit development: past, present, and future. Front Neurosci 6:51.

Bergeron S, Rompre PP (2013) Blockade of ventral midbrain NMDA receptors enhances brain stimulation reward: a preferential role for GluN2A subunits. Eur Neuropsychopharmacol 23:1623-1635.

Bianco IH, Wilson SW (2009) The habenular nuclei: a conserved asymmetric relay station in the vertebrate brain. Philos Trans R Soc Lond B Biol Sci 364:1005-1020.

Bielajew C, Shizgal P (1986) Evidence implicating descending fibers in self-stimulation of the medial forebrain bundle. J Neurosci 6:919-929.

Boye SM, Rompre PP (2000) Behavioral evidence of depolarization block of dopamine neurons after chronic treatment with haloperidol and clozapine. J Neurosci 20:1229-1239.

Gagnon D, Parent M (2014) Distribution of VGLUT3 in highly collateralized axons from the rat dorsal raphe nucleus as revealed by single-neuron reconstructions. PLoS One 9:e87709.

Gallistel CR, Leon M, Waraczynski M, Hanau MS (1991) Effect of current on the maximum possible reward. Behav Neurosci 105:901-912.

Gallistel CR, Leon M, Lim BT, Sim JC, Waraczynski M (1996) Destruction of the medial forebrain bundle caudal to the site of stimulation reduces rewarding efficacy but destruction rostrally does not. Behav Neurosci 110:766-790.

Gifuni AJ, Jozaghi S, Gauthier-Lamer AC, Boye SM (2012) Lesions of the lateral habenula dissociate the reward-enhancing and locomotor-stimulant effects of amphetamine. Neuropharmacology 63:945-957.

Gratton A, Wise RA (1983) Brain stimulation reward in the lateral hypothalamic medial forebrain bundle: mapping of boundaries and homogeneity. Brain Res 274:25-30.

Hikosaka O (2010) The habenula: from stress evasion to value-based decision-making. Nat Rev Neurosci 11:503-513.

Huston JP (1982) Searching for the neural mechanism of reinforcement (of stamping in). In: The Neural Basis of Feeding andReward, (Hoebel BG, Novin D, eds), pp 75-83. New York,: Academic Press.

Huston JP, Borbely AA (1973) Operant conditioning in forebrain ablated rats by use of rewarding hypothalamic stimulation. Brain Res 50:467-472.

Huston JP, Borbely AA (1974) The thalamic rat: general behavior, operant learning with rewarding hypothalamic stimulation, and effects of amphetamine. Physiol Behav 12:433-448.

Ikemoto S (2007) Dopamine reward circuitry: two projection systems from the ventral midbrain to the nucleus accumbens-olfactory tubercle complex. Brain Res Rev 56:27-78.

Janas JD, Stellar JR (1987) Effects of knife-cut lesions of the medial forebrain bundle in self-stimulating rats. Behav Neurosci 101:832-845.

Morissette MC, Boye SM (2008) Electrolytic lesions of the habenula attenuate brain stimulation reward. Behav Brain Res 187:17-26.

Murray B, Shizgal P (1991) Anterolateral lesions of the medial forebrain bundle increase the frequency threshold for self-stimulation of the lateral hypothalamus and ventral tegmental area in the rat. Psychobiology 19:135-146.

Murray B, Shizgal P (1994) Evidence implicating both slow- and fast-conducting fibers in the rewarding effect of medial forebrain bundle stimulation. Behav Brain Res 63:47-60.

Murray B, Shizgal P (1996a) Behavioral measures of conduction velocity and refractory period for reward-relevant axons in the anterior LH and VTA. Physiol Behav 59:643-652.

Murray B, Shizgal P (1996b) Attenuation of medical forebrain bundle reward by anterior lateral hypothalamic lesions. Behav Brain Res 75:33-47.

Omelchenko N, Bell R, Sesack SR (2009) Lateral habenula projections to dopamine and GABA neurons in the rat ventral tegmental area. Eur J Neurosci 30:1239-1250.

Ornstein K, Huston JP (1975) Influence of 6-hydroxydopamine injections in the substantia nigra on lateral hypothalamic reinforcement. Neurosci Lett 1:339-342.

Paxinos G., Watson C. (1997) The Rat Brain in Stereotaxic Coordinates. 3rd ed. Academic Press, San Diego, CA.

Poller WC, Madai VI, Bernard R, Laube G, Veh RW (2013) A glutamatergic projection from the lateral hypothalamus targets VTA-projecting neurons in the lateral habenula of the rat. Brain Res 1507:45-60.

Proulx CD, Hikosaka O, Malinow R (2014) Reward processing by the lateral habenula in normal and depressive behaviors. Nat Neurosci 17:1146-1152.

Root DH, Hoffman AF, Good CH, Zhang S, Gigante E, Lupica CR, Morales M (2015) Norepinephrine activates dopamine D4 receptors in the rat lateral habenula. J Neurosci 35:3460-3469.

Shen X, Ruan X, Zhao H (2012) Stimulation of midbrain dopaminergic structures modifies firing rates of rat lateral habenula neurons. PLoS One 7:e34323.

Simmons JM, Gallistel CR (1994) Saturation of subjective reward magnitude as a function of current and pulse frequency. Behav Neurosci 108:151-160.

Simmons JM, Ackermann RF, Gallistel CR (1998) Medial forebrain bundle lesions fail to structurally and functionally disconnect the ventral tegmental area from many ipsilateral forebrain nuclei: implications for the neural substrate of brain stimulation reward. J Neurosci 18:8515-8533.

Sutherland RJ (1982) The dorsal diencephalic conduction system: a review of the anatomy and functions of the habenular complex. Neurosci Biobehav Rev 6:1-13.

Vachon MP, Miliaressis E (1992) Dorsal diencephalic self-stimulation: a movable electrode mapping study. Behav Neurosci 106:981-991.

Varga V, Kocsis B, Sharp T (2003) Electrophysiological evidence for convergence of inputs from the medial prefrontal cortex and lateral habenula on single neurons in the dorsal raphe nucleus. Eur J Neurosci 17:280-286.

Wang RY, Aghajanian GK (1977) Physiological evidence for habenula as major link between forebrain and midbrain raphe. Science 197:89-91.

Waraczynski M, Carlton E, Perkins M (1998) Midbrain periaqueductal lesions do not degrade medial forebrain bundle stimulation reward. Behav Brain Res 95:167-177.

Waraczynski MA (1988) Basal forebrain knife cuts and medial forebrain bundle self-stimulation. Brain Res 438:8-22.

Zhang F, Zhou W, Liu H, Zhu H, Tang S, Lai M, Yang G (2005) Increased c-Fos expression in the medial part of the lateral habenula during cue-evoked heroin-seeking in rats. Neurosci Lett 386:133-137.

2.2 ARTICLE 2: Published in *Neuroscience*. 2016, 214-225.

Effect of electrolytic lesions of the dorsal diencephalic conduction system on the distribution of Fos-like immunoreactivity induced by rewarding electrical stimulation

Marc Fakhoury[1], David Voyer[2], Daniel Lévesque[2], Pierre-Paul Rompré[1,3]

[1]Department of Neurosciences, Faculty of Medicine, Université de Montréal, Montreal, Quebec, Canada

[2]Faculty of Pharmacy and FRQ-S Research Group on Central Nervous System, Université de Montréal, Montreal, Quebec, Canada

[3]FRQ-S Research Group in Behavioral Neurobiology, Concordia University, Montreal, Quebec, Canada

AUTHOR CONTRIBUTIONS

I wrote the first draft of the manuscript, conducted all the behavioral experiments in the laboratory of Dr. Pierre-Paul Rompré, and performed all the immunohistochemical analyses in the laboratory of Dr. Daniel Lévesque with the help of David Voyer.

ABSTRACT

The dorsal diencephalic conduction system (DDC) is an important pathway of the brain reward circuitry, linking together forebrain and midbrain structures. The present work was aimed at describing the effect of a DDC lesion on the distribution of Fos-like immunoreactivity (FLIR) following intracranial self-stimulation (ICSS) of the lateral hypothalamus (LH). Rats were implanted with monopolar electrodes and divided into three groups; the first two groups were trained to self-stimulate at the LH, whereas the third group received no stimulation and served as a control. Among the two groups that were trained for ICSS, one of them received a lesion at the DDC and was tested for ICSS on the subsequent 5 days. On the last day of testing, control rats were placed in operant chambers without receiving any stimulation, and the remaining rats were allowed to receive the stimulation for 1h. All rats were then processed for FLIR. As previously shown, a lesion at the DDC resulted in significant attenuations of the rewarding effectiveness of LH stimulation. Results also show a higher FLIR in several reward-related areas following LH stimulation, especially in the hemisphere ipsilateral to the stimulation electrode. Compared to non-lesioned rats, lesioned animals had lower FLIR in certain brain regions, suggesting that those regions that were activated by the rewarding stimulation may be functionally interconnected with the DDC.

Keywords: c-fos; Dorsal diencephalic conduction system; Lateral habenula; Lateral hypothalamus

INTRODUCTION

Intracranial self-stimulation (ICSS) holds great promise in understanding the neural elements involved in reward and goal-directed behaviors, and offers a valuable tool for their anatomical mapping and functional characterization. Electrical stimulation of certain regions in the brain triggers a reward signal that produces an operant response in rodents; animals will continuously self-administer the rewarding stimulation for long periods of time, neglecting other essential stimuli such as food and water. The vast majority of psychophysical studies aimed at deciphering the sites that support ICSS have focused on the medial forebrain bundle (MFB), the primary pathway connecting limbic forebrain to midbrain structures. The results of these studies show that the substrate that is directly activated by rewarding MFB stimulation includes fine, myelinated fibers with relatively fast conduction velocities, short refractory periods, and trajectories that run between the lateral hypothalamus (LH) and the ventral tegmental area (VTA) (Shizgal et al., 1980; Bielajew and Shizgal, 1986; Murray and Shizgal, 1996b, a). From single-unit recordings, we also know that axons within the LH and VTA have properties that are compatible with behaviorally derived estimates for the "first-stage" reward neurons of the MFB (Rompre and Shizgal, 1986; Shizgal et al., 1989).

Another pathway that serves as a relay between forebrain and midbrain structures is the dorsal diencephalic conduction system (DDC). The DDC is composed of three essential components: the habenula, which has a lateral and medial subdivision; the stria medullaris (SM), which receives inputs from the basal ganglia and other limbic structures involved in reward; and the fasciculus retroflexus (fr), which arises from the habenula and projects to the midbrain (Sutherland, 1982; Bianco and Wilson, 2009). The lateral habenula (LHb), which is located centrally along the DDC, has recently received widespread attention because of its ability to regulate the activity of

mesolimbic and nigrostriatal dopamine neurons (Ji and Shepard, 2007; Hong et al., 2011; Barrot et al., 2012). Several studies have shown that the DDC is anatomically connected with the LH, as evidenced by the existence of glutamatergic projections from the LH to the LHb (Poller et al., 2013; Stamatakis et al., 2016). If, indeed, first-stage neurons stimulated at the level of the LH send their projections through the DDC, then it might be expected that a lesion within the DDC will impair the reinforcing effect induced by stimulation of reward-relevant neurons in the LH. Recently, this hypothesis had led to a series of behavioral studies employing lesions along this pathway. Previous work by our group and others showed that electrolytic lesions at the LHb and/or the SM produce large and long-lasting attenuations in the rewarding effectiveness of LH stimulation (Morissette and Boye, 2008; Fakhoury et al., 2016). Although the results of these studies suggest that the DDC is involved in the brain reward circuitry, they don't provide any information on the populations of neurons that are activated by the rewarding stimulation and functionally disconnected by the lesion. The present study was aimed at filling this gap by combining electrolytic lesions at the DDC with immunolabeling for Fos protein, which serves as an index of neuronal activity (Hoffman et al., 1993).

Expression of Fos, an immediate early gene product, is rapidly induced by a variety of stimuli, and has been extensively used to visualize neurons that are activated by ICSS. Studies using this neuronal marker have shown that the LH stimulation increases Fos-like immunoreactivity (FLIR) in several forebrain and midbrain nuclei including the medial prefrontal cortex (mPFC), the nucleus accumbens (NAc), the bed nucleus of the stria terminalis (BNST), the caudate-putamen (CPu) and the ventral tegmental area (VTA) (Flores et al., 1997; Hunt and McGregor, 1998, 2002; Aldavert-Vera et al., 2013). In the present work, we sought to determine whether the brain regions that are activated by LH stimulation continue to be active following a lesion at the DDC. A

particular attention was given to regions within the forebrain, midbrain and brainstem that are involved in brain stimulation reward or that are anatomically connected with the DDC (Herkenham and Nauta, 1977; Araki et al., 1988). If the DDC participates in the transmission of the reward signal, then a lesion within this pathway should significantly reduce the level of Fos in brain regions that are subserved by its activity.

MATERIAL AND METHODS

Subjects

A total of 28 male rats of the Long-Evans strain (Charles river, QC, Canada), weighing 300-400 g at the time of surgery, served as experimental subjects. Animals were housed individually in a temperature and humidity controlled room with a 12-h light–dark cycle and ad libitum access to food and water. All experiments were carried out in compliance with the ethical guidelines of the Canadian Council on Animal Care, and were approved by the institutional animal care committee. Effort was made to minimize the number of animals used and their discomfort.

Surgical procedure

The animals were allowed at least 5 days of acclimatization to the housing conditions before the beginning of surgery. At the day of surgery, rats were put under general anesthesia with a mixture of isoflurane (5%) and oxygen (0.6 L/min), and mounted in a stereotaxic apparatus. An analgesic, Rimadyl (5 mg/kg), was then administered by subcutaneous injection, and the level of anesthesia was gradually reduced to 2.5-3.5%. After making a small incision on the scalp, a stainless steel wire attached to a male Amphenol connector was wrapped around four to five miniature screws that were threaded into the cranium. This served as the anodal current path for the stimulation.

Stainless steel electrodes coated with Epoxylite, except for the dome-shaped tip, were then implanted ipsilaterally at the LH (anterior: -2.5 mm, lateral: +1.7 mm, ventral: -8.6 mm) and DDC (anterior: -3.3 mm, lateral: +0.65 mm, ventral: -4.5 mm) using coordinates from the Paxinos and Watson atlas of the rat brain (Paxinos and Watson, 1997). The electrode assembly was then secured to the skull with acrylic dental cement. At the end of surgery, rats received another dose of analgesic and were allowed 7 days of recovery prior to behavioral training.

Group designation

Of the 28 rats that were initially used in this study, 7 rats were excluded from data analysis either because of brain tissue damage (n=3), removal of the electrode assembly after surgery (n=2), or severe post-surgical pain (n=2). The remaining 21 rats that completed the experiment were equally divided into three groups designated as follow: “no lesion”, “lesion” and “sham (n=7/group). Rats from the “no lesion” group, which will be referred to as “non-lesioned rats”, consist of lesion-naïve animals that were trained and tested for LH self-stimulation. This group was used to characterize the distribution of FLIR following the stimulation. Rats from the “lesion” group were trained for LH self-stimulation similar to non-lesioned rats, but received a lesion at the DDC and were tested for the stimulation on the subsequent days. This group was used to determine whether the same set of neurons that are active in non-lesioned rats continue to be active following a lesion. Finally, animals in the “sham” group consist of surgically-operated rats that did not received any stimulation nor lesion. This group served as a control for ICSS and was used to account for extrinsic factors such as daily manipulation of animals.

Behavioral training

One week after surgery, rats were placed individually in self-stimulation cages made from polymer walls and one front Plexiglas wall to allow constant viewing. Each chamber was encased in ventilated melamine boxes to minimize disturbance from external noise, and was equipped with a nose poke opening (3 cm wide and 3 cm deep) located 2 cm above the metal rod floor **(Figure 1A)**. Each nose poke triggered the delivery of a single 400-ms train of rectangular cathodal pulses of 0.1 ms in duration, followed by a period of 600 ms during which no pulses could be generated. Lesioned and non-lesioned rats were trained to self-administer a train of pulses using a FR1 schedule, whereas sham rats were left in the self-stimulating boxes without receiving any stimulation. At the beginning of the training, the current intensity was set at 250 μA, and a fixed frequency of 41 pulses per train was used for LH stimulation. The current intensity was subsequently increased in increments of 100 μA (up to 900 μA) in rats that were not responding to the initial parameters of stimulation. Once the operant response was acquired, rats were allowed to self-stimulate freely for at least 2 days at constant stimulation parameters so as to support consistent rates of responding with minimal motoric side effects. Rats were then allowed to self-administer the electrical stimulation during discrete 55 s trials separated by 15 s intervals during which no stimulation could be delivered **(Figure 1A)**. Five trains of non-contingent priming stimulation (1 Hz), followed by a 5 s adaptation period, were used to signal the beginning or the onset of each discrete trial **(Figure 1A)**. The pulse number within each train was systematically reduced by approximately 0.1 $\log_{10}$ unit after each trial, and at the end of the last trial, a plot of the response rate as a function of the pulse number was generated. A single session consisted of 12 different trials with stimulation frequencies ranging from 12-41 pulses per train. The reward threshold (M50), defined as the pulse number supporting a response rate equal to 50% of the

maximal response, was measured from each response-frequency (R/F) curve to assess the rewarding effectiveness of the stimulation.

Behavioral testing and electrolytic lesions

Lesioned and non-lesioned rats were tested for LH self-stimulation through nose-poke responding. The current intensity of the stimulation was adjusted so as to obtain a M50 of approximately 20 pulses per train in every rat. Each testing session began with a warm-up phase that was excluded from data analysis, followed by 3 consecutive sets of trials from which R/F curves were obtained. A single R/F curve consisted of a plot of the total number of nose pokes per trial at different stimulation frequencies. Rats from all the groups were manipulated at the same time in order to avoid differences due to extraneous factors such as the effect of order. After at least 4 days of stable operant response (M50 ~ 20 pulses per train), rats in the lesion group received a lesion at the DDC by means of an electrolytic anodal direct current (100 μA for 30 s). They were then tested 24 h later for 5 consecutive days for LH self-stimulation, as were rats from the "no lesion" group. On the final test day, lesioned and non-lesioned rats were placed in self-stimulation cages and were allowed to administer the rewarding LH stimulation for 1h at the same current intensity used in previous tests, but with a frequency of stimulation corresponding to the M50 plus 0.1 $\log_{10}$ units. Rats in the sham group were put in the stimulation cages during the same time period as the other two groups, but were not allowed to self-stimulate. A timeline of the experimental protocol is illustrated in **Figure 1B**.

Fos immunohistochemistry

Fifteen minutes after the end of the last test session, rats were anesthetized with a single intraperitoneal injection of urethane (1.4–2.0 g/kg), and the stimulation sites were marked by means of a direct anodal current (0.1 mA during 60 s). Rats were then immediately perfused with 0.9% saline followed by a formaldehyde solution that contains 3% potassium hexacyanoferrate II, 3% potassium hexacyanoferrate III and 0.5% trichloroacetic acid. When the perfusion was complete, the brains were taken out, post-fixed in 10% formalin, and stored in 30% sucrose solution for two days. They were then quickly frozen in 2-methylpentane on dry ice and kept in -80°C. During brain slicing, a small puncture was made with a knife along the rostral–caudal axis of the hemisphere contralateral to the stimulation to enable its differentiation from the other hemisphere. The brains were subsequently cut at -20°C into 30 μm coronal sections and processed for FLIR as previously described (Marcangione and Rompre, 2008). Briefly, sections were first rinsed with phosphate-buffered saline (PBS) and incubated in 0.3% hydrogen peroxide for 30 min. After three additional washes in PBS, sections were incubated with 10% goat serum in antibody diluent (0.1 M PBS containing 0.05% Tween 20 and 1% bovine serum albumin) for 30 min and then immunostained with an affinity-purified rabbit anti-c-Fos polyclonal antibody overnight at 4°C. On the following day, sections were washed three times with PBS and incubated in a biotinylated goat anti-rabbit antibody for 90 min at room temperature. After three subsequent washes with PBS, sections were incubated in an avidin-biotin-horseradish-peroxidase complex (Vectastain Standard ABC kit, Vector Laboratories) for 90 min at room temperature. The tissues were then rinsed in PBS and Tris buffer, and developed with 0.05% 3,3'-diamino-benzidine with 0.015% hydrogen peroxide (DAB substrate kit for peroxidase, Vector Laboratories). Finally, sections were washed three times with PBS, mounted onto gelatin-coated glass slides (Ultident Scientific), and allowed to air-dry overnight. They were then dehydrated, cleared in xylene and

coverslipped with Permount media (Fisher Scientfific). A negative control with no primary antibody was included in the study.

Histology

Sections were mounted onto gel-coated slides and air-dried for at least 1 day prior to being rinsed in distilled water, dehydrated in ethanol, and stained for Nissl substance using Thionin. Slices were then cleared in xylene, coverslipped with Permount, and analyzed under light microscopy. The location of each electrode tip was determined through the positioning of structural landmarks, and drawings of the stimulation site and lesion size were made using the Paxinos and Watson atlas of the rat brain (Paxinos and Watson, 1997).

Data analysis

Mean values of M50 and maximal response rates were calculated daily for each rat using the last three R/F curves obtained during the behavioral test. Post-lesion values for the M50 and maximal response rate in rats were expressed as a percentage of the baseline, which was calculated by averaging the corresponding values obtained during the 4 days preceding the lesion. Differences in M50 and maximal response rate values were assessed by using a repeated measures analysis of variance (ANOVA) with a level of significance set at $p < 0.05$. Tukey's honestly significant difference (HSD) was used as a post-hoc test for multiple comparison.

Regional differences in FLIR between treatment groups were assessed by comparing mean cell count using two to three consecutive sections from the following brain regions of each rat: the pedunculopontine tegmental nucleus (PPTg: -7.8 to -8.0), the dorsal raphe (DR: -7.6 to -7.8), the pontine nuclei (PN: -7.0 to -7.3), the interpeduncular nucleus (IPN: -6.3 to -6.6), the rostromedial

tegmental nucleus (RMTg: -6.3 to -6.6), the posterior VTA (VTAp: -5.6 to -5.8), the anterior VTA (VTAa: -5.2 to -5.3), the substantia nigra pars reticulata (SNr: -5.2 to -5.4), the substantia nigra pars compacta (SNc: -5.2 to -5.4), the basolateral amygdala (BLA: -2.8 to -3.1), the BNST (-0.2 to -0.3), the CPu (+0.7 to +1.0), the NAc (+1.0 to +1.2), the mPFC(+2.5 to +2.7) and the orbitofrontal cortex (OFC: +2.7 to +3.2), with coordinates expressed in mm relative to Bregma. These brain regions were selected on the basis of their anatomical connectivity with the DDC and/or their implication in the rewarding effect of LH stimulation.

FLIR was viewed under a microscope (10X ocular lens and 10X objective lens) coupled to a digital camera (Moticam 2500), and was analyzed with a computerized image analysis system (imageJ 1.48v software, Wayne Rasband, NIH). For each structure, brain regions were delineated in accordance with the structure boundaries defined in the Paxinos and Watson atlas of the rat brain (Paxinos and Watson, 1997). For image analysis, an intensity-based threshold was determined so that the maximum number of Fos-positive cells was counted without inclusion of the background staining. The number of FLIR positive cells were then separately analyzed for each brain region of interest using a two-way ANOVA with treatment groups as the between subjects variable (no lesion, lesion, and sham) and hemisphere (ipsilateral and contralateral) as the within subject variable. Tukey's HSD was used as a post-hoc test for multiple comparison and the level of significance was set at $p < 0.05$. To account for the lack of normal distribution and variance homogeneity, original data were transformed using the Box–Cox transformation. Normal distribution of the data and homogeneity of variance were tested by means of the Kolmogorov-Smirnov (KS) and the Levene's Test for Equality of Variances respectively, with a level of significance set at $p < 0.05$. All data fitted normal distribution and variance homogeneity after transformation ($p > 0.05$). We also examined effect sizes to compare the mean values between

treatment groups with respect to the magnitude of the difference. The results are reported as partial eta squared (ηp^2) values. A ηp^2 value of 0.01, 0.06, and 0.14 are considered as small, medium, and large effect sizes respectively (Lakens, 2013).

RESULTS

Histological analysis and behavioral testing

Location tips of the LH stimulation electrodes for lesioned and non-lesioned rats are shown in **Figure 2A**, on tracings of coronal plates taken from the Paxinos and Watson atlas of the rat brain (Paxinos and Watson, 1997). Stimulation sites were located approximately 2.12–2.80 mm posterior to Bregma, near or within the defined boundaries of the LH. **Figure 2B** shows cross-sections of the brain of lesioned rats (n=7) where the largest area of the lesion was observed. The lesions had two-dimensional sizes ranging from approximately 0.06 to 0.28 mm^2, and appeared to substantially target regions within the SM and LHb, while leaving the medial habenula (MHb) intact or minimally damaged.

To determine the overall group effect of a DDC lesion on the rewarding effectiveness of LH stimulation, mean values of M50 and maximal response rates were obtained from R/F curves before the lesion and up to 5 days thereafter. As shown in a previous report from our group (Fakhoury et al., 2016), electrolytic lesions at the DDC resulted in substantial increases in M50 during LH stimulation **(Figure 3A)**. Notably, damage within the DDC produced a gradual increase in M50 (up to 22.4%), with significant effects observed starting the third test day following the lesion ($p < 0.05$) **(Figure 3A)**. The lesion had no effect on the maximal response rate ($p > 0.05$) **(Figure 3B)**. The M50 and maximal response rates were also obtained from non-lesioned rats. While no changes in M50 were observed during the 5 days of testing in this group of rats **(Figure**

2A), a significant increase in the maximal response rate was observed at day 4 post-lesion **(Figure 3B)**.

Fos induction following ICSS

In this study, Fos-immunohistochemistry was used to identify the brain regions that were activated by the electrical stimulation of the LH. **Figure 4** depicts representative micrographs of FLIR in the contralateral and ipsilateral hemispheres of the BNST and VTAa from one subject in each treatment group.

We first examined the effect of LH stimulation on FLIR in the ipsilateral and contralateral hemispheres of several brain regions. Following LH stimulation, numerous brain regions were found to exhibit FLIR, with the highest level in the BLA, SNc and PN (> 50 cells/mm^2), and the lowest level in the CPu (< 5 cell counts/mm^2) (Table 1). We also examined FLIR in non-lesioned rats compared to sham rats in several structures of the forebrain, midbrain and brainstem **(Figures 5-7)**. FLIR was significantly higher in non-lesioned rats compared to sham rats in all of the structures analyzed, in both the ipsilateral and contralateral hemispheres ($p < 0.05$).

We next sought to determine the effect of a DDC lesion on FLIR following LH stimulation **(Figures 5-7)**. Significant decreases in FLIR were observed in the BNST [$F_{(2, 36)}$=22.67; ηp^2=0.55; p=0.047], NAc core [$F_{(2, 36)}$=30.61; ηp^2=0.62; p=0.0089], NAc shell [$F_{(2, 36)}$=26.25; ηp^2=0.59; p=0.034], BLA [$F_{(2, 36)}$=37.18; ηp^2=0.67; p=0.0067], IPN [$F_{(2, 36)}$=10.14; ηp^2=0.36; p=0.0024], PN [$F_{(2, 36)}$=44.53; ηp^2=0.71; p=0.0024], and DR [$F_{(2, 26)}$=29.37; ηp^2=0.62; p=0.012] of lesioned rats compared to non-lesioned rats irrespective of the hemisphere. In the IPN and DR, the lesion was able to reduce FLIR to a level similar to that observed in sham-operated rats in both hemispheres,

whereas in the remaining structures, the level of Fos in lesioned rats was significantly higher to that observed in sham-operated rats ($p < 0.05$).

Interhemispheric analysis of brain regions revealed that FLIR was generally higher on the ipsilateral side of the stimulation, though statistical significance was only obtained in the BNST [$F_{(1, 36)}=6.32$; $\eta p^2=0.14$; $p=0.016$], NAc core [$F_{(1, 36)}=5.15$; $\eta p^2=0.12$; $p=0.029$], NAc shell [$F_{(1, 36)}=7.73$; $\eta p^2=0.17$; $p=0.0086$], BLA [$F_{(1, 36)}=5.92$; $\eta p^2=0.14$; $p=0.020$] and SNc [$F_{(1, 36)}=9.42$; $\eta p^2=0.20$; $p=0.0042$] independent of any level of treatment **(Figures 5-6)**. In the sham group, analysis of sections revealed very sparse FLIR (fewer than 5 Fos-positive cells) in most of the brain regions assessed **(Figures 5-7)**. No FLIR was evident in control experiments after omission of the primary antibody (not shown).

DISCUSSION

The overarching goal of this study was to use Fos immunohistochemistry to characterize the functional connectivity between the DDC and brain regions that are activated by rewarding electrical stimulation of the LH. To our knowledge, this is the first report combining Fos immunolabeling with electrolytic lesions at the DDC to determine the neural elements that are still active following LH self-stimulation. A particular attention was given to forebrain sites that are directly activated by LH or MFB self-stimulation (Flores et al., 1997; Nakahara et al., 1999), and to midbrain sites that are functionally interconnected with the DDC (Bianco and Wilson, 2009). The present behavioral data demonstrate that a lesion at the DDC produces long-lasting attenuations of the rewarding effectiveness of LH self-simulation with no effect on the maximal response rate. In addition, our immunohistochemical results show that the lesion reduced the level

of Fos in multiple brain structures related to reward, suggesting that these regions that are activated by the rewarding stimulation may be functionally interconnected with the DDC.

Effect of a DDC lesion on LH stimulation

We first investigated the functional link between the DDC and the LH by examining the effect of a DDC lesion on the rewarding effectiveness of LH self-stimulation. No significant changes in the mean values of the maximum response rates were observed following the lesion, suggesting that the motor capacity of the animals to self-administer the stimulation remained intact. However, damage to the DDC resulted in long-lasting increases in M50 that developed progressively after the lesion. The pattern of effects observed in the present study are in line with earlier investigations showing that electrolytic lesions of the DDC result in changes in M50 with no or minimal changes in the maximal response rate (Morissette and Boye, 2008; Fakhoury et al., 2016). Our finding also supports the notion that the DDC is functionally linked to reward-relevant sites along the MFB, and is in accordance with studies showing the existence of functional connections between the LHb and the LH (Poller et al., 2013; Stamatakis et al., 2016).

The lesions made in our study mostly encompassed two regions of the DDC: the LHb and the SM. Although all rats from the lesion group shared common regions of damage, the magnitude of the increase in M50 observed was different among each subject, and there were no correlation between the lesion size and the resultant effect on M50 (results not shown). The inconsistency observed in lesion effect across rats with apparently similar damage patterns has already been reported in previous studies (Bielajew et al., 2002; Boye, 2005; Morissette and Boye, 2008) and could reflect the anatomically diffuse, collateralized and heterogeneous nature of the reward substrate (Arvanitogiannis et al., 1996a; Simmons et al., 1998).

FLIR: Methodological considerations

In the present study, we used Fos immunohistochemistry to visualize brain regions that were activated by rewarding LH stimulation. The use of this technique offers significant advantages compared to other imaging methods used in previous studies to detect neural activity. The more traditional ones include measures of 2-deoxyglucose, cytochrome oxidase, or glycogen phosphorylase activities. These metabolic measures are related to glucose and oxygen consumption as an index of cellular activity. Although they have been successfully used to reveal brain regions metabolically activated by rewarding brain stimulation (Gallistel et al., 1985; Bielajew, 1991; Konkle et al., 1999), FLIR seems to better reflect antidromic activation of somata obtained following ICSS (Flores et al., 1997; Arvanitogiannis et al., 2000). In addition, Fos immunohistochemistry allows the detection of transsynaptically stimulated neurons downstream of reward-related systems, thus enabling the mapping of functional reward pathways (Sagar et al., 1988). Despite its benefits, however, there are several constraints in interpreting the results of Fos immunohistochemistry. For instance, FLIR does not enable the distinction between reward-relevant neurons and other stimulated cells (Sagar et al., 1988). As a result, the population of stained cells is very likely to include neurons subserving functions not involved in reward (Arvanitogiannis et al., 1996b; Flores et al., 1997). Finally, there is a possibility that the capacity for c-fos expression might not be universal among all neurons, which could lead to false interpretations since some regions activated by the rewarding stimulation will not exhibit FLIR (Bullitt, 1990; Flores et al., 1997; Kovacs, 1998).

Effect of LH stimulation on FLIR

Analysis of brain regions revealed increased FLIR following rewarding LH stimulation, with the highest expression in the hemisphere ipsilateral to the stimulation. Significant increases in Fos-immunolabeled cells were observed in structures from the forebrain (mPFC, OFC, BNST, NAc core, NAc shell, BLA), midbrain (SNr, SNc, VTAa, VTAp, RMTg, IPN) and brainstem (PN, DR, PPTg). Thus, based on these findings, it is suitable to conclude that these regions that are activated by the stimulation are tightly related to the neural substrate subserving the rewarding effect of LH stimulation. These findings are in agreement with the view that some of the directly activated MFB fibers arise from forebrain nuclei (Rompre and Shizgal, 1986), run between the LH and VTA (Bielajew and Shizgal, 1982, 1986; Murray and Shizgal, 1996a), and extend further beyond the midbrain (Fletcher et al., 1995; Boye, 2005). In addition, the increased FLIR observed in the PPTg is in line with studies showing that cholinergic neurons within this region play a critical role in LH self-stimulation reward by activating midbrain dopamine cells (Yeomans et al., 1993; Chen et al., 2006). However, as discussed above, not all structures that showed increased FLIR after LH stimulation are equally implicated in the rewarding effectiveness of ICSS. The results of the present study showed increased level of FLIR in the BLA and NAc in non-lesioned rats. Nonetheless, previous reports have shown that the rewarding efficacy of LH stimulation was not diminished by electrolytic lesions of the amygdala complex (Waraczynski et al., 1990) or excitotoxic lesions of the NAc (Johnson and Stellar, 1994), suggesting that FLIR in these regions might be due to activation of neurons that are not involved in the rewarding efficacy of ICSS. Similarly, the increased FLIR observed in the PN in response to LH stimulation is not likely attributable to brain stimulation reward, but rather to the motor activity inherent to ICSS (Gasbarri et al., 2003).

Previous studies employing LH stimulation have shown that FLIR was significantly higher in the hemisphere ipsilateral to the stimulating electrode (Arvanitogiannis et al., 1996b; Arvanitogiannis et al., 1997; Flores et al., 1997). In our study, however, interhemispheric analysis of brain structures revealed increased FLIR in the ipsilateral part of only the BNST, NAc core and shell, BLA and SNc. In the remaining structures, no interhemispheric differences were observed, suggesting that LH stimulation activated an approximately equal proportion of fibers within each hemisphere. This finding initially appeared surprising given the predominance of ipsilateral projections in the MFB (Nieuwenhuys et al., 1982; Veening et al., 1982). However, bilateral FLIR could still arise inasmuch as some of the ascending and descending projections of the MFB decussate in the midline to reach the contralateral side (Malette and Miliaressis, 1995). The symmetrical pattern of FLIR observed in midbrain structures such as the SNr, VTAa, VTAp and RMTg is also in agreement with anatomical findings suggesting the existence of interhemispheric nigrostriatal projections originating from these regions (Fass and Butcher, 1981; Pritzel et al., 1983).

Effect of a DDC lesion on FLIR

Notwithstanding the problems of interpretation in FLIR, the findings reported here provide new and interesting insights regarding the anatomical and functional connectivity of the DDC. Following an electrolytic lesion at the DDC, a significant reduction in FLIR was observed in the BNST, NAc core and shell, BLA, IPN, PN and DR. The level of FLIR in the BNST, NAc core and shell, BLA and PN of lesioned rats remained significantly higher from that in the sham group, suggesting that some subsets of cells within these regions were still activated by the stimulation, even after damaging the DDC. In the IPN and DR, FLIR was reduced to a level comparable to that

in the sham group, indicating that a significant proportion of neurons within these regions are functionally connected with the DDC. These findings are in agreement with previous anatomical studies aimed at deciphering the relationship of the DDC with other brain areas involved in reward. For instance, studies employing immunohistochemical or axonal tracing in rats revealed the presence of anatomical contacts between the habenula and multiple brain structures including the amygdala (Akagi and Powell, 1968), BNST (McLean et al., 1983; Li et al., 1993), NAc (Powell and Leman, 1976), substantia nigra (Omelchenko et al., 2009), IPN (Kim, 2009) and raphe (Herkenham and Nauta, 1977). To our knowledge, no anatomical connections between the DDC and the PN have been documented so far, however, given the existence of functional projections from the habenula and the IPN (Kim, 2009; Antolin-Fontes et al., 2015), and excitatory feedback projections from the IPN to the PN (Campolattaro et al., 2011), the reduced FLIR observed in the latter structure may be due to transsynaptic rather than direct reduction of neuronal activity. Also noteworthy to mention are behavioral studies showing that lesions at the DDC significantly reduce the rewarding effectiveness of self-stimulation within multiple brain regions, including the LH, VTA and DR (Morissette and Boye, 2008; Fakhoury et al., 2016).

Our data revealed no differences in FLIR in the mPFC, OFC, and PPTg of lesioned and non-lesioned rats, suggesting that these regions might share minimal axonal connections with the DDC. The lack of effect observed in these structures may be due to either their distal anatomical locations with respect to the lesion site, or their rostral anatomical locations with respect to the stimulation site. Results also showed that a lesion at the DDC had no effect on FLIR in midbrain regions such as the SNc, SNr, VTAa, VTAp and RMTg. These findings were surprising at first given the wide array of studies showing the existence of excitatory glutamatergic connections from the LHb to the RMTg (Brinschwitz et al., 2010; Stamatakis and Stuber, 2012), and inhibitory GABAergic

inputs from the RMTg to midbrain dopamine neurons (Matsui and Williams, 2011; Lecca et al., 2012). However, in addition to exerting an indirect inhibitory effect on dopaminergic neurons of the VTA, the LHb also sends direct excitatory glutamatergic projections to this structure (Omelchenko et al., 2009; Goncalves et al., 2012). Therefore, the lack of differences in FLIR observed between the VTA of lesioned and non-lesioned rats could be the result of a compensatory effect between inhibitory and excitatory inputs originating from the LHb. Our data obtained in the VTA also seem to contradict a recent report showing that optical activation of LHb inputs to the midbrain is accompanied by sparse (<12%) FLIR in dopaminergic neurons of the VTA, and high (approximately 80%) FLIR in non-dopaminergic neurons of the RMTg (Lammel et al., 2012). A possible cause for the observed discrepancies, however, is that the lesions employed in our study were centered on the SM and LHb, and did not encroach the fr. As such, afferent connections originating from the LHb and projecting to the midbrain remained intact. Also noteworthy to mention is that the use of single Fos immunolabeling in our study did not enable us to determine what type of neurons (dopaminergic, glutamatergic or GABAergic) remained active following the lesion.

CONCLUSION

In summary, the present data showed that LH self-stimulation results in increased FLIR in multiple brain regions, particularly in the hemisphere ipsilateral to the stimulation electrode. A lesion at the DDC was accompanied by significant attenuations of the rewarding effectiveness of the stimulation, and resulted in substantial decreases of FLIR in multiple brain regions. These findings bolster the notion that the DDC is involved in mediating the transmission of reward-

related signals, and provide an interesting view on the functional projections that exist between this pathway and brain regions activated by ICSS.

ACKNOWLEDGMENTS

This study was supported by a Discovery Grant from the Natural Sciences and Engineering Research Council (NSERC) of Canada to PPR (#GRPIN-2015-05018). The authors would also like to acknowledge the help of Dr. Giovanni Hernandez for data analysis and presentation.

FIGURE AND TABLE LEGENDS

Table 1: Relative distribution of FLIR following LH stimulation. This table illustrates the average cell count per mm^2 in the ipsilateral hemisphere of non-lesioned rats (n = 7), as well as their interhemispheric ratio (ipsilateral/contralateral). The cell density is illustrated by ‘‘-” (sparse: 0–5 cells/mm^2), ‘‘+” (low density: 5–20 cells/mm^2), ‘‘++” (medium density: 20–50 cells/mm^2) and ‘‘+++” (high density: 50–100 cells/mm^2).

Figure 1: Schematic illustration of the experimental protocol. (A) Lesioned and non-lesioned rats were allowed to self-administer the stimulation during discrete 55 s trials preceded by non-contingent delivery of five trains of priming stimulation and a 5-s adaptation period. (B) Lesioned and non-lesioned rats were trained and tested for LH stimulation, whereas rats in the sham group were placed in the stimulation cages for the same amount of time required for training and testing, but received no stimulation.

Figure 2: (A) Location of the tips of the stimulation electrodes of lesioned and non-lesioned rats (n=7 rats/group). (B) Electrolytic lesions in rats from the lesion group (n=7 rats). Coordinates are expressed in mm relative to bregma. In all figures, illustrations of brain structures represent modified drawings taken from the Paxinos and Watson atlas of the rat brain (Paxinos and Watson, 1997). Abbreviations: supraoptic decussation (sox); optical tract (opt); fornix (f).

Figure 3: Effect of a DDC lesion on the mean values of the M50 (A) and maximum response rate (B). Mean values are expressed in percentage (%) of baseline values that preceded the lesion. Error bars correspond to the standard error of the mean (S.E.M). n=7 rats/group. For comparison with the baseline, * indicates $p<0.05$.

Figure 4: Representative figures showing FLIR in selected areas of the BNST (A) and the VTAa (B) of an individual rat from each treatment group, in both ipsilateral and contralateral

hemispheres. Pictures were taken under a total magnification of 400x (left panels; scale bar 50 μm) and 100x (right panels; scale bar 200 μm).

Figure 5: Ipsilateral and contralateral FLIR in selected regions of the forebrain in each treatment group (n=7 rats/group). Schematic diagrams of only the ipsilateral hemisphere are shown for the purpose of simplicity. Values represent the mean of the total cell count in the entire surface of each structure, and error bars correspond to the S.E.M. For comparison between treatment group, * indicates $p<0.05$, and ** indicates $p<0.01$. For interhemispheric comparison within treatment groups, ǂ indicates $p<0.05$ and ǂǂ indicates $p<0.01$.

Figure 6: Ipsilateral and contralateral FLIR in selected regions of the midbrain in each treatment group (n=7 rats/group). Schematic diagrams of only the ipsilateral hemisphere are shown for the purpose of simplicity. Values represent the mean of the total cell count in the entire surface of each structure, and error bars correspond to the S.E.M. For comparison between treatment group, * indicates $p<0.05$, and ** indicates $p<0.01$. For interhemispheric comparison within treatment groups, ǂǂ indicates $p<0.01$.

Figure 7: Ipsilateral and contralateral FLIR in the selected regions of the brainstem in each treatment group (n=7 rats/group). Schematic diagrams of only the ipsilateral hemisphere are shown for the purpose of simplicity. Values represent the mean of the total cell count in the entire surface of each structure, and error bars correspond to the S.E.M. For comparison between treatment group, * indicates $p<0.05$, and ** indicates $p<0.01$. No differences were observed between the ipsilateral and contralateral hemispheres.

Brain region	Ipsilateral cell density	Ratio (ipsilateral/contralateral)
OFC	++	3.0
mPFC	+	1.55
CPu	-	-
Nac core	+	2.49
Nac shell	++	2.45
BNST	++	2.71
BLA	+++	2.96
SNr	+	1.47
SNc	+++	2.84
VTAa	++	1.68
VTAp	++	1.38
RMTg	++	1.44
IPN	+	1.45
PN	+++	1.73
DR	++	1.31
PPTg	+	1.70

Table 1

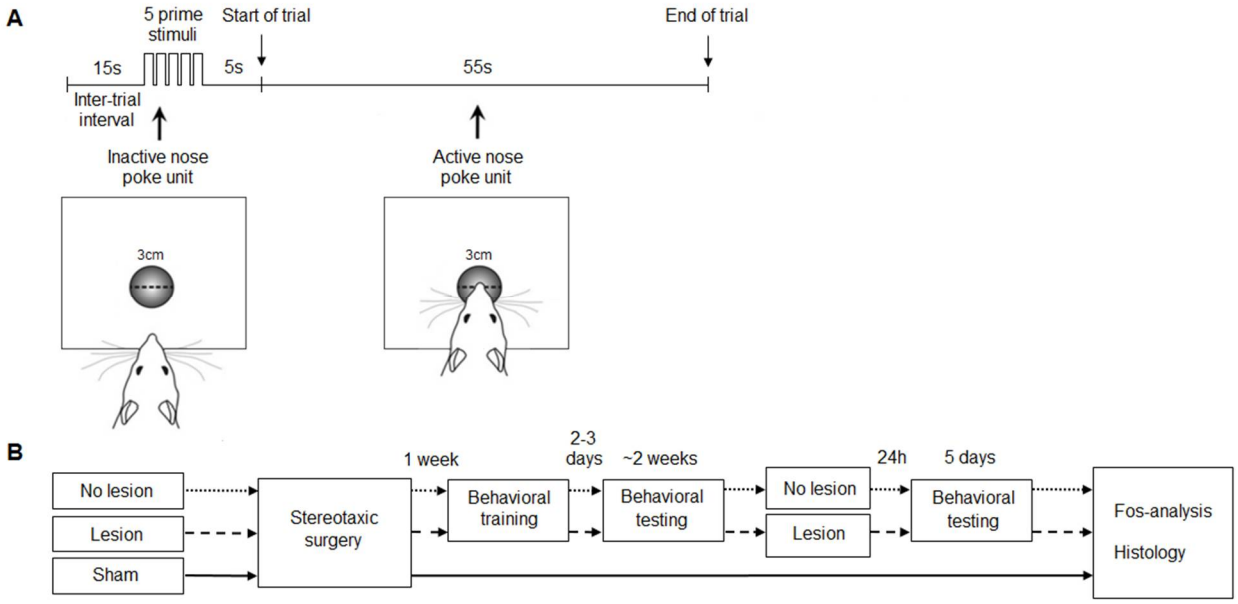
A
5 prime stimuli
Start of trial
End of trial
15s
5s
55s
Inter-trial interval
Inactive nose poke unit
Active nose poke unit
3cm
3cm
B
1 week
2-3 days
~2 weeks
24h
5 days
No lesion
Lesion
Sham
Stereotaxic surgery
Behavioral training
Behavioral testing
No lesion
Lesion
Behavioral testing
Fos-analysis
Histology

Figure 1

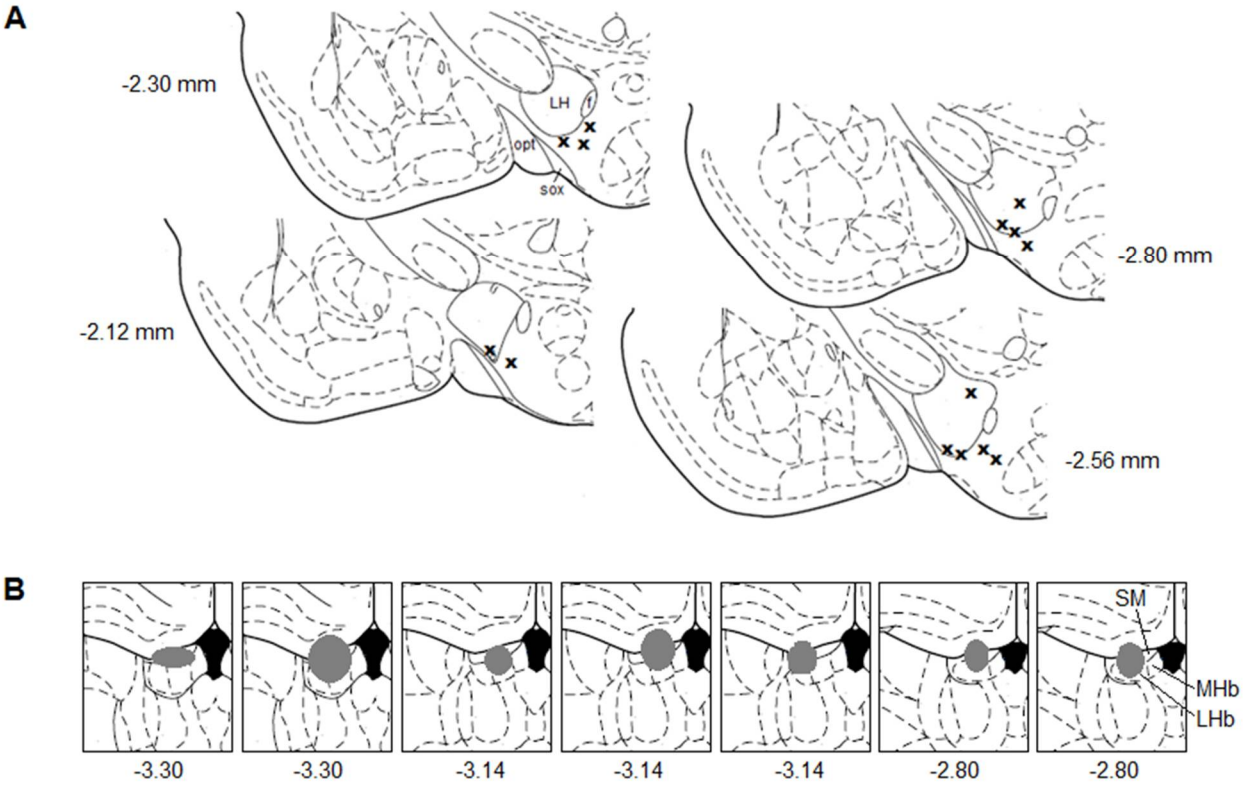
A
-2.30 mm
LH
opt
sox
-2.12 mm
-2.80 mm
-2.56 mm
B
SM
MHb
LHb
-3.30
-3.30
-3.14
-3.14
-3.14
-2.80
-2.80

Figure 2

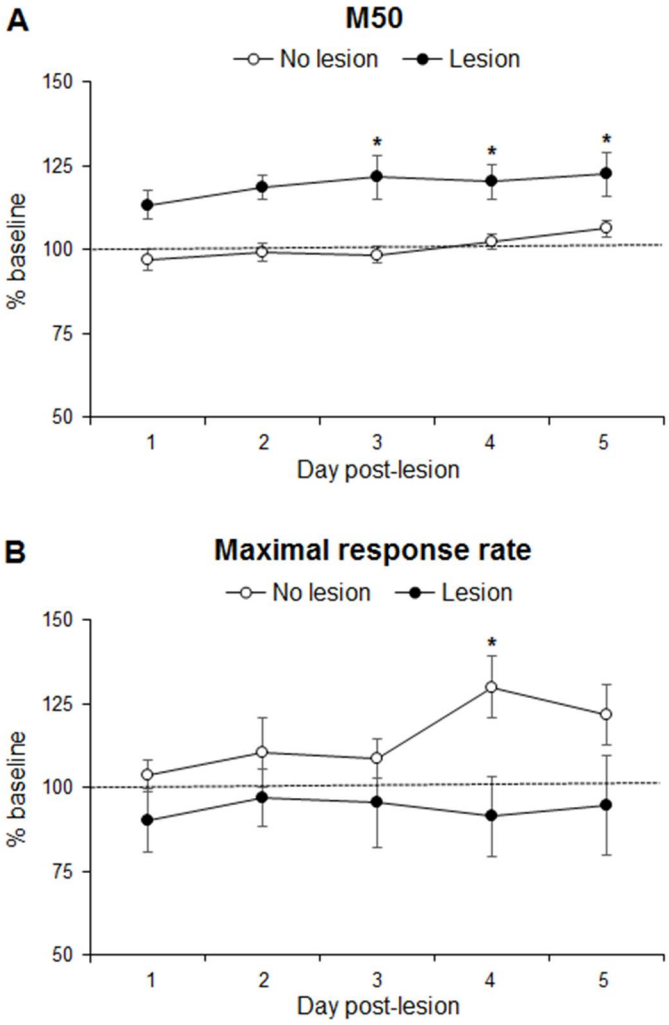
A
M50
No lesion
Lesion
150
125
100
75
50
% baseline
*
*
*
1
2
3
4
5
Day post-lesion
B
Maximal response rate
No lesion
Lesion
150
125
100
75
50
% baseline
*
1
2
3
4
5
Day post-lesion

Figure 3

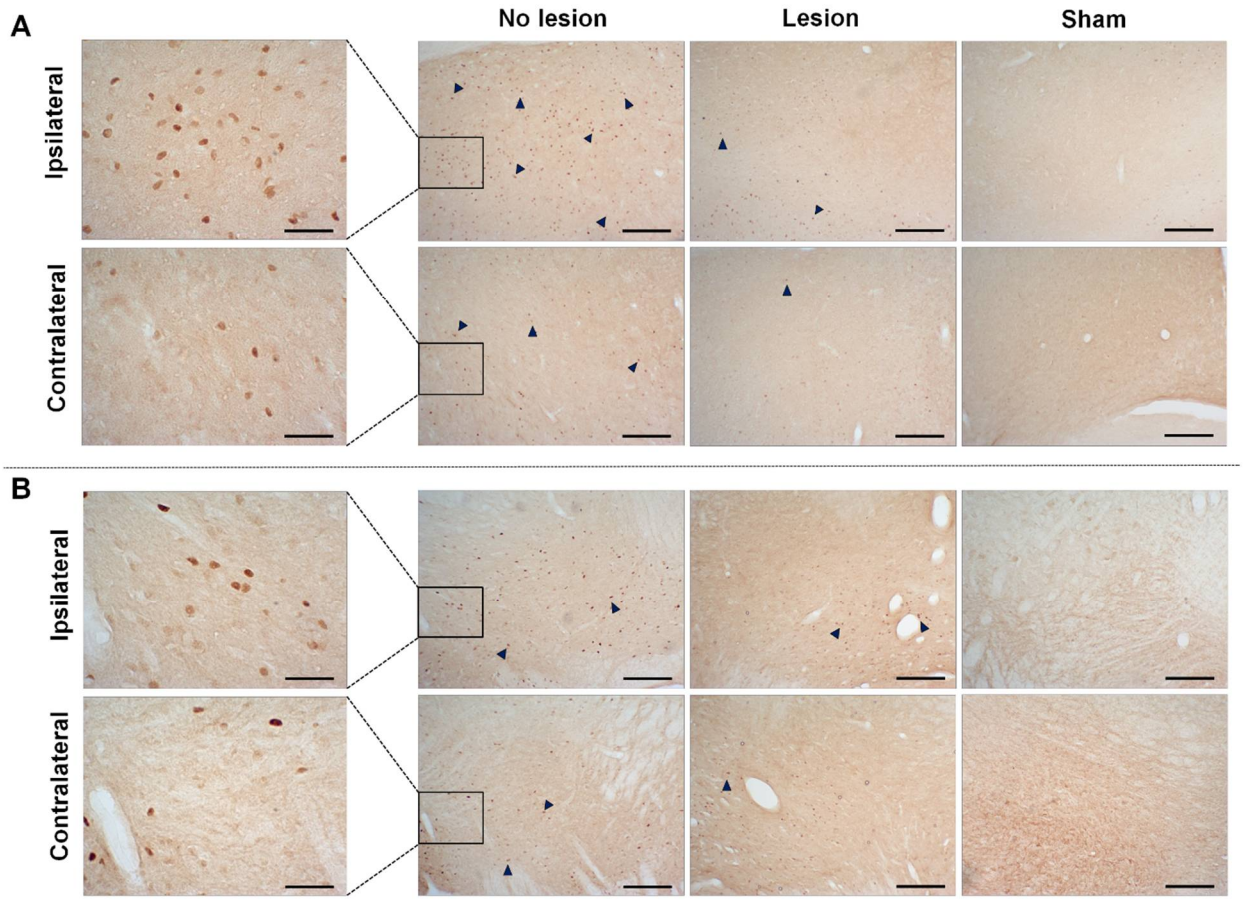
A
No lesion
Lesion
Sham
Ipsilateral
Contralateral
B
Ipsilateral
Contralateral

Figure 4

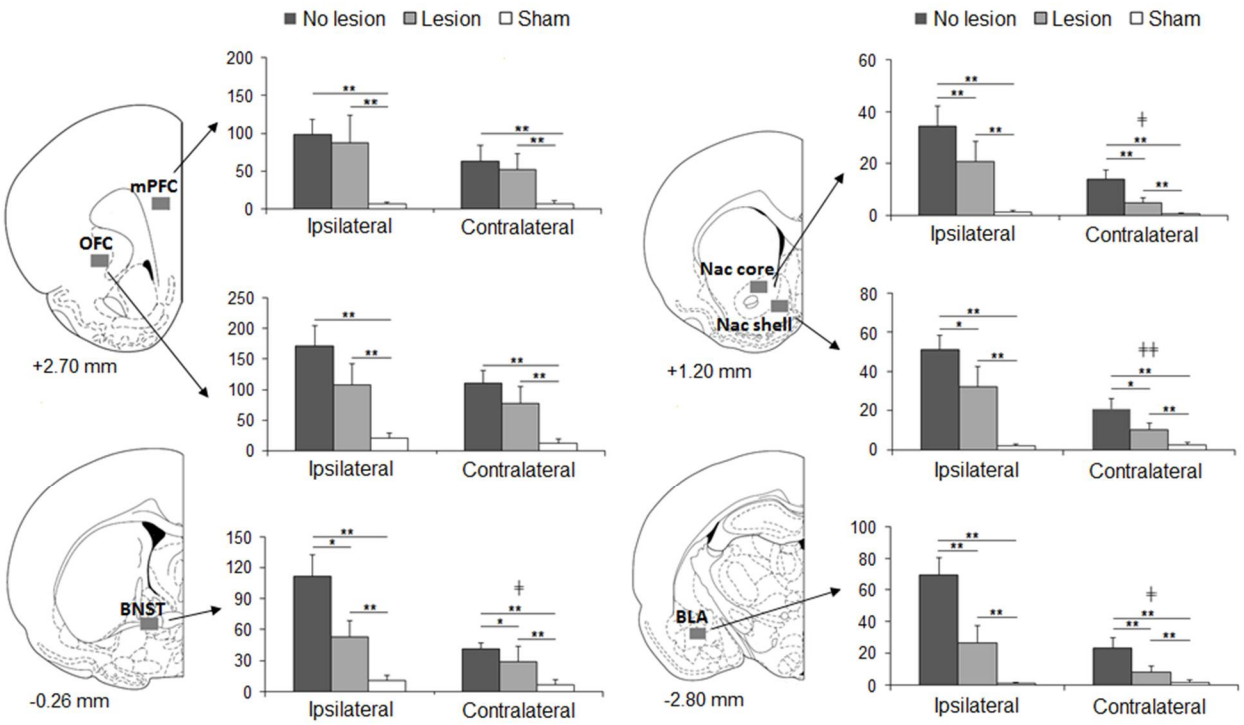
No lesion
Lesion
Sham
mPFC
OFC
+2.70 mm
Ipsilateral
Contralateral
Nac core
Nac shell
+1.20 mm
BNST
-0.26 mm
BLA
-2.80 mm

Figure 5

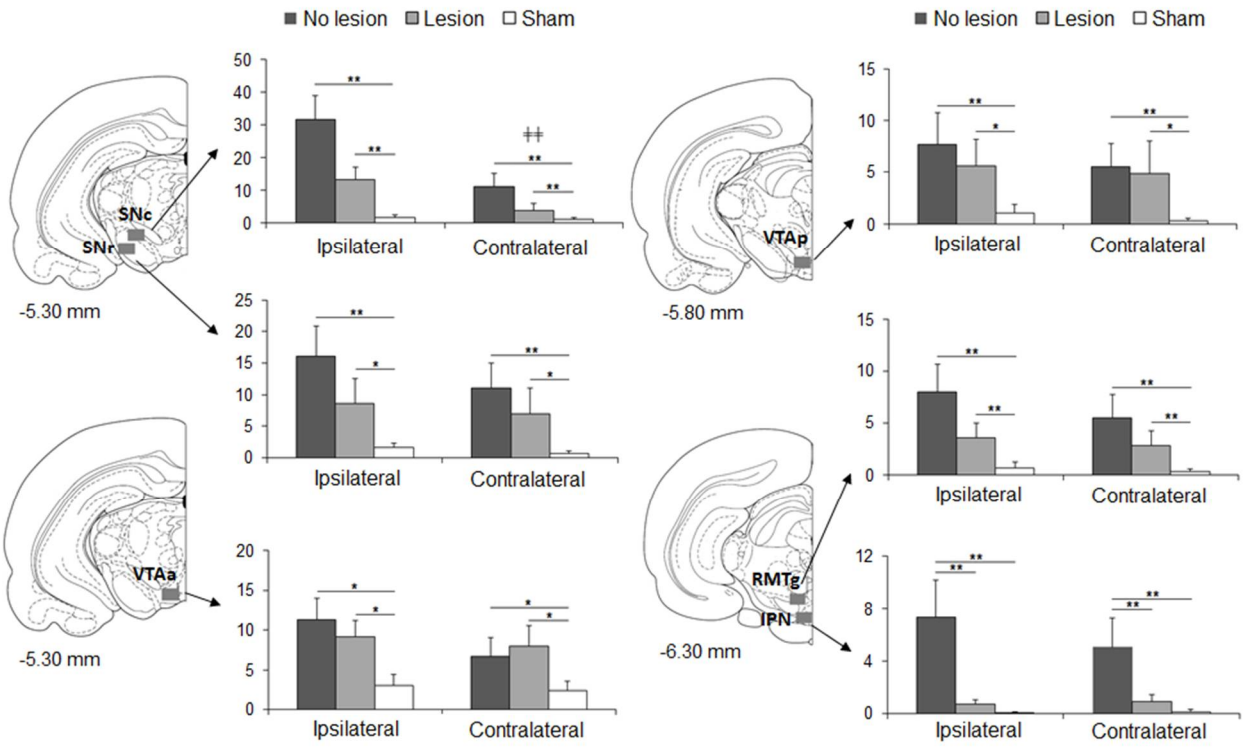
No lesion
Lesion
Sham
SNc
SNr
-5.30 mm
Ipsilateral
Contralateral
VTAp
-5.80 mm
VTAa
-5.30 mm
RMTg
IPN
-6.30 mm

Figure 6

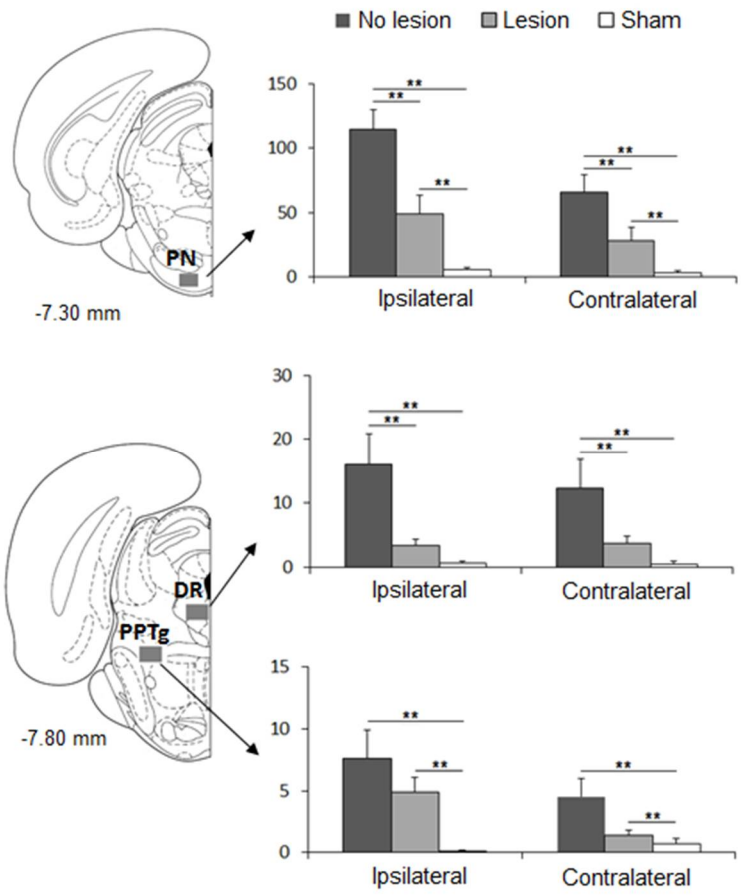
No lesion
Lesion
Sham
PN
-7.30 mm
150
100
50
0
Ipsilateral
Contralateral
DR
PPTg
-7.80 mm
30
20
10
0
Ipsilateral
Contralateral
15
10
5
0
Ipsilateral
Contralateral

Figure 7

REFERENCES

Akagi K, Powell EW (1968) Differential projections of habenular nuclei. J Comp Neurol 132:263-274.

Aldavert-Vera L, Huguet G, Costa-Miserachs D, Ortiz SP, Kadar E, Morgado-Bernal I, Segura-Torres P (2013) Intracranial self-stimulation facilitates active-avoidance retention and induces expression of c-Fos and Nurr1 in rat brain memory systems. Behav Brain Res 250:46-57.

Antolin-Fontes B, Ables JL, Gorlich A, Ibanez-Tallon I (2015) The habenulo-interpeduncular pathway in nicotine aversion and withdrawal. Neuropharmacology 96:213-222.

Araki M, McGeer PL, Kimura H (1988) The efferent projections of the rat lateral habenular nucleus revealed by the PHA-L anterograde tracing method. Brain Res 441:319-330.

Arvanitogiannis A, Waraczynski M, Shizgal P (1996a) Effects of excitotoxic lesions of the basal forebrain on MFB self-stimulation. Physiol Behav 59:795-806.

Arvanitogiannis A, Flores C, Shizgal P (1997) Fos-like immunoreactivity in the caudal diencephalon and brainstem following lateral hypothalamic self-stimulation. Behav Brain Res 88:275-279.

Arvanitogiannis A, Flores C, Pfaus JG, Shizgal P (1996b) Increased ipsilateral expression of Fos following lateral hypothalamic self-stimulation. Brain Res 720:148-154.

Arvanitogiannis A, Tzschentke TM, Riscaldino L, Wise RA, Shizgal P (2000) Fos expression following self-stimulation of the medial prefrontal cortex. Behav Brain Res 107:123-132.

Barrot M, Sesack SR, Georges F, Pistis M, Hong S, Jhou TC (2012) Braking dopamine systems: a new GABA master structure for mesolimbic and nigrostriatal functions. J Neurosci 32:14094-14101.

Bianco IH, Wilson SW (2009) The habenular nuclei: a conserved asymmetric relay station in the vertebrate brain. Philos Trans R Soc Lond B Biol Sci 364:1005-1020.

Bielajew C, Shizgal P (1982) Behaviorally derived measures of conduction velocity in the substrate for rewarding medial forebrain bundle stimulation. Brain Res 237:107-119.

Bielajew C, Shizgal P (1986) Evidence implicating descending fibers in self-stimulation of the medial forebrain bundle. J Neurosci 6:919-929.

Bielajew C, Miguelez M, Shiao R (2002) Electrolytic lesions of the cortical and adjacent nuclei in the amygdala differentially influence thresholds for rewarding medial forebrain bundle stimulation. Behav Neurosci 116:660-671.

Bielajew CH (1991) Distribution of cytochrome oxidase in response to rewarding brain stimulation: effect of different pulse durations. Brain Res Bull 26:379-384.

Boye SM (2005) Mesencephalic substrate of reward: lesion effects. Behav Brain Res 156:31-43.

Brinschwitz K, Dittgen A, Madai VI, Lommel R, Geisler S, Veh RW (2010) Glutamatergic axons from the lateral habenula mainly terminate on GABAergic neurons of the ventral midbrain. Neuroscience 168:463-476.

Bullitt E (1990) Expression of c-fos-like protein as a marker for neuronal activity following noxious stimulation in the rat. J Comp Neurol 296:517-530.

Campolattaro MM, Kashef A, Lee I, Freeman JH (2011) Neuronal correlates of cross-modal transfer in the cerebellum and pontine nuclei. J Neurosci 31:4051-4062.

Chen J, Nakamura M, Kawamura T, Takahashi T, Nakahara D (2006) Roles of pedunculopontine tegmental cholinergic receptors in brain stimulation reward in the rat. Psychopharmacology (Berl) 184:514-522.

Fakhoury M, Rompre PP, Boye SM (2016) Role of the dorsal diencephalic conduction system in the brain reward circuitry. Behav Brain Res 296:431-441.

Fass B, Butcher LL (1981) Evidence for a crossed nigrostriatal pathway in rats. Neurosci Lett 22:109-113.

Fletcher PJ, Tampakeras M, Yeomans JS (1995) Median raphe injections of 8-OH-DPAT lower frequency thresholds for lateral hypothalamic self-stimulation. Pharmacol Biochem Behav 52:65-71.

Flores C, Arvanitogiannis A, Shizgal P (1997) Fos-like immunoreactivity in forebrain regions following self-stimulation of the lateral hypothalamus and the ventral tegmental area. Behav Brain Res 87:239-251.

Gallistel CR, Gomita Y, Yadin E, Campbell KA (1985) Forebrain origins and terminations of the medial forebrain bundle metabolically activated by rewarding stimulation or by reward-blocking doses of pimozide. J Neurosci 5:1246-1261.

Gasbarri A, Pompili A, Pacitti C, Cicirata F (2003) Comparative effects of lesions to the ponto-cerebellar and olivo-cerebellar pathways on motor and spatial learning in the rat. Neuroscience 116:1131-1140.

Goncalves L, Sego C, Metzger M (2012) Differential projections from the lateral habenula to the rostromedial tegmental nucleus and ventral tegmental area in the rat. J Comp Neurol 520:1278-1300.

Herkenham M, Nauta WJ (1977) Afferent connections of the habenular nuclei in the rat. A horseradish peroxidase study, with a note on the fiber-of-passage problem. J Comp Neurol 173:123-146.

Hoffman GE, Smith MS, Verbalis JG (1993) c-Fos and related immediate early gene products as markers of activity in neuroendocrine systems. Front Neuroendocrinol 14:173-213.

Hong S, Jhou TC, Smith M, Saleem KS, Hikosaka O (2011) Negative reward signals from the lateral habenula to dopamine neurons are mediated by rostromedial tegmental nucleus in primates. J Neurosci 31:11457-11471.

Hunt GE, McGregor IS (1998) Rewarding brain stimulation induces only sparse Fos-like immunoreactivity in dopaminergic neurons. Neuroscience 83:501-515.

Hunt GE, McGregor IS (2002) Contrasting effects of dopamine antagonists and frequency reduction on Fos expression induced by lateral hypothalamic stimulation. Behav Brain Res 132:187-201.

Ji H, Shepard PD (2007) Lateral habenula stimulation inhibits rat midbrain dopamine neurons through a GABA(A) receptor-mediated mechanism. J Neurosci 27:6923-6930.

Johnson PI, Stellar JR (1994) N-methyl-D-aspartic acid-induced lesions of the nucleus accumbens and/or ventral pallidum fail to attenuate lateral hypothalamic self-stimulation reward. Brain Res 646:73-84.

Kim U (2009) Topographic commissural and descending projections of the habenula in the rat. J Comp Neurol 513:173-187.

Konkle AT, Wilson P, Bielajew C (1999) Histochemical mapping of the substrate for brain-stimulation reward with glycogen phosphorylase. J Neurosci Methods 93:111-119.

Kovacs KJ (1998) c-Fos as a transcription factor: a stressful (re)view from a functional map. Neurochem Int 33:287-297.

Lakens D (2013) Calculating and reporting effect sizes to facilitate cumulative science: a practical primer for t-tests and ANOVAs. Front Psychol 4:863.

Lammel S, Lim BK, Ran C, Huang KW, Betley MJ, Tye KM, Deisseroth K, Malenka RC (2012) Input-specific control of reward and aversion in the ventral tegmental area. Nature 491:212-217.

Lecca S, Melis M, Luchicchi A, Muntoni AL, Pistis M (2012) Inhibitory inputs from rostromedial tegmental neurons regulate spontaneous activity of midbrain dopamine cells and their responses to drugs of abuse. Neuropsychopharmacology 37:1164-1176.

Li YQ, Takada M, Shinonaga Y, Mizuno N (1993) The sites of origin of dopaminergic afferent fibers to the lateral habenular nucleus in the rat. J Comp Neurol 333:118-133.

Malette J, Miliaressis E (1995) Interhemispheric links in brain stimulation reward. Behav Brain Res 68:117-137.

Marcangione C, Rompre PP (2008) Topographical Fos induction within the ventral midbrain and projection sites following self-stimulation of the posterior mesencephalon. Neuroscience 154:1227-1241.

Matsui A, Williams JT (2011) Opioid-sensitive GABA inputs from rostromedial tegmental nucleus synapse onto midbrain dopamine neurons. J Neurosci 31:17729-17735.

McLean S, Skirboll LR, Pert CB (1983) Opiatergic projection from the bed nucleus to the habenula: demonstration by a novel radioimmunohistochemical method. Brain Res 278:255-257.

Morissette MC, Boye SM (2008) Electrolytic lesions of the habenula attenuate brain stimulation reward. Behav Brain Res 187:17-26.

Murray B, Shizgal P (1996a) Attenuation of medical forebrain bundle reward by anterior lateral hypothalamic lesions. Behav Brain Res 75:33-47.

Murray B, Shizgal P (1996b) Behavioral measures of conduction velocity and refractory period for reward-relevant axons in the anterior LH and VTA. Physiol Behav 59:643-652.

Nakahara D, Ishida Y, Nakamura M, Kuwahara I, Todaka K, Nishimori T (1999) Regional differences in desensitization of c-Fos expression following repeated self-stimulation of the medial forebrain bundle in the rat. Neuroscience 90:1013-1020.

Nieuwenhuys R, Geeraedts LM, Veening JG (1982) The medial forebrain bundle of the rat. I. General introduction. J Comp Neurol 206:49-81.

Omelchenko N, Bell R, Sesack SR (2009) Lateral habenula projections to dopamine and GABA neurons in the rat ventral tegmental area. Eur J Neurosci 30:1239-1250.

Paxinos G, Watson C (1997) The rat brain in stereotaxic coordinates, 3rd ed. Edition. San Diego, CA: Academic Press.

Poller WC, Madai VI, Bernard R, Laube G, Veh RW (2013) A glutamatergic projection from the lateral hypothalamus targets VTA-projecting neurons in the lateral habenula of the rat. Brain Res 1507:45-60.

Powell EW, Leman RB (1976) Connections of the nucleus accumbens. Brain Res 105:389-403.

Pritzel M, Sarter M, Morgan S, Huston JP (1983) Interhemispheric nigrostriatal projections in the rat: bifurcating nigral projections and loci of crossing in the diencephalon. Brain Res Bull 10:385-390.

Rompre PP, Shizgal P (1986) Electrophysiological characteristics of neurons in forebrain regions implicated in self-stimulation of the medial forebrain bundle in the rat. Brain Res 364:338-349.

Sagar SM, Sharp FR, Curran T (1988) Expression of c-fos protein in brain: metabolic mapping at the cellular level. Science 240:1328-1331.

Shizgal P, Schindler D, Rompre PP (1989) Forebrain neurons driven by rewarding stimulation of the medial forebrain bundle in the rat: comparison of psychophysical and electrophysiological estimates of refractory periods. Brain Res 499:234-248.

Shizgal P, Bielajew C, Corbett D, Skelton R, Yeomans J (1980) Behavioral methods for inferring anatomical linkage between rewarding brain stimulation sites. J Comp Physiol Psychol 94:227-237.

Simmons JM, Ackermann RF, Gallistel CR (1998) Medial forebrain bundle lesions fail to structurally and functionally disconnect the ventral tegmental area from many ipsilateral forebrain nuclei: implications for the neural substrate of brain stimulation reward. J Neurosci 18:8515-8533.

Stamatakis AM, Stuber GD (2012) Activation of lateral habenula inputs to the ventral midbrain promotes behavioral avoidance. Nat Neurosci 15:1105-1107.

Stamatakis AM, Van Swieten M, Basiri ML, Blair GA, Kantak P, Stuber GD (2016) Lateral Hypothalamic Area Glutamatergic Neurons and Their Projections to the Lateral Habenula Regulate Feeding and Reward. J Neurosci 36:302-311.

Sutherland RJ (1982) The dorsal diencephalic conduction system: a review of the anatomy and functions of the habenular complex. Neurosci Biobehav Rev 6:1-13.

Veening JG, Swanson LW, Cowan WM, Nieuwenhuys R, Geeraedts LM (1982) The medial forebrain bundle of the rat. II. An autoradiographic study of the topography of the major descending and ascending components. J Comp Neurol 206:82-108.

Waraczynski M, Ton MN, Shizgal P (1990) Failure of amygdaloid lesions to increase the threshold for self-stimulation of the lateral hypothalamus and ventral tegmental area. Behav Brain Res 40:159-168.

Yeomans JS, Mathur A, Tampakeras M (1993) Rewarding brain stimulation: role of tegmental cholinergic neurons that activate dopamine neurons. Behav Neurosci 107:1077-1087.

2.3 ARTICLE 3

Modulation of brain stimulation reward and locomotor activity by ionotropic glutamate and mu opioid receptors of the tail of the ventral tegmental area

Marc Fakhoury [a], Giovanni Hernandez [a,b], Daniel Lévesque [b], Pierre-Paul Rompré [a, c]

[a] Department of Neurosciences, Faculty of Medicine, Université de Montréal, Montreal, Quebec, Canada

[b] Faculty of Pharmacy, Université de Montréal, Montreal, Quebec, Canada

[c] FRQ-S Research Group in Behavioral Neurobiology, Concordia University, Montreal, Quebec, Canada

AUTHOR CONTRIBUTIONS

I wrote the first draft of the manuscript and conducted all the behavioral experiments in the laboratory of Dr. Pierre-Paul Rompré. Western Blot analysis was performed by Giovanni Hernandez in the laboratory of Dr. Daniel Lévesque.

ABSTRACT

The rostromedial tegmental nucleus also referred to as the tail of the ventral tegmental area (tVTA) contains a cluster of gamma-aminobutyric acid (GABA)ergic neurons that receive dense glutamatergic afferents from the lateral habenula (LHb), and project to dopamine (DA) neurons of the VTA and substantia nigra pars compacta (SNc). In light of previous evidence implicating glutamate transmission in the regulation of midbrain DA neuronal activity, we first assessed the impact of intra-tVTA microinjection of NBQX (0.8 nmol/side) and PPPA (0.825 nmol/side), respectively AMPA and NMDA receptor antagonists on reward induced by intracranial self-stimulation (ICSS) and on locomotor activity. Since the tVTA contains a large concentration of mu opioid receptors, additional measures were obtained following microinjection of endomorphin-1 (EM-1, 1 nmol/side). Then, using the small interfering RNAs (siRNAs) that target the GluN1 subunit of the NMDA receptor, we tested the effect of tVTA downregulation of these receptors on reward and locomotor activity. Results show that NBQX, PPPA and EM-1 all enhance reward and locomotor activity, effects that were of different magnitude in rostral and intermediate parts of the tVTA. On the other hand, a reduction in GluN1 receptors caused a marked decrease in operant responding for ICSS, but failed to alter ICSS reward and the reward-enhancing effect of PPPA. Our results support a role for the tVTA as a main inhibitory component of DA-dependent behavioral measures, and suggest that tVTA NMDA receptors that modulate reward are most likely expressed on tVTA afferent terminals.

Keywords: AMPA receptors; endomorphin-1; locomotor activity; NMDA receptors, reward; tVTA

INTRODUCTION

The rostromedial tegmental nucleus, also known as the tail of the VTA (tVTA), is a newly identified structure that receives strong excitatory glutamatergic inputs from the lateral habenula (LHb) (Jhou et al., 2009b; Brinschwitz et al., 2010; Goncalves et al., 2012) and that sends gamma-aminobutyric acid (GABA)ergic inhibitory projections to dopamine (DA) neurons of the VTA and substantia nigra pars compacta (SNc) (Jhou et al., 2009b; Balcita-Pedicino et al., 2011). The tVTA has been proposed to convey critical motivational signals to midbrain DA neurons by translating the LHb signal into a DA negative-reward signal (Barrot et al., 2012). Evidence in support of this hypothesis comes from electrophysiological findings showing that tVTA neurons, similar to LHb neurons, are activated following the delivery of aversive stimuli or the omission of expected reward delivery, and inhibited following the delivery of rewards or reward predicting cues (Matsumoto and Hikosaka, 2007; Jhou et al., 2009a; Hong et al., 2011). These patterns of activity are inverse to those found in putative DA neurons of the VTA and SNc (Ungless et al., 2004; Pan et al., 2005; Matsumoto and Hikosaka, 2007), suggesting that the tVTA may act as a hub between brain regions that process reward signals of opposite motivational states. In light of the dense glutamatergic inputs from the LHb to the tVTA (Brinschwitz et al., 2010), the characterization of the modulatory role of glutamate transmission in the tVTA is of great interest for better understanding the neural mechanisms underlying adaptive and maladaptive behaviors.

Glutamate signalling plays a key role in shaping the activity of midbrain DA neurons. Through its direct action on DA cells, glutamate mediates the switch from pacemaker tonic to phasic burst firing of DA neuronal activity (Grace and Bunney, 1984; Overton and Clark, 1997; Lodge and Grace, 2006), a mode that is associated with enhanced DA release (Gonon, 1988) and incentive motivation (Horvitz, 2002). Consistently, pharmacological activation of NMDA and AMPA

glutamate receptors in the VTA increases mesolimbic DA release (Suaud-Chagny et al., 1992; Karreman et al., 1996) and exploratory motor behavior (Kretschmer, 1999) in rodents. However, other studies have reported increased DA release and burst firing of DA neurons (French et al., 1993; Mathe et al., 1998), as well as enhanced locomotor activity (Narayanan et al., 1996; Cornish et al., 2001) following blockade of VTA NMDA or AMPA receptors, suggesting an opposite modulatory role of glutamate on DA neuronal activity. Prior reports from our group have also shown that blockade of VTA NMDA receptors enhances brain stimulation reward (Bergeron and Rompre, 2013; Ducrot et al., 2013; Hernandez et al., 2016), whereas the opposite effect is observed following blockade of VTA AMPA receptors (Ducrot et al., 2013).

Besides directly innervating DA neurons, glutamatergic afferents to the VTA also establish synaptic connections with local GABAergic interneurons that exert a negative modulation on DA neuronal activity (Omelchenko et al., 2009; Dobi et al., 2010). Thus, blockade of ionotropic glutamate receptors in GABAergic neurons of the VTA could conceivably remove the inhibitory tone on DA neurons, resulting in increased locomotor activity and brain stimulation reward; two DA-dependent behavioral measures. Given the strong inhibitory influence of the tVTA on midbrain DA neuron activity (Bourdy et al., 2014; Brown et al., 2017), the present study was aimed at investigating whether changes in locomotor activity and brain stimulation reward could be observed following blockade of AMPA or NMDA receptors in the tVTA using NBQX or PPPA, respectively. Brain stimulation reward and locomotor activity were also assessed following activation of mu opioid receptors (MORs) with endomorphine-1 (EM-1) owing to previous evidence showing that tVTA neurons show a strong density of MORs (Jhou et al., 2009b), and that activation of these receptors in the tVTA inhibits the activity of midbrain DA neurons (Jalabert et al., 2011; Matsui and Williams, 2011). Finally, the present study was aimed at exploring the

rewarding and locomotor stimulant effect of tVTA downregulation of NMDA receptors using a small interferon RNA (siRNA) against GluN1, an obligatory NMDA receptor subunit, and determining whether such manipulation alters the reward-enhancing effect of PPPA.

MATERIAL AND METHODS

Subjects and surgery

Male Long-Evans rats (Charles river, QC, Canada) weighing between 300-400g at the time of surgery served as experimental subjects. Upon arrival, all animals were housed two per cage in a temperature (22 ºC) and humidity (40%) controlled room with a 12-h light–dark cycle (lights on at 6 am) and ad libitum access to food and water, and allowed 1 week of acclimatization. The surgical procedure is described in the Suppl. Methods. The electrodes of stimulation were bilaterally directed at the LH (AP: -2.5 mm, ML: ±1.7 mm, DV: -8.6 mm), and the guide cannulas (26-gauge) bilaterally directed at the tVTA (AP: -6.6 to -7.0 mm, ML: ±2.1 mm at a 10º angle, DV: -6.3 mm). Coordinates are expressed in reference to bregma in accordance to the Paxinos and Watson atlas of the rat brain (Paxinos and Watson, 1997). After surgery, all animals were housed individually and were allowed 1 week of recovery. All experiments were approved by the institutional animal care committee and were carried out in compliance with the ethical guidelines of the Canadian Council on Animal Care (CCAC).

ICSS: Drug/peptide and siRNA injection

Rats were placed in operant chambers and were trained to receive pulses of electrical stimulation at one of the two LH stimulation sites through nose-poke responding **(Suppl. Methods)**. The stimulation was delivered at a constant intensity and different pulse frequencies so as to obtain

Response/Frequency curves **(Suppl. Figure 2 and 3)** correlating the number of nose-pokes per trial to the stimulation frequency. The reward threshold (M50), defined as the pulse frequency sustaining a half-maximal rate of responding, was measured to assess the reinforcing properties of ICSS. After at least 4 days of stable reward threshold (~ 20 pulses per train), a 0.5 µl solution of 0.9% saline was bilaterally microinjected into the tVTA of all rats to habituate them to the injection procedure **(Suppl. Methods)**. Behavioral testing began 5 days later. For the drug and peptide injection study, rats were bilaterally injected with either PPPA (0.825 nmol), NBQX (0.8 nmol) or the vehicle (0.9% saline) in a counterbalanced design, followed by an injection of EM-1 (1 nmol), with 4-5 days interval between two injections **(Suppl. Figure 1B)**. After each injection, rats were immediately put in operant chambers and allowed to self-stimulate for 75 min. The reward thresholds and maximum response rates were obtained immediately before and after each injection. For the siRNA injection study, rats were retested for ICSS to obtain at least 4 days of stable reward threshold, after which one group was injected with siRNA against GluN1 (10 mg/ml), and another one with siRNA against a non-active RNA sequence (10 mg/ml) bilaterally into the tVTA for three consecutive days. Twenty-four hours after the last siRNA injection, all rats received a bilateral injection of PPPA (0.825 nmol) into the tVTA. Reward thresholds and maximum response rates were measured 24 h after each siRNA injection and immediately following PPPA injection.

Locomotor activity: Drug/peptide and siRNA injection

The experimental paradigm consisted of a habituation phase of 3 days **(Suppl. Methods)**, followed by a test phase. For the drug and peptide injection experiment, rats were tested for locomotor activity in test cages 24 h following the last habituation day, for 30 min, and were then

injected with either PPPA (0.825 nmol), NBQX (0.8 nmol) or vehicle (0.9% saline) in a counterbalanced design, followed by an injection of EM-1 (1 nmol) **(Suppl. Figure 1B)**. Rats received only one injection per test day, and there was a minimum of 5 days interval between two consecutive injections. After each injection, the subjects were immediately placed into the test cages and locomotor activity was assessed for another 75 min. For the siRNA injection experiment, rats were tested for locomotor activity 3 days after the last habituation day for two consecutive days. Immediately after, one group of rats was injected with siRNA against GluN1 (0.825 nmol), and another group with siRNA against a non-active RNA sequence bilaterally into the tVTA for three consecutive days **(Figure 5F)**. Locomotor activity was assessed for 75 min 24 h after each siRNA injection and compared with baseline values obtained during the test day that preceded the first siRNA injection.

Western Blot

Immediately after the last behavioral test, rats that received a siRNA treatment were decapitated, and their brains removed and placed onto an ice-cooled plate. Brain tissues were carefully dissected from a 0.75-1 mm thick slice using a 15-gauge tissue punch, and kept in -80°C until further processing. To assess the total protein concentration, brain tissues were mechanically homogenized in a lysis buffer (1M Tris-HCL pH 6.8, 10% SDS and protease inhibitor cocktail) and protein levels were measured using a BCA assay kit (Pierce, USA). For separation by gel electrophoresis, equal amounts of protein (10µg) were dissolved into 25 µl lysis buffer (5X loading buffer and β –mercapto-ethanol) and loaded into the wells of an SDS-PAGE gel (8% polyacrylamide), along with molecular weight markers. Proteins were then transferred to a PVDF membrane (Bio-Rad Laboratories) and blocked for 1 h in TBST with 5% dry milk. For the

detection of GluN1, proteins were incubated with rabbit anti-GluN1 antibody (1 : 500, Novus Biological) overnight at 4 °C, followed by 4 times rinsing with TBST for 5 min, and a second incubation with HRP-conjugated goat anti-mouse IgG (1 : 20000, Millipore). For the detection of MORs, proteins were incubated with anti-MORs (1: 500, Abcam) overnight at 4 °C, followed by 4 times rinsing with TBST for 5 min, and a second incubation with HRP-conjugated goat anti-rabbit IgG (1 : 10000, Millipore) for 1 h. Mouse anti-β-actin (1 : 20000, Millipore) and HRP-conjugated goat anti-rabbit IgG (1 : 40000, Millipore) were used to detect the loading control protein (β-actin). Protein bands were revealed with ECL western blotting system (PerkinElmer) and visualized on an X-ray film. The band densities were measured with an image analysis system (ImageJ 1.48v software, Wayne Rasband, NIH) and normalized to β-actin.

Histology

At the end of the behavioral tests, rats that receive the drug and peptide injections were deeply anesthetized with a single intraperitoneal injection of urethane (1.4–2.0 g/kg of bodyweight), and the stimulation and injection sites were marked by passing an anodal current (0.1 mA, 60 s) through the electrodes and injection cannulae. Rats were then transcardially perfused with 0.9% saline followed by a 10% formalin solution containing 3% potassium ferrocyanide, 3% potassium ferricyanide and 0.5% trichloroacetic acid. Brains were harvested and kept in the latter solution for 24 h, and were then rinsed and stored in a 10% formalin solution for several days. They were subsequently frozen and sliced in 40 μm sections with a cryostat, mounted onto gelatine-coated slides, and stained for Nissl substance with thionin. The location of the stimulation electrodes of rats tested for ICSS are illustrated in **Suppl. Figure 4**. Because cannula placements varied among rats tested for ICSS and locomotor activity, subjects were divided into two groups; those that

received the injections at rostral sites of the tVTA (between -5.8mm and -6.2 mm with respect to bregma), and those that received the injections at intermediate sites of the tVTA (between -6.3 mm to -6.8 mm with respect to bregma).

Drug, peptide and siRNA

Pharmacological blockade of AMPA and NMDA receptors was achieved with 0.825 nmol of NBQX (2,3,-Dioxo-6-nitro-1,2,3,4-tetrahydrobenzo(f)quinoxaline-7-sulfonamide) and 0.825 nmol of PPPA [(2R,4S)-4-(3-Phosphopropyl)-2-piperidinecarboxylic acid], respectively (Tocris Bioscience, Ellisville, MI,USA), whereas activation of MORs was achieved with 1 nmol of the endogenous peptide, EM-1 (Tocris). Drug and peptide solutions were dissolved in sterile 0.9% saline to obtain the desired final concentrations, which were chosen based on previous studies (Zangen et al., 2002; Ducrot et al., 2013). Downregulation of GluN1 subunits was achieved using a mixture of pre-validated siRNA sequences against GluN1 (Cat. #4390816 ID s127804-s127806). A non-active siRNA with a nonsense/scrambled sequence served as control. The siRNA sequences were purchased from Thermo Fisher Scientific and were mixed with a cationic lipid transfection carrier N-[1-(2,3-Dioleoyloxy)-propylX-N,N,N-trimethyl-ammonium methylsulfate (DOTAP) (Roche Applied Sciences, Indianapolis, IN). The final solution contained 10 µg of the active or inactive siRNA and 1 µg of DOTAP per µl. This procedure has previously been shown to effectively reduce protein level in the midbrain (Hernandez et al., 2015).

Data analysis

Changes in mean reward threshold and maximum response rate were analysed with a two-way analysis of variance (ANOVA) for repeated measures (Treatment x Time, with 'Treatment' as a

between-subjects variable and 'Time' as a within-subjects variable), followed by Duncan's multiple range tests for post hoc comparison. Changes in total locomotor activity were analysed with a one-way ANOVA followed by Tukey HSD post-hoc test. An unpaired t-test was used to compare the EM-1 and vehicle treated groups, to analyze the changes in locomotor activity at a specific time after the injection, and to assess differences in protein levels. The level of significance was set at $p < 0.05$. When assessing differences in protein level, the Grubbs' test for a single outlier was used for identifying the outliers within groups.

RESULTS

PPPA and EM-1, but not NBQX, injection into the rostral tVTA enhance brain stimulation reward

The rewarding effects of NBQX, PPPA and EM-1 injections into the rostral tVTA were assessed by measuring changes in reward thresholds and maximum response rates **(Figure 1; Suppl. Figure 2A)**. The ANOVA performed on mean changes in reward threshold yielded a significant effect of treatment [$F_{(2,24)} = 5.23$, $p < 0.05$] but no treatment by time interaction [$F_{(8,96)} = 1.26$, $p > 0.05$] **(Figure 1A)**. Post-hoc test showed that PPPA, but not NBQX, reduced the mean reward threshold compared to vehicle. On the other hand, the ANOVA performed on mean changes in maximum response rate yielded no significant effect of treatment [$F_{(2,24)} = 5.80$, $p > 0.05$] and no treatment by time interaction [$F_{(8,96)} = 1.73$, $p > 0.05$] **(Figure 1C)**. T-tests performed at time 15 min post-injection show a strong trend toward significance for both NBQX [$t_{(16)} = 2.10$, $p > 0.05$] and PPPA [$t_{(16)} = 2.09$, $p > 0.05$] treatment. Because EM-1 is rapidly degraded by enzymes in brain tissue (Perlikowska et al., 2009), we analyzed its effects during the first 15 min of ICSS testing only.

Treatment with EM-1 reduced the reward threshold [$t_{(16)} = 4.72$, $p < 0.01$] (Figure 1A) but had no effect on the maximum response rate [$t_{(16)} = 0.024$, $p > 0.05$] **(Figure 1C)**.

NBQX, PPPA and EM-1 injection into the rostral tVTA enhance locomotor activity

The locomotor stimulant effect of NBQX, PPPA and EM-1 injections into the rostral tVTA were assessed by measuring changes in horizontal, vertical and stereotypic-like movements **(Figure 2)**. The ANOVA performed on total horizontal [$F_{(2,27)} = 3.47$, $p < 0.05$] **(Figure 2A)** and stereotypic-like [$F_{(2,27)} = 4.09$, $p < 0.05$] **(Figure 2C)** movements yielded a significant effect of treatment. Post-hoc test showed that NBQX, but not PPPA, increased the total horizontal movements post-injection. On the other hand, the ANOVA performed on total vertical movements yielded no significant effect of treatment [$F_{(2,27)} = 2.70$, $p > 0.05$] **(Figure 2B)**. Finally, treatment with EM-1 increased total horizontal movements [$t_{(18)} = 2.18$, $p < 0.05$] **(Figure 2A)**, but had no effect on total vertical [$t_{(18)} = 1.31$, $p > 0.05$] **(Figure 2B)** or stereotypic-like [$t_{(18)} = 1.24$, $p > 0.05$] movements **(Figure 2C)**.

NBQX, PPPA and EM-1 injection into the intermediate tVTA enhance brain stimulation reward

The rewarding effects of NBQX, PPPA and EM-1 injections into the intermediate tVTA were assessed by measuring changes in reward thresholds and maximum response rates **(Figure 3; Suppl. Figure 2B)**. The ANOVA performed on mean changes in reward threshold yielded a significant effect of treatment [NBQX: $F_{(2,18)} = 5.04$, $p < 0.05$; PPPA: $F_{(2,18)} = 5.04$, $p < 0.001$] and a significant treatment by time interaction [$F_{(8,72)} = 6.06$, $p < 0.01$] **(Figure 3A)**. Post-hoc test showed that both PPPA and NBQX reduced the mean reward threshold compared to vehicle. On

the other hand, the ANOVA performed on mean changes in maximum response rate yielded no significant effect of treatment [$F_{(2,17)} = 0.090$, $p > 0.05$] and no treatment by time interaction [$F_{(8,68)} = 1.53$, $p > 0.05$] **(Figure 3C)**. Finally, treatment with EM-1 reduced the reward threshold [$t_{(12)} = 2.98$, $p < 0.05$] **(Figure 3A)** but had no effect on the maximum response rate [$t_{(12)} = 0.1.99$, $p > 0.05$] **(Figure 3C)**.

NBQX, but not PPPA or EM-1, injection into the intermediate tVTA enhance locomotor activity

The locomotor stimulant effects of NBQX, PPPA and EM-1 injections into the intermediate tVTA were assessed by measuring changes in horizontal, vertical and stereotypic-like movements **(Figure 4)**. The ANOVA performed on total horizontal [$F_{(2,21)} = 4.82$, $p < 0.05$] **(Figure 4A)**, vertical [$F_{(2,21)} = 4.37$, $p < 0.05$] **(Figure 4B)**, and stereotypic-like [$F_{(2,21)} = 4.66$, $p < 0.05$] **(Figure 4C)** movements yielded a significant effect of treatment. Post-hoc test showed that NBQX, but not PPPA, increased the total horizontal, vertical and stereotypic-like movements post-injection. On the other hand, treatment with EM-1 had no effect on total horizontal [$t_{(14)} = 2.08$, $p > 0.05$] **(Figure 4A)**, vertical [$t_{(14)} = 1.21$, $p > 0.05$] **(Figure 4B)**, and stereotypic-like [$t_{(14)} = 0.98$, $p > 0.05$] **(Figure 4C)** movement.

siRNA-mediated downregulation of tVTA GluN1 subunits attenuates the maximum rate of ICSS responding without reducing locomotor activity

To validate the effect of the siRNA treatment on tVTA NMDA receptor level, the density of the obligatory GluN1 subunit was assessed from tVTA tissue homogenates. Injection of siRNA against GluN1 yielded a significant decrease in the expression of the GluN1 subunit of NMDA

receptors in rats tested for ICSS [$t_{(9)} = 2.70$, $p < 0.05$] and locomotor activity [$t_{(10)} = 2.34$, $p < 0.05$] **(Figure 5B)**. This effect was specific to NMDA receptors since the density of MORs remained unchanged in the tVTA **(Suppl. Figure 5F)**. To evaluate the rewarding effect of the siRNA treatment, ICSS was assessed following each of the three consecutive siRNA injections. The ANOVA performed on mean changes in reward threshold following the siRNA treatment yielded no significant effect of treatment [$F_{(1,60)} = 1.21$, $p > 0.05$] and no treatment by time interaction [$F_{(2,65)} = 0.59$, $p > 0.05$] **(Figure 5A)**. On the other hand, the ANOVA performed on mean changes in maximum response rate yielded a significant effect of treatment [$F_{(1,60)} = 20.12$, $p < 0.01$] and no treatment by time interaction [$F_{(2,65)} = 0.11$, $p > 0.05$] **(Figure 5A)**. Post-hoc test showed that the siRNA treatment reduced the mean maximum response rate compared to vehicle. In another group of rats, locomotor activity was assessed following the same siRNA treatment. The ANOVA performed on total horizontal, vertical and stereotypic-like movements yielded no significant effect of treatment [$F_{(1,30)} = 3.81$, $p > 0.05$; $F_{(1,30)} = 1.41$, $p > 0.05$; $F_{(1,30)} = 3.22$, $p > 0.05$, respectively] an no treatment by time interaction [$F_{(2,35)} = 0.24$, $p > 0.05$; $F_{(2,35)} = 1.02$, $p > 0.05$; $F_{(2,35)} = 0.55$, $p > 0.05$, respectively] **(Figure 5E)**. T-test performed 24h after the first siRNA injection show a significant effect on horizontal movements compared to control [$t_{(10)} = 6.24$, $p < 0.01$] **(Figure 5E)**.

siRNA-mediated downregulation of GluN1 subunits in the tVTA fails to alter the rewarding effects of PPPA

To test whether the reduction in the expression of tVTA NMDA receptors would impact the rewarding effect of PPPA, reward thresholds and maximum response rates were measured before and after bilateral intra-tVTA injection of PPPA in siRNA-treated rats **(Figure 5C)**. Compared to

baseline, PPPA increased the maximum reduction in reward threshold in rats treated with the GluN1 [$t_{(10)} = 3.37$, $p < 0.01$] or control [$t_{(10)} = 4.67$, $p < 0.01$] siRNA, indicating enhanced brain stimulation reward **(Figure 5C)**. However, the ANOVA performed on mean changes in reward threshold yielded no significant effect by treatment [$F_{(1,100)} = 2.79$, $p > 0.05$] and no treatment by time interaction [$F_{(4,100)} = 1.34$, $p > 0.05$] **(Figure 5C)**. Likewise, the ANOVA performed on mean changes in maximum response rates yielded no significant effect by treatment [$F_{(1,100)} = 2.14$, $p > 0.05$] and no effect by time interaction [$F_{(4,100)} = 0.47$, $p > 0.05$] **(Figure 5C)**.

DISCUSSION

In the present study, we examined the effect of intra-tVTA injection of the AMPA antagonist, NBQX, and the NMDA antagonist, PPPA, on the reward signal induced by ICSS. A large body of evidence suggests that the reinforcing effect of ICSS is largely dependent on mesolimbic DA transmission. Rewarding electrical stimulation leads to increased mesolimbic DA release (You et al., 2001; Yavich and Tanila, 2007; Hernandez et al., 2012) and midbrain DA cell firing (Moisan and Rompre, 1998), and pharmacological manipulations that activate (Gilliss et al., 2002) or block (Nakajima and McKenzie, 1986; Benaliouad et al., 2007) DA receptors enhance or attenuate the rewarding effect of ICSS, respectively. Our results show that NBQX injection into the intermediate, but not the rostral, tVTA produces a significant enhancement in the rewarding effect triggered by ICSS; effect that was also observed following PPPA injection into both the rostral and intermediate tVTA. Treatment with NBQX or PPPA had no effect on the maximum response rate, indicating that the capacity of rats to self-stimulate remained intact. Given the strong GABAergic inhibitory projections from the tVTA to DA neurons of the VTA/SNc complex (Jhou et al., 2009b), the most likely hypothesis to account for the rewarding effect of tVTA AMPA and

NMDA receptors blockade is the removal of the GABAergic inhibition on midbrain DA neuronal firing. In support of this hypothesis, neurotoxic lesions and electrical stimulation of the tVTA were shown to attenuate the LHb-induced inhibition of midbrain DA cells (Brown et al., 2017) and supress the activity of midbrain DA neurons (Lecca et al., 2011; Lecca et al., 2012; Bourdy et al., 2014), respectively. Also consistent with our results are findings showing that pharmacological activation of the tVTA by local AMPA injections produce robust conditioned place aversion in rats, thus indicating that glutamate transmission in the tVTA signals aversive events (Jhou et al., 2013).

The present study also sought to examine the effect of intra-tVTA injection of NBQX and PPPA on locomotor activity. Much evidence supports the inference that this behavioral measure is largely mediated by mesocorticolimbic DA transmission. Administration of DA or DA receptor agonists into the nucleus accumbens enhances locomotor activity (Pijnenburg et al., 1976; Ikemoto, 2002), whereas blockade of DA receptors (Ahlenius et al., 1987; Johnson et al., 1996) or 6-hydroxydopamine lesion of DA neurons (Koob et al., 1978; Koob et al., 1981) of the mesocorticolimbic pathway supresses spontaneous and psychostimulant-induced locomotion. Our results show that injection of NBQX into the rostral and/or intermediate tVTA enhances horizontal, vertical and stereotypic-like behavior, while injection of PPPA into the rostral, but not the intermediate, tVTA enhances stereotypic-like behavior. We speculate that blockade of glutamatergic afferents into the tVTA enhance some measures of locomotion by increasing the activity of midbrain DA neurons through a disinhibition process. These findings are consistent with our results obtained from ICSS and with previous evidence showing that neurotoxic lesions of the tVTA enhance motor performance on a rotarod (Bourdy et al., 2014) or open field (Brown et al., 2017) test. They also agree with prior reports showing increased spontaneous or drug-

induced locomotor activity following lesions of the LHb (Gifuni et al., 2012) or its efferent projections to the tVTA (Murphy et al., 1996), and following optogenetic (Jhou et al., 2013) or GABA-mediated (Huff and LaLumiere, 2015; Lavezzi et al., 2015) inhibition of the tVTA.

NBQX and PPPA produced different rewarding and locomotor effects when injected at different sites of the tVTA, pointing to anatomical and/or functional heterogeneity among tVTA neurons. These data parallel previous findings showing that drugs have different propensities to produce a rewarding effect when administered into rostral or caudal regions of the VTA (Ikemoto et al., 1997, 1998). Another important finding of the present study is that brain stimulation reward and locomotor activity were differentially regulated by AMPA and NMDA receptor activity. While blockade of tVTA NMDA receptors produced the highest enhancement in brain stimulation reward, the highest enhancement in locomotor activity was achieved following blockade of tVTA AMPA receptors. This finding parallels a previous report showing that animals that are trained to respond for rewarding ICSS show decreased expression of the GluR1 subunit of AMPA receptor in the VTA, with no effect on the expression of NMDA receptors (Carlezon et al., 2001). Elevated GluR1 in the midbrain is, on the other hand, a primary trigger to synaptic changes underlying increased sensitization to drug-induced locomotor activity (Carlezon et al., 1997; Carlezon and Nestler, 2002). These findings, along with ours, suggest that the effect of ICSS and locomotor activity are subserved by different mechanisms; the former is more sensitive to changes in NMDA receptor activity, and the latter is more sensitive to changes in AMPA receptor activity.

We next sought to examine the effect of intra-tVTA injection of EM-1 on brain stimulation reward and locomotor activity. EM-1 was used in this study because of its strong selectivity for MORs (Zadina et al., 1997) and its short half-life in brain tissue (Perlikowska et al., 2009), thus limiting the likelihood of diffusion to adjacent sites of the tVTA. EM-1 injection into the rostral

and intermediate tVTA reduced ICSS reward thresholds without altering the maximum response rate; an effect that is interpreted as rewarding. In light of prior electrophysiological findings indicating that opiates activate VTA DA neurons by inhibiting GABAergic terminals in the VTA (Jalabert et al., 2011; Matsui and Williams, 2011; Lecca et al., 2012; Hjelmstad et al., 2013), we postulate that the rewarding effect of intra-tVTA injection of EM-1 results from increased midbrain DA neuronal activity via disinhibition. Our results also show that activation of MORs in the rostral tVTA increases horizontal locomotor activity, which is in agreement with prior reports showing that intra-tVTA infusion of morphine (Wasserman et al., 2013; Wasserman et al., 2016; Steidl et al., 2017) or the MOR agonist, DAMGO (Kotecki et al., 2015), increases open-field locomotion. However, injection of EM-1 into the intermediate tVTA failed to alter locomotor activity in the present study, which further points to anatomical and/or functional heterogeneity within the tVTA. Such heterogeneity has also been reported along the rostrocaudal axis of the VTA, where robust increases in locomotor activity were observed following MOR activation into the posterior, but not the anterior, VTA (Zangen et al., 2002).

The present study finally examines the behavioral effects of tVTA NMDA receptor downregulation using a siRNA treatment against GluN1. The silencing machinery required for gene silencing by RNA interference is primarily located in the nucleus (Carthew and Sontheimer, 2009). Therefore, intra-tVTA infusion of siRNA against GluN1 will only downregulate the level of NMDA receptors on cells that have their cell bodies located in the tVTA, without altering the level of receptors located on afferent terminals. Our results show that the siRNA-mediated downregulation of tVTA NMDA receptors fails to alter ICSS reward thresholds, but causes a marked decrease in the maximal rate of responding. A downward shift in the maximal rate of ICSS responding is typically interpreted as a reduced performance capacity of rats to self-stimulate

(Miliaressis et al., 1986). However, it may also indicate a deficit in incentive salience (i.e., the strength of an animal's motivation or "wanting" to obtain the rewarding stimulation) (Edmonds et al., 1974). Because no reduction in locomotor activity was observed following the siRNA treatment, the reduced maximal rate of ICSS responding in siRNA-treated rats is more likely to result from deficits in incentive salience, thus implicating NMDA receptors that are located on tVTA cell bodies in motivation and approach behaviors.

The results obtained with the siRNA experiment also indicate a lack of differences in reward thresholds and maximum response rates following PPPA injection between rats treated with control or GluN1 siRNA. PPPA injection into the tVTA following the siRNA treatment enhanced brain stimulation reward in both groups, albeit transiently. Thus, despite the downregulation of NMDA receptors in tVTA cell bodies, the reward-enhancing effect of PPPA remained unaltered. A plausible explanation for this effect is that PPPA acts presynaptically on glutamate-releasing afferent terminals, and not on tVTA cell bodies, to enhance the reward signal induced by ICSS. Because PPPA shows a stronger affinity towards the GluN2A subunit of NMDA receptors, our data suggest that GluN2A-containing NMDA receptors are located on presynaptic glutamatergic terminals of the tVTA. These data parallel a previous finding in the VTA showing that GluN2A-containing NMDA receptors located on local afferent terminals are a likely source of inhibition on the reward signal initiated by electrical brain stimulation (Hernandez et al., 2015).

In conclusion, our results show that glutamate and opioid transmission in the tVTA are major inhibitors of DA-dependent behavioral measures, and suggest that NMDA receptors that are located in tVTA cell bodies are implicated in incentive salience, while those that are located on afferent terminals are more likely involved in brain stimulation reward. These findings could shed new light on the mechanisms underlying reward and goal directed behaviors, and may have

important implications for psychiatric conditions associated with associated with dysregulated reward circuitry function including depression and substance use disorder.

ACKNOWLEDGMENTS

This study was supported by a Discovery Grant from the Natural Sciences and Engineering Research Council (NSERC) of Canada to PPR (#GRPIN-2015-05018).

SUPPLEMENTARY METHODS

Surgery

One week after the acclimatization period, rats were anesthetized with isoflurane (5%, O_2 0.6 L/min) and mounted on a stereotaxic apparatus. An analgesic (Rimadyl; 5 mg/kg) was then administered by subcutaneous injection, and the level of anesthesia was gradually reduced to 2.5–3.5%. After making a small incision on the scalp, a stainless steel wire attached to a male Amphenol connector was wrapped around four stainless steel screws drilled into the skull. This served as the anodal current path for the stimulation. Rats were then implanted with two monopolar stainless-steel stimulation electrodes bilaterally directed at the LH (AP: -2.5 mm, ML: ±1.7 mm, DV: -8.6 mm) and two guide cannulas (26-gauge) bilaterally directed at the tVTA (AP: -6.6 to -7.0 mm, ML: ±2.1 mm at a 10º angle, DV: -6.3 mm). Coordinates are expressed in reference to bregma in accordance to the Paxinos and Watson atlas of the rat brain (Paxinos and Watson, 1997). The stimulation electrode was made from 0.25 mm diameter rod coated with Epoxylite except for the dome-shaped tip. Acrylic dental cement was used to anchor the final cannula/electrode assembly to the skull. At the end of the surgery, rats received an antibiotic (Duplocillin LA, i.m.) and another dose of analgesic, and were allowed 7 days of post-operative recovery during which their body weights were daily monitored.

ICSS: behavioral training

One week following the surgery, rats were placed in operant chambers and were trained to receive pulses of electrical stimulation at one of the two LH stimulation sites through nose-poke responding. The stimulation electrode that sustained the highest rate of operant responding was used for subsequent tests. The operant chambers were made from polymer walls and one front

Plexiglas wall to allow constant viewing. Each chamber was encased in ventilated melamine boxes to minimize disturbance from external noise, and was equipped with a nose poke opening (3 cm wide and 3 cm deep) located 2 cm above the metal rod floor. Each nose poke triggered a constant-current pulse generator that delivered a single 400-ms train of rectangular cathodal pulses of 0.1 ms in duration, followed by a period of 600 ms during which the pulse generator could not be triggered. A current intensity of 250 μA and a fixed stimulation frequency of 41 pulses per train were initially used for the establishment of the ICSS behavior. If the rat did not respond to the initial parameters of stimulation, the current intensity was increased in increments of 100 μA and up to 1000 μA until a consistent operant response was obtained. Following this period of shaping, rats were trained to self-stimulate during 12 discrete 55 sec trials, each signaled by 5 trains of non-contingent priming stimulation (1 Hz), and separated by a 15 sec inter-trial interval during which the stimulation was not available **(Suppl. Figure S1A)**. At the end of each trial, the number of pulses per train was systematically reduced in approximately 0.05-0.1 $\log_{10}$ unit steps so as to obtain a Response/Frequency curve correlating the number of nose pokes per trial to the stimulation frequency. After operant responding had been measured at each of the 12 different trials (a "pass"), the procedure was repeated such that each rat was given four passes per day. The first pass served as a warm up and was excluded from data analysis.

Intracranial injection procedure

Bilateral injections were made by inserting injection cannulae (Model C315I HRS Scientific, Montreal, Canada) directly into the guide cannulae. Each injection cannula extended 2 mm beyond the guide cannula tip, and was connected to a 5 ml Hamilton micro-syringe via polyethylene tubing. A volume of 0.5 μl containing the desired solution was simultaneously injected into each

hemisphere over a 60 sec period with a micro-infusion pump (Harvard Instruments, Holliston, MA). The injection cannulae were left in place for an additional 60 sec to allow for proper diffusion into the brain, after which rats were immediately tested for ICSS or locomotor activity.

Locomotor activity: apparatus and habituation tests

Locomotor activity was assessed in test cages that consist of a wire-mesh floor surrounded by four Plexiglas walls (43 cm wide, 43 cm long and 33 cm high). Each cage was equipped with two arrays of 15 infrared photocells located 1.5 cm above the floor to detect horizontal movements, and a third array of 15 photocells located 14.5 cm above the floor to detect vertical movements. Horizontal (total distance traveled), vertical (total independent interruptions of an elevated array of beams), and stereotypic-like (total duration of restricted and repetitive movements) movements were monitored in 5-min intervals using an Opto-Varimex Auto Track System (Columbus Instruments, Columbus, OH, USA). The experimental paradigm consisted of a habituation phase of 3 days, followed by a test phase. On the first habituation day (H1), animals were individually placed in the test cages for 45 min without receiving any injection. At H2, rats received a bilateral injection of 0.9% saline into the tVTA (0.5 µl injected over 60 sec), and were tested for locomotor activity for a period of 75 min. At H3, rats were put in the test cages for 105 min without any injection. The test phase for the drug/peptide or siRNA injection experiment began 1-3 days later.

FIGURE LEGENDS

Figure 1: Rewarding effect of NBQX, PPPA and EM-1 infusions into the rostral tVTA. Changes in reward thresholds (A) and maximum response rates (C) during individual ICSS trials (left panels) and the overall test session (middle and right panels). (B) Location of injections sites. (D) Thionin staining of a representative coronal brain section from an individual rat (Scale bar 200 µm). Data are represented as mean ± sem (n=9). For statistical comparison with control, * indicates $p < 0.05$ and ** indicates $p < 0.01$. In all figures, illustrations of brain structures represent modified drawings taken from the Paxinos and Watson atlas of the rat brain (Paxinos and Watson, 1997), with coordinates expressed in mm from bregma.

Figure 2: Locomotor stimulant effect of NBQX, PPPA and EM-1 infusions into the rostral tVTA. Changes in horizontal (A), vertical (B) and stereotypic-like (C) movements measured over 5-min intervals (left panels) or during the entire test session post-injection (middle and right panels). (D) Location of injections sites. (E) Thionin staining of a representative coronal brain section from an individual rat (Scale bar 200 µm). Data are represented as mean ± sem (n=10). For statistical comparison with control, * indicates $p < 0.05$ and ** indicates $p < 0.01$. For left panels, grey and black asterisks are for NBQX and PPPA treatment, respectively.

Figure 3: Rewarding effect of NBQX, PPPA and EM-1 infusions into the intermediate tVTA. Changes in reward thresholds (A) and maximum response rates (C) during individual ICSS trials (left panels) and the overall test session (middle and right panels). Data are represented as mean ± sem (n=7). For statistical comparison with control, * indicates $p < 0.05$ and ** indicates $p < 0.01$. (B) Location of injections sites. (D) Thionin staining of a representative coronal brain section from an individual rat (Scale bar 200 µm).

Figure 4: Locomotor stimulant effect of NBQX, PPPA and EM-1 infusions into the intermediate tVTA. Changes in horizontal (A), vertical (B) and stereotypic-like (C) movements measured over 5-min intervals (left panels) or during the entire test session post-injection (middle and right panels). (D) Location of injections sites. (E) Thionin staining of a representative coronal brain section from an individual rat (Scale bar 200 μm). Data are represented as mean ± sem (n=8). For statistical comparison with control, * indicates $p < 0.05$ and ** indicates $p < 0.01$. For left panels, grey and black asterisks are for NBQX and PPPA treatment, respectively.

Figure 5: Effect of the siRNA treatment on ICSS, locomotor activity, and intra-tVTA injection of PPPA. (A) Changes in reward threshold (left panel) and maximum response rate (right panel) following the siRNA injections (n=11/group). (B) Validation of the siRNA treatment effect on the GluN1 NMDA receptor subunit level in rats tested for ICSS (left panel; Control siRNA n=6; GluN1 siRNA n=5) and locomotor activity (right panel; Control siRNA n=6; GluN1 siRNA n=6). The bar histograms show the normalized level of protein against control. The remaining subjects from the ICSS experiment were used for determining the location of the cannulae. (C) Changes in reward threshold and maximum response rate during individual ICSS trials (left and middle panels) and the overall test session (right panel) following intra-tVTA injection of PPPA in rats that previously received a control of GluN1 siRNA treatment (n=11/group). (D) Treatment design for the ICSS experiment. (E) Changes in total horizontal (left panel), vertical (middle panel) and stereotypic-like (right panel) movements following the siRNA injections (Control siRNA n=6; GluN1 siRNA n=6). (F) Treatment design for the locomotor activity experiment. Data are represented as mean ± sem. For statistical comparison with control, * indicates $p < 0.05$ and ** indicates $p < 0.01$. For statistical comparison with baseline, # indicates $p < 0.01$.

Supplementary Figure 1: (A) ICSS protocol. Rats are trained to self-stimulate at one the two LH stimulation electrode at a fixed current intensity and varying stimulation frequencies. The trial begins by the delivery of 5 trains of non-contingent priming stimulation (1 Hz) followed by a 5 sec adaptation period during which the stimulation is not available. Rats are then allowed to self-stimulate during discrete 55 sec trials, after which the stimulation frequency is reduced. A 15 sec time-out period separates each trial. (B) Treatment design for the drug/peptide injection experiment. Each rat received 2 stimulation electrodes bilaterally aimed at the LH, and 2 cannulae bilaterally aimed at the tVTA. Rats that failed to self-stimulate at the LH were used for the locomotor activity study. The treatment consisted of injecting bilaterally into the tVTA either saline, PPPA or NBQX in a counterbalanced order, followed by EM-1.

Supplementary Figure 2: Representative Response/Frequency curves for selected subjects showing the effect of saline, PPPA, NBQX and EM-1 injection into the rostral (A) and intermediate (B) tVTA. Rats were tested for 75 min post-injection so as to generate 5 different Response/Frequency curves. Compared to baseline, treatment with PPPA, NBQX or EM-1 produced a leftward displacement of the Response/Frequency curve. Because EM-1 is rapidly degraded in brain tissue, only the curve obtained at 15 min post-injection was used for data analysis. In each Response/Frequency curve, the response rate represents the number of nose poke during each of the 55 sec trials of self-stimulation, and the pulse frequency represents the number of pulses per train of stimulation.

Supplementary Figure 3: (A) Representative Response/Frequency curves for selected subjects showing the effect of the control or GluN1 siRNA treatment. Individual Response/Frequency curves represent the average of 3 different curves that were obtained immediately before the first siRNA injection (black curve) or 24 h later each siRNA injection (colored curves). Compared to

baseline, the siRNA treatment produced a downward displacement of the Response/Frequency curve. (B) Representative Response/Frequency curves for selected subjects showing the effect of intra-tVTA injection of PPPA in siRNA-treated rats. (C) Location of injections sites in a subset of rats (n=11) that received the siRNA treatment. The remaining subjects from the experiment were used for protein analysis.

Supplementary Figure 4: Location of the stimulation electrodes in rats tested for ICSS. (A) Rats that received the saline, NBQX, PPPA and EM-1 injections into the rostral tVTA (n=9). (B) Rats that received the saline, NBQX, PPPA and EM-1 injections into the intermediate tVTA (n=7). (C) Subgroup of rats that received the control siRNA injection (n=5). (D) Subgroup of rats that received the GluN1 siRNA injection (n=6). The remaining subjects from the siRNA experiment were used for protein analysis.

Supplementary Figure 5: Representative Western blot immuno-reactive signals obtained with antibodies directed against GluN1 and MORs in siRNA-treated rats tested for ICSS (A-B) and locomotor activity (C-D). (E) Scatterplot illustrating the changes in maximum response rate (left panel, n=5) or horizontal movements (right panel, n=6) with the reduction in GluN1 in rats that received the siRNA treatment. There is no positive correlation ($p > 0.05$) between the amount of change in maximum response rate or horizontal movement and the reduction in GluN1. (F) Bar histogram showing the normalized level of MOR against control in siRNA-treated rats tested for ICSS (left panel) and locomotor activity (right panel). The siRNA treatment failed to alter the density of MORs in the tVTA of rats tested for ICSS [left panel: $t_{(8)} = 0.58$, $p > 0.05$] or locomotor activity [right panel: $t_{(10)} = 2.23$, $p > 0.05$].

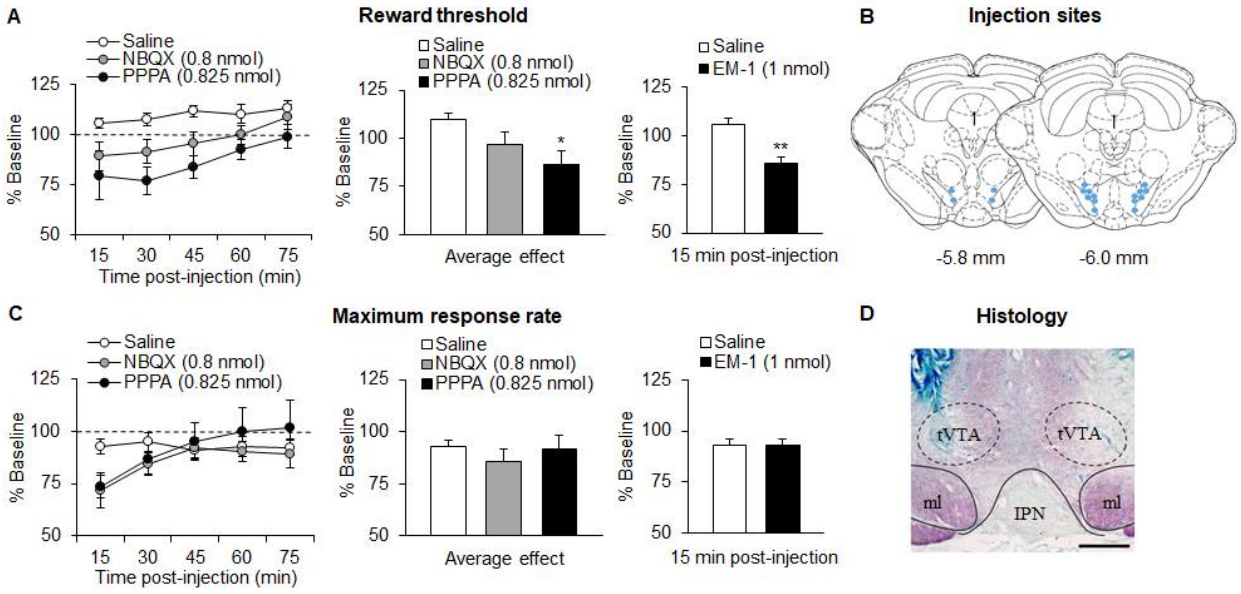
A
Saline
NBQX (0.8 nmol)
PPPA (0.825 nmol)
% Baseline
Time post-injection (min)
Reward threshold
Average effect
15 min post-injection
EM-1 (1 nmol)
B
Injection sites
-5.8 mm
-6.0 mm
C
Maximum response rate
D
Histology
tVTA
ml
IPN

Figure 1

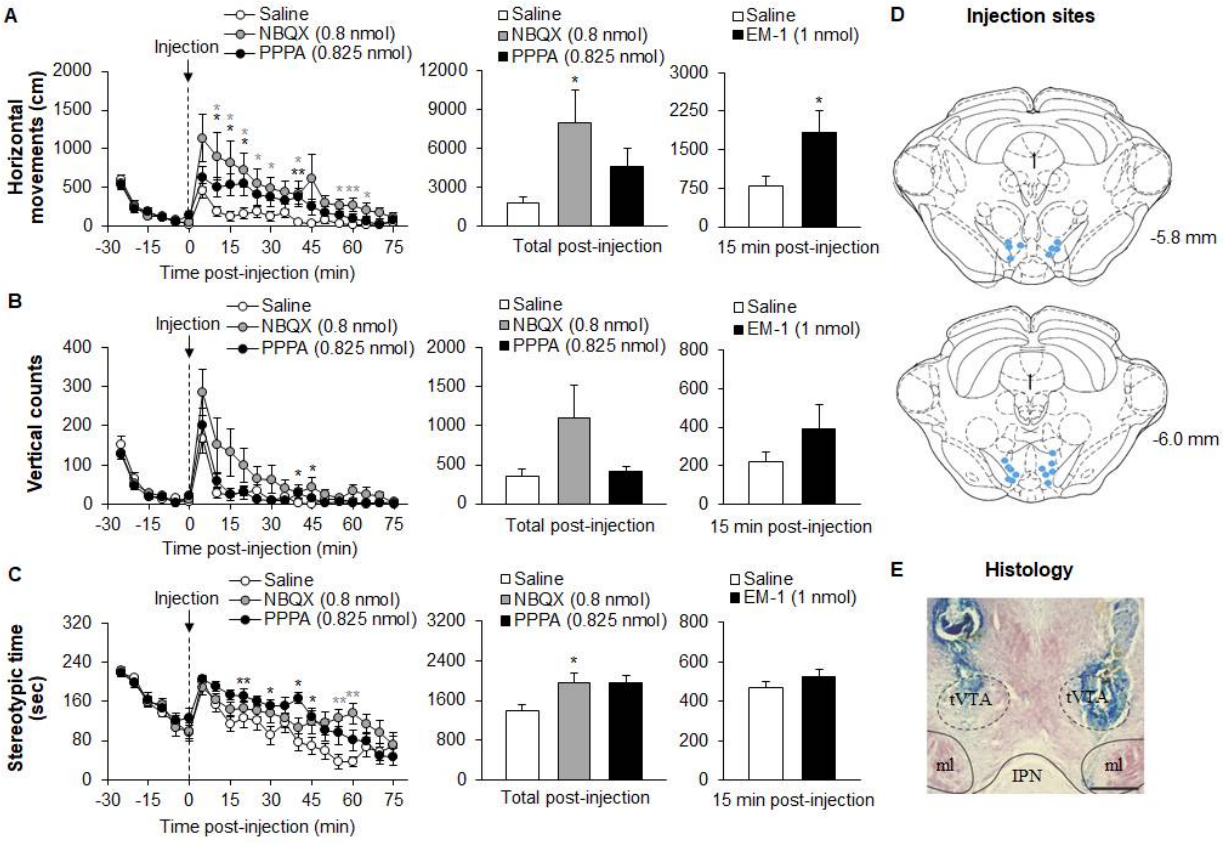
A
Saline
NBQX (0.8 nmol)
PPPA (0.825 nmol)
Injection
Horizontal movements (cm)
Time post-injection (min)
Saline
NBQX (0.8 nmol)
PPPA (0.825 nmol)
Total post-injection
Saline
EM-1 (1 nmol)
15 min post-injection
B
Vertical counts
C
Stereotypic time (sec)
D
Injection sites
-5.8 mm
-6.0 mm
E
Histology
tVTA
tVTA
ml
IPN
ml

Figure 2

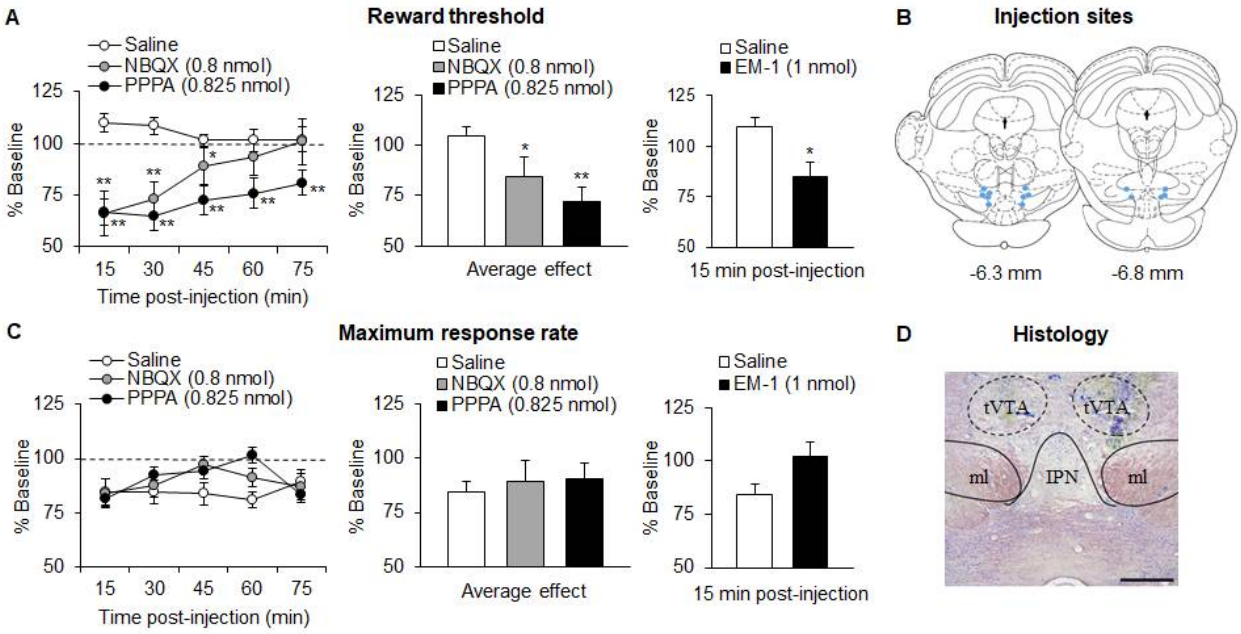
A
Saline
NBQX (0.8 nmol)
PPPA (0.825 nmol)
% Baseline
Time post-injection (min)
Reward threshold
Saline
NBQX (0.8 nmol)
PPPA (0.825 nmol)
Average effect
Saline
EM-1 (1 nmol)
15 min post-injection
B
Injection sites
-6.3 mm
-6.8 mm
C
Maximum response rate
D
Histology
tVTA
tVTA
ml
IPN
ml

Figure 3

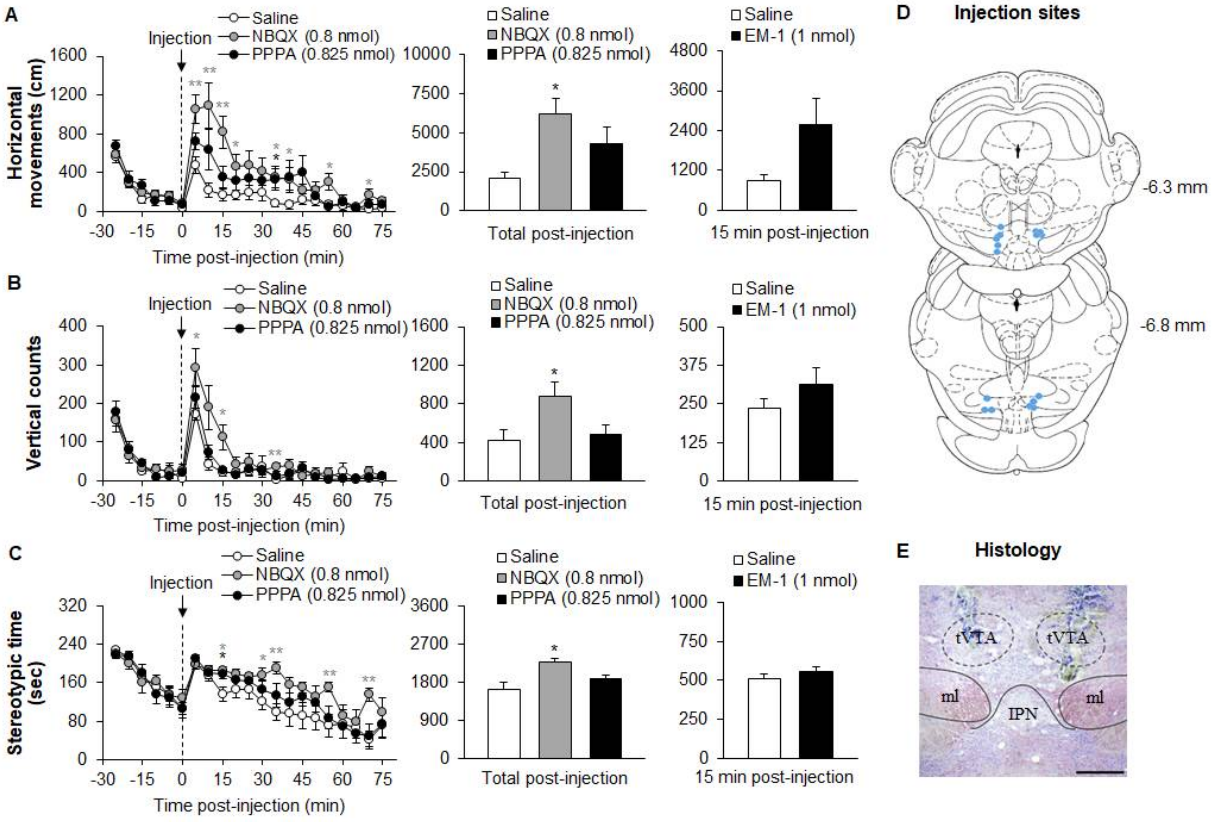
A
Saline
NBQX (0.8 nmol)
PPPA (0.825 nmol)
Injection
Horizontal movements (cm)
Time post-injection (min)
Total post-injection
15 min post-injection
EM-1 (1 nmol)
B
Vertical counts
C
Stereotypic time (sec)
D
Injection sites
-6.3 mm
-6.8 mm
E
Histology
tVTA
ml
IPN

Figure 4

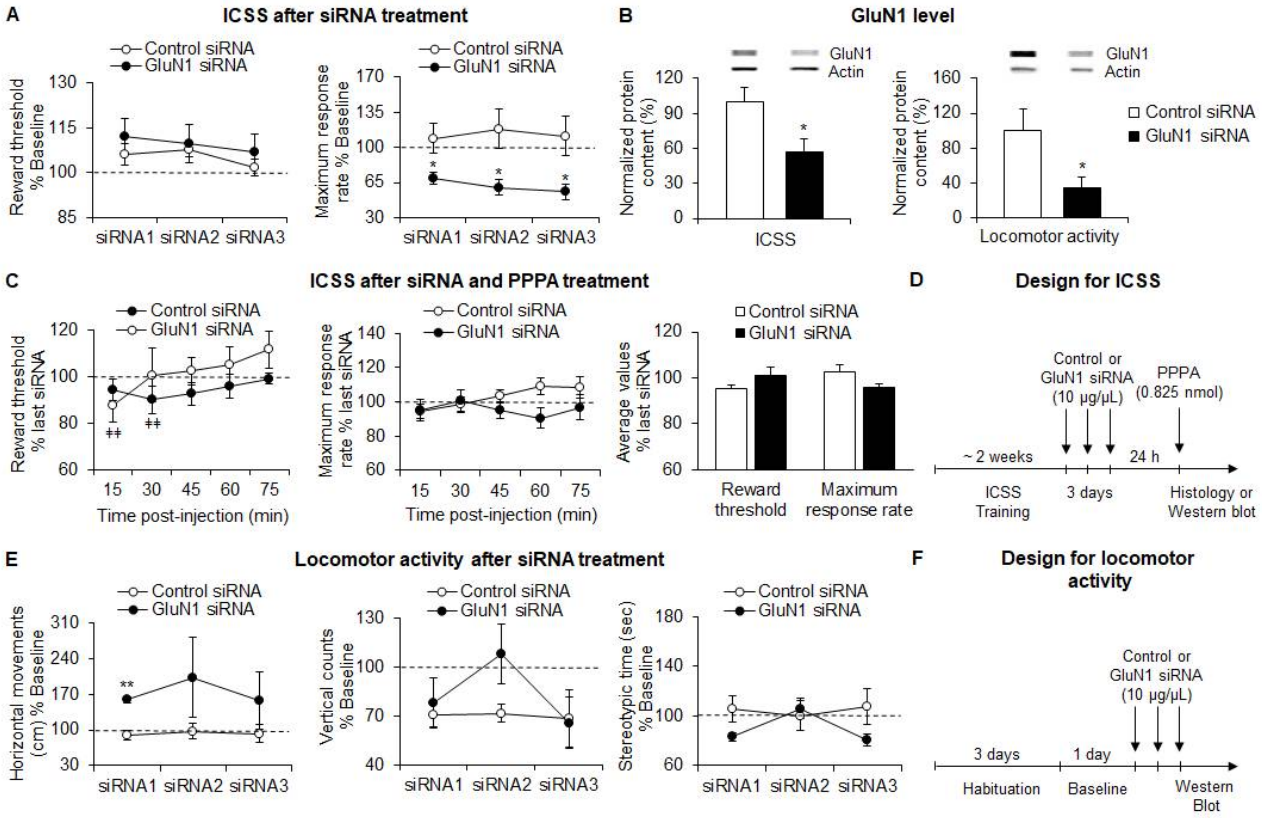
A
ICSS after siRNA treatment
Control siRNA
GluN1 siRNA
Reward threshold % Baseline
siRNA1 siRNA2 siRNA3
Maximum response rate % Baseline
B
GluN1 level
GluN1
Actin
Normalized protein content (%)
ICSS
Locomotor activity
Control siRNA
GluN1 siRNA
C
ICSS after siRNA and PPPA treatment
Reward threshold % last siRNA
Time post-injection (min)
Maximum response rate % last siRNA
Average values % last siRNA
Reward threshold
Maximum response rate
D
Design for ICSS
Control or GluN1 siRNA (10 µg/µL)
PPPA (0.825 nmol)
~ 2 weeks
24 h
ICSS Training
3 days
Histology or Western blot
E
Locomotor activity after siRNA treatment
Horizontal movements (cm) % Baseline
Vertical counts % Baseline
Stereotypic time (sec) % Baseline
F
Design for locomotor activity
3 days
1 day
Habituation
Baseline
Western Blot

Figure 5

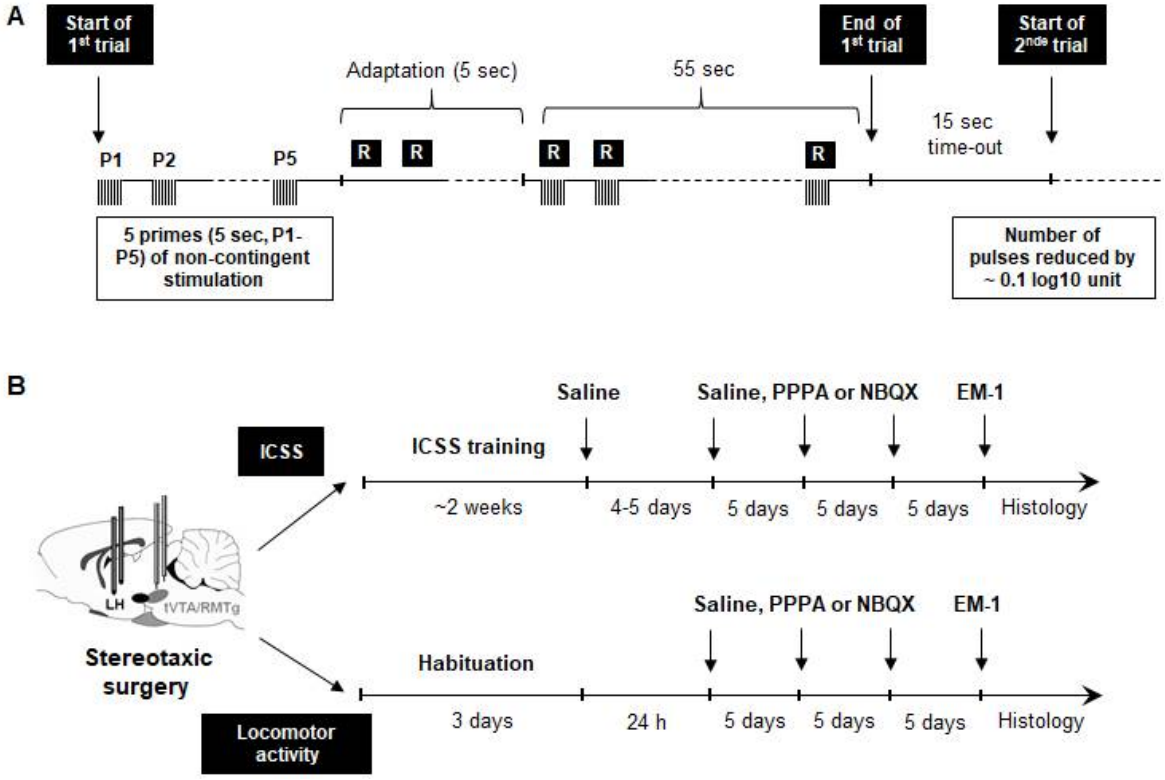

Supplementary Figure 1

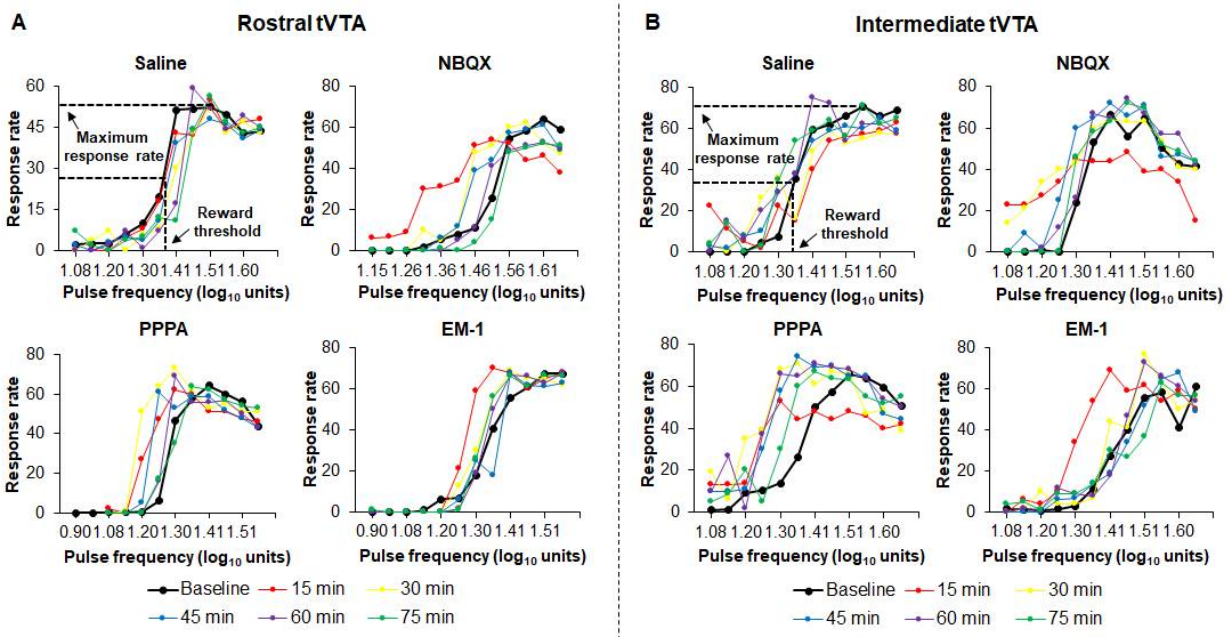

Supplementary Figure 2

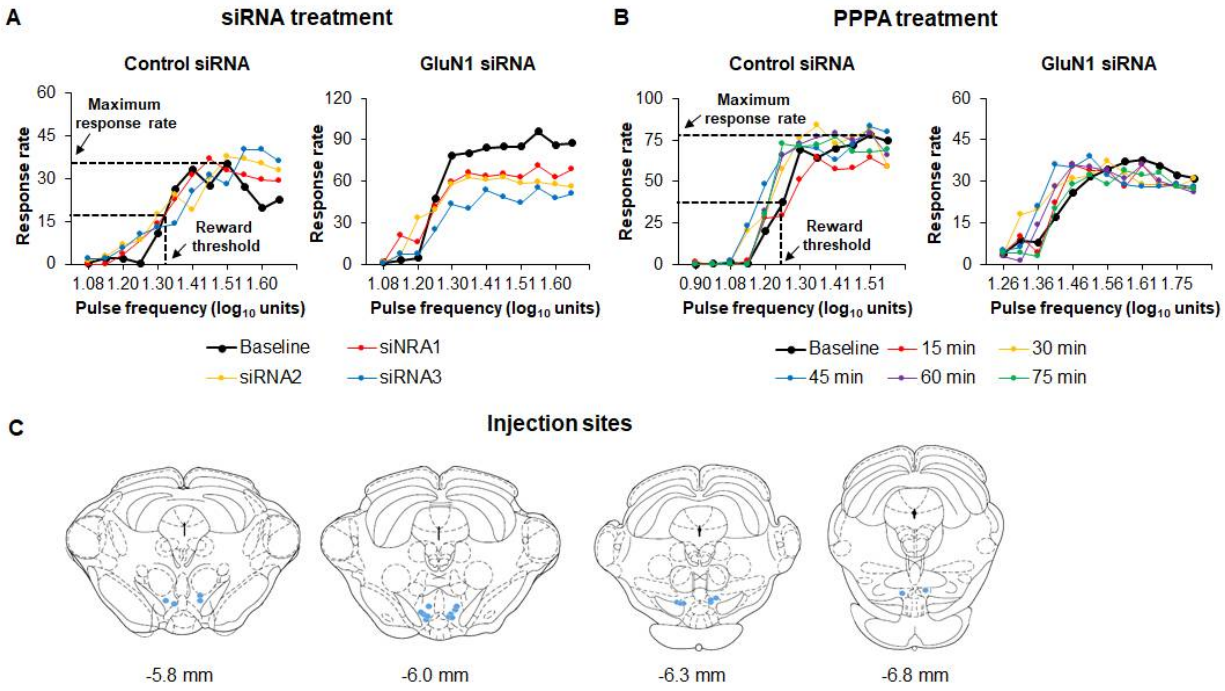

Supplementary Figure 3

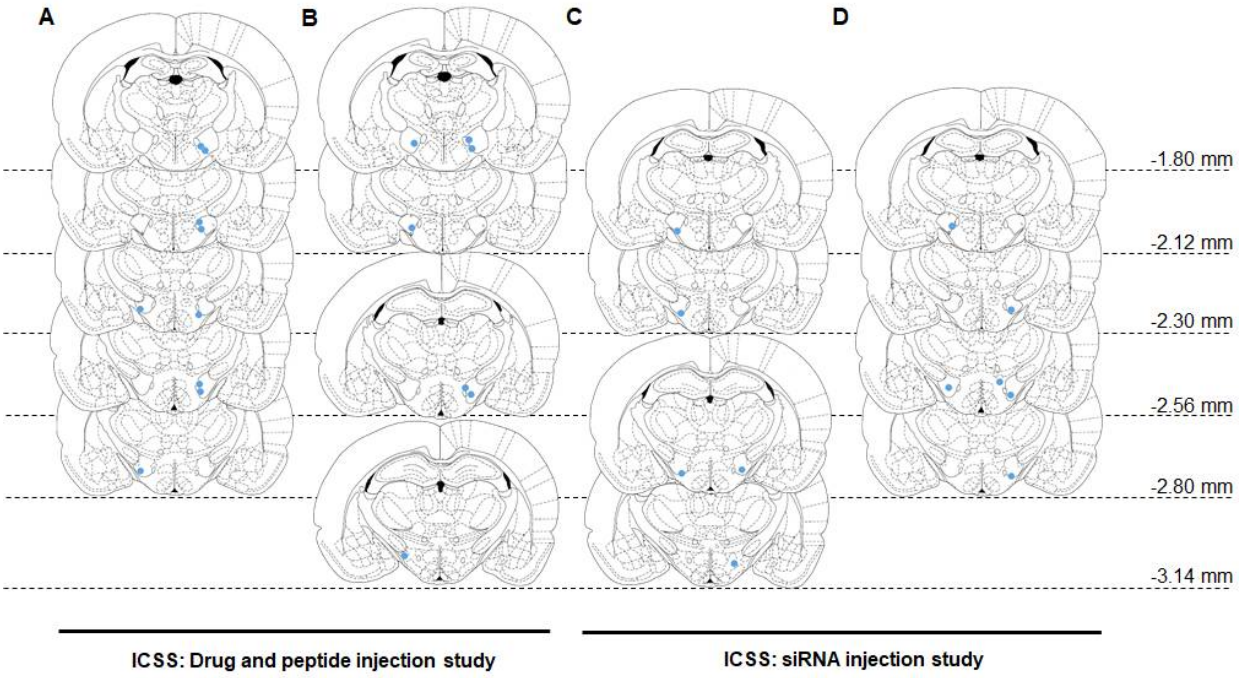

Supplementary Figure 4

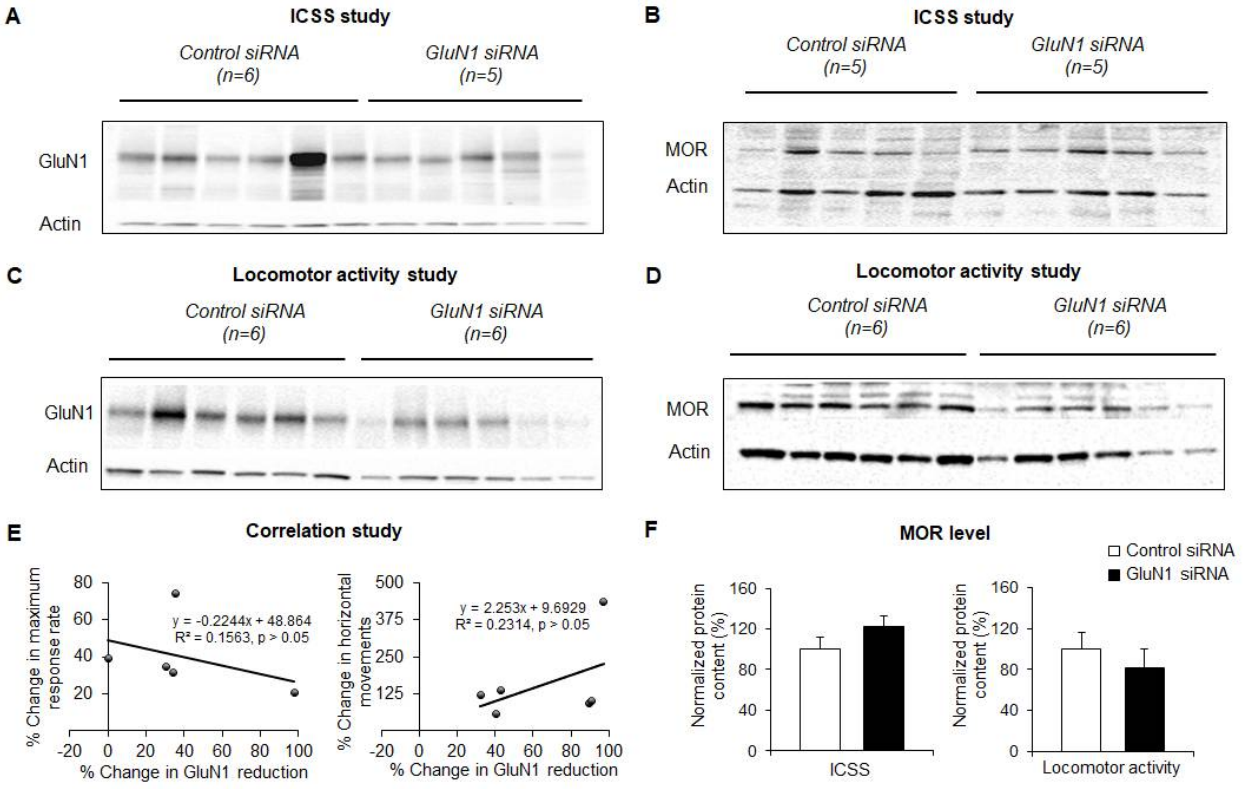

Supplementary Figure 5

REFERENCES

Ahlenius S, Hillegaart V, Thorell G, Magnusson O, Fowler CJ (1987) Suppression of exploratory locomotor activity and increase in dopamine turnover following the local application of cis-flupenthixol into limbic projection areas of the rat striatum. Brain Res 402:131-138.

Balcita-Pedicino JJ, Omelchenko N, Bell R, Sesack SR (2011) The inhibitory influence of the lateral habenula on midbrain dopamine cells: ultrastructural evidence for indirect mediation via the rostromedial mesopontine tegmental nucleus. J Comp Neurol 519:1143-1164.

Barrot M, Sesack SR, Georges F, Pistis M, Hong S, Jhou TC (2012) Braking dopamine systems: a new GABA master structure for mesolimbic and nigrostriatal functions. J Neurosci 32:14094-14101.

Benaliouad F, Kapur S, Rompre PP (2007) Blockade of 5-HT2a receptors reduces haloperidol-induced attenuation of reward. Neuropsychopharmacology 32:551-561.

Bergeron S, Rompre PP (2013) Blockade of ventral midbrain NMDA receptors enhances brain stimulation reward: a preferential role for GluN2A subunits. Eur Neuropsychopharmacol 23:1623-1635.

Bourdy R, Sanchez-Catalan MJ, Kaufling J, Balcita-Pedicino JJ, Freund-Mercier MJ, Veinante P, Sesack SR, Georges F, Barrot M (2014) Control of the nigrostriatal dopamine neuron activity and motor function by the tail of the ventral tegmental area. Neuropsychopharmacology 39:2788-2798.

Brinschwitz K, Dittgen A, Madai VI, Lommel R, Geisler S, Veh RW (2010) Glutamatergic axons from the lateral habenula mainly terminate on GABAergic neurons of the ventral midbrain. Neuroscience 168:463-476.

Brown PL, Palacorolla H, Brady D, Riegger K, Elmer GI, Shepard PD (2017) Habenula-Induced Inhibition of Midbrain Dopamine Neurons Is Diminished by Lesions of the Rostromedial Tegmental Nucleus. J Neurosci 37:217-225.

Carlezon WA, Jr., Nestler EJ (2002) Elevated levels of GluR1 in the midbrain: a trigger for sensitization to drugs of abuse? Trends Neurosci 25:610-615.

Carlezon WA, Jr., Boundy VA, Haile CN, Lane SB, Kalb RG, Neve RL, Nestler EJ (1997) Sensitization to morphine induced by viral-mediated gene transfer. Science 277:812-814.

Carlezon WA, Jr., Todtenkopf MS, McPhie DL, Pimentel P, Pliakas AM, Stellar JR, Trzcinska M (2001) Repeated exposure to rewarding brain stimulation downregulates GluR1 expression in the ventral tegmental area. Neuropsychopharmacology 25:234-241.

Carthew RW, Sontheimer EJ (2009) Origins and Mechanisms of miRNAs and siRNAs. Cell 136:642-655.

Cornish JL, Nakamura M, Kalivas PW (2001) Dopamine-independent locomotion following blockade of N-methyl-D-aspartate receptors in the ventral tegmental area. J Pharmacol Exp Ther 298:226-233.

Dobi A, Margolis EB, Wang HL, Harvey BK, Morales M (2010) Glutamatergic and nonglutamatergic neurons of the ventral tegmental area establish local synaptic contacts with dopaminergic and nondopaminergic neurons. J Neurosci 30:218-229.

Ducrot C, Fortier E, Bouchard C, Rompre PP (2013) Opposite modulation of brain stimulation reward by NMDA and AMPA receptors in the ventral tegmental area. Front Syst Neurosci 7:57.

Edmonds DE, Stellar JR, Gallistel CR (1974) Parametric analysis of brain stimulation reward in the rat: II. Temporal summation in the reward system. J Comp Physiol Psychol 87:860-869.

French ED, Mura A, Wang T (1993) MK-801, phencyclidine (PCP), and PCP-like drugs increase burst firing in rat A10 dopamine neurons: comparison to competitive NMDA antagonists. Synapse 13:108-116.

Gifuni AJ, Jozaghi S, Gauthier-Lamer AC, Boye SM (2012) Lesions of the lateral habenula dissociate the reward-enhancing and locomotor-stimulant effects of amphetamine. Neuropharmacology 63:945-957.

Gilliss B, Malanga CJ, Pieper JO, Carlezon WA, Jr. (2002) Cocaine and SKF-82958 potentiate brain stimulation reward in Swiss-Webster mice. Psychopharmacology (Berl) 163:238-248.

Goncalves L, Sego C, Metzger M (2012) Differential projections from the lateral habenula to the rostromedial tegmental nucleus and ventral tegmental area in the rat. J Comp Neurol 520:1278-1300.

Gonon FG (1988) Nonlinear relationship between impulse flow and dopamine released by rat midbrain dopaminergic neurons as studied by in vivo electrochemistry. Neuroscience 24:19-28.

Grace AA, Bunney BS (1984) The control of firing pattern in nigral dopamine neurons: burst firing. J Neurosci 4:2877-2890.

Hernandez G, Khodami-Pour A, Levesque D, Rompre PP (2015) Reduction in Ventral Midbrain NMDA Receptors Reveals Two Opposite Modulatory Roles for Glutamate on Reward. Neuropsychopharmacology 40:1682-1691.

Hernandez G, Cossette MP, Shizgal P, Rompre PP (2016) Ventral Midbrain NMDA Receptor Blockade: From Enhanced Reward and Dopamine Inactivation. Front Behav Neurosci 10:161.

Hernandez G, Trujillo-Pisanty I, Cossette MP, Conover K, Shizgal P (2012) Role of dopamine tone in the pursuit of brain stimulation reward. J Neurosci 32:11032-11041.

Hjelmstad GO, Xia Y, Margolis EB, Fields HL (2013) Opioid modulation of ventral pallidal afferents to ventral tegmental area neurons. J Neurosci 33:6454-6459.

Hong S, Jhou TC, Smith M, Saleem KS, Hikosaka O (2011) Negative reward signals from the lateral habenula to dopamine neurons are mediated by rostromedial tegmental nucleus in primates. J Neurosci 31:11457-11471.

Horvitz JC (2002) Dopamine gating of glutamatergic sensorimotor and incentive motivational input signals to the striatum. Behav Brain Res 137:65-74.

Huff ML, LaLumiere RT (2015) The rostromedial tegmental nucleus modulates behavioral inhibition following cocaine self-administration in rats. Neuropsychopharmacology 40:861-873.

Ikemoto S (2002) Ventral striatal anatomy of locomotor activity induced by cocaine, D-amphetamine, dopamine and D1/D2 agonists. Neuroscience 113:939-955.

Ikemoto S, Murphy JM, McBride WJ (1997) Self-infusion of GABA(A) antagonists directly into the ventral tegmental area and adjacent regions. Behav Neurosci 111:369-380.

Ikemoto S, Murphy JM, McBride WJ (1998) Regional differences within the rat ventral tegmental area for muscimol self-infusions. Pharmacol Biochem Behav 61:87-92.

Jalabert M, Bourdy R, Courtin J, Veinante P, Manzoni OJ, Barrot M, Georges F (2011) Neuronal circuits underlying acute morphine action on dopamine neurons. Proc Natl Acad Sci U S A 108:16446-16450.

Jhou TC, Fields HL, Baxter MG, Saper CB, Holland PC (2009a) The rostromedial tegmental nucleus (RMTg), a GABAergic afferent to midbrain dopamine neurons, encodes aversive stimuli and inhibits motor responses. Neuron 61:786-800.

Jhou TC, Geisler S, Marinelli M, Degarmo BA, Zahm DS (2009b) The mesopontine rostromedial tegmental nucleus: A structure targeted by the lateral habenula that projects to the ventral tegmental area of Tsai and substantia nigra compacta. J Comp Neurol 513:566-596.

Jhou TC, Good CH, Rowley CS, Xu SP, Wang H, Burnham NW, Hoffman AF, Lupica CR, Ikemoto S (2013) Cocaine drives aversive conditioning via delayed activation of dopamine-responsive habenular and midbrain pathways. J Neurosci 33:7501-7512.

Johnson K, Churchill L, Klitenick MA, Hooks MS, Kalivas PW (1996) Involvement of the ventral tegmental area in locomotion elicited from the nucleus accumbens or ventral pallidum. J Pharmacol Exp Ther 277:1122-1131.

Karreman M, Westerink BH, Moghaddam B (1996) Excitatory amino acid receptors in the ventral tegmental area regulate dopamine release in the ventral striatum. J Neurochem 67:601-607.

Koob GF, Stinus L, Le Moal M (1981) Hyperactivity and hypoactivity produced by lesions to the mesolimbic dopamine system. Behav Brain Res 3:341-359.

Koob GF, Riley SJ, Smith SC, Robbins TW (1978) Effects of 6-hydroxydopamine lesions of the nucleus accumbens septi and olfactory tubercle on feeding, locomotor activity, and amphetamine anorexia in the rat. J Comp Physiol Psychol 92:917-927.

Kotecki L, Hearing M, McCall NM, Marron Fernandez de Velasco E, Pravetoni M, Arora D, Victoria NC, Munoz MB, Xia Z, Slesinger PA, Weaver CD, Wickman K (2015) GIRK Channels Modulate Opioid-Induced Motor Activity in a Cell Type- and Subunit-Dependent Manner. J Neurosci 35:7131-7142.

Kretschmer BD (1999) Modulation of the mesolimbic dopamine system by glutamate: role of NMDA receptors. J Neurochem 73:839-848.

Lavezzi HN, Parsley KP, Zahm DS (2015) Modulation of locomotor activation by the rostromedial tegmental nucleus. Neuropsychopharmacology 40:676-687.

Lecca S, Melis M, Luchicchi A, Muntoni AL, Pistis M (2012) Inhibitory inputs from rostromedial tegmental neurons regulate spontaneous activity of midbrain dopamine cells and their responses to drugs of abuse. Neuropsychopharmacology 37:1164-1176.

Lecca S, Melis M, Luchicchi A, Ennas MG, Castelli MP, Muntoni AL, Pistis M (2011) Effects of drugs of abuse on putative rostromedial tegmental neurons, inhibitory afferents to midbrain dopamine cells. Neuropsychopharmacology 36:589-602.

Lodge DJ, Grace AA (2006) The laterodorsal tegmentum is essential for burst firing of ventral tegmental area dopamine neurons. Proc Natl Acad Sci U S A 103:5167-5172.

Mathe JM, Nomikos GG, Schilstrom B, Svensson TH (1998) Non-NMDA excitatory amino acid receptors in the ventral tegmental area mediate systemic dizocilpine (MK-801) induced hyperlocomotion and dopamine release in the nucleus accumbens. J Neurosci Res 51:583-592.

Matsui A, Williams JT (2011) Opioid-sensitive GABA inputs from rostromedial tegmental nucleus synapse onto midbrain dopamine neurons. J Neurosci 31:17729-17735.

Matsumoto M, Hikosaka O (2007) Lateral habenula as a source of negative reward signals in dopamine neurons. Nature 447:1111-1115.

Miliaressis E, Rompre PP, Laviolette P, Philippe L, Coulombe D (1986) The curve-shift paradigm in self-stimulation. Physiol Behav 37:85-91.

Moisan J, Rompre PP (1998) Electrophysiological evidence that a subset of midbrain dopamine neurons integrate the reward signal induced by electrical stimulation of the posterior mesencephalon. Brain Res 786:143-152.

Murphy CA, DiCamillo AM, Haun F, Murray M (1996) Lesion of the habenular efferent pathway produces anxiety and locomotor hyperactivity in rats: a comparison of the effects of neonatal and adult lesions. Behav Brain Res 81:43-52.

Nakajima S, McKenzie GM (1986) Reduction of the rewarding effect of brain stimulation by a blockade of dopamine D1 receptor with SCH 23390. Pharmacol Biochem Behav 24:919-923.

Narayanan S, Willins D, Dalia A, Wallace L, Uretsky N (1996) Role of dopaminergic mechanisms in the stimulatory effects of MK-801 injected into the ventral tegmental area and the nucleus accumbens. Pharmacol Biochem Behav 54:565-573.

Omelchenko N, Bell R, Sesack SR (2009) Lateral habenula projections to dopamine and GABA neurons in the rat ventral tegmental area. Eur J Neurosci 30:1239-1250.

Overton PG, Clark D (1997) Burst firing in midbrain dopaminergic neurons. Brain Res Brain Res Rev 25:312-334.

Pan WX, Schmidt R, Wickens JR, Hyland BI (2005) Dopamine cells respond to predicted events during classical conditioning: evidence for eligibility traces in the reward-learning network. J Neurosci 25:6235-6242.

Paxinos G, Watson C (1997) The rat brain in stereotaxic coordinates., 3rd Edition. San Deigo, CA: Academic Press.

Perlikowska R, Gach K, Fichna J, Toth G, Walkowiak B, do-Rego JC, Janecka A (2009) Biological activity of endomorphin and [Dmt1]endomorphin analogs with six-membered proline surrogates in position 2. Bioorg Med Chem 17:3789-3794.

Pijnenburg AJ, Honig WM, Van der Heyden JA, Van Rossum JM (1976) Effects of chemical stimulation of the mesolimbic dopamine system upon locomotor activity. Eur J Pharmacol 35:45-58.

Steidl S, Dhillon ES, Sharma N, Ludwig J (2017) Muscarinic cholinergic receptor antagonists in the VTA and RMTg have opposite effects on morphine-induced locomotion in mice. Behav Brain Res 323:111-116.

Suaud-Chagny MF, Chergui K, Chouvet G, Gonon F (1992) Relationship between dopamine release in the rat nucleus accumbens and the discharge activity of dopaminergic neurons during local in vivo application of amino acids in the ventral tegmental area. Neuroscience 49:63-72.

Ungless MA, Magill PJ, Bolam JP (2004) Uniform inhibition of dopamine neurons in the ventral tegmental area by aversive stimuli. Science 303:2040-2042.

Wasserman DI, Tan JM, Kim JC, Yeomans JS (2016) Muscarinic control of rostromedial tegmental nucleus GABA neurons and morphine-induced locomotion. Eur J Neurosci 44:1761-1770.

Wasserman DI, Wang HG, Rashid AJ, Josselyn SA, Yeomans JS (2013) Cholinergic control of morphine-induced locomotion in rostromedial tegmental nucleus versus ventral tegmental area sites. Eur J Neurosci 38:2774-2785.

Yavich L, Tanila H (2007) Mechanics of self-stimulation and dopamine release in the nucleus accumbens. Neuroreport 18:1271-1274.

You ZB, Chen YQ, Wise RA (2001) Dopamine and glutamate release in the nucleus accumbens and ventral tegmental area of rat following lateral hypothalamic self-stimulation. Neuroscience 107:629-639.

Zadina JE, Hackler L, Ge LJ, Kastin AJ (1997) A potent and selective endogenous agonist for the mu-opiate receptor. Nature 386:499-502.

Zangen A, Ikemoto S, Zadina JE, Wise RA (2002) Rewarding and psychomotor stimulant effects of endomorphin-1: anteroposterior differences within the ventral tegmental area and lack of effect in nucleus accumbens. J Neurosci 22:7225-7233.

CHAPTER 3: GENERAL DISCUSSION AND CONCLUSION

3.1 The DDC constitutes a route for the transmission of the reward signal triggered by ICSS

Composed of axons that travel within the habenula, SM and FR, the DDC is a pathway that provides a route for the conduction of information from limbic forebrain to limbic midbrain areas (Sutherland, 1982). Early evidence implicating this pathway in brain stimulation reward comes from lesion studies showing that damage of the habenula-IPN tract decreases the response rate for septal (Boyd and Celso, 1970) and posterior LH (Boyd and Gardner, 1967) electrical stimulation. Subsequently, it was shown that rats could learn to self-administer pulses of electrical stimulation at various sites along the DDC, including the SM, FR and the habenula (Sutherland and Nakajima, 1981; Nakajima, 1984; Blander and Wise, 1989; Vachon and Miliaressis, 1992), implying that stimulation of this pathway is rewarding. In support for a role of the DDC in brain stimulation reward, rewarding electrical stimulation of several sites within the MFB was shown to induce Fos expression (Arvanitogiannis et al., 1997; Hunt and McGregor, 1998, 2002) and increase oxidative metabolism (Bielajew, 1991) in the LHb. However, despite evidence implicating the DDC in the positive reinforcing effects of ICSS, the focus of the preponderance of behavioral studies conducted over the past few decades has been on the MFB, another pathway that links forebrain limbic to midbrain limbic areas and that is part of the reward circuitry.

In an attempt to better characterize the role of the DDC in brain stimulation reward, the first set of studies presented in the first article investigated the effect of electrolytic lesions along the DDC on the rewarding effectiveness of ICSS. Two stimulation sites were used; one in the LH, and another one in the DR, and data were analyzed on a case-by-case basis to assess the behavioral effect of different lesion size and/or location. Electrolytic lesions at the DDC produced large and long-lasting decrements in the rewarding effectiveness of both DR and LH self-stimulation, though

the magnitude of the lesion effect was higher at the LH stimulation site. The attenuation of the rewarding effectiveness of LH and DR stimulation following a DDC lesion is in accordance with findings from Morisette and Boye (2008) showing that electrolytic lesions of the habenula produce long-lasting increases in reward thresholds obtained at these two sites of stimulation. A larger effect at the LH stimulation site is consistent with prior findings showing that electrolytic lesions in caudal sites of the MFB markedly reduce the rewarding efficacy of electrical stimulation of the rostral MFB, whereas lesions in the caudal MFB fail to reduce the rewarding efficacy of electrical stimulation of the rostral MFB, even when the distance between the stimulation and lesion site is the same (Gallistel et al., 1996). Results showing that lesions at the DDC were more effective at attenuating the rewarding effectiveness of LH self-stimulation as compared to DR self-stimulation may also suggest that the DDC shares a significantly higher density of axonal connections with the LH. Accordingly, anatomical evidence shows that the habenula receives highly dense inputs from the LH, but only moderate inputs from the DR (Herkenham and Nauta, 1977).

The effect of a DDC lesion on brain stimulation reward was assessed using three different current intensities. The use of different current intensities provides insight into the location of the reward-relevant fibers near the stimulation electrode in reference with the lesioned area. Current intensities were chosen so as to yield reward thresholds of 25, 50 or 100 Hz, and were designated as “low”, “medium” or “high” current intensity, respectively. Results show that the magnitude of the increase in reward threshold following a DDC lesion was very high at low and medium current intensities, whereas only a moderate increase, or no increase at all, in reward threshold was observed at the high current intensity. A plausible interpretation of these results is that the lesioned neurons, or their efferent targets, are close to the tip of the stimulation electrode. Therefore, a high current intensity will recruit proportionally fewer lesioned fibers, whereas a low current intensity

will recruit proportionally more lesioned fibers. In the latter case, a DDC lesion will be more effective in reducing the rewarding effectiveness of the stimulation since a proportionally higher number of reward-relevant fibers would be affected. Our results are consistent with prior psychophysical studies (Murray and Shizgal, 1991, 1996a; Boye, 2005; Morissette and Boye, 2008), and suggest that a low current intensity for ICSS could constitute a more sensitive parameter for scouting lesion effects on the reward threshold.

The electrolytic lesions employed in the first study differed in size and location. First, we found no correlation between the size of the lesion and its resulting effect on reward threshold. This observation concurs with prior psychophysical findings (Waraczynski, 1988; Murray and Shizgal, 1991; Morissette and Boye, 2008) and could suggest the presence of a diffuse network of reward-relevant axons that are highly collateralized. Second, we found that DDC lesions that targeted the SM were generally more effective in attenuating brain stimulation reward compared to lesions encroaching the LHb. These findings are very informative with respect to the neural substrate of ICSS, and suggest that fibers of passage within the DDC, but not intrinsic habenula cell bodies, participate in the transmission of the reward signal induced by ICSS. This view is also supported by a set of studies from Boye and colleagues showing that destruction of DDC fibers with the use of electrolytic lesions attenuate brain stimulation reward (Morissette and Boye, 2008), whereas cell body specific lesions of the habenula fail to alter the reward-enhancing effect of amphetamine (Gifuni et al., 2012).

In light of the aforementioned findings, the DDC is well poised to act as route for the reward signal triggered by ICSS. Reward signals initiated by electrical stimulation of the LH could travel through the DDC by coursing dorsocaudally via the SM, whereas those initiated by electrical

stimulation of the DR could travel through the DDC by coursing towards the ventral midbrain and then dorsorostrally via the FR.

3.2 The DDC and MFB are functionally interconnected and merge on common reward-relevant neural elements

Previous studies combining electrolytic lesions with behavioral measures of brain stimulation reward have often yielded ambiguous results. First, in the majority of cases, prolonged attenuation of brain stimulation reward failed to be observed following electrolytic lesions (Murray and Shizgal, 1991; Waraczynski et al., 1998; Boye, 2005) or a knife cut (Janas and Stellar, 1987) of the MFB, or following electrolytic lesions of the DDC (Morissette and Boye, 2008). Second, and as mentioned earlier, there is often a discrepancy between the size of the lesion and the resultant reward degradation (Waraczynski, 1988; Murray and Shizgal, 1991; Morissette and Boye, 2008). Although the inconsistent lesion effects may be attributed to the highly collateralized and diffuse network of reward-relevant axons, they may also result from stimulation of two different brain reward pathways, the MFB and DDC, which are functionally interconnected and merge on common reward-relevant neural elements. If so, the loss of reward-relevant neurons within one pathway could be compensated by the other.

To test this hypothesis, the first article of this thesis investigated whether sequential lesions of the DDC and MFB produce additive attenuations of the rewarding effectiveness of LH and DR self-stimulation. Rats received one electrolytic lesion at the DDC and another one at the MFB in a counterbalanced order, with a 2-week interval between each lesion during which they were tested for ICSS. Our results show that sequential lesions at the DDC and MFB produce larger and longer-lasting increases in ICSS reward thresholds than lesions at either pathway alone; this effect was

most commonly observed at the low and medium current intensities and at the LH stimulation site. At the DR stimulation site, no additive effect was observed when the second lesion was done at the MFB, suggesting that the MFB and the DR may only share a modest complement of axons; this effect is consistent with post-lesion rate-frequency data showing that lesions at the DR have little effect on the rewarding effectiveness of MFB stimulation (Waraczynski et al., 1998). The additive lesion effect observed in the remaining cases suggests that the DDC and MFB are two functionally interconnected pathways that act in parallel fashion to participate in the transmission of the reward signal triggered by ICSS. At their rostral intersection, descending hypothalamic fibers travel caudally along the MFB to reach the VTA (Nieh et al., 2016), and dorsally along the DDC to reach the LHb (Stamatakis et al., 2016). At their caudal intersection, efferent fibers from the DDC reach the midbrain via the FR (Herkenham and Nauta, 1979).

The view that the MFB and DDC are functionally connected and merge on common reward-relevant neural elements is also supported by prior findings showing that habenular self-stimulation is facilitated by lesions at the MFB, and vice versa (Sutherland and Nakajima, 1981). Also noteworthy to mention are findings from Simmons and colleagues (1998) showing that rostral MFB lesions fail to disconnect all ipsilateral forebrain nuclei from the VTA either anatomically, as assessed by True Blue labeling, or functionally, as assessed by the stimulation-induced regional [^{14}C]deoxyglucose patterns. Although these findings indicate a diffuse net-like connection between forebrain nuclei and the VTA, they also suggest the stimulation of a multi-synaptic pathway, such as the DDC, which could entirely bypass the lesion done at the MFB (Simmons et al., 1998).

Altogether, our results agree with evidence showing that the MFB and DDC share similar behavioral functions, and that there is a considerable degree of overlap between their sources of

afferent inputs and efferent targets. In particular, the MFB and DDC have been shown to play crucial roles in a diverse set of behavioral systems, including but not limited to reward, motivation, emotion, endocrine system, sleep and eating habits (Sutherland, 1982; Salaberry and Mendoza, 2015; Stuber and Wise, 2016). Moreover, fibers from both the MFB and DDC innervate various structures of the limbic forebrain system and basal ganglia, and numerous brainstem regions, including the raphe nucleus and the laterodorsal tegmental nucleus (Herkenham and Nauta, 1979; Takagi et al., 1980). Therefore, both the ventral and dorsal pathway of the reward system constitute a functional route between structures located at opposite poles of the brain, and play a prominent role in the control of behavioral processes like goal-directed behaviors.

3.3 The DDC is functionally connected to brain regions activated by ICSS

The results discussed thus far provide relevant information about the neural circuitry of ICSS, and suggest that the DDC acts in parallel with the MFB to transmit the reward signal initiated by electrical stimulation of the LH and DR. The view that the DDC and MFB act in parallel fashion is also supported by a Golgi analysis showing that axons that travel along the MFB also send collaterals into the SM (Millhouse, 1969). However, the aforementioned findings failed to provide reliable information on the populations of neurons that are activated by ICSS and functionally disconnected by the lesion. To address this issue, the study presented in the second article of this thesis was aimed at assessing the effect of electrolytic lesions at the DDC on the distribution of FLIR, a marker of neuronal activity, induced by LH self-stimulation. The LH was used as a stimulation site instead of the DR because of our previous results showing that lesions at the DDC are more effective at attenuating the rewarding effectiveness of LH self-stimulation compared to DR self-stimulation. To our knowledge, this is the first study that combines FLIR with lesions and

behavioral measures of brain stimulation reward to investigate the population of neurons that remain active following damage to the DDC.

Similar to findings obtained in the first article of the present thesis and in previous experiments (Morissette and Boye, 2008), electrolytic lesions at the DDC resulted in significant increases in ICSS reward thresholds with no or minimal changes in the maximal response rate. Our data failed to show a clear correlation between the lesion size and the resultant effect on the reward threshold, indicating that the neural substrate for brain stimulation reward is anatomically diffuse, collateralized and heterogeneous. In subjects that did not receive a lesion at the DDC, the rewarding electrical stimulation of the LH induced FLIR in forebrain, midbrain and brainstem regions. Notably, high to moderate increases in FLIR were observed in the mPFC, OFC, BNST, NAc, basolateral amygdala (BLA), SNc and reticula, VTA, tVTA, IPN, pontine nuclei (PN), DR and pedunculopontine nucleus, suggesting that the activity of these regions is strongly related to the rewarding effectiveness of LH self-stimulation. It is worth mentioning that the methodological approach used in our study did not allow us to dissociate the contribution of motor activity, non-specific electrical stimulation, and rewarding electrical stimulation to the induction of FLIR. The use of a yoked control and stimulation parameters that are non-rewarding could address this issue (Marcangione and Rompre, 2008). In the majority of forebrain regions analyzed, FLIR was more prominent in the hemisphere ipsilateral to the stimulation electrode, whereas in the majority of midbrain and brainstem regions analyzed, FLIR was equally distributed between the ipsilateral and contralateral hemispheres. These data suggest that the LH reward-relevant fibers that project to the forebrain are predominantly ipsilateral, while those that project to the midbrain and brainstem are bilateral. Accordingly, a previous study employing an anterograde tracer showed that some descending hypothalamic fibers course along the MFB and decussate at several levels,

including the supramamillary decussation and pontine tegmentum, to innervate the contralateral hemisphere (Toth et al., 1999). Thus, descending LH fibers could innervate ipsilateral midbrain and brainstem regions by coursing along the MFB, and could target contralateral midbrain and brainstem regions by decussating in the midline.

Subjects that received a lesion at the DDC showed a significant reduction in stimulation-induced FLIR in certain brain regions as compared to subjects that did not receive a lesion and were trained for ICSS. Brain regions that showed reduced stimulation-induced FLIR following a DDC lesion included the BNST, NAc core and shell, BLA, IPN, PN and DR. Except for the DR and IPN, the level of FLIR in these brain regions remained significantly higher from that in the sham group, indicating that some neurons were still activated by the stimulation. However, a significantly lower proportion of neurons within the DR and IPN remained active following the lesion inasmuch as the level of FLIR in these structures was similar between lesioned and control animals. The view that certain brain regions showed reduced stimulation-induced FLIR following lesions at the DDC suggest that their activity is likely influenced by this pathway. In agreement with our findings, previous anatomical studies showed that the LHb sends dense projections to the NAc, DR and amygdala (Herkenham and Nauta, 1979; Sego et al., 2014). Anterograde tracing studies also confirmed the existence of dense MHb projections to the IPN organized in a topographical manner (Contestabile and Flumerfelt, 1981; Kawaja et al., 1988). Finally, electrolytic lesions at the MHb of cats were shown to induce degenerating fibers in the SM, which were traced to the amygdala and the BNST, demonstrating that fibers from the DDC may actually terminate into these regions by coursing through the SM (Akagi and Powell, 1968).

A reduction in stimulation-induced FLIR in certain structures following a DDC lesion implies that the corresponding brain regions are functionally disconnected from the site of stimulation.

However, our results show that a lesion at the DDC caused a marked reduction in stimulation-induced FLIR in the PN, despite the lack of anatomical connections between the PN and the DDC. A tantalizing explanation for this effect is that the reduced FLIR in the PN resulted from a transsynaptic reduction of neuronal activity following a DDC lesion via an IPN intermediate connection (Kim, 2009; Campolattaro et al., 2011). Increased FLIR in the PN following electrical stimulation of the LH was previously reported (Arvanitogiannis et al., 1997), however, this effect may be attributed to the motor activity inherent to the ICSS behavior (Gasbarri et al., 2003). Our results also indicate a lack of lesion effect on stimulation-induced FLIR in midbrain regions including the substantia nigra pars compacta and reticula, the VTA and the tVTA. These results were surprising given that the LHb, which was damaged by the lesion, exerts an inhibitory control over DA neurons of the VTA and substantia nigra (Christoph et al., 1986), and an excitatory control over GABAergic neurons of the tVTA (Brinschwitz et al., 2010). Reasons for the lack of lesion effect in these midbrain regions are diverse and include (i) the existence of direct excitatory habenular projections (whose removal will tend to reduce FLIR) onto VTA DA neurons (Omelchenko et al., 2009) in addition to the indirect inhibitory projections (whose removal will tend to increase FLIR) onto midbrain DA neurons (Balcita-Pedicino et al., 2011), and (ii) the location of the DDC electrolytic lesions, which were mainly centered on the SM and LHb and did not encroach the FR.

3.4 AMPA and NMDA receptors of the tVTA are major inhibitors of brain stimulation reward and locomotor activity

The results obtained from the first two articles of the present thesis demonstrate that the reward signal initiated by electrical stimulation of the LH is in part transmitted by the DDC, a pathway

that courses through the habenula and projects into mesencephalic regions, including the tVTA. The tVTA is a recently identified structure that was described in many species, including mice, rats and monkeys, as a cluster of GABAergic cells that convey negative reward-related information (Jhou et al., 2009b; Hong et al., 2011; Stamatakis and Stuber, 2012). Previous work has shown that AMPA and NMDA receptors located in the midbrain play a key role in the control of brain stimulation reward and locomotor activity (Kretschmer, 1999; Bergeron and Rompre, 2013; Ducrot et al., 2013). However, no investigation thus far has been performed to elucidate the role of tVTA AMPA and NMDA receptors in brain stimulation reward. Such investigation could have important implications for understanding motivational processes since tVTA neurons receive a strong glutamatergic input from the LHb (Jhou et al., 2009a; Kaufling et al., 2009; Goncalves et al., 2012) while forming inhibitory GABAergic connections with DA neurons of the VTA and SNc (Jhou et al., 2009a; Balcita-Pedicino et al., 2011; Bourdy et al., 2014). In the third article of the present thesis, ICSS and locomotor activity were assessed before and after AMPA and NMDA receptor blockade in the tVTA using the glutamate receptor antagonists NBQX and PPPA, respectively. Results show that within certain regions of the tVTA, blockade of AMPA or NMDA receptors reduces the reward threshold of LH self-stimulation without altering the maximum response rate; an effect that is interpreted as specific reward changes (Miliaressis et al., 1986). Bilateral infusion of NBQX or PPPA into certain sites of the tVTA also resulted in increased locomotor activity; an effect that has been generally associated with increased mesolimbic DA signaling (Schindler and Carmona, 2002; Alcaro et al., 2007; Palmiter, 2008). In light of previous electrophysiological findings showing that AMPA and NMDA receptor antagonists reduce the spontaneous firing activity of VTA GABAergic cells (Wang and French, 1995; Steffensen et al., 1998; Bonci and Malenka, 1999), we postulate that the rewarding and locomotor stimulant effect

of intra-tVTA injection of NBQX or PPPA are the result of a decreased GABAergic inhibitory tone onto midbrain DA cells. Our results are consistent with the view that activation of the tVTA by local AMPA injections produces conditioned place aversion in rats (Jhou et al., 2013), and are in line with previous reports demonstrating increased locomotor activity following neurotoxic lesions (Bourdy et al., 2014; Brown et al., 2017), optogenetic inhibition (Jhou et al., 2013), and GABA-mediated inhibition (Huff and LaLumiere, 2015; Lavezzi et al., 2015) of the tVTA.

An important finding of the studies presented in the third article of the present thesis is that NBQX and PPPA produced different rewarding and psychomotor stimulant effects when injected into rostral or intermediate sites of the tVTA. For instance, NBQX failed to alter ICSS reward thresholds when injected into the rostral tVTA, but produced significant decreases in reward thresholds when injected into the intermediate tVTA. Our results also show that the reward-enhancing effect of PPPA was stronger when the injection occurred in intermediates sites of the tVTA. These findings strongly point to anatomical and/or functional heterogeneity within the tVTA. Consistently, Jhou et al (2009b) found that neurons representing the rostral and caudal part of the tVTA exhibit a different pattern of functional projections to VTA DA neurons. While the rostral tVTA shows a densely packed cluster of GABAergic neurons projecting to VTA DA neurons, this density progressively declines at more caudal levels of the tVTA (Jhou et al., 2009a). Based on findings from Jhou and colleagues (2009b), one would expect to observe a higher enhancement of brain stimulation reward or locomotor activity upon blockade of glutamatergic receptors in the rostral tVTA, which seems to have a larger influence on VTA DA neuronal activity. However, this speculation appears at odds with our results showing that blockade of glutamate inputs into the intermediate tVTA produces a higher enhancement in brain stimulation reward as compared to blockade of glutamate inputs into the rostral tVTA. An attempted

explanation for the observed results is that a high proportion of neurons in the intermediate tVTA may convey negative reward signal, whereas only a few neurons in the rostral tVTA may be involved in this process. In support for this hypothesis, Perrotti and colleagues (2005) showed that ΔFosB expression is approximately 4 to 5 times higher in intermediate regions of the tVTA (6.30 and 6.72 mm from bregma) as compared to rostral regions of the tVTA (6.04 mm from bregma) following chronic administration of cocaine. Like most drugs of abuse, cocaine produces aversive effects after its initial rewarding effects have dissipated (Ettenberg, 2004; Jhou et al., 2013). The higher induction of ΔFosB observed in the intermediate tVTA (Perrotti et al., 2005) may therefore suggest that neurons in this region are more responsive to aversive stimuli and are likely to receive significantly more inputs from structures implicated in aversive responses, including the LHb (Matsumoto and Hikosaka, 2007, 2009) and the PAG (Berton et al., 2007). Finally, our results show that blockade of NMDA receptors in the tVTA produced the highest enhancement in brain stimulation reward, while blockade of AMPA receptors in the tVTA produced the highest enhancement in locomotor activity. These findings indicate that ICSS and locomotor activity are subserved by different mechanisms. While the former may be more sensitive to changes in NMDA receptor activity, the latter may be more strongly influenced by changes in AMPA receptor activity. This dissociation between reward seeking behavior and locomotor activity has also been reported with studies employing visual stimulus-induced reinforcement showing that certain drug manipulations have a stronger propensity to influence one behavior over the other (Vollrath-Smith et al., 2012; Keller et al., 2014; Talishinsky et al., 2017).

Altogether, the results obtained from the third article of the present thesis indicate that injection of NBQX and PPPA within certain sites of the tVTA enhance brain stimulation reward and locomotor activity, two behavioral measures that are largely dependent on DA neurotransmission.

These findings are consistent with anatomical studies showing that the tVTA sends GABAergic projections to DA neurons of the VTA and SNc (Jhou et al., 2009a; Balcita-Pedicino et al., 2011; Bourdy et al., 2014), and are in line with electrophysiological findings showing that electrical stimulation of the tVTA supresses the activity of midbrain DA neurons (Lecca et al., 2011; Lecca et al., 2012; Bourdy et al., 2014). They also agree with findings obtained from optogenetic studies showing that glutamatergic excitation of VTA DA neurons reinforces instrumental behavior and establishes conditioned place preference (McDevitt et al., 2014; Qi et al., 2014). Finally, the view that treatment with NBQX or PPPA yielded different rewarding and locomotor stimulant effects in the rostral and intermediate tVTA indicates some degree of heterogeneity in the tVTA. However, given that research on the tVTA is still in its infancy, the aforementioned explanations for the observed results are only speculative. Future work is needed to investigate the heterogeneity of the tVTA along its rostro-caudal axis with respect to differences in cellular composition and connectivity.

3.5 MORs of the tVTA are major enhancers of brain stimulation reward and locomotor activity

Because the tVTA shows very dense immunoreactivity for MORs (Jhou et al., 2009a; Jalabert et al., 2011), ICSS and locomotor activity were also assessed following intra-tVTA injection of EM-1, a selective agonist for these receptors. EM-1 was chosen in this study because of its short half-life (~6 min in rat brain homogenate) (Perlikowska et al., 2009), hence limiting the effect of diffusion to sites adjacent to the tVTA. The results obtained in the third article of the present thesis show that injection of EM-1 into both the rostral and intermediate tVTA is rewarding, as indicated by the leftward displacement of the curve that relates response rate to stimulation frequency. Our

results also show that EM-1 increases horizontal movements only when injected into the rostral tVTA. Treatment with EM-1 had no effect on vertical and stereotypic-like movements. Increased brain stimulation reward has typically been correlated with increased mesolimbic DA release and DA cell firing (Moisan and Rompre, 1998; You et al., 2001; Hernandez et al., 2012). On the other hand, horizontal and vertical locomotor activities are linked to changes in DA mesocorticolimbic transmission (Kalivas et al., 1988; Johnson et al., 1996; Ikemoto, 2002), while stereotypic movements can been interpreted as an exaggerated dopaminergic transmission (Fibiger et al., 1973; Wallace et al., 1999; Yates et al., 2007). Given that MOR-mediated activity changes are inhibitory (Meyer and Quenzer, 2005; Matsui and Williams, 2011), a likely explanation for the rewarding and horizontal locomotor stimulant effect of EM-1 injection into the tVTA is that this treatment increased the activity of midbrain DA neurons by inhibiting the activity of tVTA GABAergic neurons.

The view that intra-tVTA injection of EM-1 increased brain stimulation reward and horizontal locomotor activity is in line with prior reports showing that EM-1 injection into the posterior VTA—defined by a region representing the rostral tVTA in our study—or the tVTA induces conditioned place preference (Zangen et al., 2002; Jhou et al., 2012), forward locomotion (Zangen et al., 2002), and positive reinforcement in a self-administration setting (Jhou et al., 2012). The lack of treatment effect on vertical and stereotypic-like movements in our study may be due to several factors, though the most likely explanation is the dose of EM-1 (1 nmol/0.05 μL) that was chosen and/or the experimental approach employed. Increased vertical movement following EM-1 injection into the posterior VTA with a dose similar to the one used in our study was previously reported by Zangen et al. (2002), however, in this study, rats received the injection and were then tested for locomotor activity, whereas in our study, rats were placed in the test cages for 30 min

before receiving the injections and being tested for locomotor activity. Our results are also consistent with studies showing that injection of morphine or MOR agonists into the tVTA increases open-field locomotion (Wasserman et al., 2013; Kotecki et al., 2015; Wasserman et al., 2016; Steidl et al., 2017) and with electrophysiological findings showing that activation of tVTA MORs decreases the tVTA-evoked suppression of midbrain DA neuron firing in vitro (Matsui and Williams, 2011) or in vivo (Lecca et al., 2012). In parallel with our findings in the tVTA, several studies have also implicated VTA MORs in reward, showing that activation of these receptors with morphine or MOR agonists supports self-administration (Bozarth and Wise, 1981; Devine and Wise, 1994; Zangen et al., 2002; Jhou et al., 2012) and produces conditioned place preference (Bals-Kubik et al., 1993; Nader and van der Kooy, 1997).

In summary, our findings indicate that activation of MORs in certain regions of the tVTA enhances brain stimulation reward and locomotor activity. These results are consistent with the observation that morphine and opioids target the tVTA to increase the activity of VTA DA neurons (Jalabert et al., 2011; Matsui and Williams, 2011), and are in line with the revisited disinhibition model of opioid action on midbrain DA neurons proposed by Bourdy and Barrot (2012). This model postulates that opioids enhance VTA DA neuron activity by inhibiting tVTA GABA neurons or terminals, as opposed to the original disinhibition model in which opioids act on GABAergic interneurons of the VTA (Bourdy and Barrot, 2012). The tVTA is therefore well poised to act as a neuromodulatory target for a number of psychiatric and neurological disorders where DA transmission is dysregulated, including substance use disorder, schizophrenia and Parkinson's disease.

3.6 NMDA receptors of the tVTA are involved in incentive salience and brain stimulation reward

The third article of the present thesis finally examines the rewarding effect of intra-tVTA injection of PPPA, a preferred GluN2A-containing NMDA receptor antagonist, following siRNA-mediated downregulation of the obligatory GluN1 subunit of NMDA receptors in the tVTA. A siRNA mediated against NMDA receptors, and not AMPA receptors, was used because of results showing that blockade of NMDA receptors with PPPA produces marked increases in brain stimulation reward in both the rostral and intermediate tVTA, unlike NBQX, which only enhanced brain stimulation reward when injected into the intermediate tVTA. The rationale behind using a siRNA-mediated gene silencing approach is that the required silencing machinery is primarily located in the nucleus (Carthew and Sontheimer, 2009), as such, downregulation of the targeted protein will only occur on cells that have their cell bodies located in the tVTA, and will not alter the level of receptors located on afferent terminals. Previous work from our lab have shown that the rewarding effect of intra-VTA injection of PPPA is likely mediated by NMDA receptors located on afferent terminals (Hernandez et al., 2015). In light of these findings, we speculated that the rewarding effect of intra-tVTA injection of PPPA is also mediated by NMDA receptors that are located on afferent terminals. If this is true, then the siRNA-mediated downregulation of NMDA receptors in the tVTA should not change the rewarding effect of intra-tVTA injection of PPPA since only receptors that are located on cell bodies of the tVTA will be downregulated.

To test this hypothesis, ICSS was assessed following injection of a control siRNA or a siRNA that target GluN1 for 3 consecutive days. Our results show that the siRNA-mediated downregulation of NMDA receptors in the tVTA reduces the maximum rate of ICSS responding without altering the reward threshold. The same siRNA treatment failed to produce deficits in

motor performance as assessed by locomotor activity. A reduction in maximum response rate for ICSS has typically been interpreted as a deficit in motor performance (Miliaressis et al., 1986). However, it may also result from a deficit in incentive salience, that is, the motivation of the animal to obtain the rewarding stimulation. Indeed, work by Edmonds et al. (1974) showed that the speed at which the animal runs in a runway to receive a rewarding stimulation increases with increasing current intensity for the priming stimulation. Thus, in light of our findings showing that the siRNA treatment reduces the maximum response rate for ICSS without producing deficits in locomotor activity, we suggest that the NMDA receptors that are located on tVTA cell bodies are implicated in motivation and approach behaviors. Such claim could be further supported by future experiments testing the same siRNA treatment in a runway instead of an operant box. Our results also show that the siRNA-mediated downregulation of NMDA receptors in the tVTA failed to alter the reward-enhancing effect of intra-tVTA injection of PPPA. Therefore, despite the marked reduction of NMDA receptors on tVTA cell bodies, PPPA injection into the tVTA was still effective in enhancing—albeit transiently—the reward signal initiated by ICSS. We thus suggest that PPPA acts on NMDA receptors that are located on afferent terminals, but not on cell bodies, of the tVTA. These findings parallel previous work from our group showing that the rewarding effect of intra-VTA injection of PPPA is likely mediated by NMDA receptors that are located on afferent terminals (Hernandez et al., 2015). However, a question that remains to be answered is: which NMDA receptor subunit is involved in the rewarding effect of intra-tVTA injection of PPPA? Reverse transcription-polymerase chain reaction (RT-PCR) and western blot analysis of tVTA tissue homogenates indicates that the GluN2A, GluN2B, GluN2C and GluN2D subunits of NMDA receptors are expressed in the tVTA, with a higher expression of the GluN2C subunit (results not shown). Thus, although PPPA shows a preferred action on the GluN2A subunit (Feng

et al., 2005), any of the GluN2A-D subunits of NMDA receptors could be involved in the rewarding effect of intra-tVTA injection of PPPA. Further research is warranted before a firm conclusion can be drawn.

3.7 Conclusion: implications for psychiatric diseases

In summary, results of the first article of this thesis show that the DDC is involved in the transmission of the reward signal initiated by electrical stimulation of the LH and the DR, and that this pathway merges with the MFB on a common reward integrator **(Figure 1A)**. In the second article of this thesis, Fos-immunohistochemistry was used to determine whether the same nuclei that are activated by ICSS continue to be active following a lesion at the DDC. Results show that electrolytic lesions at the DDC reduce stimulation-induced FLIR in the NAc, BNST, BLA, IPN, PN and DR of rats, suggesting the existence of functional connections between the DDC and these brain regions **(Figure 1B)**. Finally, the findings presented in the third article of the present thesis show that glutamate and opioid transmissions in the tVTA are important regulators of brain stimulation reward and locomotor activity **(Figure 1C)**. Results obtained with the siRNA treatment also suggest that the reward-relevant NMDA receptors are likely located on presynaptic terminals of the tVTA, and that NMDA receptors located on tVTA cell bodies are involved in incentive salience **(Figure 1C)**.

In light of our findings and previous studies showing that the DDC is involved in reward and goal-directed behaviors (Nakajima, 1984; Blander and Wise, 1989; Vachon and Miliaressis, 1992; Morissette and Boye, 2008), experimental manipulations that alter its activity could have potential implications in the treatment of disorders characterized by aberrant reward circuitry function, including substance use disorder and depression. One approach that has been explored for the

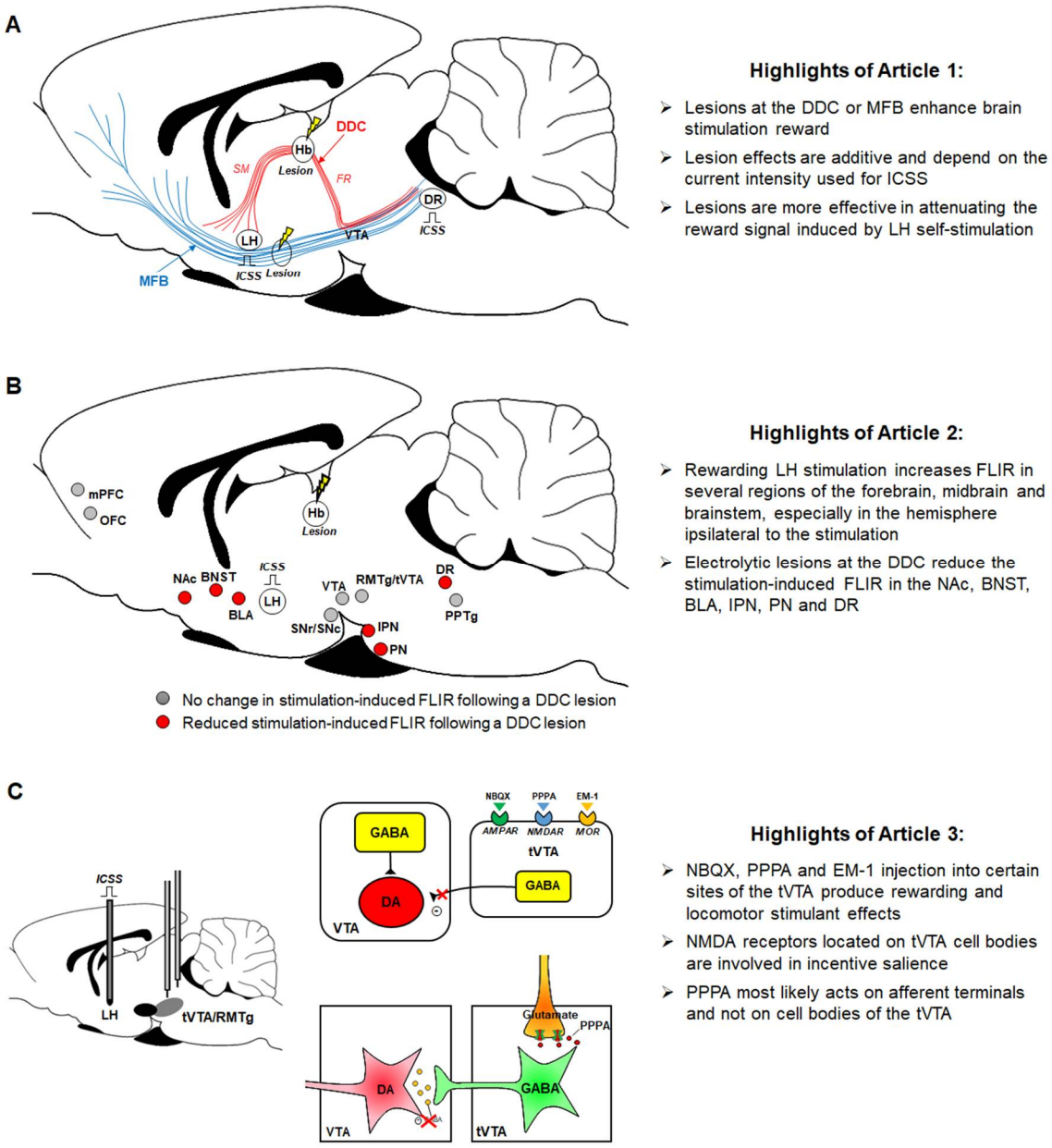

Figure 1: Schematic overview of article 1, 2, and 3 of the present thesis. (A) The rewarding effect of LH and DR self-stimulation were assessed following sequential electrolytic lesions at the DDC and MFB. (B) The distribution of FLIR, a marker of neuronal activity, was assessed following electrolytic lesions at the DDC and rewarding electrical stimulation of the LH. (C) LH self-stimulation and locomotor activity were assessed following pharmacological blockade of AMPA and NMDA receptors, pharmacological activation of MORs, and siRNA-mediated downregulation of NMDA receptors in the tVTA. The reward-enhancing effects of PPPA were also investigated following siRNA-mediated downregulation of NMDA receptors in the tVTA.

treatment of psychiatric diseases is the use of DBS. For instance, DBS of the LHb was shown to reduce cocaine self-administration in rats (Friedman et al., 2010; Lax et al., 2013), and resulted in marked attenuations of cocaine-induced increases in midbrain NMDA and AMPA receptors (Friedman et al., 2010). In animal models of depression, DBS of the LHb improved depressive-like symptoms in open-field (Meng et al., 2011) and forced-swim tests (Li et al., 2011; Kim et al., 2016), and caused marked increases in peripheral and local brain concentrations of monoamines, including DA, serotonin and norepinephrine (Meng et al., 2011). These findings have also been extended to humans inasmuch as DBS of the SM, the main afferent bundle of the LHb, yielded significant improvements in depressive symptoms in one patient with treatment-resistant MDD (Sartorius et al., 2010) and in 2 patients with severe therapy-refractory depression (Kiening and Sartorius, 2013). However, due to the invasive nature of DBS, this approach has only been tested in a small number of patients, and more work is needed to better understand its long term efficacy and safety.

Our results showing that the tVTA regulates brain stimulation reward and locomotor activity, together with the view that various drugs of abuse, including morphine, nicotine and cannabinoids, alter its electrophysiological activity (Jalabert et al., 2011; Lecca et al., 2011; Matsui and Williams, 2011), place the tVTA as a major modulator of the reward system and a potential therapeutic target for psychiatric disorders. In rats, lesions or optogenetic inactivation of the tVTA attenuates cocaine-induced avoidance behavior at a period when cocaine exhibits aversive effects, suggesting that the tVTA could act as a therapeutic target for substance use disorder (Jhou et al., 2013). In light of evidence indicating the existence of anatomical connections between the LHb and the tVTA (Jhou et al., 2009a; Kaufling et al., 2009), together with previous reports showing that DBS

of the LHb yields antidepressant effects in treatment-resistant patients (Sartorius et al., 2010; Kiening and Sartorius, 2013), also suggest that the tVTA may be considered as a potential therapeutic target in depression. However, given that the tVTA is a relatively newly identified brain region, research on this structure is still in its infancy, and more work is needed to go from fundamental theories to clinical applications.

Last but not least, the view that siRNA-mediated downregulation of NMDA receptors in the tVTA reduced the maximal response rate for ICSS without yielding deficits in locomotor activity indicates that NMDA receptors located on tVTA cell bodies are involved in incentive salience, (i.e., the motivation or "wanting" to receive the rewarding stimulation). Results with the siRNA experiment also indicate that NMDA receptors that are located on tVTA afferent terminals are the likely source of inhibition on the reward signal induced by ICSS. Together, these findings suggest that NMDA receptors of the tVTA might represent an interesting target for the treatment of depressive symptoms, and are in line with previous reports of clinical trials showing that single (Berman et al., 2000; Zarate et al., 2006; Murrough et al., 2013) or repeated (aan het Rot et al., 2010; Murrough et al., 2013; Rasmussen et al., 2013; Diamond et al., 2014) subanesthetic dose infusion of the NMDA receptor antagonist, ketamine, produces rapid and potent antidepressant effects in patients with major depression.

Overall, the articles presented in this thesis help extend the boundary of the known neuronal circuitry involved in brain stimulation reward, and could have insightful impacts on future drug development and therapeutic strategies in psychiatry. Our results showing that the DDC is involved in brain stimulation reward could prompt future studies on exploring the possibility of using this pathway as a therapeutic target for disorders associated with dysregulated reward circuitry function, notably mood disorders, schizophrenia, and substance use disorder. Similarly,

our finding that NMDA receptors located on tVTA afferent terminals are the likely source of inhibition of brain stimulation reward may influence future research to develop antidepressant agents that specifically target these receptors. As research on the DDC and tVTA is developing at a rapid pace, the next few years will see a tremendous growth in this field and will sharpen our understanding of the neural substrate underlying appetitive and aversive behaviors.

BIBLIOGRAPHY

aan het Rot M, Collins KA, Murrough JW, Perez AM, Reich DL, Charney DS, Mathew SJ (2010) Safety and efficacy of repeated-dose intravenous ketamine for treatment-resistant depression. Biol Psychiatry 67:139-145.

Adinoff B (2004) Neurobiologic processes in drug reward and addiction. Harv Rev Psychiatry 12:305-320.

Admon R, Pizzagalli DA (2015) Dysfunctional Reward Processing in Depression. Curr Opin Psychol 4:114-118.

Agmo A, Gomez M (1991) Conditioned place preference produced by infusion of Met-enkephalin into the medial preoptic area. Brain Res 550:343-346.

Aizawa H, Cui W, Tanaka K, Okamoto H (2013) Hyperactivation of the habenula as a link between depression and sleep disturbance. Front Hum Neurosci 7:826.

Aizawa H, Kobayashi M, Tanaka S, Fukai T, Okamoto H (2012) Molecular characterization of the subnuclei in rat habenula. J Comp Neurol 520:4051-4066.

Akagi K, Powell EW (1968) Differential projections of habenular nuclei. J Comp Neurol 132:263-274.

Alcaro A, Huber R, Panksepp J (2007) Behavioral functions of the mesolimbic dopaminergic system: an affective neuroethological perspective. Brain Res Rev 56:283-321.

Amorapanth P, Nader K, LeDoux JE (1999) Lesions of periaqueductal gray dissociate-conditioned freezing from conditioned suppression behavior in rats. Learn Mem 6:491-499.

Andres KH, von During M, Veh RW (1999) Subnuclear organization of the rat habenular complexes. J Comp Neurol 407:130-150.

Andrew RJ (1967) Intracranial self-stimulation in the chick. Nature 213:847-848.

Araki M, McGeer PL, McGeer EG (1984) Retrograde HRP tracing combined with a pharmacohistochemical method for GABA transaminase for the identification of presumptive GABAergic projections to the habenula. Brain Res 304:271-277.

Araki M, McGeer PL, Kimura H (1988) The efferent projections of the rat lateral habenular nucleus revealed by the PHA-L anterograde tracing method. Brain Res 441:319-330.

Arias-Carrion O, Poppel E (2007) Dopamine, learning, and reward-seeking behavior. Acta Neurobiol Exp (Wars) 67:481-488.

Arvanitogiannis A, Shizgal P (2008) The reinforcement mountain: allocation of behavior as a function of the rate and intensity of rewarding brain stimulation. Behav Neurosci 122:1126-1138.

Arvanitogiannis A, Waraczynski M, Shizgal P (1996a) Effects of excitotoxic lesions of the basal forebrain on MFB self-stimulation. Physiol Behav 59:795-806.

Arvanitogiannis A, Flores C, Shizgal P (1997) Fos-like immunoreactivity in the caudal diencephalon and brainstem following lateral hypothalamic self-stimulation. Behav Brain Res 88:275-279.

Arvanitogiannis A, Flores C, Pfaus JG, Shizgal P (1996b) Increased ipsilateral expression of Fos following lateral hypothalamic self-stimulation. Brain Res 720:148-154.

Arvanitogiannis A, Tzschentke TM, Riscaldino L, Wise RA, Shizgal P (2000) Fos expression following self-stimulation of the medial prefrontal cortex. Behav Brain Res 107:123-132.

Balazsfi DG, Zelena D, Farkas L, Demeter K, Barna I, Cserep C, Takacs VT, Nyiri G, Goloncser F, Sperlagh B, Freund TF, Haller J (2017) Median raphe region stimulation alone generates remote, but not recent fear memory traces. PLoS One 12:e0181264.

Balcita-Pedicino JJ, Omelchenko N, Bell R, Sesack SR (2011) The inhibitory influence of the lateral habenula on midbrain dopamine cells: ultrastructural evidence for indirect mediation via the rostromedial mesopontine tegmental nucleus. J Comp Neurol 519:1143-1164.

Ball GG, Micco DJ, Jr., Berntson GG (1974) Cerebellar stimulation in the rat: complex stimulation-bound oral behaviors and self-stimulation. Physiol Behav 13:123-127.

Bals-Kubik R, Ableitner A, Herz A, Shippenberg TS (1993) Neuroanatomical sites mediating the motivational effects of opioids as mapped by the conditioned place preference paradigm in rats. J Pharmacol Exp Ther 264:489-495.

Barone FC, Wayner MJ, Scharoun SL, Guevara-Aguilar R, Aguilar-Baturoni HU (1981) Afferent connections to the lateral hypothalamus: a horseradish peroxidase study in the rat. Brain Res Bull 7:75-88.

Barroso-Chinea P, Castle M, Aymerich MS, Perez-Manso M, Erro E, Tunon T, Lanciego JL (2007) Expression of the mRNAs encoding for the vesicular glutamate transporters 1 and 2 in the rat thalamus. J Comp Neurol 501:703-715.

Barrot M, Thome J (2011) Discovering a new anatomical structure in the brain: implications for neuropsychiatry and therapy. World J Biol Psychiatry 12 Suppl 1:19-22.

Batalla A, Homberg JR, Lipina TV, Sescousse G, Luijten M, Ivanova SA, Schellekens AFA, Loonen AJM (2017) The role of the habenula in the transition from reward to misery in substance use and mood disorders. Neurosci Biobehav Rev 80:276-285.

Bauco P, Wang Y, Wise RA (1993) Lack of sensitization or tolerance to the facilitating effect of ventral tegmental area morphine on lateral hypothalamic brain stimulation reward. Brain Res 617:303-308.

Beal MF (1998) Excitotoxicity and nitric oxide in Parkinson's disease pathogenesis. Ann Neurol 44:S110-114.

Bean AJ, Roth RH (1991) Extracellular dopamine and neurotensin in rat prefrontal cortex in vivo: effects of median forebrain bundle stimulation frequency, stimulation pattern, and dopamine autoreceptors. J Neurosci 11:2694-2702.

Beaulieu JM, Gainetdinov RR (2011) The physiology, signaling, and pharmacology of dopamine receptors. Pharmacol Rev 63:182-217.

Bechtholt-Gompf AJ, Walther HV, Adams MA, Carlezon WA, Jr., Ongur D, Cohen BM (2010) Blockade of astrocytic glutamate uptake in rats induces signs of anhedonia and impaired spatial memory. Neuropsychopharmacology 35:2049-2059.

Benaliouad F, Kapur S, Rompre PP (2007) Blockade of 5-HT2a receptors reduces haloperidol-induced attenuation of reward. Neuropsychopharmacology 32:551-561.

Benarroch E (2012) Endogenous opioid systems

Neurology 79:807-814.

Beretta CA, Dross N, Guiterrez-Triana JA, Ryu S, Carl M (2012) Habenula circuit development: past, present, and future. Front Neurosci 6:51.

Berg BA, Schoenbaum G, McDannald MA (2014) The dorsal raphe nucleus is integral to negative prediction errors in Pavlovian fear. Eur J Neurosci 40:3096-3101.

Bergeron S, Rompre PP (2013) Blockade of ventral midbrain NMDA receptors enhances brain stimulation reward: a preferential role for GluN2A subunits. Eur Neuropsychopharmacol 23:1623-1635.

Berman RM, Cappiello A, Anand A, Oren DA, Heninger GR, Charney DS, Krystal JH (2000) Antidepressant effects of ketamine in depressed patients. Biol Psychiatry 47:351-354.

Bernstein JG, Boyden ES (2011) Optogenetic tools for analyzing the neural circuits of behavior. Trends Cogn Sci 15:592-600.

Berthoud HR, Munzberg H (2011) The lateral hypothalamus as integrator of metabolic and environmental needs: from electrical self-stimulation to opto-genetics. Physiol Behav 104:29-39.

Berton O, Covington HE, 3rd, Ebner K, Tsankova NM, Carle TL, Ulery P, Bhonsle A, Barrot M, Krishnan V, Singewald GM, Singewald N, Birnbaum S, Neve RL, Nestler EJ (2007) Induction of deltaFosB in the periaqueductal gray by stress promotes active coping responses. Neuron 55:289-300.

Bianco IH, Wilson SW (2009) The habenular nuclei: a conserved asymmetric relay station in the vertebrate brain. Philos Trans R Soc Lond B Biol Sci 364:1005-1020.

Bielajew C, Trzcinska M (1998) Activation of reward-relevant neurons in the caudate-putamen influences the development of medial prefrontal cortex self-stimulation: a moveable electrode mapping study. Acta Neurobiol Exp (Wars) 58:189-198.

Bielajew C, Miguelez M, Shiao R (2002) Electrolytic lesions of the cortical and adjacent nuclei in the amygdala differentially influence thresholds for rewarding medial forebrain bundle stimulation. Behav Neurosci 116:660-671.

Bielajew CH (1991) Distribution of cytochrome oxidase in response to rewarding brain stimulation: effect of different pulse durations. Brain Res Bull 26:379-384.

Birtwistle J, Baldwin D (1998) Role of dopamine in schizophrenia and Parkinson's disease. Br J Nurs 7:832-834, 836, 838-841.

Bishop MP, Elder ST, Heath RG (1963) Intracranial self-stimulation in man. Science 140:394-396.

Bjorklund A, Dunnett SB (2007) Dopamine neuron systems in the brain: an update. Trends Neurosci 30:194-202.

Black D, Trevethick M (1998) The kappa opioid receptor is associated with the perception of visceral pain. Gut 43:312-313.

Blander A, Wise RA (1989) Anatomical mapping of brain stimulation reward sites in the anterior hypothalamic area: special attention to the stria medullaris. Brain Res 483:12-16.

Bonci A, Malenka RC (1999) Properties and plasticity of excitatory synapses on dopaminergic and GABAergic cells in the ventral tegmental area. J Neurosci 19:3723-3730.

Boulos LJ, Darcq E, Kieffer BL (2017) Translating the Habenula-From Rodents to Humans. Biol Psychiatry 81:296-305.

Bourdy R, Barrot M (2012) A new control center for dopaminergic systems: pulling the VTA by the tail. Trends Neurosci 35:681-690.

Bourdy R, Sanchez-Catalan MJ, Kaufling J, Balcita-Pedicino JJ, Freund-Mercier MJ, Veinante P, Sesack SR, Georges F, Barrot M (2014) Control of the nigrostriatal dopamine neuron activity and motor function by the tail of the ventral tegmental area. Neuropsychopharmacology 39:2788-2798.

Boyd ES, Gardner LC (1967) Effect of some brain lesions on intracranial self-stimulation in the rat. Am J Physiol 213:1044-1052.

Boyd ES, Celso MB (1970) Effect of some brain lesions on septal intracranial self-stimulation in the rat. Am J Physiol 219:734-741.

Boye SM (2005) Mesencephalic substrate of reward: lesion effects. Behav Brain Res 156:31-43.

Boye SM, Rompre PP (1996) Effect of pimozide on self-stimulation threshold under a continuous and fixed-interval schedule of reinforcement. Behav Brain Res 78:243-245.

Bozarth MA, Wise RA (1981) Intracranial self-administration of morphine into the ventral tegmental area in rats. Life Sci 28:551-555.

Brinschwitz K, Dittgen A, Madai VI, Lommel R, Geisler S, Veh RW (2010) Glutamatergic axons from the lateral habenula mainly terminate on GABAergic neurons of the ventral midbrain. Neuroscience 168:463-476.

Broekkamp CL, Phillips AG (1979) Facilitation of self-stimulation behavior following intracerebral microinjections of opioids into the ventral tegmental area. Pharmacol Biochem Behav 11:289-295.

Bromberg-Martin ES, Hikosaka O (2011) Lateral habenula neurons signal errors in the prediction of reward information. Nat Neurosci 14:1209-1216.

Bromberg-Martin ES, Matsumoto M, Hikosaka O (2010) Dopamine in motivational control: rewarding, aversive, and alerting. Neuron 68:815-834.

Brown PL, Shepard PD (2013) Lesions of the fasciculus retroflexus alter footshock-induced cFos expression in the mesopontine rostromedial tegmental area of rats. PLoS One 8:e60678.

Brown PL, Palacorolla H, Brady D, Riegger K, Elmer GI, Shepard PD (2017) Habenula-Induced Inhibition of Midbrain Dopamine Neurons Is Diminished by Lesions of the Rostromedial Tegmental Nucleus. J Neurosci 37:217-225.

Brownstein MJ (1993) A brief history of opiates, opioid peptides, and opioid receptors. Proc Natl Acad Sci U S A 90:5391-5393.

Bruijnzeel AW (2009) kappa-Opioid receptor signaling and brain reward function. Brain Res Rev 62:127-146.

Bursten B, Delgado JM (1958) Positive reinforcement induced by intracerebral stimulation in the monkey. J Comp Physiol Psychol 51:6-10.

Bushnik T, Bielajew C, Konkle AT (2000) The substrate for brain-stimulation reward in the lateral preoptic area. I. Anatomical mapping of its boundaries. Brain Res 881:103-111.

Campolattaro MM, Kashef A, Lee I, Freeman JH (2011) Neuronal correlates of cross-modal transfer in the cerebellum and pontine nuclei. J Neurosci 31:4051-4062.

Carlezon WA, Jr., Beguin C, DiNieri JA, Baumann MH, Richards MR, Todtenkopf MS, Rothman RB, Ma Z, Lee DY, Cohen BM (2006) Depressive-like effects of the kappa-opioid receptor agonist salvinorin A on behavior and neurochemistry in rats. J Pharmacol Exp Ther 316:440-447.

Carthew RW, Sontheimer EJ (2009) Origins and Mechanisms of miRNAs and siRNAs. Cell 136:642-655.

Chang SY, Kim U (2004) Ionic mechanism of long-lasting discharges of action potentials triggered by membrane hyperpolarization in the medial lateral habenula. J Neurosci 24:2172-2181.

Charnay Y, Leger L (2010) Brain serotonergic circuitries. Dialogues Clin Neurosci 12:471-487.

Chergui K, Charlety PJ, Akaoka H, Saunier CF, Brunet JL, Buda M, Svensson TH, Chouvet G (1993) Tonic activation of NMDA receptors causes spontaneous burst discharge of rat midbrain dopamine neurons in vivo. Eur J Neurosci 5:137-144.

Chou MY, Amo R, Kinoshita M, Cherng BW, Shimazaki H, Agetsuma M, Shiraki T, Aoki T, Takahoko M, Yamazaki M, Higashijima S, Okamoto H (2016) Social conflict resolution regulated by two dorsal habenular subregions in zebrafish. Science 352:87-90.

Christoph GR, Leonzio RJ, Wilcox KS (1986) Stimulation of the lateral habenula inhibits dopamine-containing neurons in the substantia nigra and ventral tegmental area of the rat. J Neurosci 6:613-619.

Colle LM, Wise RA (1988) Effects of nucleus accumbens amphetamine on lateral hypothalamic brain stimulation reward. Brain Res 459:361-368.

Colussi-Mas J, Geisler S, Zimmer L, Zahm DS, Berod A (2007) Activation of afferents to the ventral tegmental area in response to acute amphetamine: a double-labelling study. Eur J Neurosci 26:1011-1025.

Concha ML, Wilson SW (2001) Asymmetry in the epithalamus of vertebrates. J Anat 199:63-84.

Conrad LC, Leonard CM, Pfaff DW (1974) Connections of the median and dorsal raphe nuclei in the rat: an autoradiographic and degeneration study. J Comp Neurol 156:179-205.

Contestabile A, Flumerfelt BA (1981) Afferent connections of the interpeduncular nucleus and the topographic organization of the habenulo-interpeduncular pathway: an HRP study in the rat. J Comp Neurol 196:253-270.

Contestabile A, Villani L, Fasolo A, Franzoni MF, Gribaudo L, Oktedalen O, Fonnum F (1987) Topography of cholinergic and substance P pathways in the habenulo-interpeduncular system of the rat. An immunocytochemical and microchemical approach. Neuroscience 21:253-270.

Corbett D, Wise RA (1979) Intracranial self-stimulation in relation to the ascending noradrenergic fiber systems of the pontine tegmentum and caudal midbrain: a moveable electrode mapping study. Brain Res 177:423-436.

Corbett D, Wise RA (1980) Intracranial self-stimulation in relation to the ascending dopaminergic systems of the midbrain: a moveable electrode mapping study. Brain Res 185:1-15.

Corbett D, Fox E, Milner PM (1982) Fiber pathways associated with cerebellar self-stimulation in the rat: a retrograde and anterograde tracing study. Behav Brain Res 6:167-184.

Cornish JL, Nakamura M, Kalivas PW (2001) Dopamine-independent locomotion following blockade of N-methyl-D-aspartate receptors in the ventral tegmental area. J Pharmacol Exp Ther 298:226-233.

Cornish JL, Hunt GE, Robins L, McGregor IS (2012) Regional c-Fos and FosB/DeltaFosB expression associated with chronic methamphetamine self-administration and methamphetamine-seeking behavior in rats. Neuroscience 206:100-114.

Crow TJ (1972a) A map of the rat mesencephalon for electrical self-stimulation. Brain Res 36:265-273.

Crow TJ (1972b) Catecholamine-containing neurones and electrical self-stimulation. 1. A review of some data. Psychol Med 2:414-421.

Cuello AC, Emson PC, Paxinos G, Jessell T (1978) Substance P containing and cholinergic projections from the habenula. Brain Res 149:413-429.

D'Souza MS (2015) Glutamatergic transmission in drug reward: implications for drug addiction. Front Neurosci 9:404.

Danna CL, Shepard PD, Elmer GI (2013) The habenula governs the attribution of incentive salience to reward predictive cues. Front Hum Neurosci 7:781.

David V, Durkin TP, Cazala P (1998) Rewarding effects elicited by the microinjection of either AMPA or NMDA glutamatergic antagonists into the ventral tegmental area revealed by an intracranial self-administration paradigm in mice. Eur J Neurosci 10:1394-1402.

Delgado JM, Anand BK (1953) Increase of food intake induced by electrical stimulation of the lateral hypothalamus. Am J Physiol 172:162-168.

Deneau G, Yanagita T, Seevers MH (1969) Self-administration of psychoactive substances by the monkey. Psychopharmacologia 16:30-48.

Descarries L, Watkins KC, Garcia S, Beaudet A (1982) The serotonin neurons in nucleus raphe dorsalis of adult rat: a light and electron microscope radioautographic study. J Comp Neurol 207:239-254.

Devine DP, Wise RA (1994) Self-administration of morphine, DAMGO, and DPDPE into the ventral tegmental area of rats. J Neurosci 14:1978-1984.

Devine DP, Leone P, Pocock D, Wise RA (1993) Differential involvement of ventral tegmental mu, delta and kappa opioid receptors in modulation of basal mesolimbic dopamine release: in vivo microdialysis studies. J Pharmacol Exp Ther 266:1236-1246.

Di Chiara G, Imperato A (1988) Opposite effects of mu and kappa opiate agonists on dopamine release in the nucleus accumbens and in the dorsal caudate of freely moving rats. J Pharmacol Exp Ther 244:1067-1080.

Diamond PR, Farmery AD, Atkinson S, Haldar J, Williams N, Cowen PJ, Geddes JR, McShane R (2014) Ketamine infusions for treatment resistant depression: a series of 28 patients treated weekly or twice weekly in an ECT clinic. J Psychopharmacol 28:536-544.

Dib B (1985) A study of intracerebroventricular self-administration of leucine or methionine enkephalin by rats in response to intermittent electric shocks. Pain 22:49-57.

Dingledine R, McBain CJ (1999) Glutamate and Aspartate Are the Major Excitatory Transmitters in the Brain. In: Basic Neurochemistry: Molecular, Cellular and Medical Aspects. 6th edition. Philadelphia: Lippincott-Raven.

Dobi A, Margolis EB, Wang HL, Harvey BK, Morales M (2010) Glutamatergic and nonglutamatergic neurons of the ventral tegmental area establish local synaptic contacts with dopaminergic and nondopaminergic neurons. J Neurosci 30:218-229.

Duchesne V, Boye SM (2013) Differential contribution of mesoaccumbens and mesohabenular dopamine to intracranial self-stimulation. Neuropharmacology 70:43-50.

Ducrot C, Fortier E, Bouchard C, Rompre PP (2013) Opposite modulation of brain stimulation reward by NMDA and AMPA receptors in the ventral tegmental area. Front Syst Neurosci 7:57.

Dunlop BW, Nemeroff CB (2007) The role of dopamine in the pathophysiology of depression. Arch Gen Psychiatry 64:327-337.

Durkin MM, Gunwaldsen CA, Borowsky B, Jones KA, Branchek TA (1999) An in situ hybridization study of the distribution of the GABA(B2) protein mRNA in the rat CNS. Brain Res Mol Brain Res 71:185-200.

Duvauchelle CL, Fleming SM, Kornetsky C (1997) DAMGO and DPDPE facilitation of brain stimulation reward thresholds is blocked by the dopamine antagonist cis-flupenthixol. Neuropharmacology 36:1109-1114.

Edmonds DE, Gallistel CR (1974) Parametric analysis of brain stimulation reward in the rat: III. Effect of performance variables on the reward summation function. J Comp Physiol Psychol 87:876-883.

Ettenberg A (2004) Opponent process properties of self-administered cocaine. Neurosci Biobehav Rev 27:721-728.

Fakhoury M (2016) Revisiting the Serotonin Hypothesis: Implications for Major Depressive Disorders. Mol Neurobiol 53:2778-2786.

Fakhoury M (2017) The habenula in psychiatric disorders: More than three decades of translational investigation. Neurosci Biobehav Rev 83:721-735.

Fakhoury M, Rompre PP, Boye SM (2016a) Role of the dorsal diencephalic conduction system in the brain reward circuitry. Behav Brain Res 296:431-441.

Fakhoury M, Voyer D, Levesque D, Rompre PP (2016b) Effect of electrolytic lesions of the dorsal diencephalic conduction system on the distribution of Fos-like immunoreactivity induced by rewarding electrical stimulation. Neuroscience 334:214-225.

Faulkner P, Deakin JF (2014) The role of serotonin in reward, punishment and behavioural inhibition in humans: insights from studies with acute tryptophan depletion. Neurosci Biobehav Rev 46 Pt 3:365-378.

Feenstra MG, Botterblom MH, van Uum JF (1998) Local activation of metabotropic glutamate receptors inhibits the handling-induced increased release of dopamine in the nucleus accumbens but not that of dopamine or noradrenaline in the prefrontal cortex: comparison with inhibition of ionotropic receptors. J Neurochem 70:1104-1113.

Fenalti G, Law RH, Buckle AM, Langendorf C, Tuck K, Rosado CJ, Faux NG, Mahmood K, Hampe CS, Banga JP, Wilce M, Schmidberger J, Rossjohn J, El-Kabbani O, Pike RN, Smith AI, Mackay IR, Rowley MJ, Whisstock JC (2007) GABA production by glutamic acid decarboxylase is regulated by a dynamic catalytic loop. Nat Struct Mol Biol 14:280-286.

Feng B, Morley RM, Jane DE, Monaghan DT (2005) The effect of competitive antagonist chain length on NMDA receptor subunit selectivity. Neuropharmacology 48:354-359.

Ferraro G, Montalbano ME, Sardo P, La Grutta V (1996) Lateral habenular influence on dorsal raphe neurons. Brain Res Bull 41:47-52.

Fesrter CB, Skinner BF (1957) Schedules of reinforcement. New York: Appleton-Century-Crofts.

Fibiger HC, Fibiger HP, Zis AP (1973) Attenuation of amphetamine-induced motor stimulation and stereotypy by 6-hydroxydopamine in the rat. Br J Pharmacol 47:683-692.

Fibiger HC, Carter DA, Phillips AG (1976) Decreased intracranial self-stimulation after neuroleptics or 6-hydroxydopamine: evidence for mediation by motor deficits rather than by reduced reward. Psychopharmacology (Berl) 47:21-27.

Fibiger HC, LePiane FG, Jakubovic A, Phillips AG (1987) The role of dopamine in intracranial self-stimulation of the ventral tegmental area. J Neurosci 7:3888-3896.

Fisher MT, Fisher JL (2014) Contributions of different kainate receptor subunits to the properties of recombinant homomeric and heteromeric receptors. Neuroscience 278:70-80.

Flores C, Arvanitogiannis A, Shizgal P (1997) Fos-like immunoreactivity in forebrain regions following self-stimulation of the lateral hypothalamus and the ventral tegmental area. Behav Brain Res 87:239-251.

Fouriezos G (1995) Temporal integration in self-stimulation: a paradox lost? Behav Neurosci 109:965-971.

Fouriezos G, Wise RA (1984) Current-distance relation for rewarding brain stimulation. Behav Brain Res 14:85-89.

Fouriezos G, Bielajew C, Pagotto W (1990) Task difficulty increases thresholds of rewarding brain stimulation. Behav Brain Res 37:1-7.

Frank RA, Williams HP (1985) Both response effort and current intensity affect self-stimulation train duration thresholds. Pharmacol Biochem Behav 22:527-530.

Friedman A, Lax E, Dikshtein Y, Abraham L, Flaumenhaft Y, Sudai E, Ben-Tzion M, Yadid G (2011) Electrical stimulation of the lateral habenula produces an inhibitory effect on sucrose self-administration. Neuropharmacology 60:381-387.

Friedman A, Lax E, Dikshtein Y, Abraham L, Flaumenhaft Y, Sudai E, Ben-Tzion M, Ami-Ad L, Yaka R, Yadid G (2010) Electrical stimulation of the lateral habenula produces enduring inhibitory effect on cocaine seeking behavior. Neuropharmacology 59:452-459.

Furman DJ, Gotlib IH (2016) Habenula responses to potential and actual loss in major depression: preliminary evidence for lateralized dysfunction. Soc Cogn Affect Neurosci 11:843-851.

Gallistel CR (1974) Note on temporal summation in the reward system. J Comp Physiol Psychol 87:870-875.

Gallistel CR (1978) Self-stimulation in the rat: quantitative characteristics of the reward pathway. J Comp Physiol Psychol 92:977-998.

Gallistel CR, Karras D (1984) Pimozide and amphetamine have opposing effects on the reward summation function. Pharmacol Biochem Behav 20:73-77.

Gallistel CR, Freyd G (1987) Quantitative determination of the effects of catecholaminergic agonists and antagonists on the rewarding efficacy of brain stimulation. Pharmacol Biochem Behav 26:731-741.

Gallistel CR, Leon M (1991) Measuring the subjective magnitude of brain stimulation reward by titration with rate of reward. Behav Neurosci 105:913-925.

Gallistel CR, Shizgal P, Yeomans JS (1981) A portrait of the substrate for self-stimulation. Psychol Rev 88:228-273.

Gallistel CR, Gomita Y, Yadin E, Campbell KA (1985) Forebrain origins and terminations of the medial forebrain bundle metabolically activated by rewarding stimulation or by reward-blocking doses of pimozide. J Neurosci 5:1246-1261.

Gallistel CR, Leon M, Lim BT, Sim JC, Waraczynski M (1996) Destruction of the medial forebrain bundle caudal to the site of stimulation reduces rewarding efficacy but destruction rostrally does not. Behav Neurosci 110:766-790.

Gao DM, Hoffman D, Benabid AL (1996) Simultaneous recording of spontaneous activities and nociceptive responses from neurons in the pars compacta of substantia nigra and in the lateral habenula. Eur J Neurosci 8:1474-1478.

Gardon O, Faget L, Chu Sin Chung P, Matifas A, Massotte D, Kieffer BL (2014) Expression of mu opioid receptor in dorsal diencephalic conduction system: new insights for the medial habenula. Neuroscience 277:595-609.

Gasbarri A, Pompili A, Pacitti C, Cicirata F (2003) Comparative effects of lesions to the ponto-cerebellar and olivo-cerebellar pathways on motor and spatial learning in the rat. Neuroscience 116:1131-1140.

Gass JT, Olive MF (2008) Glutamatergic substrates of drug addiction and alcoholism. Biochem Pharmacol 75:218-265.

Geisler S, Andres KH, Veh RW (2003) Morphologic and cytochemical criteria for the identification and delineation of individual subnuclei within the lateral habenular complex of the rat. J Comp Neurol 458:78-97.

Geisler S, Derst C, Veh RW, Zahm DS (2007) Glutamatergic afferents of the ventral tegmental area in the rat. J Neurosci 27:5730-5743.

Geisler S, Marinelli M, Degarmo B, Becker ML, Freiman AJ, Beales M, Meredith GE, Zahm DS (2008) Prominent activation of brainstem and pallidal afferents of the ventral tegmental area by cocaine. Neuropsychopharmacology 33:2688-2700.

George SR, Zastawny RL, Briones-Urbina R, Cheng R, Nguyen T, Heiber M, Kouvelas A, Chan AS, O'Dowd BF (1994) Distinct distributions of mu, delta and kappa opioid receptor mRNA in rat brain. Biochem Biophys Res Commun 205:1438-1444.

Gifuni AJ, Jozaghi S, Gauthier-Lamer AC, Boye SM (2012) Lesions of the lateral habenula dissociate the reward-enhancing and locomotor-stimulant effects of amphetamine. Neuropharmacology 63:945-957.

Gilliss B, Malanga CJ, Pieper JO, Carlezon WA, Jr. (2002) Cocaine and SKF-82958 potentiate brain stimulation reward in Swiss-Webster mice. Psychopharmacology (Berl) 163:238-248.

Giustino TF, Maren S (2015) The Role of the Medial Prefrontal Cortex in the Conditioning and Extinction of Fear. Front Behav Neurosci 9:298.

Goeders NE, Smith JE, Lane JD (1984a) Intracranial self-administration of the endocoid methionine-enkephalin. J Am Osteopath Assoc 84:148-151.

Goeders NE, Lane JD, Smith JE (1984b) Self-administration of methionine enkephalin into the nucleus accumbens. Pharmacol Biochem Behav 20:451-455.

Golden SA, Heshmati M, Flanigan M, Christoffel DJ, Guise K, Pfau ML, Aleyasin H, Menard C, Zhang H, Hodes GE, Bregman D, Khibnik L, Tai J, Rebusi N, Krawitz B, Chaudhury D, Walsh JJ, Han MH, Shapiro ML, Russo SJ (2016) Basal forebrain projections to the lateral habenula modulate aggression reward. Nature 534:688-692.

Gomita Y, Gallistel CR (1982) Effects of reinforcement-blocking doses of pimozide on neural systems driven by rewarding stimulation of the MFB: a 14C-2-deoxyglucose analysis. Pharmacol Biochem Behav 17:841-845.

Goncalves L, Sego C, Metzger M (2012) Differential projections from the lateral habenula to the rostromedial tegmental nucleus and ventral tegmental area in the rat. J Comp Neurol 520:1278-1300.

Gonon FG (1988) Nonlinear relationship between impulse flow and dopamine released by rat midbrain dopaminergic neurons as studied by in vivo electrochemistry. Neuroscience 24:19-28.

Good CH, Wang H, Chen YH, Mejias-Aponte CA, Hoffman AF, Lupica CR (2013) Dopamine D4 receptor excitation of lateral habenula neurons via multiple cellular mechanisms. J Neurosci 33:16853-16864.

Goto M, Swanson LW, Canteras NS (2001) Connections of the nucleus incertus. J Comp Neurol 438:86-122.

Gottesfeld Z (1983) Origin and distribution of noradrenergic innervation in the habenula: a neurochemical study. Brain Res 275:299-304.

Grace AA, Bunney BS (1984a) The control of firing pattern in nigral dopamine neurons: single spike firing. J Neurosci 4:2866-2876.

Grace AA, Bunney BS (1984b) The control of firing pattern in nigral dopamine neurons: burst firing. J Neurosci 4:2877-2890.

Grady SR, Moretti M, Zoli M, Marks MJ, Zanardi A, Pucci L, Clementi F, Gotti C (2009) Rodent habenulo-interpeduncular pathway expresses a large variety of uncommon nAChR subtypes, but only the alpha3beta4* and alpha3beta3beta4* subtypes mediate acetylcholine release. J Neurosci 29:2272-2282.

Groenewegen HJ, Ahlenius S, Haber SN, Kowall NW, Nauta WJ (1986) Cytoarchitecture, fiber connections, and some histochemical aspects of the interpeduncular nucleus in the rat. J Comp Neurol 249:65-102.

Gruber C, Kahl A, Lebenheim L, Kowski A, Dittgen A, Veh RW (2007a) Dopaminergic projections from the VTA substantially contribute to the mesohabenular pathway in the rat. Neurosci Lett 427:165-170.

Gruber SA, Silveri MM, Yurgelun-Todd DA (2007b) Neuropsychological consequences of opiate use. Neuropsychol Rev 17:299-315.

Han LN, Zhang L, Li LB, Sun YN, Wang Y, Chen L, Guo Y, Zhang YM, Zhang QJ, Liu J (2015) Activation of serotonin(2C) receptors in the lateral habenular nucleus increases the expression of depression-related behaviors in the hemiparkinsonian rat. Neuropharmacology 93:68-79.

Harris GC, Aston-Jones G (2003) Critical role for ventral tegmental glutamate in preference for a cocaine-conditioned environment. Neuropsychopharmacology 28:73-76.

Harris GC, Wimmer M, Byrne R, Aston-Jones G (2004) Glutamate-associated plasticity in the ventral tegmental area is necessary for conditioning environmental stimuli with morphine. Neuroscience 129:841-847.

Hayakawa T, Ito H, Zyo K (1993) Neuroanatomical study of afferent projections to the supramammillary nucleus of the rat. Anat Embryol (Berl) 188:139-148.

Heilig M, Goldman D, Berrettini W, O'Brien CP (2011) Pharmacogenetic approaches to the treatment of alcohol addiction. Nat Rev Neurosci 12:670-684.

Heneka MT, Kummer MP, Stutz A, Delekate A, Schwartz S, Vieira-Saecker A, Griep A, Axt D, Remus A, Tzeng TC, Gelpi E, Halle A, Korte M, Latz E, Golenbock DT (2013) NLRP3 is

activated in Alzheimer's disease and contributes to pathology in APP/PS1 mice. Nature 493:674-678.

Herkenham M, Nauta WJ (1977) Afferent connections of the habenular nuclei in the rat. A horseradish peroxidase study, with a note on the fiber-of-passage problem. J Comp Neurol 173:123-146.

Herkenham M, Nauta WJ (1979) Efferent connections of the habenular nuclei in the rat. J Comp Neurol 187:19-47.

Hernandez G, Shizgal P (2009) Dynamic changes in dopamine tone during self-stimulation of the ventral tegmental area in rats. Behav Brain Res 198:91-97.

Hernandez G, Khodami-Pour A, Levesque D, Rompre PP (2015) Reduction in Ventral Midbrain NMDA Receptors Reveals Two Opposite Modulatory Roles for Glutamate on Reward. Neuropsychopharmacology 40:1682-1691.

Hernandez G, Cossette MP, Shizgal P, Rompre PP (2016) Ventral Midbrain NMDA Receptor Blockade: From Enhanced Reward and Dopamine Inactivation. Front Behav Neurosci 10:161.

Hernandez G, Trujillo-Pisanty I, Cossette MP, Conover K, Shizgal P (2012) Role of dopamine tone in the pursuit of brain stimulation reward. J Neurosci 32:11032-11041.

Herzog E, Gilchrist J, Gras C, Muzerelle A, Ravassard P, Giros B, Gaspar P, El Mestikawy S (2004) Localization of VGLUT3, the vesicular glutamate transporter type 3, in the rat brain. Neuroscience 123:983-1002.

Hong S, Hikosaka O (2008) The globus pallidus sends reward-related signals to the lateral habenula. Neuron 60:720-729.

Hong S, Jhou TC, Smith M, Saleem KS, Hikosaka O (2011) Negative reward signals from the lateral habenula to dopamine neurons are mediated by rostromedial tegmental nucleus in primates. J Neurosci 31:11457-11471.

Hortnagl H, Tasan RO, Wieselthaler A, Kirchmair E, Sieghart W, Sperk G (2013) Patterns of mRNA and protein expression for 12 GABAA receptor subunits in the mouse brain. Neuroscience 236:345-372.

Hreib KK, Rosene DL, Moss MB (1988) Basal forebrain efferents to the medial dorsal thalamic nucleus in the rhesus monkey. J Comp Neurol 277:365-390.

Hsu YW, Wang SD, Wang S, Morton G, Zariwala HA, de la Iglesia HO, Turner EE (2014) Role of the dorsal medial habenula in the regulation of voluntary activity, motor function, hedonic state, and primary reinforcement. J Neurosci 34:11366-11384.

Huff ML, LaLumiere RT (2015) The rostromedial tegmental nucleus modulates behavioral inhibition following cocaine self-administration in rats. Neuropsychopharmacology 40:861-873.

Hunt GE, McGregor IS (1998) Rewarding brain stimulation induces only sparse Fos-like immunoreactivity in dopaminergic neurons. Neuroscience 83:501-515.

Hunt GE, McGregor IS (2002) Contrasting effects of dopamine antagonists and frequency reduction on Fos expression induced by lateral hypothalamic stimulation. Behav Brain Res 132:187-201.

Hwang EK, Chung JM (2014) 5HT(1B) receptor-mediated pre-synaptic depression of excitatory inputs to the rat lateral habenula. Neuropharmacology 81:153-165.

Hynd MR, Scott HL, Dodd PR (2004) Glutamate-mediated excitotoxicity and neurodegeneration in Alzheimer's disease. Neurochem Int 45:583-595.

Ikemoto S (2002) Ventral striatal anatomy of locomotor activity induced by cocaine, D-amphetamine, dopamine and D1/D2 agonists. Neuroscience 113:939-955.

Jaber M, Robinson SW, Missale C, Caron MG (1996) Dopamine receptors and brain function. Neuropharmacology 35:1503-1519.

Jacinto LR, Mata R, Novais A, Marques F, Sousa N (2017) The habenula as a critical node in chronic stress-related anxiety. Exp Neurol 289:46-54.

Jalabert M, Bourdy R, Courtin J, Veinante P, Manzoni OJ, Barrot M, Georges F (2011) Neuronal circuits underlying acute morphine action on dopamine neurons. Proc Natl Acad Sci U S A 108:16446-16450.

Janas JD, Stellar JR (1987) Effects of knife-cut lesions of the medial forebrain bundle in self-stimulating rats. Behav Neurosci 101:832-845.

Javitt DC (2004) Glutamate as a therapeutic target in psychiatric disorders. Mol Psychiatry 9:984-997, 979.

Jhou TC, Geisler S, Marinelli M, Degarmo BA, Zahm DS (2009a) The mesopontine rostromedial tegmental nucleus: A structure targeted by the lateral habenula that projects to the ventral tegmental area of Tsai and substantia nigra compacta. J Comp Neurol 513:566-596.

Jhou TC, Fields HL, Baxter MG, Saper CB, Holland PC (2009b) The rostromedial tegmental nucleus (RMTg), a GABAergic afferent to midbrain dopamine neurons, encodes aversive stimuli and inhibits motor responses. Neuron 61:786-800.

Jhou TC, Xu SP, Lee MR, Gallen CL, Ikemoto S (2012) Mapping of reinforcing and analgesic effects of the mu opioid agonist endomorphin-1 in the ventral midbrain of the rat. Psychopharmacology (Berl) 224:303-312.

Jhou TC, Good CH, Rowley CS, Xu SP, Wang H, Burnham NW, Hoffman AF, Lupica CR, Ikemoto S (2013) Cocaine drives aversive conditioning via delayed activation of dopamine-responsive habenular and midbrain pathways. J Neurosci 33:7501-7512.

Ji H, Shepard PD (2007) Lateral habenula stimulation inhibits rat midbrain dopamine neurons through a GABA(A) receptor-mediated mechanism. J Neurosci 27:6923-6930.

Johnson K, Churchill L, Klitenick MA, Hooks MS, Kalivas PW (1996) Involvement of the ventral tegmental area in locomotion elicited from the nucleus accumbens or ventral pallidum. J Pharmacol Exp Ther 277:1122-1131.

Johnson SW, North RA (1992) Opioids excite dopamine neurons by hyperpolarization of local interneurons. J Neurosci 12:483-488.

Johnson SW, Seutin V, North RA (1992) Burst firing in dopamine neurons induced by N-methyl-D-aspartate: role of electrogenic sodium pump. Science 258:665-667.

Kalen P, Karlson M, Wiklund L (1985) Possible excitatory amino acid afferents to nucleus raphe dorsalis of the rat investigated with retrograde wheat germ agglutinin and D-[3H]aspartate tracing. Brain Res 360:285-297.

Kalen P, Lindvall O, Bjorklund A (1989) Electrical stimulation of the lateral habenula increases hippocampal noradrenaline release as monitored by in vivo microdialysis. Exp Brain Res 76:239-245.

Kalen P, Pritzel M, Nieoullon A, Wiklund L (1986) Further evidence for excitatory amino acid transmission in the lateral habenular projection to the rostral raphe nuclei: lesion-induced decrease of high affinity glutamate uptake. Neurosci Lett 68:35-40.

Kalivas PW, Duffy P, DuMars LA, Skinner C (1988) Behavioral and neurochemical effects of acute and daily cocaine administration in rats. J Pharmacol Exp Ther 245:485-492.

Kane F, Coulombe D, Miliaressis E (1991) Amygdaloid self-stimulation: a movable electrode mapping study. Behav Neurosci 105:926-932.

Karreman M, Westerink BH, Moghaddam B (1996) Excitatory amino acid receptors in the ventral tegmental area regulate dopamine release in the ventral striatum. J Neurochem 67:601-607.

Kaufling J, Aston-Jones G (2015) Persistent Adaptations in Afferents to Ventral Tegmental Dopamine Neurons after Opiate Withdrawal. J Neurosci 35:10290-10303.

Kaufling J, Veinante P, Pawlowski SA, Freund-Mercier MJ, Barrot M (2009) Afferents to the GABAergic tail of the ventral tegmental area in the rat. J Comp Neurol 513:597-621.

Kaufling J, Veinante P, Pawlowski SA, Freund-Mercier MJ, Barrot M (2010a) gamma-Aminobutyric acid cells with cocaine-induced DeltaFosB in the ventral tegmental area innervate mesolimbic neurons. Biol Psychiatry 67:88-92.

Kaufling J, Waltisperger E, Bourdy R, Valera A, Veinante P, Freund-Mercier MJ, Barrot M (2010b) Pharmacological recruitment of the GABAergic tail of the ventral tegmental area by acute drug exposure. Br J Pharmacol 161:1677-1691.

Kawaja MD, Flumerfelt BA, Hrycyshyn AW (1988) Topographical and ultrastructural investigation of the habenulo-interpeduncular pathway in the rat: a wheat germ agglutinin-horseradish peroxidase anterograde study. J Comp Neurol 275:117-127.

Keller KL, Vollrath-Smith FR, Jafari M, Ikemoto S (2014) Synergistic interaction between caloric restriction and amphetamine in food-unrelated approach behavior of rats. Psychopharmacology (Berl) 231:825-840.

Kempadoo KA, Tourino C, Cho SL, Magnani F, Leinninger GM, Stuber GD, Zhang F, Myers MG, Deisseroth K, de Lecea L, Bonci A (2013) Hypothalamic neurotensin projections

promote reward by enhancing glutamate transmission in the VTA. J Neurosci 33:7618-7626.

Kerner B (2009) Glutamate Neurotransmission in Psychotic Disorders and Substance Abuse. Open Psychiatr J 3:1-8.

Kiening K, Sartorius A (2013) A new translational target for deep brain stimulation to treat depression. EMBO Mol Med 5:1151-1153.

Kim JJ, Rison RA, Fanselow MS (1993) Effects of amygdala, hippocampus, and periaqueductal gray lesions on short- and long-term contextual fear. Behav Neurosci 107:1093-1098.

Kim U (2009) Topographic commissural and descending projections of the habenula in the rat. J Comp Neurol 513:173-187.

Kim U, Chang SY (2005) Dendritic morphology, local circuitry, and intrinsic electrophysiology of neurons in the rat medial and lateral habenular nuclei of the epithalamus. J Comp Neurol 483:236-250.

Kim U, Chung LY (2007) Dual GABAergic synaptic response of fast excitation and slow inhibition in the medial habenula of rat epithalamus. J Neurophysiol 98:1323-1332.

Kim U, Lee T (2012) Topography of descending projections from anterior insular and medial prefrontal regions to the lateral habenula of the epithalamus in the rat. Eur J Neurosci 35:1253-1269.

Kim Y, Morath B, Hu C, Byrne LK, Sutor SL, Frye MA, Tye SJ (2016) Antidepressant actions of lateral habenula deep brain stimulation differentially correlate with CaMKII/GSK3/AMPK signaling locally and in the infralimbic cortex. Behav Brain Res 306:170-177.

Kiss J, Csaki A, Bokor H, Kocsis K, Kocsis B (2002) Possible glutamatergic/aspartatergic projections to the supramammillary nucleus and their origins in the rat studied by selective [(3)H]D-aspartate labelling and immunocytochemistry. Neuroscience 111:671-691.

Kita H, Oomura Y (1982) An HRP study of the afferent connections to rat lateral hypothalamic region. Brain Res Bull 8:63-71.

Kleckner NW, Dingledine R (1988) Requirement for glycine in activation of NMDA-receptors expressed in Xenopus oocytes. Science 241:835-837.

Koneru A, Satyanarayana S, Rizwan S (2009) Endogenous Opioids: Their Physiological Role and Receptors. Global Journal of Pharmacology 3:149-153.

Koob GF, Le Moal M (2008) Addiction and the brain antireward system. Annu Rev Psychol 59:29-53.

Kotecki L, Hearing M, McCall NM, Marron Fernandez de Velasco E, Pravetoni M, Arora D, Victoria NC, Munoz MB, Xia Z, Slesinger PA, Weaver CD, Wickman K (2015) GIRK Channels Modulate Opioid-Induced Motor Activity in a Cell Type- and Subunit-Dependent Manner. J Neurosci 35:7131-7142.

Kowski AB, Veh RW, Weiss T (2009) Dopaminergic activation excites rat lateral habenular neurons in vivo. Neuroscience 161:1154-1165.

Kretschmer BD (1999) Modulation of the mesolimbic dopamine system by glutamate: role of NMDA receptors. J Neurochem 73:839-848.

Kritis AA, Stamoula EG, Paniskaki KA, Vavilis TD (2015) Researching glutamate - induced cytotoxicity in different cell lines: a comparative/collective analysis/study. Front Cell Neurosci 9:91.

Lammel S, Lim BK, Ran C, Huang KW, Betley MJ, Tye KM, Deisseroth K, Malenka RC (2012) Input-specific control of reward and aversion in the ventral tegmental area. Nature 491:212-217.

Land BB, Bruchas MR, Schattauer S, Giardino WJ, Aita M, Messinger D, Hnasko TS, Palmiter RD, Chavkin C (2009) Activation of the kappa opioid receptor in the dorsal raphe nucleus mediates the aversive effects of stress and reinstates drug seeking. Proc Natl Acad Sci U S A 106:19168-19173.

Larsen PJ, Hay-Schmidt A, Mikkelsen JD (1994) Efferent connections from the lateral hypothalamic region and the lateral preoptic area to the hypothalamic paraventricular nucleus of the rat. J Comp Neurol 342:299-319.

Lavezzi HN, Parsley KP, Zahm DS (2012) Mesopontine rostromedial tegmental nucleus neurons projecting to the dorsal raphe and pedunculopontine tegmental nucleus: psychostimulant-elicited Fos expression and collateralization. Brain Struct Funct 217:719-734.

Lavezzi HN, Parsley KP, Zahm DS (2015) Modulation of locomotor activation by the rostromedial tegmental nucleus. Neuropsychopharmacology 40:676-687.

Lawson RP, Seymour B, Loh E, Lutti A, Dolan RJ, Dayan P, Weiskopf N, Roiser JP (2014) The habenula encodes negative motivational value associated with primary punishment in humans. Proc Natl Acad Sci U S A 111:11858-11863.

Lax E, Friedman A, Croitoru O, Sudai E, Ben-Moshe H, Redlus L, Sasson E, Blumenfeld-Katzir T, Assaf Y, Yadid G (2013) Neurodegeneration of lateral habenula efferent fibers after intermittent cocaine administration: implications for deep brain stimulation. Neuropharmacology 75:246-254.

Le Merrer J, Becker JA, Befort K, Kieffer BL (2009) Reward processing by the opioid system in the brain. Physiol Rev 89:1379-1412.

Lecca S, Melis M, Luchicchi A, Muntoni AL, Pistis M (2012) Inhibitory inputs from rostromedial tegmental neurons regulate spontaneous activity of midbrain dopamine cells and their responses to drugs of abuse. Neuropsychopharmacology 37:1164-1176.

Lecca S, Melis M, Luchicchi A, Ennas MG, Castelli MP, Muntoni AL, Pistis M (2011) Effects of drugs of abuse on putative rostromedial tegmental neurons, inhibitory afferents to midbrain dopamine cells. Neuropsychopharmacology 36:589-602.

Leone P, Pocock D, Wise RA (1991) Morphine-dopamine interaction: ventral tegmental morphine increases nucleus accumbens dopamine release. Pharmacol Biochem Behav 39:469-472.

Li B, Piriz J, Mirrione M, Chung C, Proulx CD, Schulz D, Henn F, Malinow R (2011) Synaptic potentiation onto habenula neurons in the learned helplessness model of depression. Nature 470:535-539.

Li K, Zhou T, Liao L, Yang Z, Wong C, Henn F, Malinow R, Yates JR, 3rd, Hu H (2013) betaCaMKII in lateral habenula mediates core symptoms of depression. Science 341:1016-1020.

Li YQ, Takada M, Shinonaga Y, Mizuno N (1993) The sites of origin of dopaminergic afferent fibers to the lateral habenular nucleus in the rat. J Comp Neurol 333:118-133.

Liang F, Hatanaka Y, Saito H, Yamamori T, Hashikawa T (2000) Differential expression of gamma-aminobutyric acid type B receptor-1a and -1b mRNA variants in GABA and non-GABAergic neurons of the rat brain. J Comp Neurol 416:475-495.

Liguz-Lecznar M, Skangiel-Kramska J (2007) Vesicular glutamate transporters (VGLUTs): the three musketeers of glutamatergic system. Acta Neurobiol Exp (Wars) 67:207-218.

Lisoprawski A, Herve D, Blanc G, Glowinski J, Tassin JP (1980) Selective activation of the mesocortico-frontal dopaminergic neurons induced by lesion of the habenula in the rat. Brain Res 183:229-234.

Ljungberg T, Apicella P, Schultz W (1992) Responses of monkey dopamine neurons during learning of behavioral reactions. J Neurophysiol 67:145-163.

Lodge DJ, Grace AA (2006) The laterodorsal tegmentum is essential for burst firing of ventral tegmental area dopamine neurons. Proc Natl Acad Sci U S A 103:5167-5172.

Lorens SA (1966) Effect of lesions in the central nervous system on lateral hypothalamic self-stimulation in the rat. J Comp Physiol Psychol 62:256-262.

Luo SX, Huang EJ (2016) Dopaminergic Neurons and Brain Reward Pathways: From Neurogenesis to Circuit Assembly. Am J Pathol 186:478-488.

Mague SD, Pliakas AM, Todtenkopf MS, Tomasiewicz HC, Zhang Y, Stevens WC, Jr., Jones RM, Portoghese PS, Carlezon WA, Jr. (2003) Antidepressant-like effects of kappa-opioid receptor antagonists in the forced swim test in rats. J Pharmacol Exp Ther 305:323-330.

Maier SF, Grahn RE, Kalman BA, Sutton LC, Wiertelak EP, Watkins LR (1993) The role of the amygdala and dorsal raphe nucleus in mediating the behavioral consequences of inescapable shock. Behav Neurosci 107:377-388.

Maisonneuve IM, Archer S, Glick SD (1994) U50,488, a kappa opioid receptor agonist, attenuates cocaine-induced increases in extracellular dopamine in the nucleus accumbens of rats. Neurosci Lett 181:57-60.

Malanga CJ, Riday TT, Carlezon WA, Jr., Kosofsky BE (2008) Prenatal exposure to cocaine increases the rewarding potency of cocaine and selective dopaminergic agonists in adult mice. Biol Psychiatry 63:214-221.

Maldonado-Irizarry CS, Stellar JR, Kelley AE (1994) Effects of cocaine and GBR-12909 on brain stimulation reward. Pharmacol Biochem Behav 48:915-920.

Mansour A, Khachaturian H, Lewis ME, Akil H, Watson SJ (1987) Autoradiographic differentiation of mu, delta, and kappa opioid receptors in the rat forebrain and midbrain. J Neurosci 7:2445-2464.

Mansour A, Fox CA, Burke S, Meng F, Thompson RC, Akil H, Watson SJ (1994) Mu, delta, and kappa opioid receptor mRNA expression in the rat CNS: an in situ hybridization study. J Comp Neurol 350:412-438.

Marcangione C, Rompre PP (2008) Topographical Fos induction within the ventral midbrain and projection sites following self-stimulation of the posterior mesencephalon. Neuroscience 154:1227-1241.

Mark TA, Gallistel CR (1993) Subjective reward magnitude of medial forebrain stimulation as a function of train duration and pulse frequency. Behav Neurosci 107:389-401.

Mathuru AS, Jesuthasan S (2013) The medial habenula as a regulator of anxiety in adult zebrafish. Front Neural Circuits 7:99.

Matsui A, Williams JT (2011) Opioid-sensitive GABA inputs from rostromedial tegmental nucleus synapse onto midbrain dopamine neurons. J Neurosci 31:17729-17735.

Matsumoto M, Hikosaka O (2007) Lateral habenula as a source of negative reward signals in dopamine neurons. Nature 447:1111-1115.

Matsumoto M, Hikosaka O (2009) Representation of negative motivational value in the primate lateral habenula. Nat Neurosci 12:77-84.

McCallum SE, Cowe MA, Lewis SW, Glick SD (2012) alpha3beta4 nicotinic acetylcholine receptors in the medial habenula modulate the mesolimbic dopaminergic response to acute nicotine in vivo. Neuropharmacology 63:434-440.

McCulloch J, Savaki HE, Sokoloff L (1980) Influence of dopaminergic systems on the lateral habenular nucleus of the rat. Brain Res 194:117-124.

McDevitt RA, Tiran-Cappello A, Shen H, Balderas I, Britt JP, Marino RAM, Chung SL, Richie CT, Harvey BK, Bonci A (2014) Serotonergic versus nonserotonergic dorsal raphe projection neurons: differential participation in reward circuitry. Cell Rep 8:1857-1869.

McNally GP, Westbrook RF (2006) Predicting danger: the nature, consequences, and neural mechanisms of predictive fear learning. Learn Mem 13:245-253.

Meng H, Wang Y, Huang M, Lin W, Wang S, Zhang B (2011) Chronic deep brain stimulation of the lateral habenula nucleus in a rat model of depression. Brain Res 1422:32-38.

Messer MM, Haller IV (2017) Ketamine Therapy for Treatment-resistant Depression in a Patient with Multiple Sclerosis: A Case Report. Innov Clin Neurosci 14:56-59.

Meye FJ, Lecca S, Valentinova K, Mameli M (2013) Synaptic and cellular profile of neurons in the lateral habenula. Front Hum Neurosci 7:860.

Meyer J, Quenzer L (2005) The opiates. In: Psychopharmacology: Drugs, the Brain, and Behavior, p 254. Massachusetts, USA: Sinauer Associates Inc.

Milde-Langosch K (2005) The Fos family of transcription factors and their role in tumourigenesis. Eur J Cancer 41:2449-2461.

Mileykovskiy B, Morales M (2011) Duration of inhibition of ventral tegmental area dopamine neurons encodes a level of conditioned fear. J Neurosci 31:7471-7476.

Miliaressis E, Rompre PP, Durivage A (1982) Psychophysical method for mapping behavioral substrates using a moveable electrode. Brain Res Bull 8:693-701.

Miliaressis E, Rompre PP, Laviolette P, Philippe L, Coulombe D (1986) The curve-shift paradigm in self-stimulation. Physiol Behav 37:85-91.

Miller DK, Nation JR (1997) Chronic cadmium exposure attenuates the conditioned reinforcing properties of morphine and fentanyl. Brain Res 776:162-169.

Millhouse O (1969) A Golgi study of the desending medial forebrain bundle. Brain Res 15:341-363.

Milner PM (1991) Brain-stimulation reward: a review. Can J Psychol 45:1-36.

Mirrione MM, Schulz D, Lapidus KA, Zhang S, Goodman W, Henn FA (2014) Increased metabolic activity in the septum and habenula during stress is linked to subsequent expression of learned helplessness behavior. Front Hum Neurosci 8:29.

Mogenson GJ, Takigawa M, Robertson A, Wu M (1979) Self-stimulation of the nucleus accumbens and ventral tegmental area of Tsai attenuated by microinjections of spiroperidol into the nucleus accumbens. Brain Res 171:247-259.

Moisan J, Rompre PP (1998) Electrophysiological evidence that a subset of midbrain dopamine neurons integrate the reward signal induced by electrical stimulation of the posterior mesencephalon. Brain Res 786:143-152.

Mora F, Avrith DB, Rolls ET (1980) An electrophysiological and behavioural study of self-stimulation in the orbitofrontal cortex of the rhesus monkey. Brain Res Bull 5:111-115.

Morissette MC, Boye SM (2008) Electrolytic lesions of the habenula attenuate brain stimulation reward. Behav Brain Res 187:17-26.

Murphy CA, DiCamillo AM, Haun F, Murray M (1996) Lesion of the habenular efferent pathway produces anxiety and locomotor hyperactivity in rats: a comparison of the effects of neonatal and adult lesions. Behav Brain Res 81:43-52.

Murray B, Shizgal P (1991) Anterolateral lesions of the medial forebrain bundle increase the frequency threshold for self-stimulation of the lateral hypothalamus and ventral tegmental area in the rat. Psychobiology 19(2):135-146.

Murray B, Shizgal P (1996a) Attenuation of medical forebrain bundle reward by anterior lateral hypothalamic lesions. Behav Brain Res 75:33-47.

Murray B, Shizgal P (1996b) Behavioral measures of conduction velocity and refractory period for reward-relevant axons in the anterior LH and VTA. Physiol Behav 59:643-652.

Murrough JW, Perez AM, Pillemer S, Stern J, Parides MK, aan het Rot M, Collins KA, Mathew SJ, Charney DS, Iosifescu DV (2013) Rapid and longer-term antidepressant effects of repeated ketamine infusions in treatment-resistant major depression. Biol Psychiatry 74:250-256.

Nader K, van der Kooy D (1997) Deprivation state switches the neurobiological substrates mediating opiate reward in the ventral tegmental area. J Neurosci 17:383-390.

Nakahara D, Ozaki N, Miura Y, Miura H, Nagatsu T (1989) Increased dopamine and serotonin metabolism in rat nucleus accumbens produced by intracranial self-stimulation of medial forebrain bundle as measured by in vivo microdialysis. Brain Res 495:178-181.

Nakahara D, Fuchikami K, Ozaki N, Iwasaki T, Nagatsu T (1992) Differential effect of self-stimulation on dopamine release and metabolism in the rat medial frontal cortex, nucleus accumbens and striatum studied by in vivo microdialysis. Brain Res 574:164-170.

Nakajima S (1984) Serotonergic mediation of habenular self-stimulation in the rat. Pharmacol Biochem Behav 20:859-862.

Nakajima S, McKenzie GM (1986) Reduction of the rewarding effect of brain stimulation by a blockade of dopamine D1 receptor with SCH 23390. Pharmacol Biochem Behav 24:919-923.

Narayanan S, Willins D, Dalia A, Wallace L, Uretsky N (1996) Role of dopaminergic mechanisms in the stimulatory effects of MK-801 injected into the ventral tegmental area and the nucleus accumbens. Pharmacol Biochem Behav 54:565-573.

Neckers LM, Schwartz JP, Wyatt RJ, Speciale SG (1979) Substance P afferents from the habenula innervate the dorsal raphe nucleus. Exp Brain Res 37:619-623.

Neugebauer NM, Einstein EB, Lopez MB, McClure-Begley TD, Mineur YS, Picciotto MR (2013) Morphine dependence and withdrawal induced changes in cholinergic signaling. Pharmacol Biochem Behav 109:77-83.

Neumann PA, Ishikawa M, Otaka M, Huang YH, Schluter OM, Dong Y (2014) Increased excitability of lateral habenula neurons in adolescent rats following cocaine self-administration. Int J Neuropsychopharmacol 18.

Niciu MJ, Kelmendi B, Sanacora G (2012) Overview of glutamatergic neurotransmission in the nervous system. Pharmacol Biochem Behav 100:656-664.

Nieh EH, Vander Weele CM, Matthews GA, Presbrey KN, Wichmann R, Leppla CA, Izadmehr EM, Tye KM (2016) Inhibitory Input from the Lateral Hypothalamus to the Ventral Tegmental Area Disinhibits Dopamine Neurons and Promotes Behavioral Activation. Neuron 90:1286-1298.

Nieuwenhuys R, Geeraedts LM, Veening JG (1982) The medial forebrain bundle of the rat. I. General introduction. J Comp Neurol 206:49-81.

Nishikawa T, Fage D, Scatton B (1986) Evidence for, and nature of, the tonic inhibitory influence of habenulointerpeduncular pathways upon cerebral dopaminergic transmission in the rat. Brain Res 373:324-336.

Niswender CM, Conn PJ (2010) Metabotropic glutamate receptors: physiology, pharmacology, and disease. Annu Rev Pharmacol Toxicol 50:295-322.

Ogawa SK, Cohen JY, Hwang D, Uchida N, Watabe-Uchida M (2014) Organization of monosynaptic inputs to the serotonin and dopamine neuromodulatory systems. Cell Rep 8:1105-1118.

Ohno M, Watanabe S (1995) Persistent increase in dopamine release following activation of metabotropic glutamate receptors in the rat nucleus accumbens. Neurosci Lett 200:113-116.

Olds J (1956a) A preliminary mapping of electrical reinforcing effects in the rat brain. J Comp Physiol Psychol 49:281-285.

Olds J (1956b) Runway and maze behavior controlled by basomedial forebrain stimulation in the rat. J Comp Physiol Psychol 49:507-512.

Olds J (1958a) Satiation effects in self-stimulation of the brain. J Comp Physiol Psychol 51:675-678.

Olds J (1958b) Self-stimulation of the brain; its use to study local effects of hunger, sex, and drugs. Science 127:315-324.

Olds J, Milner P (1954) Positive reinforcement produced by electrical stimulation of septal area and other regions of rat brain. J Comp Physiol Psychol 47:419-427.

Omelchenko N, Sesack SR (2010) Periaqueductal gray afferents synapse onto dopamine and GABA neurons in the rat ventral tegmental area. J Neurosci Res 88:981-991.

Omelchenko N, Bell R, Sesack SR (2009) Lateral habenula projections to dopamine and GABA neurons in the rat ventral tegmental area. Eur J Neurosci 30:1239-1250.

Ornstein K, Huston JP (1975) Influence of 6-hydroxydopamine injections in the substantia nigra on lateral hypothalamic reinforcement. Neurosci Lett 1:339-342.

Overton PG, Clark D (1997) Burst firing in midbrain dopaminergic neurons. Brain Res Brain Res Rev 25:312-334.

Ozawa S, Kamiya H, Tsuzuki K (1998) Glutamate receptors in the mammalian central nervous system. Prog Neurobiol 54:581-618.

Palmiter RD (2008) Dopamine signaling in the dorsal striatum is essential for motivated behaviors: lessons from dopamine-deficient mice. Ann N Y Acad Sci 1129:35-46.

Panagis G, Miliaressis E, Anagnostakis Y, Spyraki C (1995) Ventral pallidum self-stimulation: a moveable electrode mapping study. Behav Brain Res 68:165-172.

Paoletti P, Bellone C, Zhou Q (2013) NMDA receptor subunit diversity: impact on receptor properties, synaptic plasticity and disease. Nat Rev Neurosci 14:383-400.

Park MR (1987) Monosynaptic inhibitory postsynaptic potentials from lateral habenula recorded in dorsal raphe neurons. Brain Res Bull 19:581-586.

Pasternak GW, Pan YX (2013) Mu opioids and their receptors: evolution of a concept. Pharmacol Rev 65:1257-1317.

Pavlov I (1927) Conditioned Reflexes: An Investigation of the Physiological Activity of the Cerebral Cortex. Translated and Edited by G. V. Anrep. London: Oxford University Press. p. 142.

Peng XQ, Ashby CR, Jr., Spiller K, Li X, Li J, Thomasson N, Millan MJ, Mocaer E, Munoz C, Gardner EL, Xi ZX (2009) The preferential dopamine D3 receptor antagonist S33138 inhibits cocaine reward and cocaine-triggered relapse to drug-seeking behavior in rats. Neuropharmacology 56:752-760.

Perlikowska R, Gach K, Fichna J, Toth G, Walkowiak B, do-Rego JC, Janecka A (2009) Biological activity of endomorphin and [Dmt1]endomorphin analogs with six-membered proline surrogates in position 2. Bioorg Med Chem 17:3789-3794.

Perrotti LI, Bolanos CA, Choi KH, Russo SJ, Edwards S, Ulery PG, Wallace DL, Self DW, Nestler EJ, Barrot M (2005) DeltaFosB accumulates in a GABAergic cell population in the posterior tail of the ventral tegmental area after psychostimulant treatment. Eur J Neurosci 21:2817-2824.

Phillips AG (1970) Enhancement and inhibition of olfactory bulb self-stimulation by odours. Physiol Behav 5:1127-1131.

Phillips AG, Van Der Kooy D, Fibiger HC (1977) Maintenance of intracranial self-stimulation in hippocampus and olfactory bulb following regional depletion of noradrenaline. Neurosci Lett 4:77-84.

Phillips AG, Coury A, Fiorino D, LePiane FG, Brown E, Fibiger HC (1992) Self-stimulation of the ventral tegmental area enhances dopamine release in the nucleus accumbens: a microdialysis study. Ann N Y Acad Sci 654:199-206.

Phillipson OT, Pycock CJ (1982) Dopamine neurones of the ventral tegmentum project to both medial and lateral habenula. Some implications for habenular function. Exp Brain Res 45:89-94.

Phillipson OT, Griffiths AC (1985) The topographic order of inputs to nucleus accumbens in the rat. Neuroscience 16:275-296.

Pijnenburg AJ, Honig WM, Van der Heyden JA, Van Rossum JM (1976) Effects of chemical stimulation of the mesolimbic dopamine system upon locomotor activity. Eur J Pharmacol 35:45-58.

Pollak Dorocic I, Furth D, Xuan Y, Johansson Y, Pozzi L, Silberberg G, Carlen M, Meletis K (2014) A whole-brain atlas of inputs to serotonergic neurons of the dorsal and median raphe nuclei. Neuron 83:663-678.

Pompeiano M, Palacios JM, Mengod G (1994) Distribution of the serotonin 5-HT2 receptor family mRNAs: comparison between 5-HT2A and 5-HT2C receptors. Brain Res Mol Brain Res 23:163-178.

Porrino LJ, Domer FR, Crane AM, Sokoloff L (1988) Selective alterations in cerebral metabolism within the mesocorticolimbic dopaminergic system produced by acute cocaine administration in rats. Neuropsychopharmacology 1:109-118.

Proulx CD, Hikosaka O, Malinow R (2014) Reward processing by the lateral habenula in normal and depressive behaviors. Nat Neurosci 17:1146-1152.

Qi J, Zhang S, Wang HL, Wang H, de Jesus Aceves Buendia J, Hoffman AF, Lupica CR, Seal RP, Morales M (2014) A glutamatergic reward input from the dorsal raphe to ventral tegmental area dopamine neurons. Nat Commun 5:5390.

Qin C, Luo M (2009) Neurochemical phenotypes of the afferent and efferent projections of the mouse medial habenula. Neuroscience 161:827-837.

Quina LA, Tempest L, Ng L, Harris JA, Ferguson S, Jhou TC, Turner EE (2015) Efferent pathways of the mouse lateral habenula. J Comp Neurol 523:32-60.

Ramm P, Beninger RJ, Frost BJ (1984) Functional activity in the lateral habenular and dorsal raphe nuclei following administration of several dopamine receptor antagonists. Can J Physiol Pharmacol 62:1530-1533.

Ranck JB, Jr. (1975) Which elements are excited in electrical stimulation of mammalian central nervous system: a review. Brain Res 98:417-440.

Rasmussen KG, Lineberry TW, Galardy CW, Kung S, Lapid MI, Palmer BA, Ritter MJ, Schak KM, Sola CL, Hanson AJ, Frye MA (2013) Serial infusions of low-dose ketamine for major depression. J Psychopharmacol 27:444-450.

Reisine TD, Soubrie P, Artaud F, Glowinski J (1982) Involvement of lateral habenula-dorsal raphe neurons in the differential regulation of striatal and nigral serotonergic transmission cats. J Neurosci 2:1062-1071.

Ren J, Qin C, Hu F, Tan J, Qiu L, Zhao S, Feng G, Luo M (2011) Habenula "cholinergic" neurons co-release glutamate and acetylcholine and activate postsynaptic neurons via distinct transmission modes. Neuron 69:445-452.

Robertson SJ, Edwards FA (1998) ATP and glutamate are released from separate neurones in the rat medial habenula nucleus: frequency dependence and adenosine-mediated inhibition of release. J Physiol 508 (Pt 3):691-701.

Robertson SJ, Burnashev N, Edwards FA (1999) Ca2+ permeability and kinetics of glutamate receptors in rat medial habenula neurones: implications for purinergic transmission in this nucleus. J Physiol 518 (Pt 2):539-549.

Robinson JE, Fish EW, Krouse MC, Thorsell A, Heilig M, Malanga CJ (2012) Potentiation of brain stimulation reward by morphine: effects of neurokinin-1 receptor antagonism. Psychopharmacology (Berl) 220:215-224.

Robles CF, McMackin MZ, Campi KL, Doig IE, Takahashi EY, Pride MC, Trainor BC (2014) Effects of kappa opioid receptors on conditioned place aversion and social interaction in males and females. Behav Brain Res 262:84-93.

Roiser JP, Levy J, Fromm SJ, Nugent AC, Talagala SL, Hasler G, Henn FA, Sahakian BJ, Drevets WC (2009) The effects of tryptophan depletion on neural responses to emotional words in remitted depression. Biol Psychiatry 66:441-450.

Rolls ET (2017) The roles of the orbitofrontal cortex via the habenula in non-reward and depression, and in the responses of serotonin and dopamine neurons. Neurosci Biobehav Rev 75:331-334.

Rompre PP, Miliaressis E (1985) Pontine and mesencephalic substrates of self-stimulation. Brain Res 359:246-259.

Rompre PP, Boye S (1989) Localization of reward-relevant neurons in the pontine tegmentum: a moveable electrode mapping study. Brain Res 496:295-302.

Rompre PP, Bauco P (1990) GBR 12909 reverses the SCH 23390 inhibition of rewarding effects of brain stimulation. Eur J Pharmacol 182:181-184.

Ronnekleiv OK, Moller M (1979) Brain-pineal nervous connections in the rat: an ultrastructure study following habenular lesion. Exp Brain Res 37:551-562.

Root DH, Mejias-Aponte CA, Zhang S, Wang HL, Hoffman AF, Lupica CR, Morales M (2014) Single rodent mesohabenular axons release glutamate and GABA. Nat Neurosci 17:1543-1551.

Rotllant D, Marquez C, Nadal R, Armario A (2010) The brain pattern of c-fos induction by two doses of amphetamine suggests different brain processing pathways and minor contribution of behavioural traits. Neuroscience 168:691-705.

Routtenberg A, Lindy J (1965) Effects of the availability of rewarding septal and hypothalamic stimulation on bar pressing for food under conditions of deprivation. J Comp Physiol Psychol 60:158-161.

Sabatino M, Ferraro G, La Grutta V (1991) Relay stations and neurotransmitters between the pallidal region and the hippocampus. Electroencephalogr Clin Neurophysiol 78:302-310.

Sadowski B (1972) Intracranial self-stimulation patterns in dogs. Physiol Behav 8:189-193.

Sagar SM, Sharp FR, Curran T (1988) Expression of c-fos protein in brain: metabolic mapping at the cellular level. Science 240:1328-1331.

Salaberry NL, Mendoza J (2015) Insights into the Role of the Habenular Circadian Clock in Addiction. Front Psychiatry 6:179.

Salas R, Baldwin P, de Biasi M, Montague PR (2010) BOLD Responses to Negative Reward Prediction Errors in Human Habenula. Front Hum Neurosci 4:36.

Sanchez-Catalan MJ, Faivre F, Yalcin I, Muller MA, Massotte D, Majchrzak M, Barrot M (2017) Response of the Tail of the Ventral Tegmental Area to Aversive Stimuli. Neuropsychopharmacology 42:638-648.

Sartorius A, Kiening KL, Kirsch P, von Gall CC, Haberkorn U, Unterberg AW, Henn FA, Meyer-Lindenberg A (2010) Remission of major depression under deep brain stimulation of the lateral habenula in a therapy-refractory patient. Biol Psychiatry 67:e9-e11.

Sastry BR, Zialkowski SE, Hansen LM, Kavanagh JP, Evoy EM (1979) Acetylcholine release in interpeduncular nucleus following the stimulation of habenula. Brain Res 164:334-337.

Sattler R, Tymianski M (2001) Molecular mechanisms of glutamate receptor-mediated excitotoxic neuronal cell death. Mol Neurobiol 24:107-129.

Scammell TE, Estabrooke IV, McCarthy MT, Chemelli RM, Yanagisawa M, Miller MS, Saper CB (2000) Hypothalamic arousal regions are activated during modafinil-induced wakefulness. J Neurosci 20:8620-8628.

Schaefer GJ, Michael RP (1980) Acute effects of neuroleptics on brain self-stimulation thresholds in rats. Psychopharmacology (Berl) 67:9-15.

Schindler CW, Carmona GN (2002) Effects of dopamine agonists and antagonists on locomotor activity in male and female rats. Pharmacol Biochem Behav 72:857-863.

Schlussman SD, Zhang Y, Hsu NM, Allen JM, Ho A, Kreek MJ (2008) Heroin-induced locomotor activity and conditioned place preference in C57BL/6J and 129P3/J mice. Neurosci Lett 440:284-288.

Schultz W (2010) Dopamine signals for reward value and risk: basic and recent data. Behav Brain Funct 6:24.

Schultz W (2015) Neuronal Reward and Decision Signals: From Theories to Data. Physiol Rev 95:853-951.

Schultz W (2016) Dopamine reward prediction error coding. Dialogues Clin Neurosci 18:23-32.

Schultz W, Dayan P, Montague PR (1997) A neural substrate of prediction and reward. Science 275:1593-1599.

Schulz D, Canbeyli RS (2000) Lesion of the bed nucleus of the stria terminalis enhances learned despair. Brain Res Bull 52:83-87.

Sego C, Goncalves L, Lima L, Furigo IC, Donato J, Jr., Metzger M (2014) Lateral habenula and the rostromedial tegmental nucleus innervate neurochemically distinct subdivisions of the dorsal raphe nucleus in the rat. J Comp Neurol 522:1454-1484.

Semba K, Fibiger HC (1992) Afferent connections of the laterodorsal and the pedunculopontine tegmental nuclei in the rat: a retro- and antero-grade transport and immunohistochemical study. J Comp Neurol 323:387-410.

Seoane-Collazo P, Ferno J, Gonzalez F, Dieguez C, Leis R, Nogueiras R, Lopez M (2015) Hypothalamic-autonomic control of energy homeostasis. Endocrine 50:276-291.

Sesack SR, Deutch AY, Roth RH, Bunney BS (1989) Topographical organization of the efferent projections of the medial prefrontal cortex in the rat: an anterograde tract-tracing study with Phaseolus vulgaris leucoagglutinin. J Comp Neurol 290:213-242.

Shabel SJ, Proulx CD, Piriz J, Malinow R (2014) Mood regulation. GABA/glutamate co-release controls habenula output and is modified by antidepressant treatment. Science 345:1494-1498.

Shabel SJ, Proulx CD, Trias A, Murphy RT, Malinow R (2012) Input to the lateral habenula from the basal ganglia is excitatory, aversive, and suppressed by serotonin. Neuron 74:475-481.

Shaw PJ, Ince PG (1997) Glutamate, excitotoxicity and amyotrophic lateral sclerosis. J Neurol 244 Suppl 2:S3-14.

Shelton L, Becerra L, Borsook D (2012a) Unmasking the mysteries of the habenula in pain and analgesia. Prog Neurobiol 96:208-219.

Shelton L, Pendse G, Maleki N, Moulton EA, Lebel A, Becerra L, Borsook D (2012b) Mapping pain activation and connectivity of the human habenula. J Neurophysiol 107:2633-2648.

Shen X, Ruan X, Zhao H (2012) Stimulation of midbrain dopaminergic structures modifies firing rates of rat lateral habenula neurons. PLoS One 7:e34323.

Shepard PD, Holcomb HH, Gold JM (2006) Schizophrenia in translation: the presence of absence: habenular regulation of dopamine neurons and the encoding of negative outcomes. Schizophr Bull 32:417-421.

Shibata H, Suzuki T, Matsushita M (1986) Afferent projections to the interpeduncular nucleus in the rat, as studied by retrograde and anterograde transport of wheat germ agglutinin conjugated to horseradish peroxidase. J Comp Neurol 248:272-284.

Shih PY, Engle SE, Oh G, Deshpande P, Puskar NL, Lester HA, Drenan RM (2014) Differential expression and function of nicotinic acetylcholine receptors in subdivisions of medial habenula. J Neurosci 34:9789-9802.

Shumake J, Edwards E, Gonzalez-Lima F (2003) Opposite metabolic changes in the habenula and ventral tegmental area of a genetic model of helpless behavior. Brain Res 963:274-281.

Sidhu KS, Stellar JR, Garity D, Bruno JP (1993) 6-OHDA-treated weanling rats show normal neuroleptic sensitivity as adults on LHSS. Pharmacol Biochem Behav 44:901-905.

Simmons JM, Ackermann RF, Gallistel CR (1998) Medial forebrain bundle lesions fail to structurally and functionally disconnect the ventral tegmental area from many ipsilateral forebrain nuclei: implications for the neural substrate of brain stimulation reward. J Neurosci 18:8515-8533.

Skinner BF (1938) The behavior of organisms: An experimental analysis. New York: Appleton-Century-Crofts.

Smith Y, Seguela P, Parent A (1987) Distribution of GABA-immunoreactive neurons in the thalamus of the squirrel monkey (Saimiri sciureus). Neuroscience 22:579-591.

Soubrie P, Reisine T, Artaud F, Glowinski J (1981) Role of the lateral habenula in modulating nigral and striatal in vivo [3H]serotonin release in the cat. Brain Res 222:192-197.

Spanagel R, Herz A, Shippenberg TS (1992) Opposing tonically active endogenous opioid systems modulate the mesolimbic dopaminergic pathway. Proc Natl Acad Sci U S A 89:2046-2050.

Stamatakis AM, Stuber GD (2012) Activation of lateral habenula inputs to the ventral midbrain promotes behavioral avoidance. Nat Neurosci 15:1105-1107.

Stamatakis AM, Van Swieten M, Basiri ML, Blair GA, Kantak P, Stuber GD (2016) Lateral Hypothalamic Area Glutamatergic Neurons and Their Projections to the Lateral Habenula Regulate Feeding and Reward. J Neurosci 36:302-311.

Stamatakis AM, Jennings JH, Ung RL, Blair GA, Weinberg RJ, Neve RL, Boyce F, Mattis J, Ramakrishnan C, Deisseroth K, Stuber GD (2013) A unique population of ventral tegmental area neurons inhibits the lateral habenula to promote reward. Neuron 80:1039-1053.

Steffensen SC, Svingos AL, Pickel VM, Henriksen SJ (1998) Electrophysiological characterization of GABAergic neurons in the ventral tegmental area. J Neurosci 18:8003-8015.

Steidl S, Myal S, Wise RA (2015) Supplemental morphine infusion into the posterior ventral tegmentum extends the satiating effects of self-administered intravenous heroin. Pharmacol Biochem Behav 134:1-5.

Steidl S, Dhillon ES, Sharma N, Ludwig J (2017) Muscarinic cholinergic receptor antagonists in the VTA and RMTg have opposite effects on morphine-induced locomotion in mice. Behav Brain Res 323:111-116.

Steimer T (2002) The biology of fear- and anxiety-related behaviors. Dialogues Clin Neurosci 4:231-249.

Stern WC, Johnson A, Bronzino JD, Morgane PJ (1979) Effects of electrical stimulation of the lateral habenula on single-unit activity of raphe neurons. Exp Neurol 65:326-342.

Stoker A, Markou A (2011) The Intracranial Self-Stimulation Procedure Provides Quantitative Measures of Brain Reward Function. In: Mood and Anxiety Related Phenotypes in Mice: Characterization Using Behavioral Tests, Volume II. In: Neuromethods, vol. 63. (Gould TD, ed). New York: Humana Press, pp. 307-331.

Straub CJ, Carlezon WA, Jr., Rudolph U (2010) Diazepam and cocaine potentiate brain stimulation reward in C57BL/6J mice. Behav Brain Res 206:17-20.

Stuber GD, Wise RA (2016) Lateral hypothalamic circuits for feeding and reward. Nat Neurosci 19:198-205.

Sutherland RJ (1982) The dorsal diencephalic conduction system: a review of the anatomy and functions of the habenular complex. Neurosci Biobehav Rev 6:1-13.

Sutherland RJ, Nakajima S (1981) Self-stimulation of the habenular complex in the rat. J Comp Physiol Psychol 95:781-791.

Tachibana Y, Hikosaka O (2012) The primate ventral pallidum encodes expected reward value and regulates motor action. Neuron 76:826-837.

Takagi H, Shiosaka S, Tohyama M, Senba E, Sakanaka M (1980) Ascending components of the medial forebrain bundle from the lower brain stem in the rat, with special reference to raphe and catecholamine cell groups. A study by the HRP method. Brain Res 193:315-337.

Talishinsky AD, Nicolas C, Ikemoto S (2017) Interaction of chronic food restriction and methylphenidate in sensation seeking of rats. Psychopharmacology (Berl) 234:2197-2206.

Taraschenko OD, Shulan JM, Maisonneuve IM, Glick SD (2007) 18-MC acts in the medial habenula and interpeduncular nucleus to attenuate dopamine sensitization to morphine in the nucleus accumbens. Synapse 61:547-560.

Tchenio A, Valentinova K, Mameli M (2016) Can the Lateral Habenula Crack the Serotonin Code? Front Synaptic Neurosci 8:34.

Tempel A, Zukin RS (1987) Neuroanatomical patterns of the mu, delta, and kappa opioid receptors of rat brain as determined by quantitative in vitro autoradiography. Proc Natl Acad Sci U S A 84:4308-4312.

Thompson T, Schuster CR (1964) Morphine Self-Administration, Food-Reinforced, and Avoidance Behaviors in Rhesus Monkeys. Psychopharmacologia 5:87-94.

Thorndike EL (1911) Animal intelligence. New York: Macmillan.

Tian J, Uchida N (2015) Habenula Lesions Reveal that Multiple Mechanisms Underlie Dopamine Prediction Errors. Neuron 87:1304-1316.

Todtenkopf MS, Marcus JF, Portoghese PS, Carlezon WA, Jr. (2004) Effects of kappa-opioid receptor ligands on intracranial self-stimulation in rats. Psychopharmacology (Berl) 172:463-470.

Tomasiewicz HC, Todtenkopf MS, Chartoff EH, Cohen BM, Carlezon WA, Jr. (2008) The kappa-opioid agonist U69,593 blocks cocaine-induced enhancement of brain stimulation reward. Biol Psychiatry 64:982-988.

Toth ZE, Gallatz K, Fodor M, Palkovits M (1999) Decussations of the descending paraventricular pathways to the brainstem and spinal cord autonomic centers. J Comp Neurol 414:255-266.

Ullsperger M, von Cramon DY (2003) Error monitoring using external feedback: specific roles of the habenular complex, the reward system, and the cingulate motor area revealed by functional magnetic resonance imaging. J Neurosci 23:4308-4314.

Ungless MA, Magill PJ, Bolam JP (2004) Uniform inhibition of dopamine neurons in the ventral tegmental area by aversive stimuli. Science 303:2040-2042.

Ursin R, Ursin H, Olds J (1966) Self-stimulation of hippocampus in rats. J Comp Physiol Psychol 61:353-359.

Vachon MP, Miliaressis E (1992) Dorsal diencephalic self-stimulation: a movable electrode mapping study. Behav Neurosci 106:981-991.

Valentinova K, Mameli M (2016) mGluR-LTD at Excitatory and Inhibitory Synapses in the Lateral Habenula Tunes Neuronal Output. Cell Rep 16:2298-2307.

van Ree JM, Slangen JL, de Wied D (1978) Intravenous self-administration of drugs in rats. J Pharmacol Exp Ther 204:547-557.

Varga V, Kocsis B, Sharp T (2003) Electrophysiological evidence for convergence of inputs from the medial prefrontal cortex and lateral habenula on single neurons in the dorsal raphe nucleus. Eur J Neurosci 17:280-286.

Varga V, Szekely AD, Csillag A, Sharp T, Hajos M (2001) Evidence for a role of GABA interneurones in the cortical modulation of midbrain 5-hydroxytryptamine neurones. Neuroscience 106:783-792.

Vento PJ, Burnham NW, Rowley CS, Jhou TC (2017) Learning From One's Mistakes: A Dual Role for the Rostromedial Tegmental Nucleus in the Encoding and Expression of Punished Reward Seeking. Biol Psychiatry 81:1041-1049.

Verma A, Moghaddam B (1998) Regulation of striatal dopamine release by metabotropic glutamate receptors. Synapse 28:220-226.

Vertes RP (1991) A PHA-L analysis of ascending projections of the dorsal raphe nucleus in the rat. J Comp Neurol 313:643-668.

Vertes RP, Crane AM (1997) Distribution, quantification, and morphological characteristics of serotonin-immunoreactive cells of the supralemniscal nucleus (B9) and pontomesencephalic reticular formation in the rat. J Comp Neurol 378:411-424.

Vertes RP, Fortin WJ, Crane AM (1999) Projections of the median raphe nucleus in the rat. J Comp Neurol 407:555-582.

Vigneault E, Poirel O, Riad M, Prud'homme J, Dumas S, Turecki G, Fasano C, Mechawar N, El Mestikawy S (2015) Distribution of vesicular glutamate transporters in the human brain. Front Neuroanat 9:23.

Volkow ND, Morales M (2015) The Brain on Drugs: From Reward to Addiction. Cell 162:712-725.

Volkow ND, Fowler JS, Wang GJ, Swanson JM, Telang F (2007) Dopamine in drug abuse and addiction: results of imaging studies and treatment implications. Arch Neurol 64:1575-1579.

Volkow ND, Fowler JS, Wang GJ, Baler R, Telang F (2009) Imaging dopamine's role in drug abuse and addiction. Neuropharmacology 56 Suppl 1:3-8.

Vollrath-Smith FR, Shin R, Ikemoto S (2012) Synergistic interaction between baclofen administration into the median raphe nucleus and inconsequential visual stimuli on investigatory behavior of rats. Psychopharmacology (Berl) 220:15-25.

Wallace TL, Gudelsky GA, Vorhees CV (1999) Methamphetamine-induced neurotoxicity alters locomotor activity, stereotypic behavior, and stimulated dopamine release in the rat. J Neurosci 19:9141-9148.

Wang D, Li Y, Feng Q, Guo Q, Zhou J, Luo M (2017) Learning shapes the aversion and reward responses of lateral habenula neurons. Elife 6.

Wang DG, Gong N, Luo B, Xu TL (2006) Absence of GABA type A signaling in adult medial habenular neurons. Neuroscience 141:133-141.

Wang DV, Yau HJ, Broker CJ, Tsou JH, Bonci A, Ikemoto S (2015) Mesopontine median raphe regulates hippocampal ripple oscillation and memory consolidation. Nat Neurosci 18:728-735.

Wang RY, Aghajanian GK (1977) Physiological evidence for habenula as major link between forebrain and midbrain raphe. Science 197:89-91.

Wang T, French ED (1995) NMDA, kainate, and AMPA depolarize nondopamine neurons in the rat ventral tegmentum. Brain Res Bull 36:39-43.

Waraczynski M, Shizgal P (1995) Self-stimulation of the MFB following parabrachial lesions. Physiol Behav 58:559-566.

Waraczynski M, Ton MN, Shizgal P (1990) Failure of amygdaloid lesions to increase the threshold for self-stimulation of the lateral hypothalamus and ventral tegmental area. Behav Brain Res 40:159-168.

Waraczynski M, Conover K, Shizgal P (1992) Rewarding effectiveness of caudal MFB stimulation is unaltered following DMH lesions. Physiol Behav 52:211-218.

Waraczynski M, Carlton E, Perkins M (1998) Midbrain periaqueductal lesions do not degrade medial forebrain bundle stimulation reward. Behav Brain Res 95:167-177.

Waraczynski MA (1988) Basal forebrain knife cuts and medial forebrain bundle self-stimulation. Brain Res 438:8-22.

Ward SE, Bax BD, Harries M (2010) Challenges for and current status of research into positive modulators of AMPA receptors. Br J Pharmacol 160:181-190.

Wasserman DI, Tan JM, Kim JC, Yeomans JS (2016) Muscarinic control of rostromedial tegmental nucleus GABA neurons and morphine-induced locomotion. Eur J Neurosci 44:1761-1770.

Wasserman DI, Wang HG, Rashid AJ, Josselyn SA, Yeomans JS (2013) Cholinergic control of morphine-induced locomotion in rostromedial tegmental nucleus versus ventral tegmental area sites. Eur J Neurosci 38:2774-2785.

Watson JB (1913) Psychology as the behaviorist views it. Psychological Review 20:158-177.

Wechsler LR, Savaki HE, Sokoloff L (1979) Effects of d- and l-amphetamine on local cerebral glucose utilization in the conscious rat. J Neurochem 32:15-22.

Weeks JR (1962) Experimental morphine addiction: method for automatic intravenous injections in unrestrained rats. Science 138:143-144.

Weiss T, Veh RW (2011) Morphological and electrophysiological characteristics of neurons within identified subnuclei of the lateral habenula in rat brain slices. Neuroscience 172:74-93.

Whitton AE, Treadway MT, Pizzagalli DA (2015) Reward processing dysfunction in major depression, bipolar disorder and schizophrenia. Curr Opin Psychiatry 28:7-12.

Wilkinson HA, Peele TL (1963) Intracranial Self-Stimulation in Cats. J Comp Neurol 121:425-440.

Winter C, Vollmayr B, Djodari-Irani A, Klein J, Sartorius A (2011) Pharmacological inhibition of the lateral habenula improves depressive-like behavior in an animal model of treatment resistant depression. Behav Brain Res 216:463-465.

Wirtshafter D, Asin KE, Pitzer MR (1994) Dopamine agonists and stress produce different patterns of Fos-like immunoreactivity in the lateral habenula. Brain Res 633:21-26.

Wise RA (1981) Intracranial self-stimulation: mapping against the lateral boundaries of the dopaminergic cells of the substantia nigra. Brain Res 213:190-194.

Wise RA (1989) Opiate reward: sites and substrates. Neurosci Biobehav Rev 13:129-133.

Wise RA (2002) Brain reward circuitry: insights from unsensed incentives. Neuron 36:229-240.

Wise RA, Rompre PP (1989) Brain dopamine and reward. Annu Rev Psychol 40:191-225.

Wree A, Zilles K, Schleicher A (1981) Growth of fresh volumes and spontaneous cell death in the nuclei habenulae of albino rats during ontogenesis. Anat Embryol (Berl) 161:419-431.

Wu X, Zhao N, Bai F, Li C, Liu C, Wei J, Zong W, Yang L, Ryabinin AE, Ma Y, Wang J (2016) Morphine-induced conditioned place preference in rhesus monkeys: Resistance to inactivation of insula and extinction. Neurobiol Learn Mem 131:192-200.

Wu Y, Pearl SM, Zigmond MJ, Michael AC (2000) Inhibitory glutamatergic regulation of evoked dopamine release in striatum. Neuroscience 96:65-72.

Xie G, Zuo W, Wu L, Li W, Wu W, Bekker A, Ye JH (2016) Serotonin modulates glutamatergic transmission to neurons in the lateral habenula. Sci Rep 6:23798.

Yadid G, Gispan I, Lax E (2013) Lateral habenula deep brain stimulation for personalized treatment of drug addiction. Front Hum Neurosci 7:806.

Yamadori T (1969) Efferent fibers of the habenula and stria medullaris thalami in rats. Exp Neurol 25:541-558.

Yang Y, Cui Y, Sang K, Dong Y, Ni Z, Ma S, Hu H (2018) Ketamine blocks bursting in the lateral habenula to rapidly relieve depression. Nature 554:317-322.

Yates JW, Meij JT, Sullivan JR, Richtand NM, Yu L (2007) Bimodal effect of amphetamine on motor behaviors in C57BL/6 mice. Neurosci Lett 427:66-70.

Yavich L, Tanila H (2007) Mechanics of self-stimulation and dopamine release in the nucleus accumbens. Neuroreport 18:1271-1274.

Yeomans J, Prior P, Bateman F (1986) Current-distance relations of axons mediating circling elicited by midbrain stimulation. Brain Res 372:95-106.

Yetnikoff L, Cheng AY, Lavezzi HN, Parsley KP, Zahm DS (2015) Sources of input to the rostromedial tegmental nucleus, ventral tegmental area, and lateral habenula compared: A study in rat. J Comp Neurol 523:2426-2456.

Yizhar O, Fenno LE, Davidson TJ, Mogri M, Deisseroth K (2011) Optogenetics in neural systems. Neuron 71:9-34.

You ZB, Chen YQ, Wise RA (2001) Dopamine and glutamate release in the nucleus accumbens and ventral tegmental area of rat following lateral hypothalamic self-stimulation. Neuroscience 107:629-639.

Zahm DS, Becker ML, Freiman AJ, Strauch S, Degarmo B, Geisler S, Meredith GE, Marinelli M (2010) Fos after single and repeated self-administration of cocaine and saline in the rat: emphasis on the Basal forebrain and recalibration of expression. Neuropsychopharmacology 35:445-463.

Zangen A, Ikemoto S, Zadina JE, Wise RA (2002) Rewarding and psychomotor stimulant effects of endomorphin-1: anteroposterior differences within the ventral tegmental area and lack of effect in nucleus accumbens. J Neurosci 22:7225-7233.

Zarate CA, Jr., Singh JB, Carlson PJ, Brutsche NE, Ameli R, Luckenbaugh DA, Charney DS, Manji HK (2006) A randomized trial of an N-methyl-D-aspartate antagonist in treatment-resistant major depression. Arch Gen Psychiatry 63:856-864.

Zhang B, Gao Y, Li Y, Yang J, Zhao H (2016) Sleep Deprivation Influences Circadian Gene Expression in the Lateral Habenula. Behav Neurol 2016:7919534.

Zhou Y, Danbolt NC (2014) Glutamate as a neurotransmitter in the healthy brain. J Neural Transm (Vienna) 121:799-817.

Zilles K, Schleicher A, Wingert F (1976) [Quantitative growth analysis of limbic nuclei areas fresh volume in diencephalon and mesencephalon of an albino mouse ontogenic series. I. Nucleus habenulare]. J Hirnforsch 17:1-10.

Zuo W, Zhang Y, Xie G, Gregor D, Bekker A, Ye JH (2016) Serotonin stimulates lateral habenula via activation of the post-synaptic serotonin 2/3 receptors and transient receptor potential channels. Neuropharmacology 101:449-459.